D 2021

U.PORTO
FEUP FACULDADE DE ENGENHARIA
UNIVERSIDADE DO PORTO

STOCHASTIC NUMERICAL MODELLING OF FLUVIAL MORPHODYNAMICS

BRUNO ANDRÉ MACHADO ANDRADE OLIVEIRA
TESE DE DOUTORAMENTO APRESENTADA
À FACULDADE DE ENGENHARIA DA UNIVERSIDADE DO PORTO EM
ENGENHARIA CIVIL

U.PORTO

FEUP FACULDADE DE ENGENHARIA
UNIVERSIDADE DO PORTO

Stochastic Numerical Modelling of Fluvial Morphodynamics

Bruno André Machado Andrade Oliveira

Dissertation submitted towards the partial fulfilment of the requirements for the degree of

DOCTOR IN CIVIL ENGINEERING

Supervisor: Professor Rodrigo Maia

Co-supervisor: Professor Francesco Ballio

APRIL 2021

To my family,

To my friends

And above all

To Diana

A person who never made a mistake never tried anything new

Albert Einstein

ACKNOWLEDGEMENTS

As with most journeys, this PhD could not have been brought to fruition without the help of many people. I would like to identify and thank some of these individuals here.

To Professor Rodrigo Maia, I have to thank in particular his support and professional guidance over a very long period of time, without which none of this would have been possible. Having started relatively fresh in the world of academia, this assistance, more than anything else, was essential in this, the (most likely) most difficult task in my life.

To Professor Ballio, I have to thank, above all else, the in-depth understanding and professional opinion with which he contributed to this study. His influence was essential in maintaining a realistic setting and a realistic purpose for the work which was developed.

To my "co-workers", the researchers and PhD students at the Faculty of Engineering of the University of Porto, who have shared of my struggle, I wish the best of luck for their futures. An individual thank you is necessary to Tiago Ferradosa and Vanessa Ramos, with whom I have had the pleasure of sharing in both motivation and enthusiasm (and also some exhaustion naturally) even when not in the weight of our respective responsibilities.

To my family and particularly my father, mother and brother, I must thank their patient support for 29 years and counting. One must not forget one's own roots and these are mine.

And finally, last but definitely not least, I have to express my gratitude to my girlfriend, Diana, not just for her support, but also for her unrelenting understanding and patience as well as her unbridled care and concern for me.

This study has been developed with the support of a scholarship funded by the *Fundação para a Ciência e* Tecnologia, of Portugal, with the scholarship reference number PD/BI/128053/2016.

RESUMO

Durante a presente dissertação de doutoramento, o conceito da modelação estocástica da morfodinâmica fluvial foi desenvolvido e sistematizado tendo em vista a sua aplicação. Este estudo propôs-se superar as dificuldades inerentes a este processo de modelação, particularmente no que diz respeito à sua aplicação no contexto de um ambiente fluvial real. Este objetivo foi alcançado através da definição e da sistematização dos aspetos e metodologias conceptuais e práticas essenciais à realização da modelação estocástica da morfodinâmica fluvial numa situação real. Os objetivos correspondentes podem ser descritos como: primeiro, desenvolver uma aplicação estocástica de modelação numérica da morfodinâmica fluvial, com base e a par com a metodologia correspondente; obtendo assim uma descrição clara das distribuições de probabilidade da evolução temporal morfodinâmica de um rio; segundo, aplicar estes resultados em análises de fiabilidade/risco dentro do contexto do correspondente caso de estudo. Tanto esta descrição como a metodologia em si representam uma inovação significativa sobre o conhecimento atual.

Na área da engenharia (e particularmente no projeto de estruturas hidráulicas), a variabilidade dos diferentes parâmetros envolvidos num determinado estudo deve, na maioria das situações, ser tida em consideração, por exemplo, por meio de análises de fiabilidade /risco. Existe atualmente um crescente interesse na aplicação de metodologias probabilísticas de projeto, nomeadamente na área da geomorfologia fluvial (Scheel, et al., 2014; Snyder, et al., 2003). A clarificação dos fatores determinantes da morfodinâmica e das principais limitações e requisitos da correspondente modelação estocástica (que se propôs realizar nesta tese) pretende constituir uma fundação sólida para futuros estudos nesta área.

O estudo utilizou um modelo numérico hidro e morfodinâmico para aproximar e representar a relação entre a morfodinâmica (ou seja, a evolução da forma do leito fluvial ao longo do tempo) e as variáveis que são mais importantes para a sua definição, seja em termos da sua magnitude global como do seu respetivo padrão, ou distribuição espacial, ao longo do leito do canal. Foram feitas melhorias e otimizações das ferramentas e métodos existentes para a modelação estocástica (da morfodinâmica fluvial) em quase todos os passos integrantes deste processo, nomeadamente, i) no tratamento de dados (com a aplicação da metodologia de pré-modelação, que se revelou capaz de reduzir a incerteza nos dados de batimetria), ii) na geração dos valores das variáveis (com particular enfase na geração de séries de valores de caudais), iii) na modelação estocástica propriamente dita (através do desenvolvimento da respetiva metodologia), iv) na validação da modelação estocástica (através da aplicação e comparação da utilidade de diferentes abordagens de validação) e v) na aplicação dos resultados da modelação estocástica.

No final da presente tese é detalhada a metodologia de aplicação (desenvolvido com base e durante o desenvolvimento da presente dissertação de doutoramento) em que são clarificadas as diferentes tarefas e soluções envolvidas no processo da modelação estocástica da morfodinâmica fluvial, incluindo os

passos necessários à sua aplicação na análise de risco. Embora ainda seja expectável a necessidade de desenvolver mais profundamente alguns aspetos específicos da metodologia, nomeadamente antes que a aplicação generalizada da modelação estocástica da morfodinâmica fluvial se torne uma realidade, pretende-se que o trabalho desenvolvido neste estudo providencie um sólido alicerce para o seu desenvolvimento no futuro.

PALAVRAS-CHAVE: Morfodinâmica fluvial, Modelação estocástica, Análise de sensibilidade, Incerteza, Risco

ABSTRACT

In this PhD study, the concept of the stochastic modelling of fluvial morphodynamics was applied and systematized for application. The present study was developed in order to overcome the difficulties inherent to this process, with particular focus on a real fluvial environment. This was accomplished by way of the definition and systematization of the conceptual and practical aspects and methodologies essential to these processes in a real life situation. The corresponding goals can therefore be described as, firstly, to develop a stochastic application of numerical modelling to fluvial morphodynamics along with the corresponding methodology and, secondly, to apply these results in a related reliability and risk analysis application. The former is intended to provide a clear description of the probability distribution functions of the temporal evolution of river's morphodynamic, while the latter is intended to establish and validate the necessary methodology. Both this description and the methodology itself represent a significant novelty over the existing knowledge.

In engineering (and particularly in the design of hydraulic structures), the variability of the different parameters involved in a study should, in most situations, be taken into consideration (e.g., by way of reliability/risk analysis). Presently, there is a growing interest in the application of probabilistic design methodologies, namely in fluvial geomorphology (Scheel, et al., 2014; Snyder, et al., 2003). The clarification of the driving factors of morphodynamics, along with the limitations and requirements of the corresponding stochastic modelling is intended to provide a foundation for future studies in this area.

This study uses a numerical hydro and morphodynamic model to approximate and represent the relationship between morphodynamics (i.e., the evolution of a channel's bed shape over time) and the variables which are most important to its definition, both in terms of the overall magnitude and of the distribution/pattern along the channel bed. Improvements and enhancements on the existing tools and methods for stochastic modelling (of fluvial morphodynamics) were introduced at virtually every step of the process, including: the data treatment (with the application of a pre-modelling approach capable of reducing bed level data uncertainty), the variable generation (with particular emphasis on streamflow generation), the stochastic modelling itself (via the development of its methodology), the validation of the stochastic modelling (by applying and comparing the usefulness of different validation approaches) and in the application of the results of the stochastic modelling.

At the end of this document, a methodology (developed based on and in the context of this PhD study), clarifying and summarizing the tasks and solutions involved in the process of the stochastic modelling of fluvial morphodynamics is detailed (including the steps necessary for its application to risk analysis). Although some components of the methodology still require some further scientific development before the wide-spread use of the stochastic modelling of fluvial morphodynamics can be a possibility, the work developed in this study, by way of the systematization of the corresponding methodology, will provide a reliable and complete foundation for its development.

KEYWORDS: Fluvial morphodynamics, Stochastic modelling, Sensitivity analysis, Uncertainty, Risk

TABLE OF CONTENTS

LIST OF FIGURES

LIST OF TABLES

LIST OF SYMBOLS AND ACRONYMS

C_D – Wind drag coefficient

D – Granulometry

D_{50} – Median sediment particle diameter (mm)

$D_{'XX'}$ – Quantile *'XX'* of sediment granulometry (mm)

D_m – Mean sediment particle diameter (mm)

dH – Bed level change (m)

f – correction factor of downstream discharge

i – average longitudinal slope of the channel

k – Grain roughness (mm)

$MorFac$ – Morphological change acceleration parameter

M_{PM} – Empirical factor in the Meyer-Peter & Müller formula

n – Bed roughness (mm)

p_{al} – Thickness of the active layer (m)

R – Hydraulic radius of the flow (m)

R^2 – Square of the Pearson's correlation coefficient

Q – Streamflow (m^3/s)

Q^* - Flood parameter used in the Stylized Case Study to represent flood intensity

Q' – Optimal flow value for the pre-modelling approach (m^3/s)

Q_{bl} – Flow of bed load (Kg/s)

Q_{min} – Incipient flow (which starts sediment transport in a channel) (m^3/s)

Q_s – Flow of sediment (Kg/s)

Q_t – Flow at instant t (m^3/s)

t – an instant in time (or simulation)

α – Parameter for defining the effect of secondary currents

β – Slope effect parameter in Koch & Flokstra (1981) formula

$\Delta Q_{(t,\,t')}$ – Difference/Derivative of flow between instant t and t'.

γ – Volumetric density of water (KN/m^2)

γ_s – Dry volumetric density of the soil/terrain (KN/m^2)

γ_{wall} – Dry volumetric density of the retention wall (KN/m^2)

λ - Bed porosity (%)

λ_b - Bottom friction coefficient

θ_c – Shields Parameter

Φ_r – Sediment critical shear angle (or of repose) (degrees)

ζ - Bank erosion coefficient (part of Ikeda, et al. (1981) linear model)

ANN – Artificial Neural Networks

APA – Agência Portuguesa do Ambiente

AR – Auto-Regressive models

ARMA – Auto-Regressive Moving Average models

ARIMA – Auto-Regressive Integrated Moving Average models

ARFIMA – Auto-Regressive Fractionally Integrated Moving Average models

AutoCor – Absolute change in the streamflow's first order autocorrelation coefficient

CC – Curvature Coefficient

CDF – Cumulative Distribution Function

CFL – Courant-Friedrichs-Lewy (condition)

CS – Complete Simulations

dAVGAnnual – Percentage change in the mean yearly streamflow values

dAVG1d – Absolute change in the daily streamflow's first derivate's mean

dAVG2d – Absolute change in the streamflow's second derivate's mean

dAVG%S – Percentage change in the daily streamflow's mean

dAVG%XX – Percentage change in the mean monthly streamflow sequentially from January (Ja) to December (De)

DS – Direct Simulations

dSD%S – Percentage change in the streamflow's standard deviation

dSD%1d – Percentage change in the streamflow's first derivate's standard deviation

dSD%2d – Percentage change in the streamflow's second derivate's standard deviation

ECDF – Empirical Cumulative Distribution Function

EDP – Energias de Portugal

FEUP – Faculdade de Engenharia da Universidade do Porto

FOI – First Order Index

FOSM – First Order Second-Moment method

FS – Final Simulations

GDP – Gross Domestic Product

GSA – Global Sensitivity Analysis

GUI – Graphical User Interface

HM – Hydrodynamic and Morphodynamics (as it pertains to the numerical models and its respective simulations)

HMAC – Harmonic Mean Absolute bed level Change

ISA – Independent Sensitivity Analysis

JSA – Joint Sensitivity Analysis

KDE – Kernel Density Estimation

KNN – K-Nearest Neighbours

K-plot – Kendall plot

MASV – Spatial Variability of Morphodynamics

MaxDfPr – Maximum difference between the observed and simulated streamflow's PDF

MBB – Moving Block Bootstrap

MCS – Monte Carlo Simulation

LMAC – Localized Mean Absolute bed level Change

LMC – Localized Mean bed level Change

LQI – Life Quality Index

OECD – Organization for Economic Co-operation and Development

OMAC – Overall Mean Absolute bed level Change

OMC – Overall Mean bed level Change

PARMA – Periodic Auto-Regressive Moving Average models

PDF – Probability Density Function

PDFR – PDF Rankings of bed level change

PFA – Percentage of channel Area Flooded

QQ plot – Quantile-Quantile plot

SD – Standard Deviation

SNIRH – Sistema Nacional de Informação de Recursos Hídricos

TEI – Total Effect Index

UC – Uniformity Coefficient

1D – Uni-Dimensional (or One-Dimensional)

2D – Two-Dimensional (or in Two Dimensions)

2DH – Horizontal Two-Dimensional

3D – Three-Dimensional (or in Three Dimensions)

'X'Y – for 'X' years or for a 'X' year(s) horizon (e.g., 1Y, 2Y)

LIST OF EQUATIONS

1
INTRODUCTION

The integration of one or more of the statistical aspects of fluvial morphodynamics (and, more concretely, their uncertainty) in the study of river bed morphology has long been a desired goal in the fields of hydrodynamics and (hydraulic) structure reliability (Schielen, et al., 2007; van Vuren, et al., 2015; Huthoff, et al., 2010; Ballio & Menoni, 2009). Additionally, there is a growing interest in the application of probabilistic design methodologies, namely in fluvial geomorphology (Scheel, et al., 2014; Snyder, et al., 2003). This study, which in itself constitutes this PhD's work, aims to overcome the difficulties inherent to accomplishing these goals, namely incorporating these statistical components in the analysis of fluvial morphodynamics. This incorporation is to be accomplished by systematizing and expediting the application of stochastic modelling in fluvial morphodynamics, with a particular focus on its use in a real fluvial environment. The corresponding goals can therefore be described as, firstly, to develop a stochastic application methodology for the numerical modelling to fluvial morphodynamics along with the corresponding methodology and, secondly, to apply these results in a related reliability and risk analysis application. The former is intended to provide a clear description of the probability distribution functions of the temporal evolution of river's morphodynamic, while the latter is intended to establish and exemplifying the necessary methodology. This is to be accomplished by way of the definition (where necessary) and systematization of the conceptual and practical aspects and methodologies essential to the application of stochastic modelling in a real life situation. The underlying tasks/stages of this objective are presented in this document, along with all the relevant conclusions and improvements introduced in the currently existing knowledge base in the context of this PhD study.

The process of simulating (and particularly forecasting) fluvial morphodynamics (i.e., the evolution of bed level change – dH – over time) is always permeated by a certain amount of uncertainty. The primary cause for this uncertainty is the large complexity involved in that process, specifically due to the large number of variables involved (exemplified in Figure 1, each with its own relative degree of importance for morphodynamics) and their strong inter-dependencies, as well as, the difficulty involved in estimating their exact values and effects in the morphodynamical processes. Generally, no two channels are alike in terms of the characteristics and relative importance of these variables. As such, fluvial

morphodynamics (as a product of the erosive/deposition processes) can be considered as having a strong probabilistic nature (Hu & Guo, 2010; Turowski, 2011).

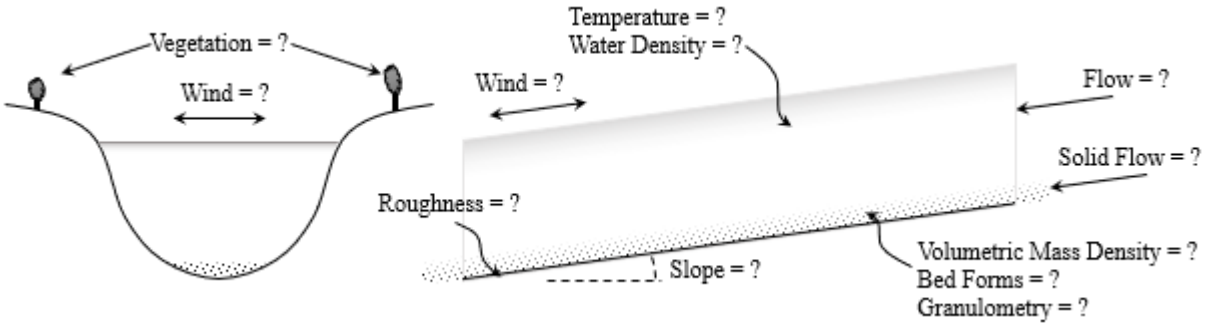

Figure 1 – Schematic cross-sectional and longitudinal representation of potential sources of uncertainty in a channel/fluvial environment.

Uncertainty in numerical modelling is generally divided into aleatory and epistemic uncertainty. Aleatory uncertainty refers to the uncertainty which is a by-product of the natural uncertainty in the values of variables and parameters of the models and is generally assumed to be unpredictable. Epistemic uncertainty on the other hand is the uncertainty which comes from the lack of precision and inaccuracies in the theoretical, mathematical, numerical and/or empirical representations of the processes to be reproduced in the models. Epistemic uncertainty while, to some extent, quantifiable and predictable is generally nearly impossible to eliminate in the context of numerical modelling by its very nature. Accordingly, this study focuses essentially on representing the aleatory uncertainty in the numerical modelling of fluvial morphodynamics. The uncertainty in question particularly pertains to the variables and parameters which are determinative for channel morphological change in a real fluvial environment and is a result of their natural spatial and temporal variability (which in turn makes it unfeasible to determine an exact numerical definition for those variables).

The use of the Monte Carlo method fostered the development of a new set of time series generation techniques and of their corresponding random or stochastic applications (i.e., involving, respectively, random or random and time-dependent variables). The concept of the Monte Carlo method consists of using randomly or stochastically generated values as a model's input, with the resulting output providing valuable information of the Probability Density Function (PDF) of other variables (Gentle, 2003). The Monte Carlo method, when applied as a form of simulation, has proven itself especially useful in the numerical modelling of uncertainty(ies) (e.g., in economics (Niederreiter, 2010), hydrology (Smith & Hebbert, 1979), structural analysis (Papadrakakis, et al., 1996) and physics (Dolgos, et al., 2012)). Other applications, with different objectives, of the Monte Carlo method can be found in study areas such as statistics (e.g., in sensitivity analysis (McNeil, 1985)) and mathematics (for approximating the value of integrals (Geweke, 1989)).

One of the main complexities in the application of the Monte Carlo method is the adequate generation of the input variables' values. Specifically, the selection and application of a proper series generation

technique can be very complex, being influenced by the nature of the variable and the assumptions involved in the generation technique. In most situations, uncertainty is integrated into the physical or numerical modelling by way of the stochastic/random generation process of the models' inputs. While other potential solutions exist for uncertainty propagation (such as the First Order Second-Moment Method), these methods are only applicable in relatively simple (potentially linear or linearizable) models, which is clearly not the case of numerical hydro-morphodynamic (HM) models. For this reason, this PhD study made use of Monte Carlo Simulation (MCS, which consists of the application of the Monte Carlo method) as a tool for modelling/representing the statistical variability of fluvial morphodynamics, opening the way for the application of this statistical data in reliability and risk analysis.

Hydrology as a field of study has also benefitted significantly from stochastic applications of its underlying models. For example, in studies on water resources management, particularly in the presence of climate change (Maia, et al., 2014; Milly, et al., 2008), stochastic applications helped in producing more complete descriptions of the potential results and to quell doubts on the importance of the uncertainty in the results. On the other hand, in applications of groundwater hydrology (Anderson, et al., 2015; Bosompemaa, et al., 2016), the inclusion of uncertainty can help in producing realistic results. In the area of fluvial morphodynamics however, there are comparatively fewer examples of uncertainty analysis. Examples of the representation of the uncertainty in morphodynamics are mostly focused on analysis on larger time scales (van Vuren, et al., 2016) or with simplified representations of streamflow variation (van Vuren, et al., 2015).

Although there have been a few attempts at the statistical representation of morphodynamics, a variety of limitations are commonly present. Some of the variables involved can be very hard to properly simulate, an example of which is streamflow, whose autocorrelation over time can be very hard to reproduce. Additionally, the amount of computational resources required in order to numerically model the behaviour of fluvial morphodynamics can be excessively large (van Vuren, 2005). Finally, the interpretation of the results of the simulation of fluvial morphodynamics, given the natural complexity of river morphology, can be difficult to perform and optimize (Mouradi, et al., 2016). These, amongst other difficulties, are the targeted enhancements which are to be introduced in this work regarding the stochastic modelling of fluvial morphodynamics.

This study uses a numerical hydro and morphodynamic (HM) model to approximate and represent the relationship between morphodynamics (i.e., the evolution of a channel's bed shape over time) and the variables which are most important to its definition, in terms of both temporal and spatial uncertainty. While this approach can produce some errors in the definition of the morphodynamical processes (due to the approximated nature of the modelling itself), these errors can be ameliorated by way of the correct definition of the model data, parameters and uncertainty, thereby producing the most correct possible representation of fluvial morphological effects for each case study. Additionally, given the extensive number of simulations required in order to represent the variability of morphodynamics (which is

geometrically proportional to the number of variables involved), the representation of fluvial morphodynamics by way of numerical HM models is the only viable option. Comparatively, physical modelling of uncertainty is a much more complex and lengthy task to perform. Accordingly, the different intermediary objectives of the work developed in this study (which are also a part of the stages of the stochastic modelling of fluvial morphodynamics) were:

- Describing and characterizing the different stages necessary for the implementation of stochastic modelling of fluvial morphodynamics in a real life situation;
- Studying and complementing existing limitations in the present literature regarding the stages of stochastic modelling of fluvial morphodynamics, be it by way of the creation of new methodologies or by systematizing the processes involved;
- The stochastic simulation of fluvial morphodynamics, namely involving the simulation of multiple combinations of different parameters'/variables' values representing the uncertainty in the morphodynamical processes. The results of these simulations are to be used for:
    - Defining the nature and characteristics of the relationship between fluvial morphodynamics and the corresponding morphodynamically-relevant variables;
    - The statistical characterization of fluvial morphodynamics, both in global terms (for an overall representation of morphodynamical variability) and in local terms (for application in reliability/risk analysis).
- To provide an example application of the results of stochastic modelling of fluvial morphodynamics to structural/terrain stability/risk analysis.

Risk, in the context of risk analysis, consists of the expected (i.e., the mean probabilistic value) cost associated with a given scenario. Accordingly, risk analysis consists of a comparison of the different potential scenarios considered in a particular case study (Bedford & Cooke, 2001). Multiple applications of risk analysis can be found in the literature (such as in, economics (Ayyub, 2014), structural design (Melchers & Beck, 2018) or hydrology (Ashofteh, et al., 2014)). However, to the best of the author's knowledge, only more simplistic applications have been performed in the areas of fluvial morphodynamics (de Kok & Grossmann, 2010). Generally speaking, the hardest component of risk analysis involves the quantification of probabilities associated with the different events involved in the analysis (often comprising the stochastic generation and simulation of a structure/system's behaviour). By systematizing the application methodology and providing an application example of the results of this same methodology, this study is intended to establish strong foundations for further studies in the subject of the stochastic modelling of fluvial morphodynamics, while exemplifying the different stages of its progression all the way from data to models and from reliability to risk. In the last section of this document, an application methodology (developed based on and in the context of this study), clarifying and summarizing the tasks and solutions involved in the process of the stochastic modelling of fluvial

morphodynamics, will be presented (including the steps necessary for its application to risk analysis). This methodology is applicable to both practical and scientific engineering works, being an innovation in and of itself. Using the proposed methodology, it will be possible to represent the uncertainty in fluvial morphodynamics for a number of other relevant applications. An example of these applications is provided in this thesis.

In this study, two case studies were considered, namely, a reach of the Mondego river (situated in Portugal) and a stylized straight channel. The first, designated as the Mondego Case Study, served as the main case study for the application of the stochastic simulation and the corresponding analysis of fluvial morphodynamics. Accordingly, the present Thesis documents the entire process of performing the stochastic simulation of fluvial morphodynamics in that particular reach of the Mondego river. The second case study, designated as the Stylized Case Study (in that it was defined based on an adaptation/simplification of channel considered the Mondego river case study), essentially served the purpose of a control/comparison case for the results obtained with the Mondego Case Study, especially regarding the sensitivity analysis of morphodynamics and the validation of the Mondego Case Study's results.

The numerical HM model used in this study was the CCHE2D (Zhang, 2005), specifically using the CCHE_GUI 3.29 and CCHE_MESH 3 programs, all of which are available at the website of the National Center for Computational Hydroscience and Engineering of the University of Mississippi (NCCHE, 2017).

1.1. METHODOLOGY

An important part of the objectives of this PhD study is the definition of the methodology for the stochastic modelling of fluvial morphodynamics. While based on the well-defined concept of the MCS, its exact definition required several attempts and optimizations. Both the development and the application of this methodology are an integral part of the work developed. Accordingly, a summary of the main stages involved in the stochastic modelling of fluvial morphodynamics is shown below, providing a logical guideline for the tasks developed and the sections which are a part of this Thesis's work.

Generally speaking, the stochastic modelling of fluvial morphodynamics follows the concept of the MCS, i.e., the stochastic modelling is performed by (1) stochastically generating the numerical HM models' inputs (or randomly, depending on the nature of the variable), (2) performing the numerical HM modelling for different combinations of the variables involved and (3) summarizing/systematizing the results to statistically describe the models' output variables. Despite its conceptual simplicity, the tasks involved in the application of stochastic modelling to the fluvial morphodynamics area are significantly more extensive. The following list (graphically represented in Figure 2) describes and justifies, in their sequential order of execution, the tasks necessary for the completion of this study's goals (and therefore for the stochastic modelling of fluvial morphodynamics):

1. Selection of the models' variables which are to be simulated (i.e., whose uncertainty is to be considered in this study). The choice has a great impact in the models' results and the relevance of the work developed. Picking the most relevant variables (for fluvial morphodynamics) is important. However, selecting an overly large number of variables not only increases the time required to perform the numerical modelling (potentially increasing exponentially with the number of variables) but it also greatly complicates the generation of the variables' values (due to, amongst other factors, the variables' dependencies).
2. Stochastic or random generation of the selected variables. This is generally performed based on existing data and the tools available for data/series generation. The selection of the generation approach must be in accordance with the nature of the corresponding variable.
3. Selection of the numerical models/packages/programs to be used in representing fluvial morphodynamics. This choice can be important given that the models' reliability in representing a channel's morphodynamical behaviour is directly proportional to the credibility of the simulations performed. Additionally, the selected models' speed will greatly impact the feasibility of the stochastic modelling of fluvial morphodynamics. In this study, the model selected was the CCHE2D (Zhang, 2005).
4. Simulation of the selected combinations of the variables' values using the numerical HM models (chosen in task 3). This stage consists of the application of the numerical model with the different combinations of variables produced in task 2. While it is a conceptually simple stage, it is overall the most time-consuming task in this study.
5. Statistical analysis and systematization of the stochastic modelling's results (obtained from task 4), namely with the purpose of performing the sensitivity analysis and statistical characterization of fluvial morphodynamics. This statistical analysis of the model's results was accomplished using the R language (Venables & Smith, 2018), namely, by programming and comparing different sets of analysis tools. The best analyses' approaches and statistics were selected and utilized in this study.

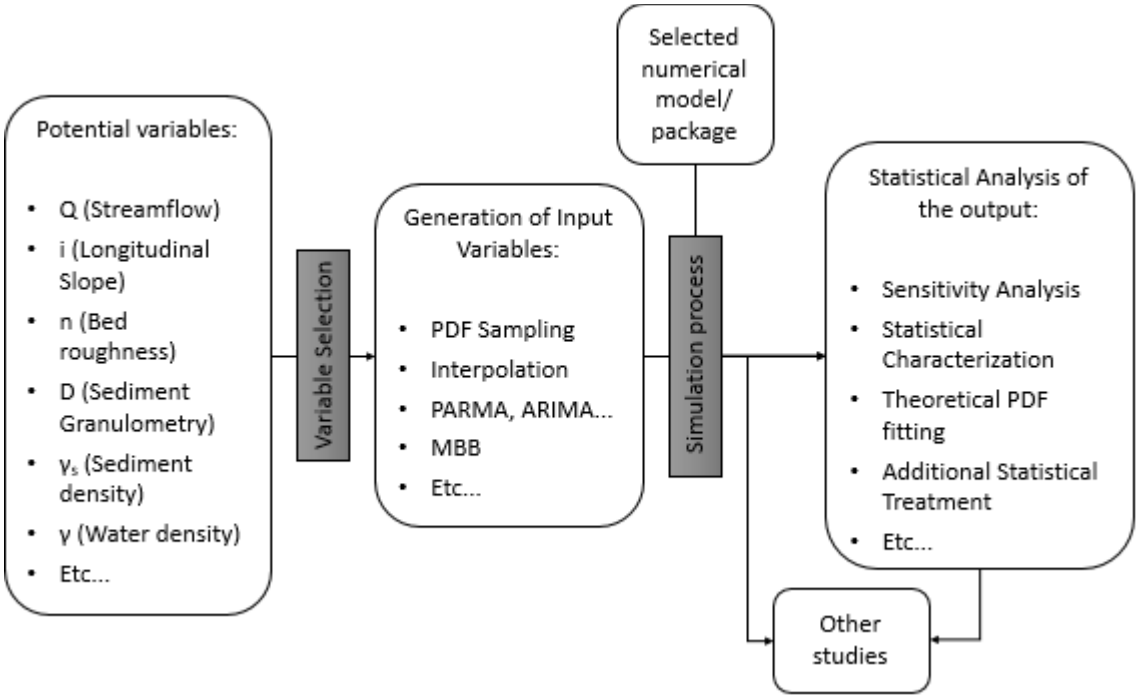

Figure 2 – Methodology applied for the stochastic modelling of fluvial morphodynamics.

As part of the simulation process developed and applied in task 4, a hot-start/pre-modelling approach to morphodynamical modelling, aimed at improving the quality of the bed level data used in numerical modelling and optimizing the stochastic modelling itself, was also presented. The underlying principles and criteria involved in the application of this pre-modelling approach are systematized and validated.

Specifically for the purpose of applying the results of the stochastic modelling in the context of reliability and risk analyses, a significant portion of the statistical analyses developed in task 5 was focused on the characterization of the case study's morphodynamical patterns. This characterization is meant to provide important information on how to translate the large quantity of results which is produced by the stochastic modelling of fluvial morphodynamics into a manageable description of the statistical progression of the channel's morphology (which can in turn be applicable to other studies). Particular emphasis was given to the analysis and generalization of 2D erosion profiles, given that they provide simple but often useful representations of the terrain.

As can be understood from the previous list, the stochastic modelling of fluvial morphodynamics requires carrying out multiple decisions, each of which has a significant influence on the results. Accordingly, this document provides a description and justification of the different choices made throughout this PhD study as a tool to facilitate the development of future, similar studies in this area. Additionally, a few tools, techniques and types of analysis have been created and/or systematized in order to make possible and speed up the stochastic modelling itself.

The variables whose uncertainty was simulated in this study were the (1) streamflow in the river (represented by the magnitude of the streamflow input to the model, *Q*), (2) the bed particle's sediment granulometry (characterized by the corresponding granulometric curves and by their median or mean

diameters, respectively, D_{50} or D_m) and (3) the channel's bed roughness (simulated as the varying Manning roughness coefficient along the channels' beds and banks and represented by its mean value, n). The sediment influx to the model (or, to be more exact, its uncertainty relative to its streamflow-based estimated value, ΔQ_s) was also considered as a random variable and simulated in the model, specifically in the Stylized Case Study (where its' inclusion was deemed to be the particularly important). While numerical HM models have a very large number of parameters involved (and even different selections of equations to solve), many of which are influential in terms of the simulated morphodynamics, most of these parameters pertain to the epistemic uncertainties involved in the numerical representation of fluvial morphodynamics. Accordingly, the selection of the relevant parameters mostly focused on the parameters which are known (from the literature) to be relevant for fluvial morphodynamical behaviour and which pertain solely to the aleatory uncertainty. Further details on the criteria for the selection of the designated variables will be presented in section 2.2. Finally, depending on the complexity of the case study, the choice of the tools and techniques used in the generation of the variables' values can have a large impact in the accuracy of the corresponding results. Accordingly, and in particular for the more complex Mondego Case Study, a significant effort was made to apply the most suitable generation tools that can properly reproduce the historical/observed nature of the selected variables.

In order to increase the reliability of the simulations performed in this study, an adaptive interface was developed for the CCHE2D model using the R language. This interface allowed for the automatic generation of the CCHE2D program's input and output files for all of the variables and case studies' characteristics, removing potential human/interface errors from the simulations. The only task performed with the CCHE2D's Graphical User Interface (GUI) was the application of the CCHE2D's numerical HM models. This interface also automatically implemented an algorithm to collect and treat the results of the simulations, allowing for its analysis in task 5.

The numerical model used in this study (CCHE2D) is a finite element numerical HM model based on the Reynolds-Averaged Navier Stokes equations, which it solves using an implicit scheme of time marching (Jia & Wang, 2001). It is capable of dynamic flow and sediment transport modelling, including various options for turbulence modelling and the calculation of bed load transport (by way of the corresponding empirical formulas). Bed level change is computed using an equilibrium sediment transport model based on the bed load transport formulas (solved using a first order upwind scheme) and adjusted by the effects of bed slope and channel curvature. The CCHE2D model is capable of simulating the behaviour of non-uniform sediment mixtures. This model has been successfully used in multiple instances in the past for the simulation of HMs in fluvial environments (Kim, et al., 2010; Negm, et al., 2010; Nassar, 2011).

CCHE2D is a hydrodynamic model for unsteady turbulent open channel flow and sediment transport simulations developed at the National Center for Computational Hydroscience and Engineering (NCCHE). This model includes a variety of capabilities, such as hydrodynamic quasi-3D modelling,

bed load and suspended sediment transport, non-uniform sediment transport, etc.. The model uses the Efficient Element Method (a form of finite element method) in an implicit scheme for time-marching, namely the fourth order Runge-Kutta. Aside from the tradition Reynolds-Averaged Navier Stokes (RANS) equations, it includes different turbulence closure schemes such as k-ε, mixing length, parabolic eddy viscosity, etc..

Regarding morphodynamics, the model is capable of simulating sediment transport solely as bed load, solely as suspended load or as a combination of the two. In order to compute sediment transport capacity, the model may the formulas of Wu et al., Ackers and White, Engelund and Hansen and SEDTRA. These formulas are paired with the sediment continuity equation.

Further information on the model's underlying equations may be consulted in its technical report No. NCCHE-TR-2001-1.

1.2. THESIS STRUCTURE AND ARTICLE PUBLICATIONS

This document was split into a total of nine sections, including the present introduction (which is section 1 of the Thesis). Section 2 of this Thesis consists of a presentation of the review which was performed regarding the existing literature on the subjects most relevant for the completion of this PhD study's goals. The remaining seven sections approximately represent, in chronological order, the different stages/tasks involved in the completion of the goals of this study (i.e., the development and application of a methodology for the stochastic modelling of fluvial morphodynamics), namely:

- Section 3 presents and systematizes the stochastic streamflow generation methodology created in the context of this work – much of which has also been presented in (Oliveira & Maia, 2018), which was necessary for the completion of task 2 of the methodology;
- Section 4 consists of a presentation of the two case studies (and associated data) used in this study for the purpose of the stochastic modelling of fluvial morphodynamics;
- Section 5 is a compilation of all of the simulations performed, as well as of all of the related considerations, assumptions and the numerical model optimization/hot-start approach – whose concept, application and assessment was summarized in (Oliveira & Maia, 2019) – corresponding to tasks 1 and 4 of the methodology;
- Section 6 presents the results of the sensitivity analyses performed based on both of the case studies and the corresponding implications and conclusions regarding the simulations – part of which was presented in (Oliveira, et al., s.d.), which is part of task 5 of the methodology;
- Section 7 presents the statistical description of fluvial morphodynamics, as produced by the stochastic simulations. Considerations regarding the extension of this description to multi-year studies and the generalization and simplification of the simulation process are also undertaken. These activities are also a part of task 5 of the methodology.

- Section 8 describes the risk analysis application developed based on the results of the simulations . The effects of morphodynamics and its uncertainty are analysed and quantified.
- Section 9 consists of the summary and conclusions of the results of this study, both in terms of its overall objectives and regarding each of its independent, intermediate tasks. A general application methodology for the implementation of the stochastic modelling of fluvial morphodynamics is presented in this section, summarizing the different inferences and conclusions attained over the course of the study.

As part of the development of this study, some journal articles have been systematized and published or submitted for that purpose. The respective publications/bibliographic references are as follows:

- *Stochastic Generation of Streamflow Time Series*. The paper presents the work developed in the context of the proposed stochastic streamflow series generation methodology, which was developed for the purpose of generating the streamflow series necessary for the stochastic application of the numerical HM models.
- *Pre-modelling as tool for optimizing morphodynamical numerical simulations*. In this paper, an optimization solution, which was adopted for the purpose of improving the quality of the results (in terms of the intelligibility and sensitivity of the individual simulations), is presented and systematized.
- *Sensitivity Analysis of Fluvial Morphodynamics*. The sensitivity analysis of the simulated morphodynamical behaviour in the Stylized Case Study (presented in this Thesis) is summarized in the paper and compared to the results obtained in related and referenced previous studies.

2
LITERATURE REVIEW

Given the natural uncertainty that is known to envelop the study of fluid morphodynamics, the stochastic modelling of fluvial morphodynamics has been a long standing ambition in the areas of risk analysis, structural stability and river rehabilitation (Schielen, et al., 2007; van Vuren, et al., 2015; van Vuren, et al., 2016). Nonetheless, given the corresponding requirements (particularly in terms of the computational capacity, amongst other limitations), this objective (of including the effects of uncertainty in the fluvial morphodynamics) has been mostly accomplished using approximated approaches and/or simplifications in the representation of the behaviour of the rivers' morphology. In the context of the objective of this PhD study, a review on several related subjects was performed, namely on:

- The existing methodologies/techniques to perform the stochastic generation of streamflow time series. Streamflow series, given their strong auto-correlation structure, are, amongst the different input variables of the numerical HM models, the hardest variables to be realistically simulated. A review on the existing approaches for this task and their respective advantages and disadvantages was therefore performed;
- The sensitivity of morphodynamics, namely in terms of the choices and results of previous studies in this area, namely with the purpose of pre-selecting the variables most important for the correct definition of morphodynamical evolution and uncertainty;
- Examples of risk analysis applied in the areas of hydrology, hydraulics and, generally speaking, studies where the hydrodynamical and morphodynamical uncertainty is taken into consideration.

2.1. STREAMFLOW SERIES GENERATION

Depending on the time-scale of a study, the generation of the streamflow series can be the most complex generation to be performed (Lall & Sharma, 1996). Streamflow combines all three different types of dependencies, namely: (1) time-dependency (often referred to as periodicity or seasonality), (2) dependency on other variables and (3) autocorrelation/serial correlation or self-dependency. Accordingly, its generation process can be equally complex. Nonetheless, many different solutions currently exist for the generation of streamflow series, each of which with its respective advantages and disadvantages. Some of these methods were designed specifically for the stochastic generation of

streamflow series while others were designed for the forecasting of time-dependent variables and adapted to streamflow generation (e.g., (Lettenmaier, 1984)). Most forecasting approaches however are not univariate and make use of other data sources to perform the forecasting itself. Alternatively, some disaggregation approaches have also been used to simulate streamflow series (e.g., by sampling yearly streamflow values and disaggregating them into monthly or daily values, as in, (Portela, et al., 2017)). This review on streamflow series generation was performed in the context of the journal paper produced on a new, proposed methodology for stochastic streamflow series generation (Oliveira & Maia, 2018).

The methods most used in univariate (streamflow) time series generation are here presented, with a particular focus on the methods capable of representing the autocorrelation structure, in accordance with the intended application's time scale:

- Autoregression (AR) Models – These models replicate the relationship between a variable's values at each instant t with the corresponding values at instants $t - 1$. An example of an AR model is a first-order Markov model where values are directly sampled from the PDF of the variable based on an autocorrelation coefficient (Van Beek, et al., 2005). Alternative versions, generalizations and adaptations for different situation also exist, including the Autoregressive Moving Average (ARMA (Musa, 2013)) Models, the Autoregressive Integrated Moving Average (ARIMA (Yurekli & Kurunc, 2005)) Models, the Periodic Autoregressive Moving Average (PARMA (Srinivas & Srinivasan, 2001)), Models and the Autoregressive Fractionally Integrated Moving Average (ARFIMA (Grimaldi, 2004; Sirangelo, et al., 2017)) Models.
- Shot Noise Models – Also known as pulse models, these are mostly used for variables with a strong and repetitive autocorrelation structure. The generated series are defined by overlapping pulses, each of which in turn represents the variable's autocorrelation structure (represented schematically in Figure 3). Common applications include, for example, a combination with a two-state Markov model (You, et al., 2014).

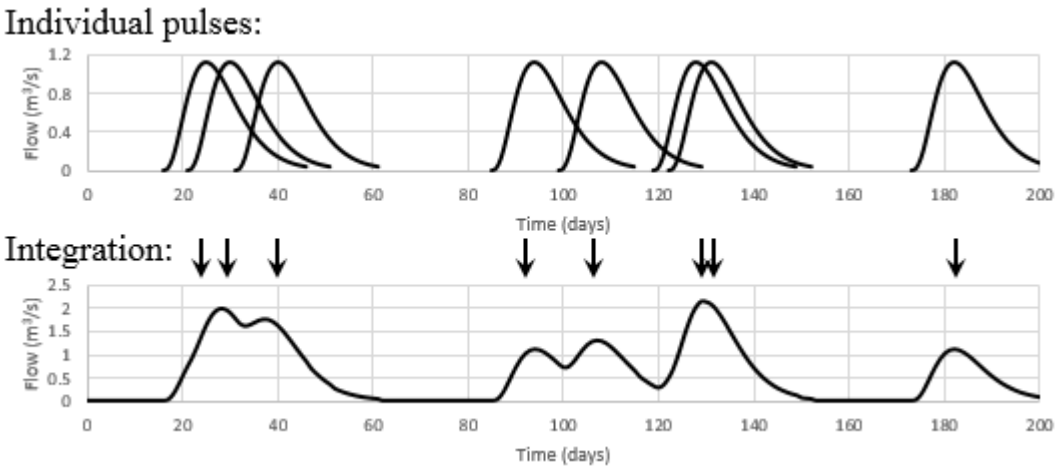

Figure 3 – Schematic representation of the construction of streamflow series via a shot noise model.

- Wavelet Models – This type of model performs a decomposition of a given time series into different frequency components which are then scaled and overlapped for constructing new time series. This approach is very similar to that of the Fourier analysis based generation, except that, in this instance, the frequencies are decomposed by way of Fourier series instead of Wavelets (Wang, et al., 2011). One of the main disadvantages of this approach is that the generated series will not be able to reproduce the skewness of the PDF of the observed time series due the method's own characteristics.
- Block Bootstrap Scheme – A model typology with many variants, it most commonly consists of a Moving Block Bootstrap (MBB) where the observed time series is divided into blocks (often in such a fashion that certain characteristics of it are preserved) which are deemed to be independent and that can therefore be resampled (schematically represented in Figure 4) (Srinivas & Srinivasan, 2005; Kalra & Ahmad, 2011). While this approach provides a reasonable solution for a variety of applications, it is, however, limited to reproducing observed sequences of values. Additionally, the nature of this technique limits the number of distinct, relevant generated series.

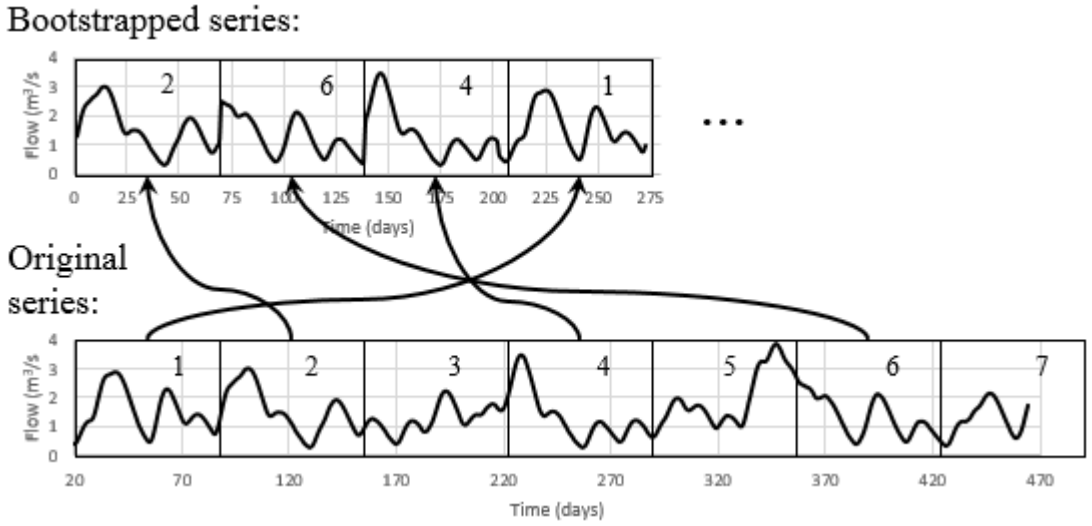

Figure 4 – Schematic representation of the construction of streamflow series via a block bootstrap scheme.

- K-Nearest Neighbour (KNN) Approach – This technique attempts to approximate, for a given variable, the dependence relationship between consecutive points in time. In order to sample a new value, the K pairs of values for instants $[t, t+1]$ are pondered as a function of the difference between the streamflow at instant t and the last value generated. Basically, the method sequentially samples (using probability weights) the variables' values in order to produce new time series (Prairie, et al., 2007; Nowak, et al., 2008).
- Artificial Neural Network (ANN) Models – While primarily a forecasting technique, the ANN's capacity for representing a variable's autocorrelation over a limited time range is very significant and it has therefore also been applied in the generation of time series (Jia & Culver, 2006; Tiwari & Chatterjee, 2010). The main issue with this approach is that it requires significant computational capacity which can render unfeasible the generation of a very large number of series.

Generally speaking, the main criticisms on existing approaches are related with parametrization (it can be complex or even excessive, e.g., ANN Models), universality (many models are limited in terms of their applicability, namely in terms of the series' time scale, e.g., AR models) and the model's limitations regarding the number and representativeness of the generated series (e.g., Block Bootstrap and Shot Noise Models).

2.2. SENSITIVITY ANALYSIS OF MORPHODYNAMICS

Sensitivity analysis is a type of analysis which is intended to provide a description of the relative importance of a model's output to each of its input variables/parameters. Accordingly, it is an important step in any stochastic application of models, as it provides important information on the relationships represented by the numerical model. At the same time, sensitivity analysis is virtually the only general-purpose tool for validating the results of stochastic modelling (Saltelli, et al., 2008). The inherent nature of stochastic modelling implies that each individual simulation is by itself meaningless and must be understood in the context of the global results. Because of this, in most cases, the validation of the stochastic modelling of a system relies on verifying whether the results' behaviour is in accordance with the system's (i.e., morphodynamical change) expected behaviour. Sensitivity analysis is generally the most appropriate tool for this task. The methodology and statistics used in sensitivity analysis must also be carefully selected in order to ensure the replicability of results across different case studies. This section summarizes the methods and results which may be used for validating stochastic modelling by way of sensitivity analysis.

The representation of the variables' uncertainty for sensitivity analysis can be performed by using a variety of methods such as, for example, the First Order Second-Moment Method – FOSM, the Second Order Reliability Methods or the Scatter Analysis (Faber, 2012). In fact, several studies (Kopmann & Schmidt, 2014; Villaret, et al., 2016) have chosen to analyse morphodynamics based on these approaches, particularly in what regards the sensitivity analysis of the (system of) equations involved in the modelling of fluvial morphodynamics. While this indeed qualifies as sensitivity analysis of morphodynamics, it generally disregards the temporal and spatial complexities involved in morphodynamical processes (Pinto, et al., 2006; Kopmann, et al., 2012). Additionally, these methods are only applicable in relatively simple (potentially linear or linearizable) models, which is clearly not the case of fluvial applications of numerical HM models (Kopmann, et al., 2012). For these reasons, in this PhD study, the Monte Carlo Simulation (MCS) was used as a tool for simulating and representing the statistical variability of fluvial morphodynamics, which, while often a costly approach to develop, provides a more complete and reliable description of the effect of the different variables' uncertainties in the HM models results.

The importance of stochastic modelling in the analysis of fluvial morphodynamics has long been recognized in the study areas of hydrology and geomorphology (van Vuren, 2005; Posner & Duan,

2012). Accordingly, many studies in the areas of hydraulics and hydrology have simulated the variables' uncertainty and analysed the sensitivity of morphodynamics in regards to its control parameters, such as the bed material shear resistance/granulometry (Zhang, et al., 2016; Kopmann & Schmidt, 2014), stochastic particle entrainment and deposition (Bohorquez & Ancey, 2015; Ancey, 2010) and the erosive action over the bed, mostly focused on small scale stochastic processes (Posner & Duan, 2012; Zhang, et al., 2015).

Different studies generally compare very different sets of variables, in accordance with the studies' own purpose/goals, data/environment (e.g., coastal, estuarine, fluvial) and limitations/conditionings. Table 1 presents an exhaustive list of all of the variables whose uncertainty in the context of bed morphodynamics has been analysed in the literature (jointly or separately from other variables), namely via the application of numerical HM model.

Table 1 – Description of the variables analysed in the sensitivity analysis studies available in the literature.

Variable/Parameter/Formula	Symbol	Observations/Descriptions	[reference]
Adaptation length	---	Parameter regulating inertia effects in HM modelling	(Moges, 2010)
Bank erosion coefficient	ζ	Part of Ikeda, et al. (1981) linear model	(Posner & Duan, 2012)
Bed load input rate	Qbl	Defined as a parameter of the corresponding rating curve	(Beckers, et al., 2016)
Bed porosity	λ	Percentage of non-solid volume in the bed	(Mouradi, et al., 2016)
Bed roughness	n	Overall manning roughness coefficient in the channel	(Schuurman, et al., 2013; Villaret, et al., 2016; Kopmann & Schmidt, 2014; Moges, 2010; Kopmann, et al., 2012; Beckers, et al., 2016; van Vuren, 2005)
Critical Shields Parameter	θc	---	(Mouradi, et al., 2016; Beckers, et al., 2016; van Vuren, 2005)
Forcing tide	---	The (harmonic) time-series of tidal variations in water level	(Bertin, et al., 2007)
Grain roughness	k	Bed roughness associated with grain size	(Mouradi, et al., 2016; Beckers, et al., 2016)
Hydrological inputs	Q	Influx of flow at the models' upstream boundaries	(Schuurman, et al., 2013; Pinto, et al., 2006; Huthoff, et al., 2010; Lambeek, et al., 2004; van Vuren, 2005)
Morphological change acceleration	MorFac	Numerical (semi-empirical) model parameter	(Schuurman, et al., 2013)
Parameter for secondary current	α	---	(Kopmann & Schmidt, 2014; Kopmann, et al., 2012; Mouradi, et al., 2016)
Sediment angle of repose	θr	---	(Mouradi, et al., 2016)

Variable/Parameter/Formula	Symbol	Observations/Descriptions	[reference]
Sediment grain size and or distribution	D	Characteristic value(s) of the sediment size distribution	(Pinto, et al., 2006; Villaret, et al., 2016; Kopmann & Schmidt, 2014; Moges, 2010; Zhang, et al., 2015; Kopmann, et al., 2012; Bertin, et al., 2007; Mouradi, et al., 2016; van Vuren, 2005; Plecha, et al., 2010)
Sediment Transport Formula	---	Including the formulas' individual parameters	(Plecha, et al., 2010; Schuurman, et al., 2013; Pinto, et al., 2006; Kopmann & Schmidt, 2014; Bertin, et al., 2007; Mouradi, et al., 2016; Beckers, et al., 2016; van Vuren, 2005)
Settling velocity	---	---	(Zhang, et al., 2015)
Slope effect parameter	β	Part of Flokstra & Koch (1981)	(Kopmann, et al., 2012; Kopmann & Schmidt, 2014; Mouradi, et al., 2016)
Thickness of the active layer	pal	---	(Kopmann, et al., 2012; Moges, 2010; Zhang, et al., 2015; Kopmann & Schmidt, 2014; Beckers, et al., 2016)

While, generally speaking, the most widely recognized sources of uncertainty in morphological change are the hydrological inputs (i.e., streamflow), other variables have also been found to be important. Different studies generally compare different sets of variables, in accordance with the studies' own purpose/goals, data/environment (e.g., coastal, estuarine, fluvial) and limitations. Table 2 displays the variables, from the list presented in Table 1, which were considered to be the most relevant in the different studies found in the literature, namely in terms of the importance of those variables' uncertainty for fluvial morphodynamics. Notice that not all of the variables were simulated in every study, a factor which can influence the choice of the variables which are most relevant for fluvial morphodynamics.

Table 2 – Most relevant variables for different studies in the literature.

Study Environment	Most important variable(s)		Number of Variables Analysed	Other important river-specific variables	[reference]
River	β	Sediment Transport Formula	4	Channel bed roughness	(Schuurman, et al., 2013)
Stylized Channel	Settling velocity		2	Sediment grain size	(Villaret, et al., 2016)
River	Adaptation length		4		(Moges, 2010)
Lagoon	Sediment Transport Formula		2	Sediment grain size	(Plecha, et al., 2010)
River	θc		8	Sediment grain size	(Mouradi, et al., 2016)
River	θc	Empirical Factor in M-PM*	6	Channel bed roughness	(Beckers, et al., 2016)
River	θc	Empirical Factor in M-PM*	5	Streamflow	(van Vuren, 2005)

*M-PM: Meyer-Peter & Müller formula for sediment transport capacity

As can be observed from Table 2, regarding river-specific variables, the literature offers no consensus regarding what variables are most important to fluvial morphodynamics. Morphodynamical sensitivities appear to be very volatile in nature and are probably not generalizable from one case study to another. Different approaches to the simulation of the variables' uncertainty also produce wildly different results. The sensitivity analysis to be performed in this study is intended to provide some clarity regarding the causes for these facts. In section 6.3, the results of the available examples of quantitative sensitivity measurements from the literature are compared with the results of this study.

For the purposes of selecting the most important variables to include in the uncertainty modelling of fluvial morphodynamics, the universe of potential variables can be simplistically defined as that of all of the variables which affect morphodynamical behavior. As a reference, to delimit this universe of variables, both dimensional analysis and a review on the variables considered in numerical HM modelling and considered in this context in the existing literature can be used. Based on principles suggested in the literature (e.g., in (Saltelli, et al., 2008; Guyon & Elisseeff, 2003)), and in the authors' experience, the best criteria for selecting the variables to be considered in the uncertainty modelling of fluvial morphodynamics are common and applicable to any type of stochastic modelling:

- Simulated variables should be demonstrably relevant, not for the modelling itself but for the uncertainty of fluvial morphodynamics. Parameters or elements of the HM model such as the Shields parameters, the adaptation length, the slope effect parameter or the choice of sediment transport formula are very likely to be virtually deterministic in real fluvial morphodynamics and therefore should not be considered when specifically analysing the sensitivity of fluvial morphodynamics;
- The independent representation of the uncertainty from significantly related variables (such as sediment grain size, density and angle of repose) should be avoided. This is because ignoring the effects of these inherent dependencies can reduce the quality of the sensitivity analysis (e.g., when

certain combinations of the variables' values are not realistic, despite the individual values being within the variables' likely variability ranges);

- Where the definition of a variable's uncertainty range is difficult (or even impossible), the corresponding variable should be excluded from consideration (due to the significant danger of over/under-estimating the variable's effects of fluvial morphodynamics). Examples of this type of uncertainty are, for example, the bathymetrical uncertainty, whose values can only be improved upon and not included in the sensitivity analysis.

In accordance with these criteria, the list of variables whose potential uncertainty should be considered can be significantly reduced. The variables whose sensitivities were analysed in this study were the (1) channel's granulometry (generally represented by its median diameter D_{50} or its mean diameter D_m), (2) the channel's bed roughness (represented by the Manning's roughness parameter n) and (3) the flood intensity/hydrograph (represented by a flood magnitude parameter or representative hydrograph). Sediment input in a reach (or to be more accurate, the uncertainty in sediment input, symbolized by ΔQ_s) may be relevant in morphodynamical uncertainty, its inclusion being dependent on the local conditions of each case study. Accordingly, its definition and uncertainty were included in the Stylized Case Study but not in the Mondego Case Study (where it was deemed to be virtually irrelevant). Nonetheless, given the relative nature of the magnitudes and relations which were to be quantified, the representation of the relative importance of the remaining variables should remain virtually unaffected by the addition of this variable (relative to the Mondego Case Study). These variables were selected because they have been shown to have a very significant influence in morphodynamics (van Vuren, 2005; Visconti, et al., 2010; Kasyi, et al., 2015) and because these are variables which specifically influence fluvial morphodynamics and not just the numerical modelling of morphodynamics itself (unlike others, such as the Shields parameter, which are numerical representations of the theoretical models' adaptations of real river sediment dynamics' mechanisms).

Adding a large number of variables in sensitivity analysis does not necessarily equal added quality to it but can instead reduce the representativeness of the simulated variables. Adding uncertainty from variables whose variability range is not well defined (as is the case with the vast majority of the variables whose uncertainty is mostly only present in the numerical HM models) tends to reduce the reliability of the sensitivity analysis of the underlying processes (Saltelli, et al., 2008). Concomitantly, regarding the excluded variables, in numerical modelling, the best option is to simply set them to their most likely/accurate value.

The analysis of a system's sensitivities can be performed either individually (by way of independent sensitivity analysis – ISA, where each variable is analysed independently from the others) or jointly (via Joint Sensitivity Analysis – JSA, where the interdependency between variables is taken into consideration in the quantification of sensitivities). ISA consists of assessing a variable's individual effect to a particular process or system (or, from another perspective, the system's sensitivity to that

variable). The definition of a system's sensitivity to a single variable is generally a relatively simple process. From a conceptual perspective, the sensitivity of a system to a single variable can be derived from the range of variability that this variable's uncertainty produces in the variability of the system. In a fluvial environment however, this is often an inadequate approach. Most variables (particularly in a fluvial environment) can often influence each other (in terms of their overall effects on a river's morphology) while other variables can produce more irregular/unpredictable effects on morphodynamics (and thereby, to some extent, have a larger relative importance for fluvial morphology) which are harder to quantify.

While studies based both on ISA and on JSA in the area of fluvial morphodynamics exist, the influence that different variables have on morphodynamics has been mostly represented by the corresponding range of possible morphologies produced by the different combinations of the variables (Lambeek, et al., 2004; Bertin, et al., 2007; Mouradi, et al., 2016; Beckers, et al., 2016). However, this measurement of sensitivity is extremely discrete (in the sense that its' value can greatly change due to a single outlier simulation/value) and, due to its simplistic nature, it is mostly incapable of capturing the complexity of the different variables' effects on morphodynamics. In addition to this, studies of JSA in morphodynamics are often limited by the large computational demands of numerical HM models (van Vuren, 2005).

As a tool to analyse the combined effect of the different variables in morphodynamics, as well as their respective interdependencies in this aspect, this study performed JSA using a variance-based application (i.e., using variance-based statistics) of Global Sensitivity Analysis (GSA). The relative importance of the variables (for a given statistic/measurement *Y* representative of *dH*) was estimated by analysing the effects of only considering one variable or discarding the effect of said variable on the overall variance of the MCS-generated morphological results (Saltelli, et al., 2008). The former corresponds to the first order – FOI – or Sobol index, represented in Eq. 1, while the latter corresponds to the total effect index – TEI – represented in Eq. 2:

$$\mathrm{FOI}(Y \mid \mathbf{X_i}) = \frac{Var\left[E[\mathrm{Y} \mid \mathbf{X_i}]\right]}{Var[\mathrm{Y}]},\ where\ i \in \{n,\ D_{50},\ Q\} \qquad \text{Eq. 1}$$

$$\mathrm{TEI}(Y \mid \mathbf{X_{\sim i}}) = \frac{E\left[Var[\mathrm{Y} \mid \mathbf{X_{\sim i}}]\right]}{Var[\mathrm{Y}]} = 1 - \frac{Var\left[E[\mathrm{Y} \mid \mathbf{X_i}]\right]}{Var[\mathrm{Y}]},\ where\ i \in \{n,\ D_{50},\ Q\} \qquad \text{Eq. 2}$$

where $\mathrm{Var}[X]$ represents the variance of X, $\mathrm{E}[X]$ is the mean/expected value of X, i can be any of the selected variables, $Y \mid \mathbf{X_{\sim i}}$ is the values of the statistic Y after the variability introduced by variable i is removed (by averaging over the corresponding simulations) and $Y \mid \mathbf{X_i}$ is the values of the statistic Y for a set value of variable i. Variance-based GSA has been used with success in the analysis of morphodynamical sensitivity (van Vuren, 2005; Mouradi, et al., 2016). However, these studies have only analysed a single statistic at a time (such as the mean *dH*), disregarding the complexity inherent to

morphological change. The present study considered multiple different statistics to represent *dH* so as to represent this same complexity.

Other studies have not quantified the relationship between morphodynamics and the different variables relating to it but have instead chosen to analyse the variables' effects graphically, based on different, visually assessable aspects of morphodynamical change (Lambeek, et al., 2004). This option is generally a result of the large complexity which is inherent to morphodynamical processes. The approach developed in this study for the purpose of sensitivity analysis is a combination of these two approaches. Both the GSA and graphical comparisons of the variables effects were combined with a multitude of morphodynamically-representative statistics in order to fully quantify and represent the complexity of morphodynamics. With this approach, both a validation of the MCS-generated morphological results and a consensus on the relative importance of the different variables (and their uncertainty) is intended.

Finally, conceptually speaking, the sensitivity analysis of a process which is represented by a numerical model is also a sensitivity analysis of the numerical model itself and not exclusively of the processes themselves (in that there may be approximations/inaccuracies in the representation of the processes by the model). However, in order to perform sensitivity analysis, assuming the exactitude of the model is a necessary step in representing the processes themselves. Particularly in the case of sensitivity analysis of morphodynamics, where performing the physical modelling of uncertainty would be a lengthy and most likely unfeasible possibility, accepting the numerical HM model to be accurate is a necessary condition to its implementation.

2.3. Uncertainty and Risk Analysis in Hydrology

Generally speaking, there are two different types of uncertainty which can be distinguished between, namely, aleatory and epistemic uncertainty. Aleatory uncertainty refers to the uncertainty which is a by-product of the natural uncertainty in the values of the variables and parameters of the models and is generally assumed to be unpredictable. Epistemic uncertainty on the other hand is a result of the lack of precision and inaccuracies or approximations in the theoretical, mathematical, numerical and/or empirical representations of the processes to be reproduced in the models. Epistemic uncertainty while, to some extent, quantifiable and predictable, is generally nearly impossible to eliminate in the context of numerical modelling by its very nature. The uncertainty of variables who (by way of empirical or theoretical relations) serve the purpose of representing real river sediment dynamics' mechanisms are generally always a part of the epistemic uncertainty of the model.

In the context of numerical modelling, oftentimes uncertainty is divided into (1) forcing uncertainty, (2) parameter uncertainty, (3) numerical uncertainty and (4) unknown uncertainty (Scheel, et al., 2014) (as is represented in Figure 5). Forcing uncertainty and parameter uncertainty pertain to the boundary conditions and boundary variables in the model and to the parameters which characterize the system's variables, respectively. Numerical uncertainty results essentially from the epistemic uncertainty (due to

the approximated nature) of the model. Unknown uncertainty corresponds to the uncertainty sources which have yet to have been identified and introduced in the modelling itself. These types of uncertainties correspond to the different types of inputs introduced in numerical models. This study primarily focused on the forcing and parameter uncertainties because, in the context of fluvial morphodynamics, they are the only types of uncertainty which are quantifiable and representable when simulating the uncertainty of morphodynamical processes.

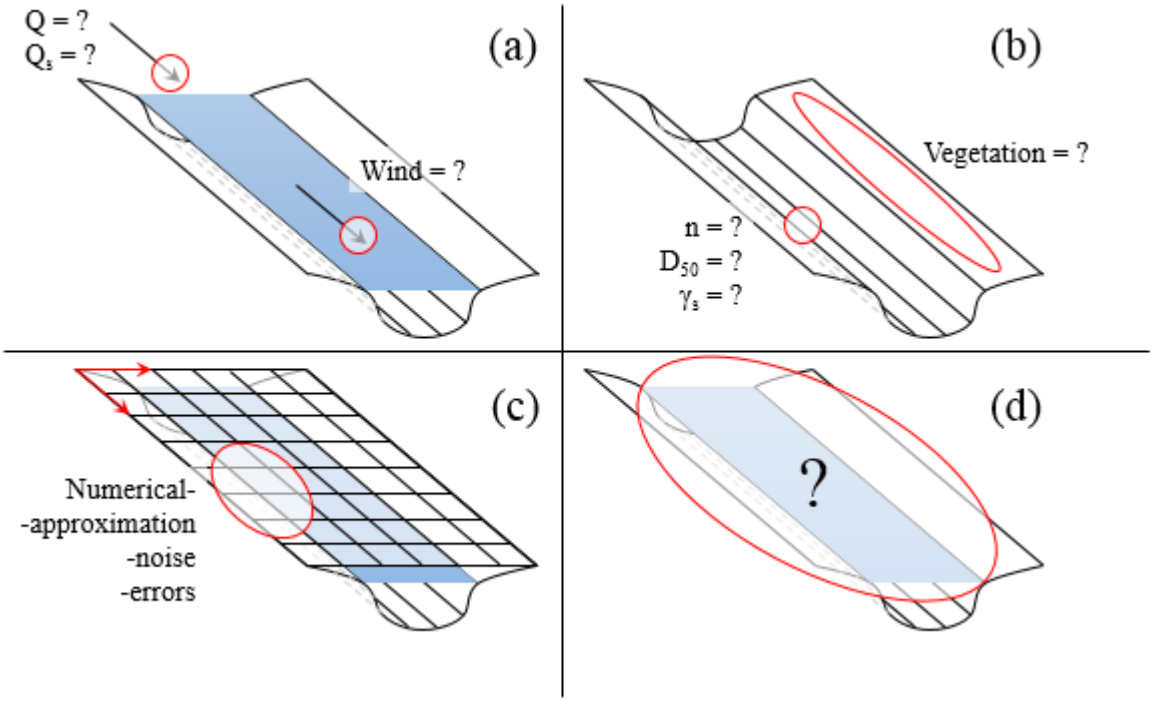

Figure 5 – Representation of the different types of uncertainty involved in the numerical modelling of morphodynamics, namely, the forcing uncertainty (in plot a), the parameter uncertainty (in plot b), the numerical uncertainty (in plot c) and unknown uncertainty (in plot d) (adapted from (Scheel, et al., 2014)).

Uncertainty analysis (or, as is referred to in some types of applications, reliability analysis) consists of simulating or representing the uncertainty inherent to a system, mostly by way of experimental or numerical modelling of the variables/parameters/processes which give birth to this uncertainty. In most cases, this representation of the uncertainty has a specific purpose, such as its own characterization, sensitivity analysis or decision-making. Uncertainty analysis has been applied in multiple fields of study such as economics (e.g., in investment assessment and decision making (Savvides, 1998)), structural engineering (as part of structural stability/reliability analysis (Faber, 2012)), and medicine (e.g., in planning and evaluating potential therapies (Albertsen, et al., 1998)). In the area of hydrology, applications are generally more recent, being linked with the advent of faster computers and more advanced monitoring and data collection tools which facilitate the application of this type of analysis. Applications can be found in water resources management (Lempert & Groves, 2010), surface and groundwater hydrology (Anderson, et al., 2015), maritime engineering (Kristiansen, 2013) and fluvial engineering (van Vuren, et al., 2015), often associated with existing or future infrastructures.

Risk, in probabilistic terms, can be understood as the expected/mean consequences (e.g., monetary costs) associated with a given system. Accordingly, the risk analysis of a system consists of taking the results of the uncertainty analysis (the likelihood of the different potential events in the system) and applying its respective costs (e.g., in terms of money, fatalities or work hours) thereby, producing the statistical mean costs associated with that system (Faber, 2012). Additionally, potential different scenarios of system interventions can be considered (where there is a change in the events, probabilities and costs of that system). Risk analysis, when involving decision-making or the comparison of scenarios can be likened to a probabilistic/uncertainty-based cost-benefit analysis. The most common application of risk analysis is precisely in decision-making, where, considering the cost criteria, a decision can be made while taking into consideration the inherent uncertainty of that system. While applications of risk analysis to hydrology are less common than applications of uncertainty analysis, some are also present, such as in the areas of water resource management (Maia, et al., 2014). However, only very few applications exist in the area of fluvial morphodynamics, primarily due to the large computational requirements associated with the numerical HM models.

A great many tools are currently in existence for the representation of the variables' uncertainty (many of which are described in section 3), as well as of the processes which these variables represent (also referred in section 6). Applying these methods in risk analysis can simply be achieved by associating the different costs linked with morphological evolution, such as property damage, terrain failure and infrastructure collapse. In order to integrate costs and the different potential events, a variety of different tools can be utilized, depending on the degree of complexity of the system in question, such as fault trees or Bayesian networks (Faber, 2012). On the other hand, and regarding the present study, as the complexity of the risk analysis case study is relatively reduced (since it only involves one type of failure and the remaining interactions of the variables involved are already represented in the models), the failure likelihoods and costs were multiplied directly and in accordance with the corresponding scenarios.

2.4. SUMMARY

In this section, the literature review performed in the context of this PhD study is summarized. The subjects presented include (1) the streamflow series generation (necessary for the stochastic generation of the numerical HM models' inputs, formally the first task involved in the stochastic modelling of fluvial morphodynamics), (2) the sensitivity analysis of fluvial morphodynamics, which is essential in determining the viability of validating the results of the proposed stochastic modelling, and (3) applications of uncertainty and risk analysis applications in a fluvial environment, providing context for the goals established for this PhD.

In general, the gaps in the knowledge represented in the literature which this thesis is intended to supplement are as follows:

- A generally applicable technique for the stochastic generation of streamflow series. Presently existing techniques are limited in some way or another and therefore an alternative must be found;
- The sensitivity of morphodynamics to the different variables involved and potential means of validating stochastic modelling. At the moment, there is no consensus in the literature as to which variables are most important for morphodynamical behaviour;
- A methodology for representing the uncertainty in fluvial morphodynamics. The proposed methodology is intended to provide the means for representing the referred uncertainty.

This information is an integral part of the application of the stochastic modelling of fluvial morphodynamics to be presented in the following sections of this Thesis, with particular emphasis in sections 3 (for context and comparison purposes) and 5 and 6 (guiding the choice of variables to be considered in the modelling of morphodynamical uncertainty).

3
STOCHASTIC GENERATION OF STREAMFLOW SERIES

Considering the need to generate inputs for the numerical HM models, and given the complex nature of the streamflow series at the time scale required to promote the stochastic simulation of fluvial morphodynamics, a novel stochastic streamflow time series generation methodology was created. This methodology was systematized and validated in Oliveira and Maia (2018). In this section, the overall principles and concept behind this new methodology are presented.

The proposed methodology is aimed at reproducing both the short and long term components of the streamflow's behaviour, with a particular focus on the autocorrelation component of its behaviour. From a conceptual point of view, the methodology consists of, when sampling new streamflow series, reproducing, from a probabilistic point-of-view, the probability distribution and dependencies of both the streamflow and its' first and higher order time derivatives. The proposed methodology was designed so as to allow for the near-limitless generation of new streamflow series using solely information from observed values. Generally speaking, this methodology can therefore be useful for any study where the variability of streamflow may be relevant to the quality of the results, such as morphody namic modelling (Beckers, et al., 2016) and water resources management (Morway, et al., 2016). At the same time, the proposed methodology can also provide a good alternative to deterministic approaches in studies involving streamflow modelling and forecasting (such as (Wang, et al., 2017; Chen, et al., 2015)). The general nature of this methodology makes it useful for virtually any area of series generation, even in climate change analysis or financial and health-related studies

3.1. STOCHASTIC TIME SERIES

The proposed methodology aims to generate streamflow series with an overall behaviour identical to that of observed/historical recorded data. Streamflow is a stochastic variable and can therefore be said to be both random and, to a certain extent, dependent. This dependency can be expressed in different forms and have different origins. For most types of time series (including streamflow), the types of dependencies which are relevant to their variability can often be split into 3 different components:

- Time dependency – the variable varies as a function of a particular frequency, i.e., periodicity;
- Dependency on other variables – the variable varies as a function of other existing variables;

- Dependency on itself – the variable varies as a function of its own prior values. This component is often referred to as autocorrelation.

Independently, the first two components are relatively well studied in literature, with a variety of techniques available for each of them (e.g., Differentiation, Multilinear Regression, Artificial Neural Networks, etc.). However, the autocorrelation component can often be harder to model due to the complex non-linear effects that it involves. Additionally, the different forms of dependency can often overlap and may be imbued of a strong probabilistic nature.

The relevance of the different components in streamflow which defines the time series' variability varies greatly from location to location and is dependent on the timescale of the series. The autocorrelation component in particular is predominantly relevant for series with smaller timescales, such as hourly and daily streamflow series (such as series necessary for the application of stochastic representation of morphodynamics). The primary challenge in streamflow generation (at small timescales) is therefore the representation of this autocorrelation component due to its non-linear and probabilistic nature. The proposed methodology was developed precisely to handle this difficulty, specifically, by directly representing this statistical relationship using a joint PDF which can be used to relate the variables' values from a probabilistic point of view.

Streamflow is a result of the streamflow/runoff process continuity and its behaviour regarding autocorrelation on smaller timescales can be understood as a form of inertia (which limits the ranges of variation of streamflow and its derivates). As the dependency/autocorrelation between consecutive pairs of values of streamflow increases, then so does its inertia. The inertia of any given streamflow series is dependent on a variety of factors relating to the corresponding hydrometric station's location, e.g. upstream basin area, shape and slope, local climate conditions, groundwater storage capacity and the time scale/time resolution of the data (i.e., smaller time scales/resolutions usually imply higher inertia/dependency between consecutive values of the series). Generally speaking, common streamflow series are composed of a base flow (for non-ephemeral rivers; which is a very slowly varying component and mostly results from the behaviour of the surface and groundwater storage mechanisms in the basin) and direct runoff which translates into flood wave-like hydrograms (for all rivers; generated by precipitation-runoff events and which vary very quickly), as is represented in Figure 6. The flood waves, due to their higher flow values are generally the main responsible for bed-level change in fluvial channels. In addition, unlike the base flow, these flood waves, given their rapidly varying rate of change (generally composed of a faster varying increase in streamflow up to its maximum value, followed by a slower decrease back to "normal" values – Figure 6), can be very hard to mimic precisely. Conversely, the methodology will focus particularly on representing flood waves, as their behaviour can be mostly characterized as driven by autocorrelation.

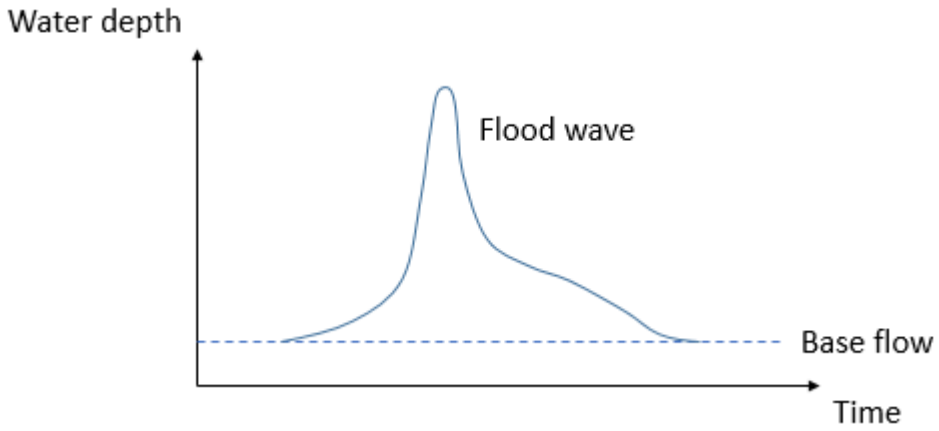

Figure 6 – Schematic representation of a typical flood wave hydrograph.

The proposed approach is not intended as a physically-based method. At the moment, there are a large number of physically-based methods in existence and improvements upon these are unlikely to be significant. At the same time, physically-based methods often require a significant amount of inputs from external variables, make significant assumptions or both. These facts make any one of these individual methods limited for general application. Conversely, the proposed methodology, which is statistically-based, is less restricted in these aspects. Its goal is to produce streamflow series with realistic behaviour, undistinguishable from real, measured series for any given location and without any external information sources outside of the streamflow series themselves.

3.2. CONCEPT

Autocorrelation, which is the primary focus of the proposed methodology, can be described as the interdependence between different values in a series. Specifically in the case of streamflow, this dependency is often expressed over time and is particularly visible between consecutive values of small time scale series (e.g., hourly or daily values). It is one of the main defining characteristics of the streamflow's behaviour. Conceptually, the proposed methodology for the generation of streamflow series is built upon the idea of expressing autocorrelation as a probabilistic dependence between consecutive values in time. Alternatively, the dependence between consecutive values can also be understood as a dependence between the streamflow's magnitudes and its derivates over time.

If streamflow were to be sampled directly from its PDF, the resulting autocorrelation structure would be non-existent, with each new value having complete freedom to oscillate independently from the rest of the series. The proposed methodology stems from the idea that, by statistically restraining the generation of new values according to previously generated values, the autocorrelation structure of the observed streamflow series can be transported to the generated series. Figure 7 illustrates an example of the effect of the addition of derivatives to the streamflow generation and the changes that it introduces in the PDF's considered for the generation of each new consecutive value in a generated series. In this example, the autocorrelation (defined as a statistical example) leads to new values not being able to change freely along the streamflow's PDF, but in fact being restricted as a function of prior values.

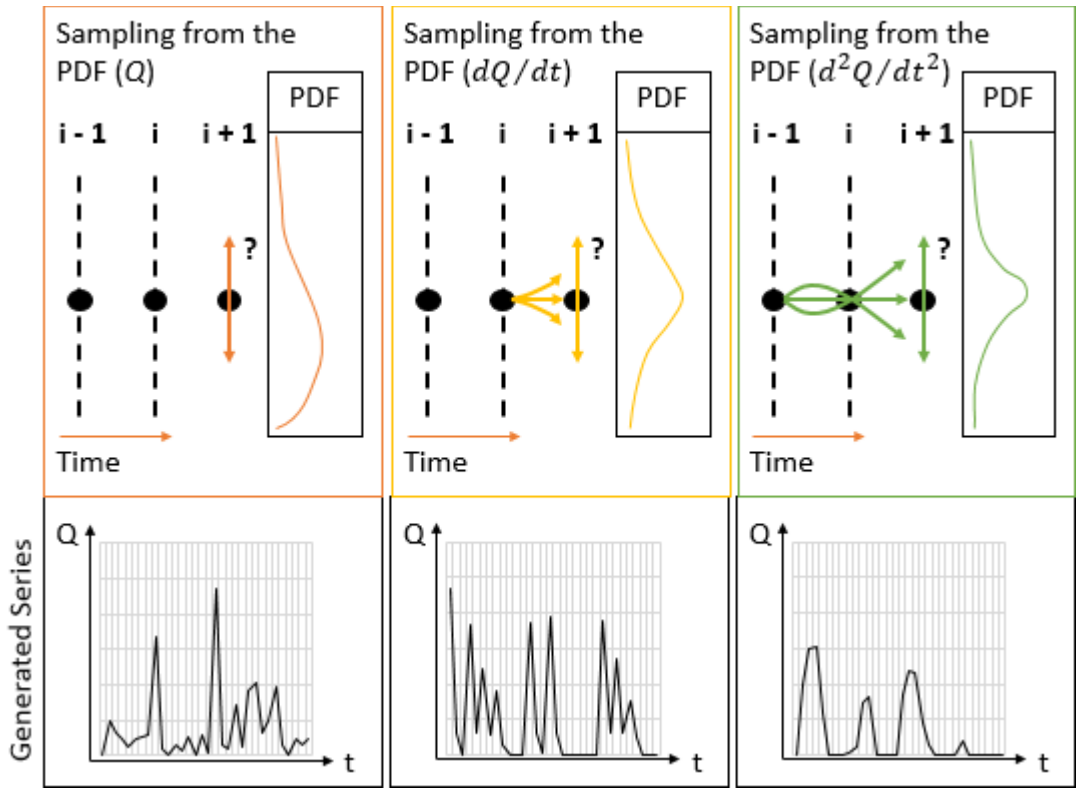

Figure 7 – Schematic representation of the influence of derivative superposition in series generation

The autocorrelation structure of the streamflow is to be represented using a joint PDF, i.e., a multi-dimensional Probability Distribution Function which contains both the PDFs of the streamflow and its derivatives and the dependence structure between them. Naturally, the autocorrelation structure (and corresponding joint PDF) is site-specific, as it is a result of the processes which generate the streamflow itself. The shape and dimensionality of the joint PDF may change between sites as a function of local geomorphological and hydrological characteristics, as well as of the time scale of the data itself (e.g., hourly, daily or monthly scales). The concept of simulating the joint PDF to represent the streamflow's variability and autocorrelation structure has in fact already been applied in previous works (e.g., Lee & Salas, 2011) but not, to the best of the author's knowledge, for the time scales here proposed.

3.3. Basic Assumptions

A set of general assumptions comes associated with the methodology. These assumptions are meant to completely describe the type of variable for which the methodology is to be applied and are necessary for its application. The target variable can be generally described as non-periodic, unbounded (i.e., infinite over time), discrete or continuous, stochastic variable. Specifically regarding streamflow, while it is generally periodic, the periodicity itself can be easily reproduced with other methods, most of them straightforwardly integrable with the proposed methodology.

The assumptions upon which this approach is based are as follows:

- Periodicity aside, the variable is assumed to be the result of a continuous phenomenon, thereby implying that the dependency between different values of the time series reduces as the separation/distance (in time) between those values increases (as represented in Figure 8). This assumption allows for this technique to use only a limited number of derivates (as higher order derivates have little to no impact on the series generation);
- The values of the variable and of its derivates are interdependent. This assumption (which is equivalent to not assuming their independence) implies that the PDF's cannot be sampled directly and must be sampled as a joint PDF;
- The relationship linking the variable and its derivates is of a purely statistical nature (i.e., it is non-deterministic). Therefore, there should be no mathematical function which can be used to fully describe this relationship;
- The variable results from a process stationary in time (aside from the seasonality's effect, which should be reproduced by a suitable technique applied alongside the proposed methodology), therefore implying that each new generation can be performed from the same joint PDF (i.e., streamflow, its derivates and dependencies are time-independent).

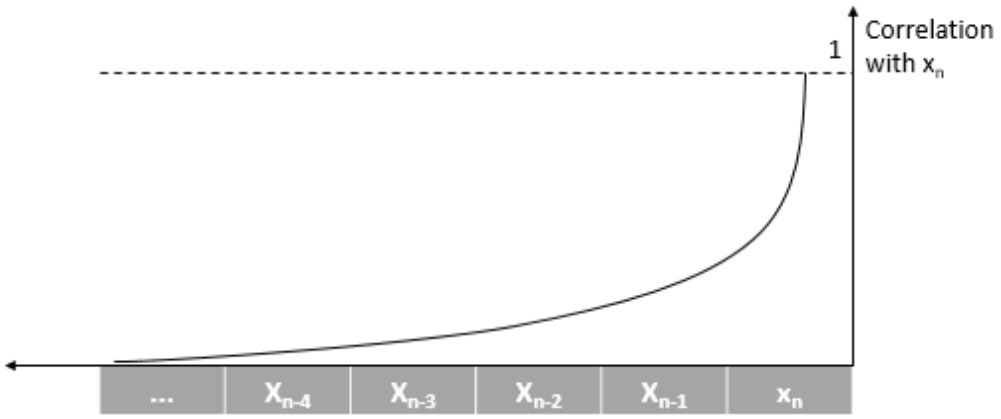

Figure 8 – Schematic representation of the influence of derivative superposition in series generation

These assumptions have been verified as correct for several types of commonly studied variables (particular those which originate in nature, such as streamflow). This technique aims to generate new series of streamflow values from a minimal amount of assumptions, being therefore potentially applicable to other variables besides streamflow (such as precipitation and temperature), as long as they follow the above referred assumptions.

3.4. METHODOLOGY

Generally speaking, the proposed methodology for streamflow generation consists of using a probabilistically-defined dependence structure to produce new streamflow values based on prior values. Each new value is therefore sequentially and randomly sampled based on a joint PDF (which represents the probabilistic dependence structure) conditioned by the prior values.

In order to remove the series seasonality/periodicity, the adopted approach consisted of dividing and multiplied the streamflow series by yearly daily scale factors (e.g., taken from 30-day moving averages of the observed streamflow series). These daily scale factors were calculated based on the available data. Seasonality can, from a statistical point-of-view, obscure the autocorrelation structure of streamflow and should therefore be handled separately. Other methods to remove periodicity (e.g., such as PARMA or differentiation, as described in (Chatfield, 2016)) are also acceptable.

The primary stages of methodology's application therefore are:

- Decomposition of historical streamflow data into deseasonalized series (i.e., observed streamflow removed of its periodicity) and its seasonal component (e.g., defined by the corresponding period and the moving average scale factors). ;
- Construction of the streamflow's joint PDF (from the deseasonalized streamflow series). Both the streamflow's autocorrelation structure (the dependency between streamflow and its derivates) and variability are represented by this joint PDF;
- Starting from a few random initial streamflow values, sequentially generate streamflow values (at a reference instant in time *t*) by:
    - Defining a conditional PDF from the joint PDF conditioned by prior values of streamflow (i.e., the values of streamflow/derivates for instants *t-1*, *t-2*, etc.);
    - Define the new streamflow value for instant *t* by randomly sampling from the conditional PDF;
    - Repeat for instant *t=t+1* (i.e., where the instant *t* becomes part of the prior values in the generation for instant *t+1*).
- Transformation of the generated streamflow series to incorporate seasonality (i.e., reverse application of the decomposition process applied in the first stage, e.g., scaling the streamflow by 30-day moving averages).

These stages are represented in Figure 9 for an n-dimensional joint PDF.

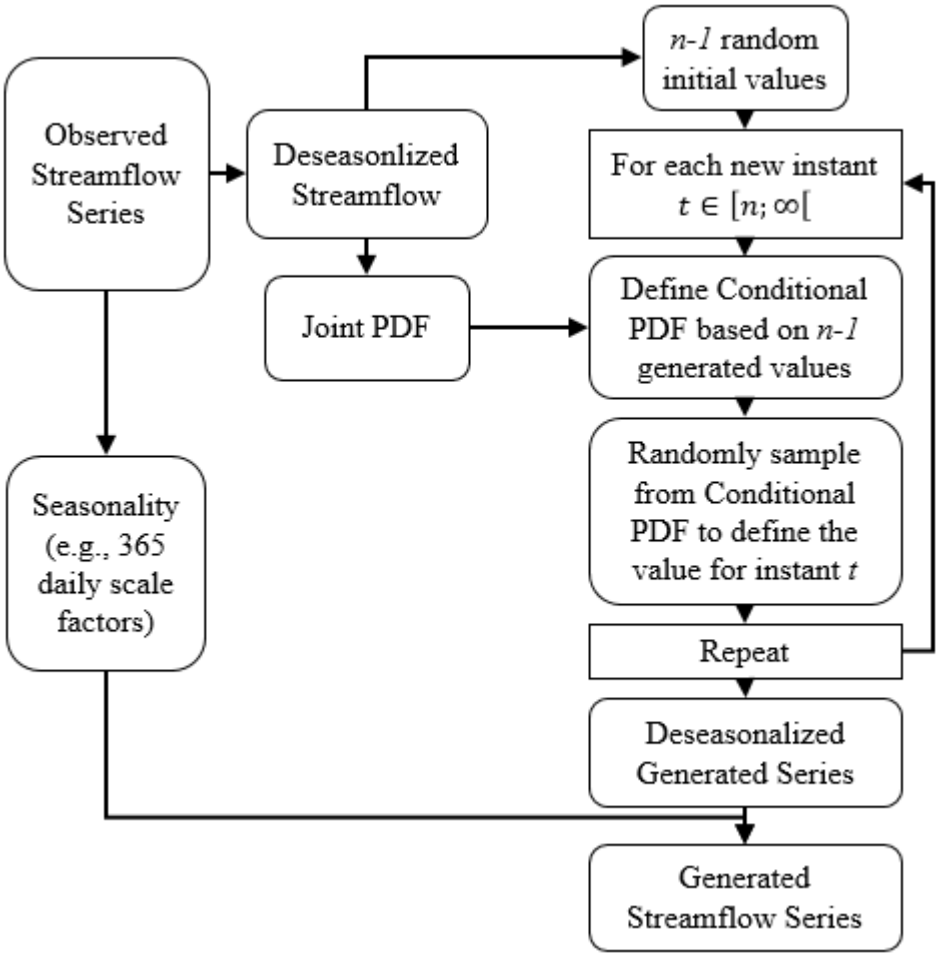

Figure 9 – The different stages which define the time series generation procedure.

3.4.1. JOINT PDF

The most important information obtained from the observed data (which represents the behaviour that is to be replicated) is the joint PDF of the streamflow and its derivates (i.e., the probability density function which describes the probabilistic relationship of these variables). Taking into advantage of the assumptions previously referred in Section 3.3 (specifically, the one which states that the relationship between streamflow and its derivates is uniquely of a statistical nature), it becomes possible to define the probability distribution of new streamflow derivates from the joint PDF conditioned to previously generated streamflow values and derivates. Taking into account that the derivates are defined based on the streamflow's values for the previously generated instants, this process is equivalent to defining each new value as a function of prior values.

3.4.1.1. Defining a Joint PDF

A few different techniques are available for defining the joint (i.e., multi-dimensional) PDF. The main techniques available in the literature for this task (specifically, those which require virtually no user input) are:

- Copulas (Trivedi & Zimmer, 2005). Consists of a parametric approach to the modelling of joint parametric distributions. The copulas themselves correspond to functions connecting the marginal functions which compose a multivariate PDFs. Generally speaking, applying copulas consists of (1) determining the corresponding marginal probability distributions, (2) selecting the appropriate copula function to use, (3) setting the parameter which determines the degree of dependence between the variables and (4) applying the copula. One of the main advantages of this solution is that maximum likelihood can be used for selecting the copula and defining the parameters.
- Kernel Density Estimation (KDE) (Scott, 2015). Consists of a non-parametric approach which uses kernels to average the probability density over a defined smoothing bandwidth. KDE utilizes Euclidian distances as a measure of probability density along an evenly spaced grid. Because this approach is purely data-based and the probability density is defined by means of discrete values on a grid, the KDE can be easily applied for defining joint PDFs, even when complex dependencies are involved.

Alternatively, artificially defined conditional PDFs (i.e., probability distributions whose parameters change as a function of streamflow) and Markov chains (useful when multi-stage behaviour can be detected in the streamflow series, such as for hydrometric stations situated downstream of reservoirs) may also be used where necessary in order to fully define the Joint PDF. However, these solutions can only be applied on a case-by-case basis and were therefore excluded from this study.

Although, in some instances, the Copula approach may be suitable for representing the streamflow's joint PDF, the complex autocorrelation structure of streamflow makes it less suitable for general application than the KDE. An example application of the two methods (to one of the streamflow series later used in the validation of this methodology), along with the distribution of observed data, is shown in Figure 10.

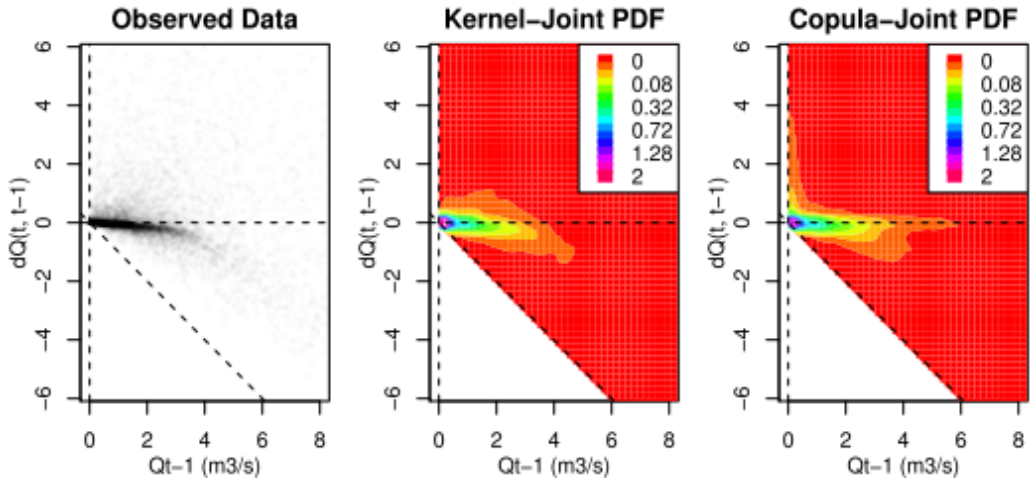

Figure 10 – Comparison between the observed pairs of Q and dQ (on the left), the joint PDF defined by the Copula approach (on the right) and the Kernel approach (at the centre). t is a reference point in time, meaning that these PDFs represent the pairs of values of Q_{t-1} versus Q_t - Q_{t-1}.

Comparing the observed distribution of point concentration (in Figure 10a) with the magnitudes of probability density described by the PDF's (in Figure 10b and Figure 10c), the PDF of the Copula (a Tawn type 1, selected by way of the maximum likelihood method) is not quite as capable of representing the distribution of the pairs of observed streamflows and their derivates as the KDE. Specifically, the Copula produces a significant concentration of points around both the x and y-axis which is not compatible with the observations.

While the Copula has the potential for producing good results (depending on the streamflow autocorrelation structure), for general application to all of the available streamflow data, the KDE was chosen as the tool for representing the joint PDFs. Nevertheless, in some instances during the streamflow generation process, depending on the number and distribution of points in the data, the KDE approach may prove unruly near the very extremes of the PDF and, in those instances, the conditional PDF can be estimated locally, i.e., by directly sampling from the closest observations.

3.4.1.2. Dimensionality of the Joint PDF

The dimension of the joint PDF (i.e., the number of derivates to consider towards representing the streamflow's autocorrelation structure) should be equal to the number of derivates which are relevant to describe the streamflow's behaviour (stronger autocorrelation structures imply more derivates and vice-versa). In simple terms, the larger is the number of independent consecutive pairs of derivates, the larger is the number of derivates which should be included in the methodology's application. If derivate i and derivate i+1 are highly dependent, then the derivate i+1 should not be simulated. Accordingly, if derivate j and derivate j+1 are independent, then both of them should be included in the generation process.

In order to define the number of derivates relevant for the representation of the streamflow's autocorrelation structure, it is necessary to assess the dependency (or lack thereof) between the different pairs of derivates and/or streamflow. Assessing variable dependency can generally be performed by way of statistics or of graphical methods. However, seeing as, due to their simplistic nature, statistics can be deceiving (particularly, when complex forms of dependency are involved, such as is the case here), graphical methods are advised. Two examples of practical graphical methods are the Chi-plot (Fisher & Switzer, 2001) and the Kendall plot (Genest & Boies, 2003).

Alternatively, as a (graphical) method for assessing specifically the dependency of consecutive derivates, the author suggests a comparison between the PDF of the observed derivates' values and their simulated counterparts taken from differentiated randomly sampled derivates with an order of -1 (as described in Eq. 3). For example, if there is a significant difference between the PDF of the streamflow's first derivate and the PDF of differentiated randomly sampled values of streamflow, then there is most likely some level of dependence between streamflow and its first derivate. An example application of the Kendall plot (also referred to as K-plot) and of the suggested method is presented in section 3.5 of this Thesis.

$$If\ PDF\left(\frac{d^iQ(t)}{dt^i}\right) \neq PDF\left(\frac{d\left(\frac{d^{i-1}Q(t)}{dt^{i-1}}\right)}{dt}\right), then\ d^iQ = f\left(d^{i-1}Q\right) \qquad \text{Eq. 3}$$

Generally speaking, after the number of relevant derivates is selected, different solutions can be used for representing the derivates and the derivate dependency structure in the joint PDF. For example, for 3 derivates, the joint PDF is 4-dimensional, and it can be represented just as well as $f(Q_t, Q_{t-1}, Q_{t-2})$ or as $f(\Delta Q_{(t,t-1)}, Q_{t-1}, \Delta Q_{(t-1,t-2)})$. In order to enhance the perceptibility of the derivates/streamflow dependency, the author has chosen to use the representation defined in Eq. 4 for n dimensions. The resulting PDF should be, for example, for 2 derivates $f(\Delta Q_{(t,t-1)}, Q_{t-1})$, for 3 derivates $f(\Delta Q_{(t,t-1)}, Q_{t-1}, \Delta Q_{(t-1,t-2)})$, for 4 derivates $f(\Delta Q_{(t,t-1)}, Q_{t-1}, \Delta Q_{(t-1,t-2)}, \Delta Q_{(t-1,t-3)})$ and so on. In this solution, the value sampled is the ΔQ (or dQ), which is summed with Q_{t-1} in order to define the new streamflow value, Q_t.

$$PDF^{\,n-Dimension}(Q) = f\left(\Delta Q_{(t,t-1)}, Q_{t-1}, \Delta Q_{(t-1,t-i)}\right) \forall\, i \in [2;n] \qquad \text{Eq. 4}$$

The number of relevant derivates changes as a function of the characteristics of the drainage basin upstream from the river section in which the hydrometric stations is located, such as, surface area, average slope, soil occupation, etc.. Since the autocorrelation structure is dependent on these characteristics, the application of the streamflow generation methodology for a given site must be based on data from that same hydrometric station or on scaled streamflow records from a hydrometric station with similar geomorphological and hydrological characteristics.

3.4.2. Sampling Process

The sampling process of the proposed methodology is performed on a sequential, value-by-value basis. For each instant t (for which a new streamflow value is to be generated), a conditional PDF is defined by constraining (e.g., using Eq. 5) the joint PDF based on prior values of the generated time series (*t-1*, *t-2*, etc.). From this conditional PDF, the value of the streamflow variation, ΔQ, is sampled from the corresponding conditional Cumulative Density Function (CDF), and added to Q_{t-1} in order to define the new streamflow value, Q_t. Alternatively, depending on the definition of the joint PDF, the value of the streamflow for the instant t (Q_t) may be directly sampled from the conditional PDF. The sampling process is then repeated for the following instants (i.e., *t+1* and *t+2* and so on) until the desired streamflow series length is achieved.

$$PDF_{dQ,\ Q}(dq|Q=q) = \frac{PDF_{dQ,\ Q}(dq,q)}{f_Q(q)} \qquad \text{Eq. 5}$$

The potential length of the generated streamflow series is virtually limitless. However, if a very large number of values is generated (several times the number of values recorded in the observed data), some

issues with the representativeness of the generated series may arise due to the representativeness (or lack thereof) of the observed streamflow data itself.

Since the generation process is based on the sampling of the derivates themselves and not just on the observed streamflow magnitudes, and depending on the definition of the joint PDF, new values of streamflow may be generated. These new values are, however, in accordance with the streamflow's PDF, due to the methodology's own sampling process. Negative values may be generated but they are generally very small and may therefore be simply rounded to zero. Conversely, values above the maximum streamflow on record have been observed but are mostly rare and are generally situated only slightly above the maximum.

3.5. VALIDATION

An example application of the proposed methodology was used to analyse the methodology's output. This example was based on a large record of daily streamflow values for multiple different locations all over mainland Portugal.

The generation of streamflow was performed based on the methodology described in the previous section (3.4). The deseasonalization and reseasonalization processes were performed by, respectively, dividing and multiplying the daily values by a coefficient corresponding to its yearly mean daily values.

For comparison purposes, the KNN and ARFIMA approaches were also applied to this set of streamflow data, providing a better assessment of the quality of the proposed methodology.

3.5.1. THE DATA

The analysis of the methodology was accomplished based on daily streamflow data from a total of 203 hydrometric stations in Portugal. The daily streamflow's high degree of autocorrelation is especially useful for demonstrating the usefulness of the proposed methodology. These data were collected from Portugal's National System on Water Resources Information (SNIRH – *Sistema Nacional de Informação de Recursos Hídricos*), from all available hydrometric stations.

The data used in this study were taken from hydrometric stations situated all over Portugal (Figure 11a). Given this fact, these stations belong to hydrometric stations and rivers from various river typologies (from ephemeral to perennial) and some distinct types of climate (mainly split between marine, continental and mediterranean climate - Figure 11b).

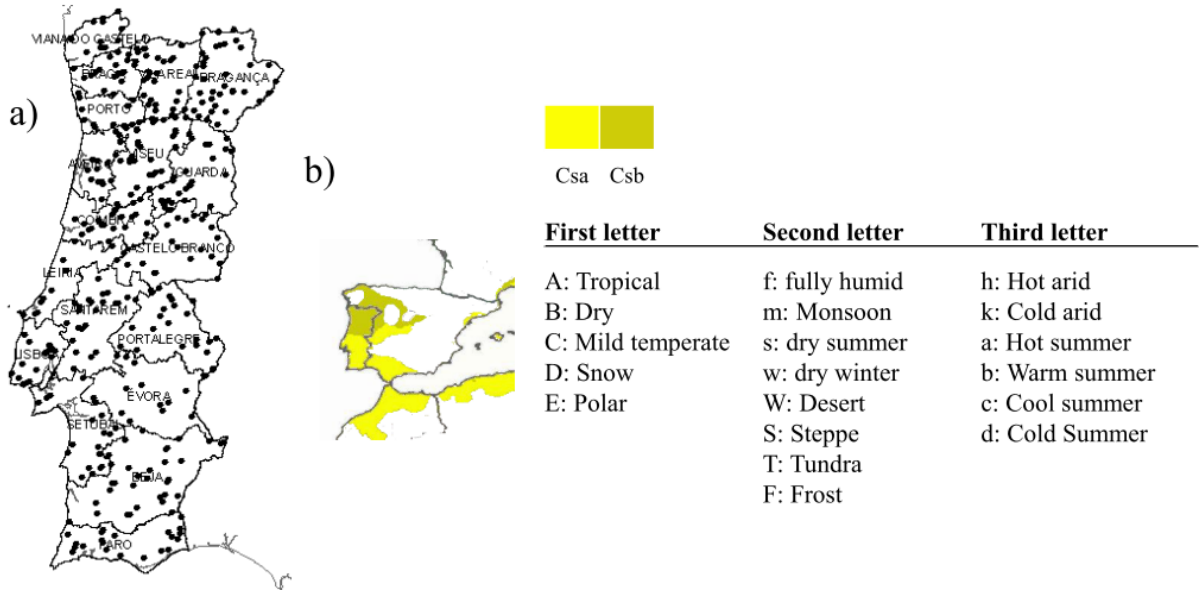

Figure 11 a (left) and b (right) – Respectively, location of hydrometric stations and climate typology distribution in Portugal (adapted from SNIRH – http://snirh.apambiente.pt/ – and Chen & Chen, 2013).

Data set lengths for each station vary greatly, ranging from 337 to 18835 daily values (or 51.6 years) on record and only four stations with a year's worth of data or less. Station record's lengths have a median of 4311 daily values or 11.8 years. For application purposes, and in accordance with common practice principles in the field of hydrology, only stations with more than 2 years-worth of data were considered, reducing the number of usable stations to 161. The stations were identified by their name (in capital letters) and their identification code, as defined by the SNIRH (generically, *XXX*/*XX*H, for example, 19F/01H).

3.5.2. Analysis of the data

Streamflow presents a significant degree of autocorrelation which defines the number of relevant derivates to be considered in the streamflow generation process. In order to assess the magnitude of the autocorrelation structure of the streamflow (and the number of derivates relevant to the definition of streamflow's joint PDF), the methodologies proposed in Section 3.4 were applied. As referred before, graphical methods, while relatively subjective, present a clearer picture of the dependence of the different pairs of daily streamflow/derivates.

Figure 12 presents the overlapped Kendall plots (commonly referred to as K-plots) for all of the stations considered.

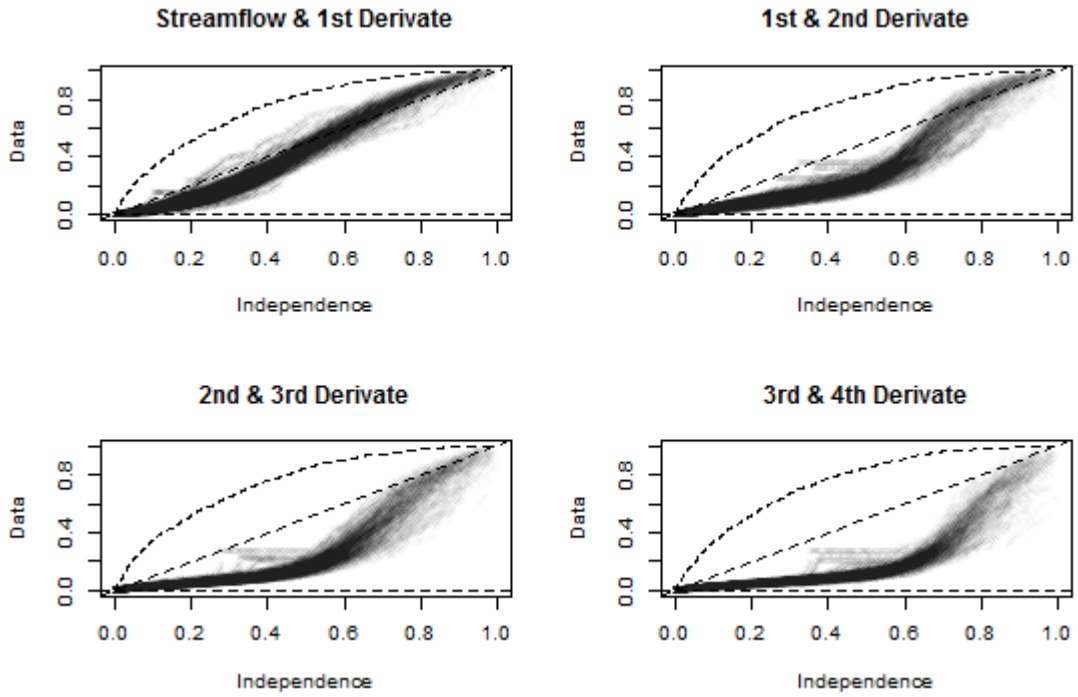

Figure 12 – K-plots analysing the relative dependency of streamflow and its derivates.

Generally speaking, in a K-plot, the data pairs are said to be independent if the points line up along the 45º line. Conversely, if the data pairs line up along the top curve or the bottom line, they are estimated to be, respectively, positively or negatively dependent. Accordingly, as can be observed in Figure 12, the results indicate that the streamflow and the 1st derivate are mostly independent (and therefore both contribute to the streamflow's variability). On the other hand, the pairs of derivates of 1st/2nd, 2nd/3rd and 3rd/4th order show an increasing dependency, with the first pair already displaying a very strong dependence between the corresponding derivates. These results indicate that the PDFs of the 2nd, 3rd and 4th derivates can likely be reproduced by generating their corresponding lower order derivates.

Figure 13 presents the overlapped Quantile-Quantile (QQ) plots comparing PDFs of the observed derivates' values and their simulated (differentiated randomly sampled derivates with an order of -1) counterparts, as described in Section 3.4. Overall, and in agreement with the results of the K-plot, the 2nd, 3rd and 4th derivates overall tendency indicate that the dependency between derivates is likely to be random, in that the different QQ lines centre around the 45° line, indicating that the observed PDFs are identical to the randomly sampled PDFs. The results regarding the 1st derivate however, consistently deviate from the 45° line, proving that the 1st derivate and the streamflow (i.e., the 0th derivate) have a strong dependence structure (which defines a significant amount of the streamflow's behaviour).

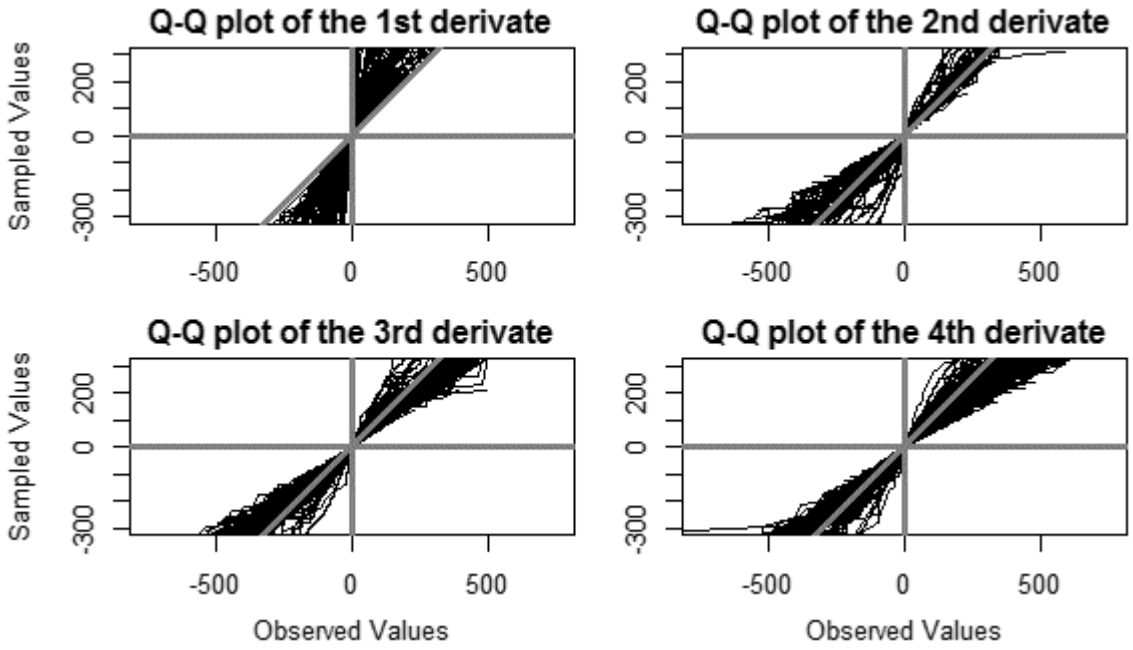

Figure 13 – Q-Q plots comparing randomly sampled and observed streamflow and derivate distributions (in m^3/s).

Additionally, some of the previously referred assumptions can also be considered as having been explicitly verified for the set of streamflow data analysed in this study, specifically:

- The streamflow derivates' importance in the definition of the streamflow's behaviour reduces as the order of the derivate increases;
- Derivates have also been shown to be inter-dependent up to a certain degree.

Taking these results into consideration, and for the purposes of this study, only the first derivate of the streamflow, as well as the streamflow itself and their respective dependencies, will be considered in the streamflow series generation. This means that the sampling process will use a 3 dimensional joint PDF of shape $f(\Delta Q_{(t,\,t-1)},\, Q_{t-1})$.

3.5.3. Application of the Methodology

Figure 14 exemplifies the application of the proposed methodology to the case study data. Figure 14 presents, on the bottom, an example of a 5-year-long portion of the original daily time series (for the CIDADELHE (08O/02H) station) and, on the top, an example of a 5-year-long series generated using the time-series generation methodology.

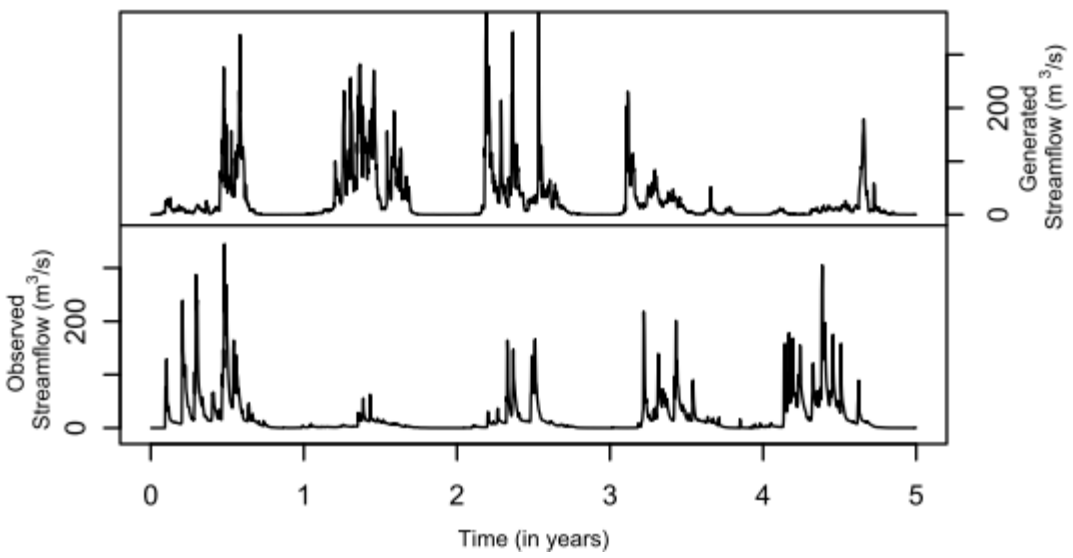

Figure 14 – Example of observed (on the bottom, corresponding to the axis on the left) versus generated daily flow time series (on the top, corresponding to the axis on the right) comparison for the CIDADELHE (08O/02H) station.

Notice that the generated streamflow series' values are in no way supposed to be identical to the values in the observed series but must instead have the same behaviour (sequencing-wise) and probability distribution of the observed series. A more detailed analysis of the results is presented in the following section. The evaluation of the quality of the proposed methodology was performed based on the entire set of streamflow series available.

Additionally, for the purpose of further validating this methodology, a comparison was established between the proposed methodology and the KNN and ARFIMA approaches. Since the ARFIMA approach generally implies the application of a logarithmic or a Box-Cox data transformation, it is usually limited to being applicable to series without null values. However, only some of the streamflow series in the database available obey this limitation and, therefore, the comparison with the ARFIMA and KNN approaches was performed based on one example of these series (which provided a clear distinction between the ARFIMA and the rest of the approaches). Finally, since the KNN produced the results most similar to those of the proposed methodology, a comparison based on the entire set of streamflow series was also produced.

3.5.3.1. Analysis of the results

As can be observed in Figure 14, the behaviour of the original and the generated series is quite similar. Specifically, the shape of the flood waves is virtually identical between the observed and generated series.

For a more quantitative analysis of the proposed methodology's capability for reproducing the sequencing/autocorrelation structure of the historical streamflow data, statistics were developed regarding streamflow's probability distribution and autocorrelation, based on the entire set of selected 161 daily streamflow series. These statistics (whose distribution boxplots comparing the observed and simulated series are represented in Figure 15) are:

- dAVG%S – Percentage change in the daily streamflow's mean;
- dAVG1d – Absolute change in the daily streamflow's first derivate's mean;
- dAVG2d – Absolute change in the streamflow's second derivate's mean;
- dSD%S – Percentage change in the streamflow's standard deviation;
- dSD%1d – Percentage change in the streamflow's first derivate's standard deviation;
- dSD%2d – Percentage change in the streamflow's second derivate's standard deviation;
- MaxDfPr – Maximum difference between the observed and simulated streamflow's PDF;
- AutoCor – Absolute change in the streamflow's first order autocorrelation coefficient.

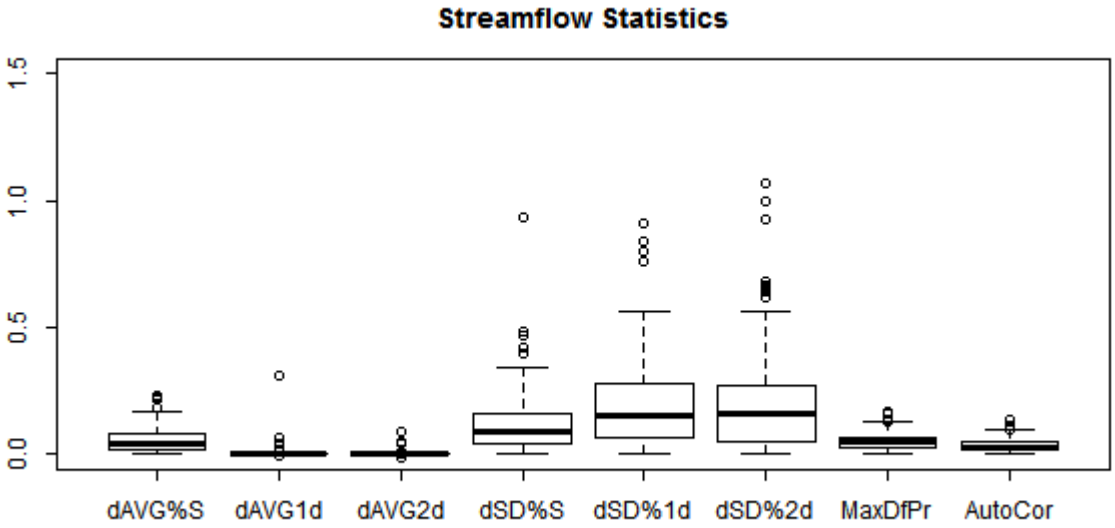

Figure 15 – Boxplots of generated daily streamflow statistics for the complete dataset of the 161 hydrometric stations.

Additionally, monthly and yearly statistics were also calculated for the entire set of streamflow series (Figure 16). The statistics (comparing the observed and simulated series) calculated were:

- dAVG%*XX* – Percentage change in the mean monthly streamflow sequentially from January (Ja) to December (De);
- dAVGAnnual – Percentage change in the mean yearly streamflow values;

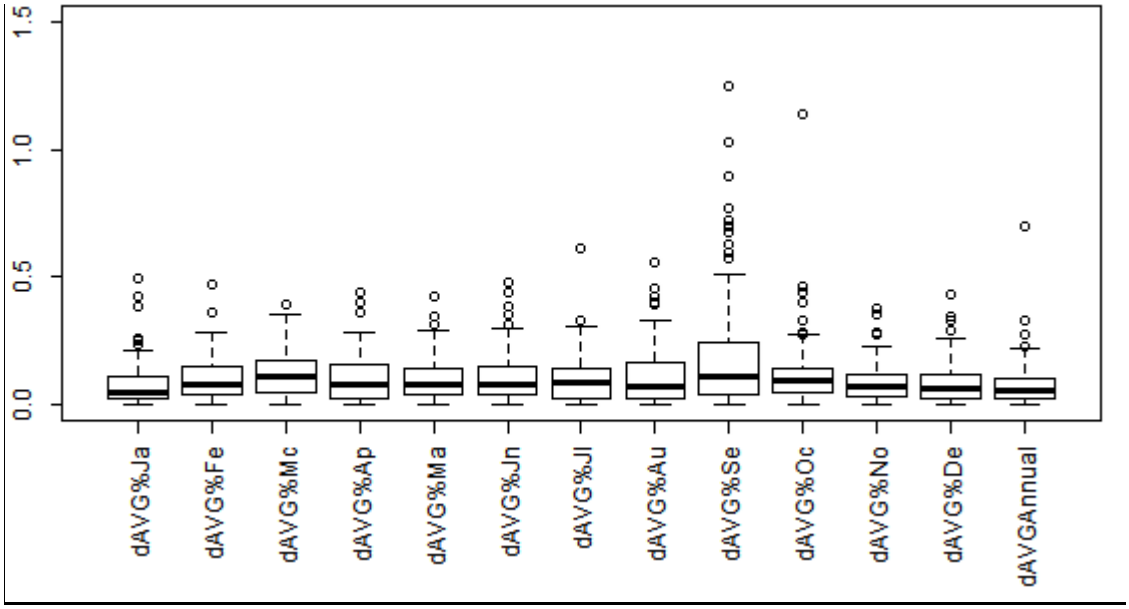

Figure 16 – Boxplots of generated monthly and yearly streamflow statistics for the complete dataset of the 161 hydrometric stations.

Generally speaking, these results indicate a very good agreement between the observations and the generated series, with only relatively small deviations observed in terms of the streamflow statistics. Regarding the daily streamflow statistics (Figure 15), the 75% quantile reaches a maximum of 25% change in the standard deviation of daily streamflow and its derivates. Additionally, the change in mean daily streamflow remains generally below 5% and the remaining statistics have barely no change between observed and simulated streamflow series, including the autocorrelation (a clear sign of the methodology's capability to reproduce autocorrelation).

Regarding the monthly and yearly statistics, there is a larger disparity between observed and generated series but the vast majority of the results (aside from September (Se)) present errors below 10%. Deviations in these long term statistics primarily indicate periodical bias in the generated series, specifically in the coupled technique used to remove seasonality.

The proposed methodology very rarely produced negative values, on average 1 in every 10000 values, and, when that occurred, they were rounded to zero, as negative values were always very small (below 1% of the respective streamflow series variability range). Regarding the presence of abnormally high values, the methodology did produce streamflow values above the maximum of the observed series. However, on average, the proposed methodology produced "abnormal values" at a pace of around 1 to 3 values for every 10000 values generated, a relatively small number which can therefore be easily limited to the observed streamflow's range (if deemed necessary).

Regarding the data requirements of the proposed methodology, for the available daily data (which is a mixture of all the different river typologies), visual analysis of the generated series showed no significant distortion of the behaviour of streamflow for historical records larger than (approximately) 3.5 years. For stations with only a small number of null values per year (primarily situated in perennial rivers), it is likely for the methodology's data requirements to be smaller. However, as a general rule, using less

than 5 years' worth of data is not advised (primarily due to the resulting reduced representativeness of the generated streamflow's PDF). If the approach used to define the joint PDF was the copulas or a conditional PDF, the data requirements would automatically drop significantly (at least by half). The KDE (which was the approach applied to the data), due to its discrete representation of the joint PDF, is the approach that requires the most data in order to correctly generate streamflow series.

3.5.3.2. Comparison of the proposed methodology with other approaches

Figure 17 presents an example the series generated by each of the different selected methods.

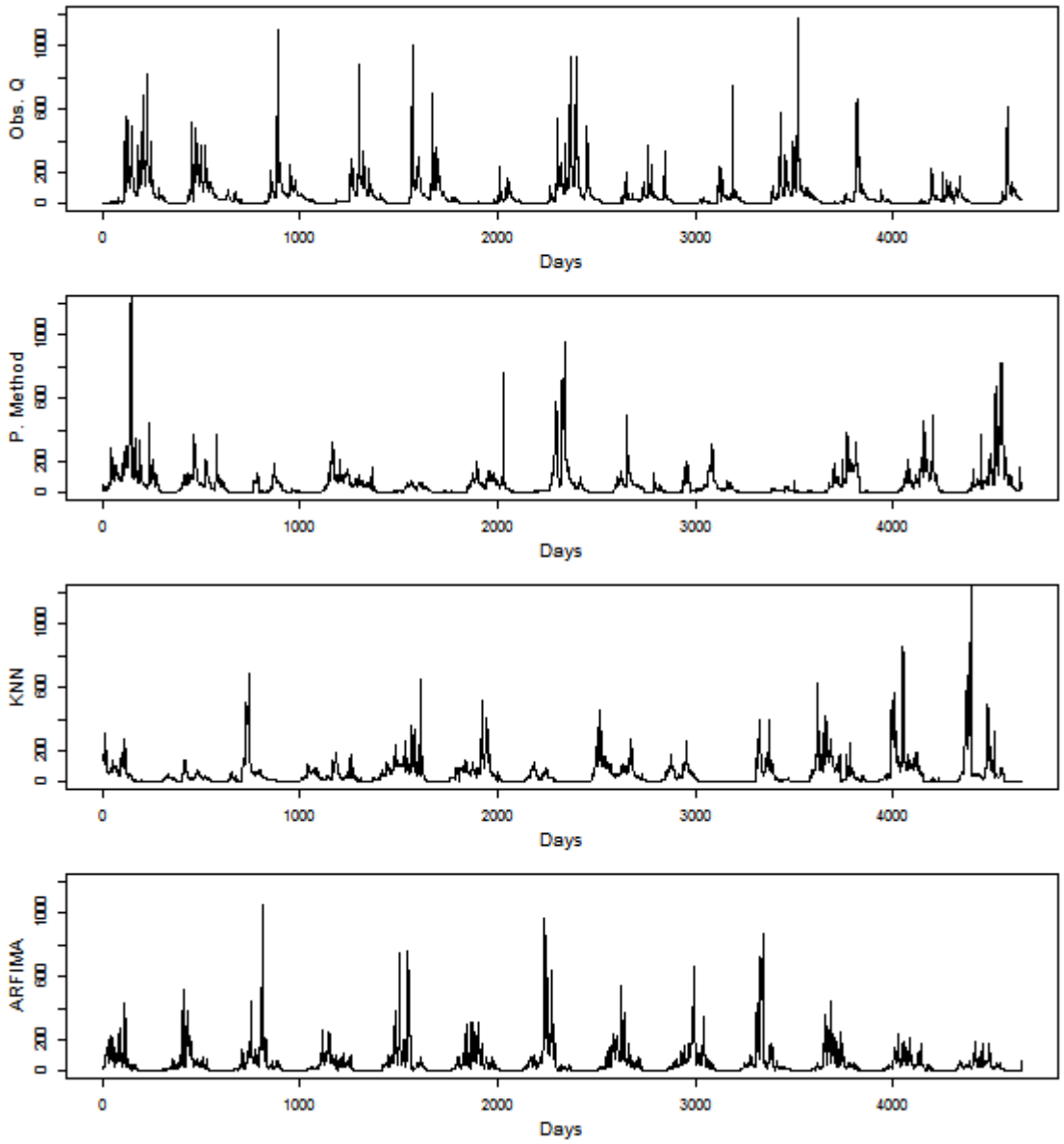

Figure 17 - Comparison of observed versus generated daily streamflow series for the different methods compared (from top to bottom, the graphics show the observed, the proposed methodology, the KNN and the ARFIMA's series, respectively), for the ALBERNOA (26J/01H) station.

The KNN and the ARFIMA approach were used as a term of comparison for the quality of the proposed methodology in what regards the reproduction of the autocorrelation component of the streamflow time

series. This application of the KNN was based on the work of Lall & Sharma (1996). The ARFIMA approach was applied by using the corresponding functions made available in the package "ARFIMA", in R. The example application was performed for the station ALBERNOA (26J/01H).

In order to compare the different methods in terms of the short term representation of autocorrelation, Figure 18 represents the different joint PDFs produced by applying the methodologies to the data. These joint PDFs relate streamflow and its first derivate, thereby representing the streamflow's autocorrelation structure.

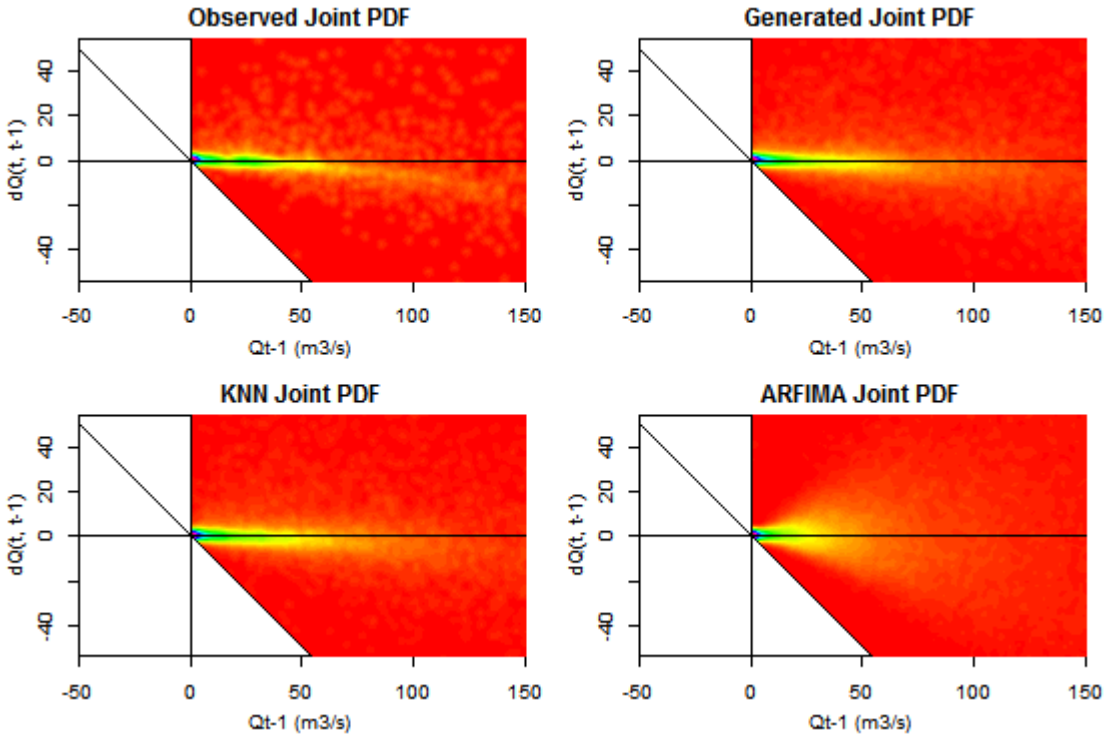

Figure 18 – Comparison of the observed joint PDF and the joint PDFs produced by the proposed methodology, the KNN and the ARFIMA, for the ALBERNOA (26J/01H) station.

Comparing the magnitudes of observed probability density (in the top left of Figure 18) with the probability densities produced by way of the proposed methodology (on the top right) and the KNN and ARFIMA approaches (presented on the bottom), only the ARFIMA approach displays a significant distortion of the joint PDF. Comparing with the observed probability densities, where larger values of Q_t produce smaller values of $\Delta Q_{(t,t-1)}$, the ARFIMA appears to produce an overly symmetric Joint PDF (relative to the x-axis).

Figure 19 displays the observed and simulated CDFs for streamflow and its first derivate. In this aspect, as can be observed from the visual analysis of the cumulative probability in Figure 19, all of the methods used are capable of representing the streamflow's probability distribution.

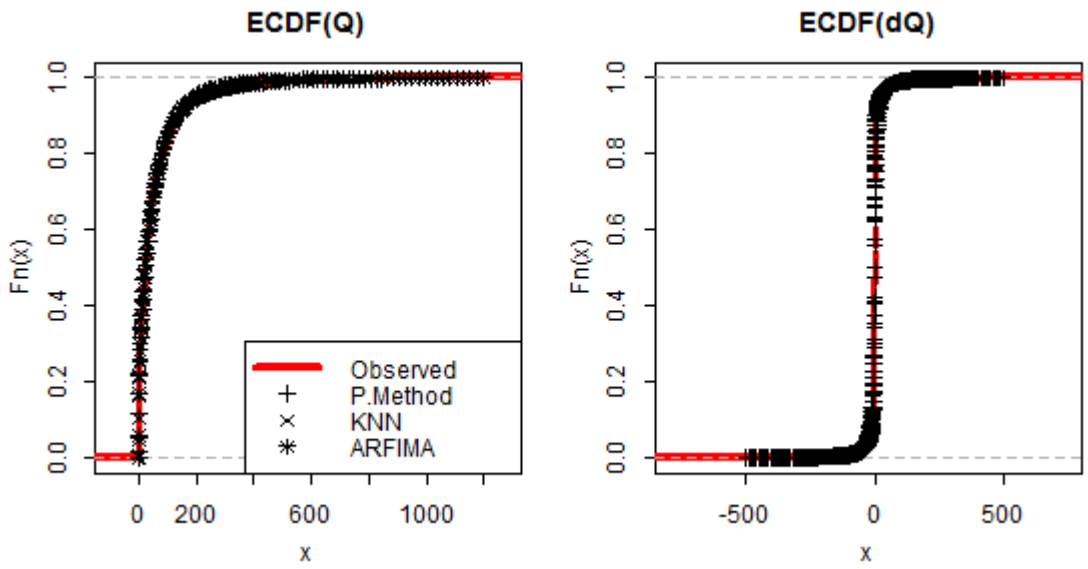

Figure 19 – Comparison of the PDFs produced by the proposed methodology, the KNN and the ARFIMA, for the ALBERNOA (26J/01H) station.

Finally, Figure 20 represents the average of the monthly streamflows, as produced by the different methodologies. Generally speaking, all three approaches reasonably reproduce the monthly variability of streamflow.

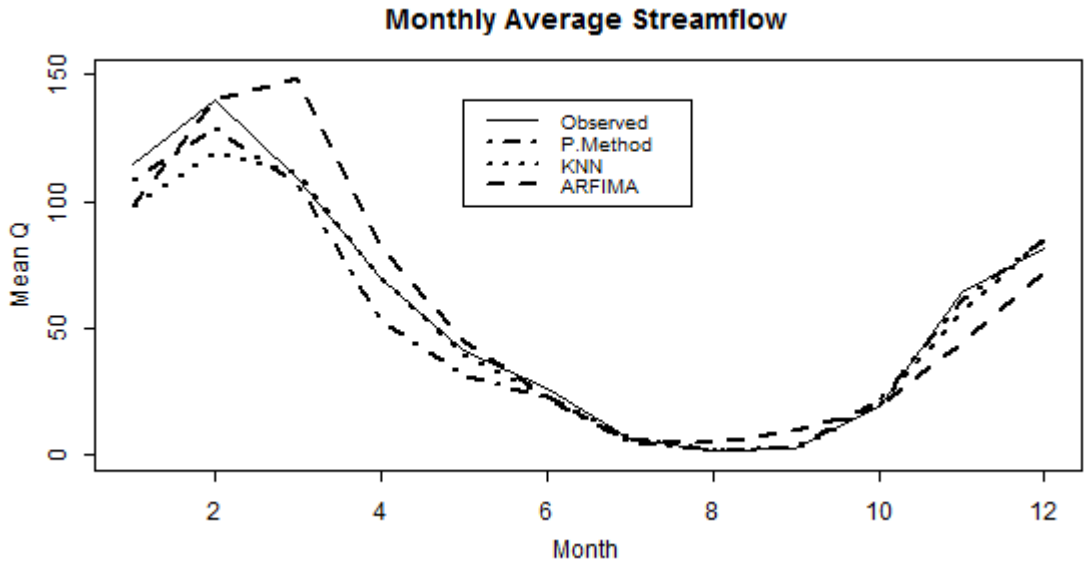

Figure 20 – Comparison of the average of the monthly streamflows produced by the different methods, for the ALBERNOA (26J/01H) station.

All of the three approaches were capable of reproducing the streamflow's daily and seasonal probability distribution. However, the proposed methodology and the KNN approach proved themselves especially capable of reproducing the statistical dependency between the streamflow and its derivates. Given the similarity between the KNN and the proposed approach, the KNN approach was applied, not just for the previous example, but also for the entirety of the available data set of streamflow series. The box plots

of streamflow statistics for the KNN approach are presented in Figure 21. Comparing the KNN and the proposed methodology (i.e., Figure 21 vs. Figure 15), the latter of the two produced smaller overall changes in terms of the reproduced mean and standard deviations of the streamflow and its derivates, thereby providing a more reliable reproduction of the streamflow's auto correlation.

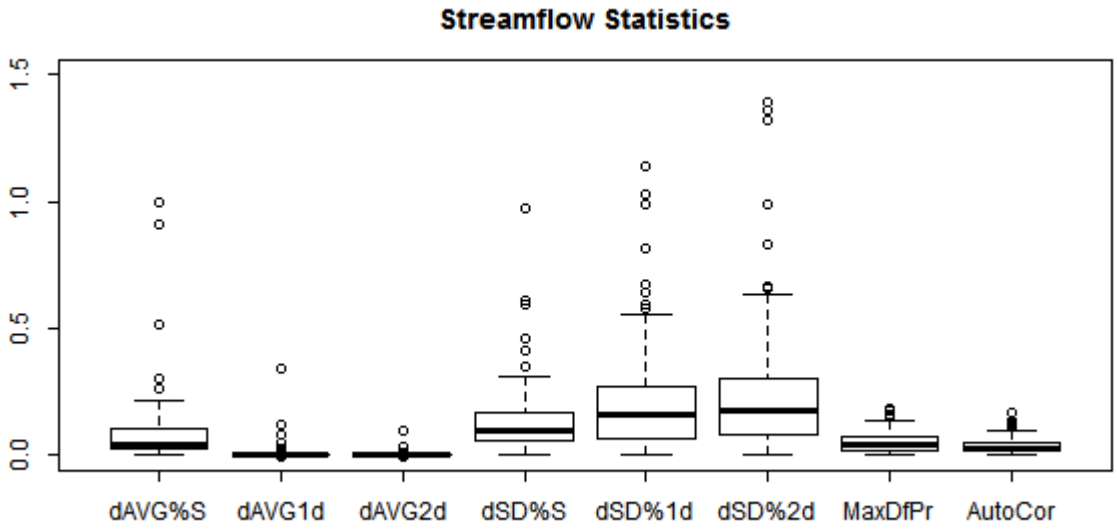

Figure 21 – Box plots of streamflow statistics as produced by the KNN approach for the complete dataset of the 161 hydrometric stations.

As can be observed from these results, all of the approaches here compared perform well in reproducing both the streamflow's PDF and its periodicity (where the differences between the approaches are practically negligible). Nonetheless, the proposed methodology performs better in what regards to the reproduction of the observed series short-term correlation, as can be observed in the joint PDF and the streamflow statistics (Figure 18 and Figure 21, respectively).

Including the entire generation process, the author observed relatively similar application times (in terms of the time necessary for execution) for the ARFIMA approach and the proposed methodology, with the KNN being a bit slower (approximately by one third). In fact, not considering the deseasonalization (which is identical between approaches), on average, and in order to generate 20000 values, the proposed methodology took 30 seconds, the ARFIMA approach took 22 seconds and the KNN took 49 seconds.

In terms of the data requirements for the proper application of the 3 techniques, while it was not possible to perform a direct quantitative measurement of their respective requirements, some conclusions can be drawn from the corresponding application methods. From a theoretical point-of-view, the ARFIMA approach undoubtedly requires the least amount of data (i.e., consecutive streamflow values) in order to generate series (due to its parameter-based approach). Depending on the approach used to represent the joint PDF in the proposed methodology's application, the KNN may require more (for a copula or conditional PDF based approach) or less (for the KDE approach) data.

3.6. SUMMARY

A variety of different time series generation methods are known to correctly reproduce the magnitude and PDF of most given variables. However, most methods in existence are significantly less successful at reproducing the complex sequencing/autocorrelation structures in the series, such as those which are commonly present in streamflow series. In this section, a simple and generally applicable methodology (which can produce a virtually infinite number of streamflow time series using information taken solely from observed data) was systematized and validated. Generally speaking, this methodology is capable of independently reproducing the characteristics of non-periodic time series affected by autocorrelation.

The resulting stochastic streamflow series generation methodology originates in the concept of probabilistically decomposing the variability of historical series in terms of the streamflow and its derivates (and their respective dependency) and then sampling them together. The idea of reproducing the probabilistic structure of the streamflow is meant to allow for an appropriate representation of the autocorrelation component of the streamflow's variability. The technique, however, makes no considerations regarding other time dependencies (e.g., periodicity) which must therefore be removed prior to the technique's application.

The validation of some assumptions (referred in section 3.3) is necessary for the technique to be applicable and, accordingly, these assumptions were appropriately validated for the entire data set (i.e., including all of the available hydrometric stations) used in the application example of the proposed methodology. At the same time, daily streamflow, as a variable, was shown to have a strong degree of autocorrelation, with the dependency between consecutive values being both complex and of a strong probabilistic nature.

Nonetheless, the application example using the whole of the available streamflow data set demonstrated that the proposed methodology is fully capable of producing good overall results. The methodology visibly reproduced known, complex sequencing/autocorrelation structures (with small deviations in the corresponding PDFs, further validating the KDE for representing the joint PDF), as well as the daily, monthly and annual variabilities of the streamflow itself (observable in the small deviations present in terms of the corresponding means and standard deviations, mostly below 10%). Using one derivate, specifically for this application example, was shown to be sufficient to reproduce to a significant extent the streamflow's autocorrelation structure. Overall, the method provides very good results for the stochastic generation of streamflow series and is suitable for application to other variables with a similar behaviour (i.e., variables with a strong autocorrelation component, such as precipitation). The streamflow's first derivates and autocorrelation coefficient presented only small deviations from the observed values, representing the methodology's capability to reproduce the streamflow's autocorrelation structure.

It should be noted that the application of this methodology is significantly data dependent, i.e., in order to produce quality results, the methodology primarily requires data from the hydrometric station's location for which the streamflow is being generated. Alternatively, data from other sites can be used to

represent streamflow variability, as long as the upstream basin presents geomorphological and hydrological characteristics similar to the basin upstream of the site for which streamflow is to be generated.

The proposed methodology opens up the possibility of performing stochastic model applications in areas where it was not previously possible to do so. This is particularly true for heavily time-dependent autocorrelated variables (such as streamflow), a type of variable which is found very commonly in nature or which is the result of nature-originated processes.

4
CASE STUDY DATA

The work presented in this study was developed based on the data of two separate case studies. The first case study corresponds to a real reach of the Mondego river and the second case study is a theoretical example of a simplified/stylized representation of a river channel (constructed based on a simplification on the data from the Mondego river).

The Mondego case study was used throughout the PhD study, namely for the sensitivity analysis, the statistical characterization of morphodynamics and the risk analysis application of the stochastic simulation of fluvial morphodynamics. The theoretical/stylized case study was used as part of the sensitivity analysis of morphodynamics, providing a useful term of comparison for the Mondego case study, particularly regarding the validation of the simulations and the associated corollaries.

Both of the previously referred case studies are presented and described in this section.

4.1. MONDEGO RIVER

The area which is part of this case study corresponds to a reach of the Mondego river, in Portugal. The headwater of this river is in the Estrela mountain range in Portugal and drains into the Atlantic Ocean near the city of Figueira da Foz. This is a considerably regulated river, with 11 large dams, 2 of which spill directly upstream from the study reach (namely, out of the Raiva and Fronhas dams, situated approximately at 23 and 40 kilometres upstream from the Palheiros levee along the Mondego and Alva rivers, respectively). The river has multiple levees along its path.

The reach of the Mondego river which was here analysed is situated between the Palheiros levee (the upstream boundary of the model) and the Portela bridge (the downstream boundary of the model), situated about 4 km upstream from the centre of Coimbra city, whose locations are represented in Figure 22.

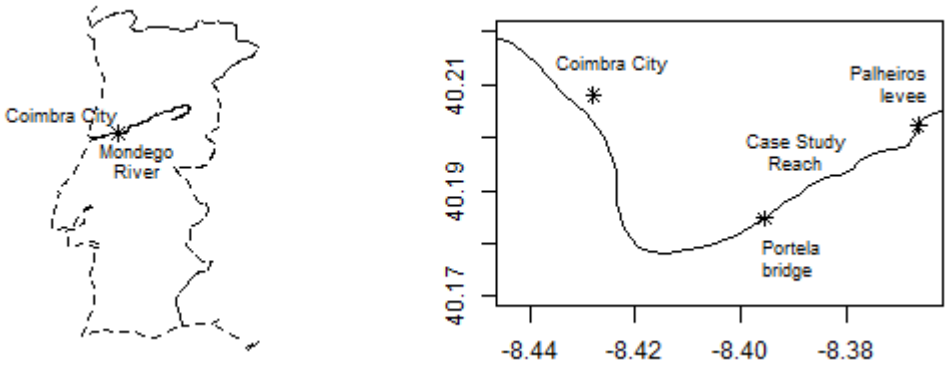

Figure 22 – Schematic representation of overall location of the Mondego river reach which is part of the case study. The coordinate data corresponds to the PT-TM06/ETRS89 coordinate system.

4.1.1. Study Reach

The reach of the Mondego river which is part of the case study is approximately 3350 meters long, with an average width of 50 meters and an average water depth of 3.5 meters, and is represented in Figure 23. The river channel is mostly straight, with a sinuosity index (Mueller, 1968) of 1.075 and an average longitudinal slope of 0.066%. The channel in this section of the river is largely composed of granular material (sand), albeit a small amount of organic soil can be found in the flood plains. The entirety of the reach was simulated as part of the HM modelling.

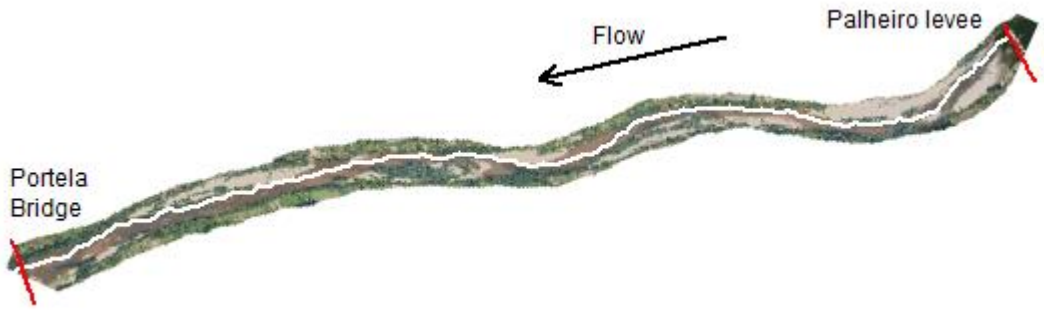

Figure 23 – Aerial map of the case study's Mondego river reach (rotated 25º for visualization purposes). The white line represents the river's thalweg and the red lines represent the study reach's boundaries.

For future reference, due to practical aspects of the representation of the study reach (i.e., the significant extensiveness of the reach), its graphical representation will be split into three areas, namely, areas a, b and c. The limits of these areas are represented in Figure 24. Photographs of the river from the Portela Bridge and of the Palheiros levee can be found in the annex of this Thesis.

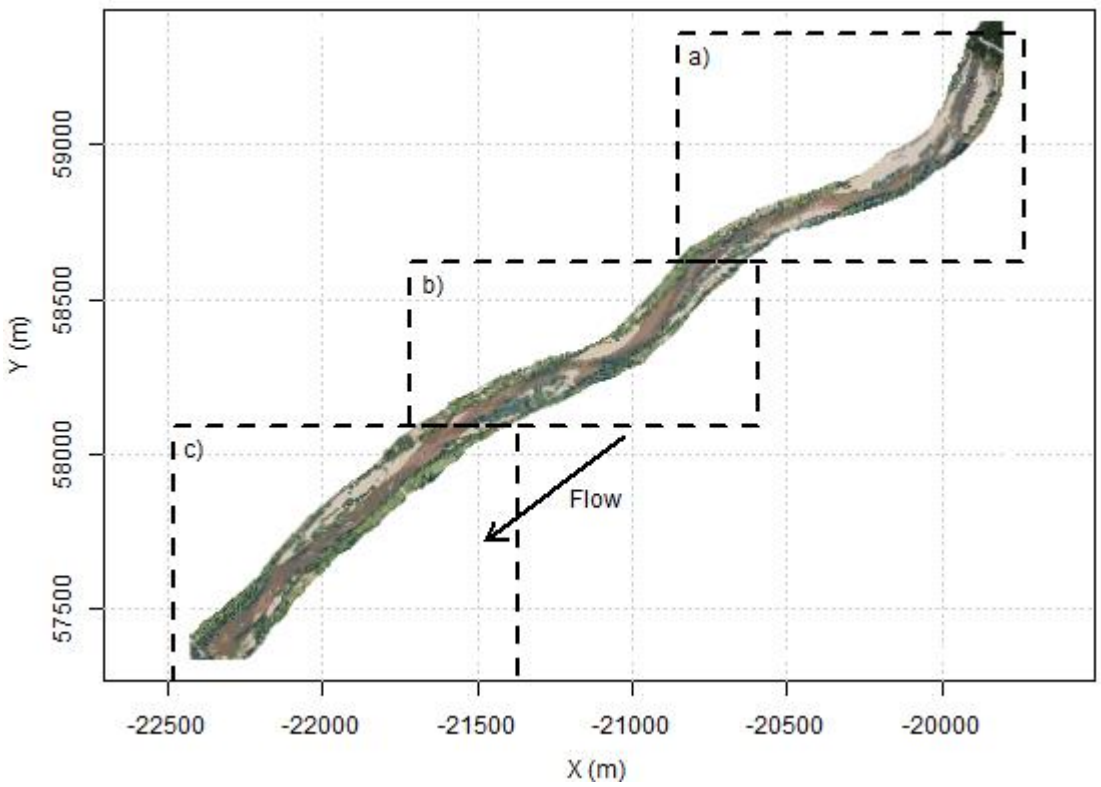

Figure 24 – Geo-referenced aerial map of the Mondego Case Study's reach. The dashed rectangles marked by the letters a, b and c designate the limits of the areas a, b and c of the study reach. The coordinate data corresponds to the PT-TM06/ETRS89 coordinate system.

Nonetheless, in certain parts of this study (referred in the corresponding text), in order to more clearly represent the evolution of morphodynamics, particular focus was put into analysing the models' output in a specific study segment of the reach which has been signalled (as part of previous studies) as being particularly active from a morphological point of view. This study segment constitutes the latter half of area b. The purpose of analysing this particular stretch of the river (which is located close to the middle of the study reach) is to avoid potential boundary effects from the numerical HM models which might affect the quality of the results. The study segment is delimited in Figure 25 (which represents an aerial map of area b of the study reach) and Figure 28b (showing the corresponding bathymetry). This study segment of the reach starts 1400 meters from the upstream boundary and is 900 meters long. By analysing a morphodynamically active middle area of the reach, it should be possible to obtain a clearer description of morphodynamics, given that it is mostly unaffected by boundary conditions (particularly for the purposes of the sensitivity analysis of fluvial morphodynamics).

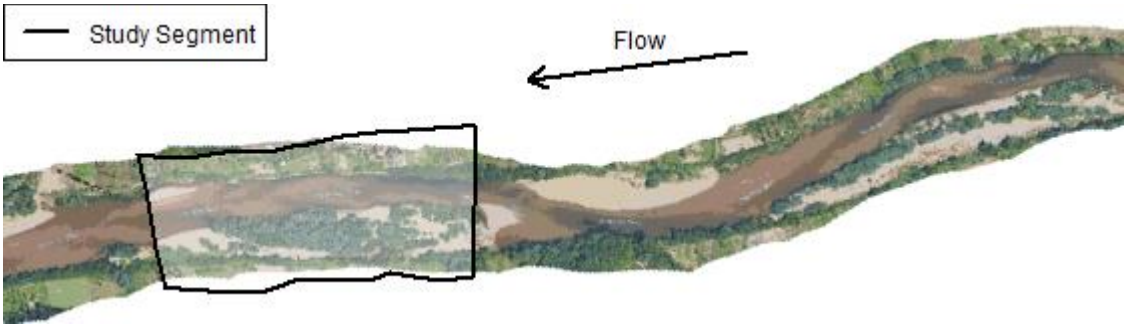

Figure 25 – Location of the Mondego Case Study's study segment, relative to the area b of the study reach.

The study segment was mostly relevant to the implementation of the sensitivity analysis, as it was observed to provide clearer results than by considering the entire study reach. Nonetheless, all of the simulations performed in the context of this research were based on the entire study reach as a whole, from the Palheiros levee to the Portela bridge. Accordingly, the statistical characterization of morphodynamics (carried out in section 7 of this Thesis) and the risk analysis application of the stochastic modelling of fluvial morphodynamics (carried out in section 8 of this Thesis) were also based on the simulations for the whole of the study reach.

4.1.2. Available Data

In order to fully represent the Mondego Case Study, data was used from multiple sources, namely:

- Bathymetric and topographic data (defined relative to the topographic zero) was obtained from a combination of topographic measurements using a total station and a sonar on a boat for bathymetric measurements (produced in the context of a partnership between the Faculty of Engineering of the University of Porto – FEUP and *Agência Portuguesa do Ambiente* – APA). This data was collected in 2016;
- *Energias de Portugal* (EDP) – Responsible for the management of the reservoirs upstream from the study reach, EDP provided data regarding the reservoirs' discharges on an hourly time scale for the period of January 2010 to May 2014.
- The granulometric data, along with the locations of the corresponding measurements, was taken from Volume 1 of the Phase 2 of the Sediment Extraction Plan for the Mondego and Vouga rivers (Instituto da Água, s.d.). This data was collected in 2012;
- Bed roughness was estimated based on the available literature and supported by in-situ observations and satellite photography of the study reach (taken from Google Maps).

The bathymetric and topographic measurements used in this study to represent the Mondego river's morphology are presented in Figure 26.

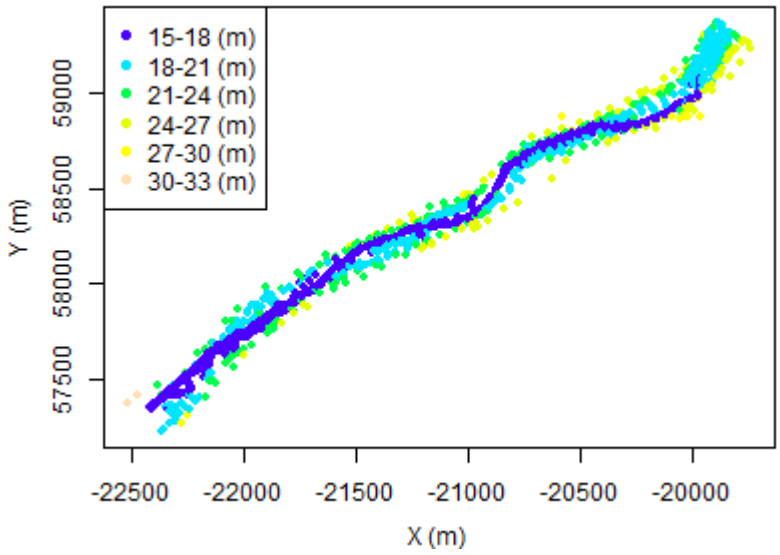

Figure 26 – Bathymetric and topography measurements obtained for the study reach of the Mondego Case Study. The coordinate data corresponds to the PT-TM06/ETRS89 coordinate system.

The corresponding longitudinal profile of the study reach (along with the longitudinal limits of the study segment) can be observed in Figure 27. Figure 28 presents an overlap of the corresponding topography/bathymetry and an aerial map for each of the areas of the reach. For ease of presentation, the plots in Figure 28 were rotated (by 25º). The bathymetric measurements (represented in Figure 26) were interpolated using a common interpolation technique (viz., the triangular interpolation (Renka, et al., 1984)) and then optimized via the pre-modelling approach described in section 5.3 of this Thesis (further details on this can be found in the corresponding section). The corrected bed level data was used as part of the initial conditions of all of the simulations in this study.

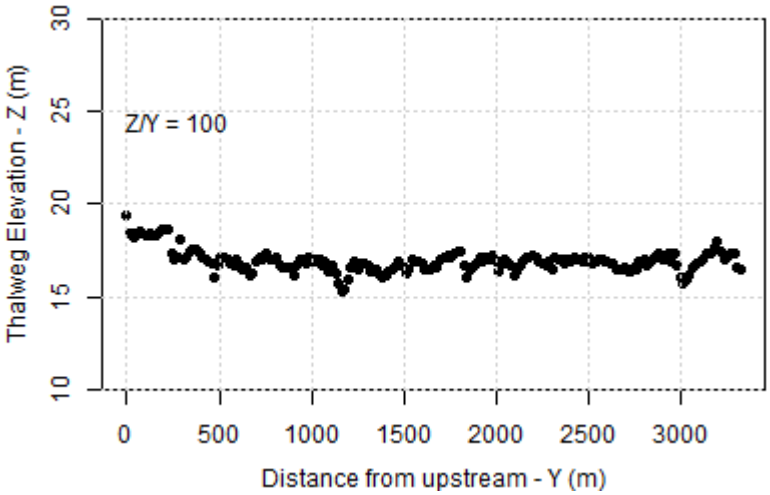

Figure 27 – Longitudinal profile of the Mondego Case Study river reach.

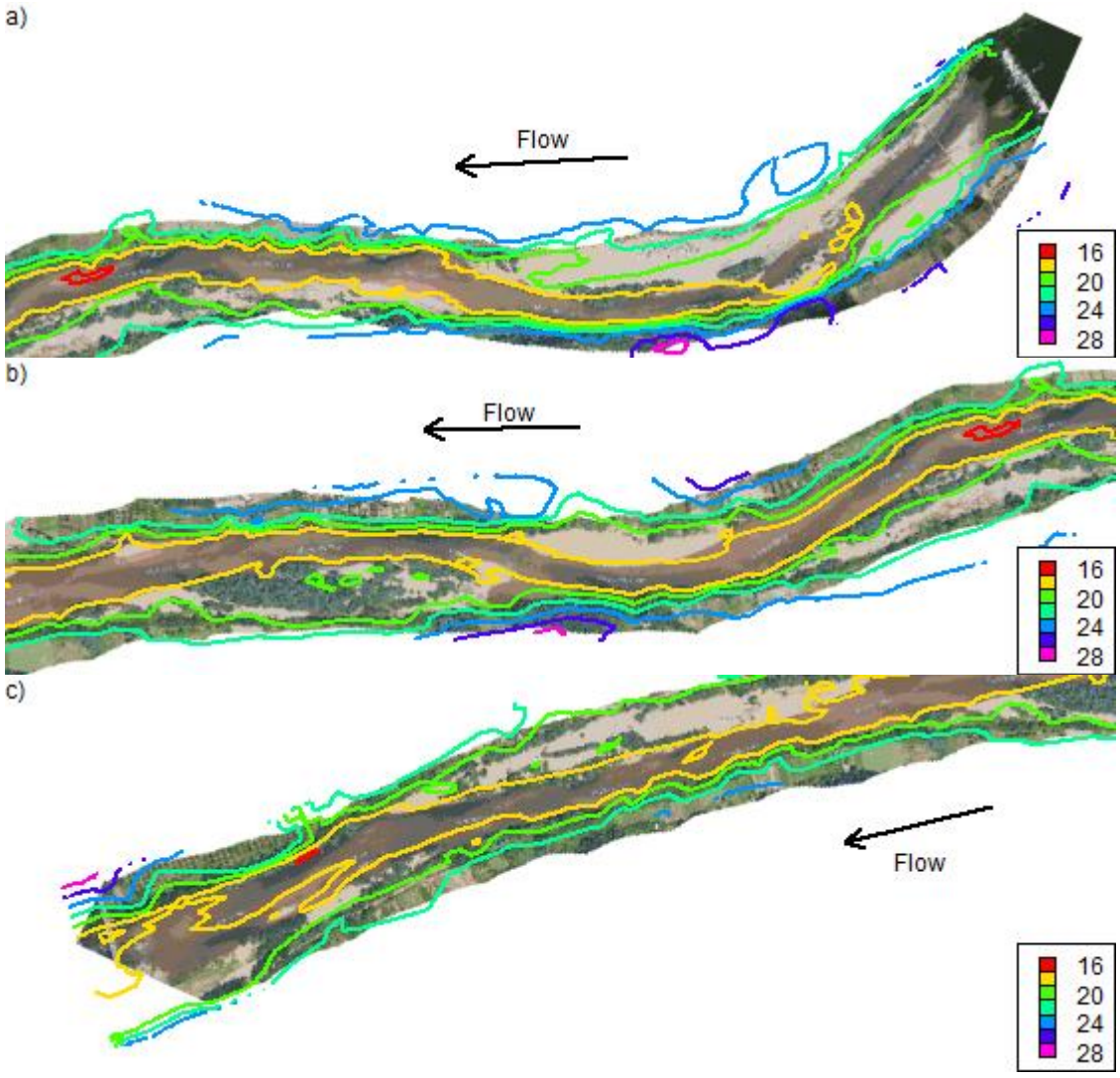

Figure 28 – Rotated overlap of aerial map of the Mondego Case Study's reach and representation (using color-coded lines) the elevation of the reach's channel bed (where the letters a, b and c coincide with the areas a, b and c of the study reach, delimited in Figure 24).

The data regarding the reservoirs' discharges provided by EDP was used to represent the streamflow series at the upstream boundary of the study reach. As a solution to speed-up the numerical HM simulations, only the wetter periods of each hydrological year were considered in the simulations. This choice was made under the assumption that this is the period of time where the vast majority of morphodynamical changes are known to occur, as has in fact been confirmed in other studies. (van Vuren, 2005). These periods generally centre on the months of January, February and March. The resulting streamflow series obtained from the historical data are graphically represented in Figure 29.

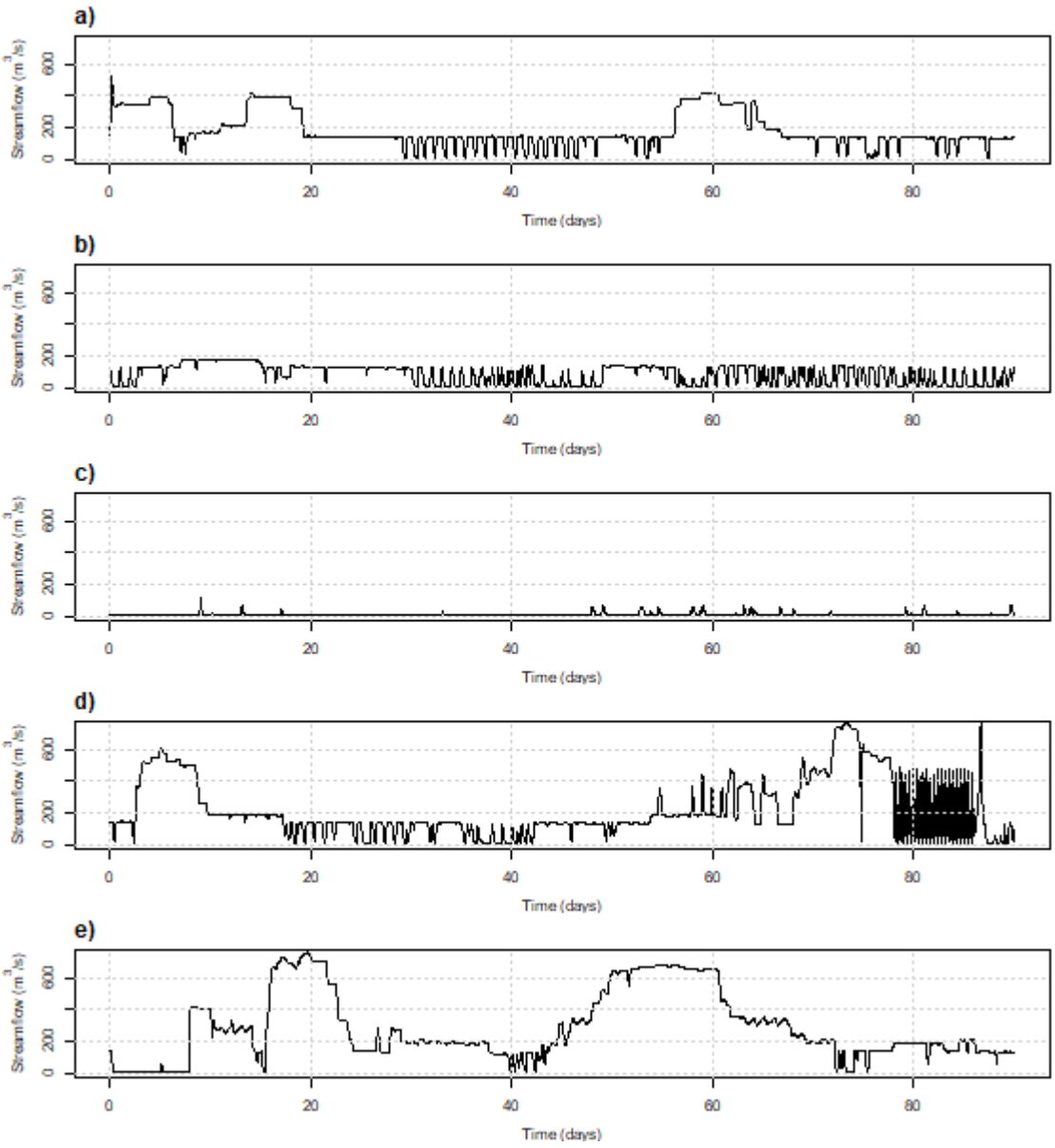

Figure 29 – Recorded streamflow series for the wettest 3 months in the hydrological years of 2010 to (and including) 2014, respectively corresponding to plots a) through e).

Values of streamflow magnitude range from virtually zero and 760 m^3/s at the hourly time scale. Yearly maximums range from values of 143 m^3/s to 760 m^3/s. From driest to wettest (defined proportionally to the mean annual streamflow), the order of the years is 2012, 2011, 2010, 2013, 2014.

The granulometric data corresponds to a series of granulometric measurements taken from several locations along the Mondego river (with one measurement taken at the downstream end of the study reach, referenced as P26 in the original report (Instituto da Água, s.d.), where the number 26 corresponds to the distance in kilometres to the Mondego river's mouth). From the eight granulometric curves available in the data, only the six curves measured nearest to the case study's study reach have been considered (with a maximum distance from the reach of approximately 20 km). Of the six selected curves, three are situated downstream from the reach and three are situated upstream from the reach.

The selection of the correct granulometric curves is important given that they will represent the range of granulometric variability to be considered in this study's numerical HM simulations. The two previously referred granulometric measurements were disqualified because they showed much more significant thinning and should therefore not be considered for representing the variability of granulometry in the study reach. Granulometry was represented as non-uniform (i.e., it is composed of different sizes of particles) curve identical for the entire reach.

Table 3 displays the median (D_{50}), the mean particle diameters (D_m), the classification (in accordance with the standards of the Unified Soil Classification System, the ASTM D 2487 (Howard, 1984)) and the location of the different granulometric curves considered for representing the variability space of granulometry. Included in Table 3 are also the Uniformity Coefficient (UC) and the Curvature Coefficient (CC), which are useful characteristics for understanding the variability of the granulometric curves. The corresponding granulometric curves are graphically represented in Figure 30.

Table 3 – Description of the measured granulometric curves and their respective characteristics.

Curve	D_{50} (mm)	D_m (mm)	UC	CC	Classification (ASTM D 2487-85)	Km	Location
P9	1.64	2.03	3.30	1.04	SP	20.41	Downstream
P20	5.56	7.83	8.26	0.77	SP	34.946	Downstream
P26	26.62	25.07	16.22	2.26	SW	43.322	Downstream Boundary
P30	2.74	3.27	3.95	0.95	SP	49.456	Upstream
P35	29.65	30.45	21.70	0.90	SP	55.726	Upstream
P42	20.56	22.11	94.27	10.69	SP	64.525	Upstream

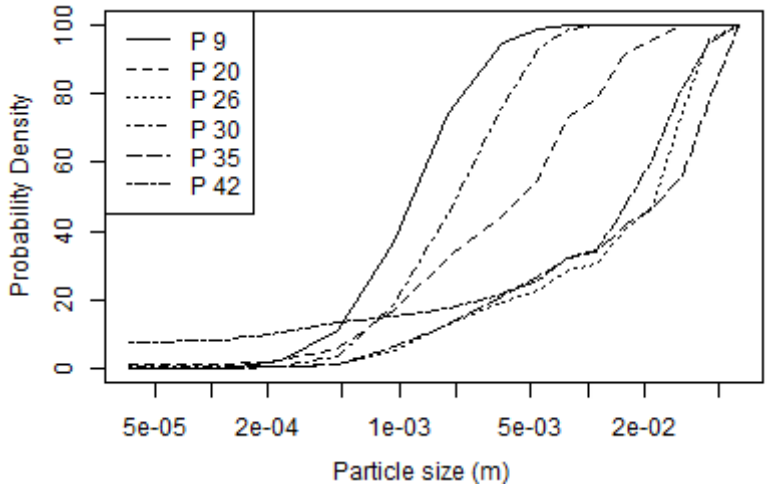

Figure 30 – Granulometric curves considered to represent the variability of granulometry for the HM simulations to be performed (detailed in Table 3).

Other options for defining granulometry, such as adopting a variability range around a single measured curve are generally worse in terms of the justification for the adopted values. The adopted approach is based solely on observed data, while such approaches would ordinarily require the arbitration of values, thereby reducing their significance.

As previously mentioned, the bed roughness values along the river bed were estimated based on the available literature (such as, (Schall, et al., 2008; Arcement & Schneider, 1984; Chow, 1959)) and supported by in-situ observations (of vegetation cover over the river banks and sediment particle size for the main channel) and satellite photography. Figure 31 displays the spatial distribution of the bed roughness magnitude along the study reach's channel bed. This same spatial variability was used in representing bed roughness for each individual grid node along the reach.

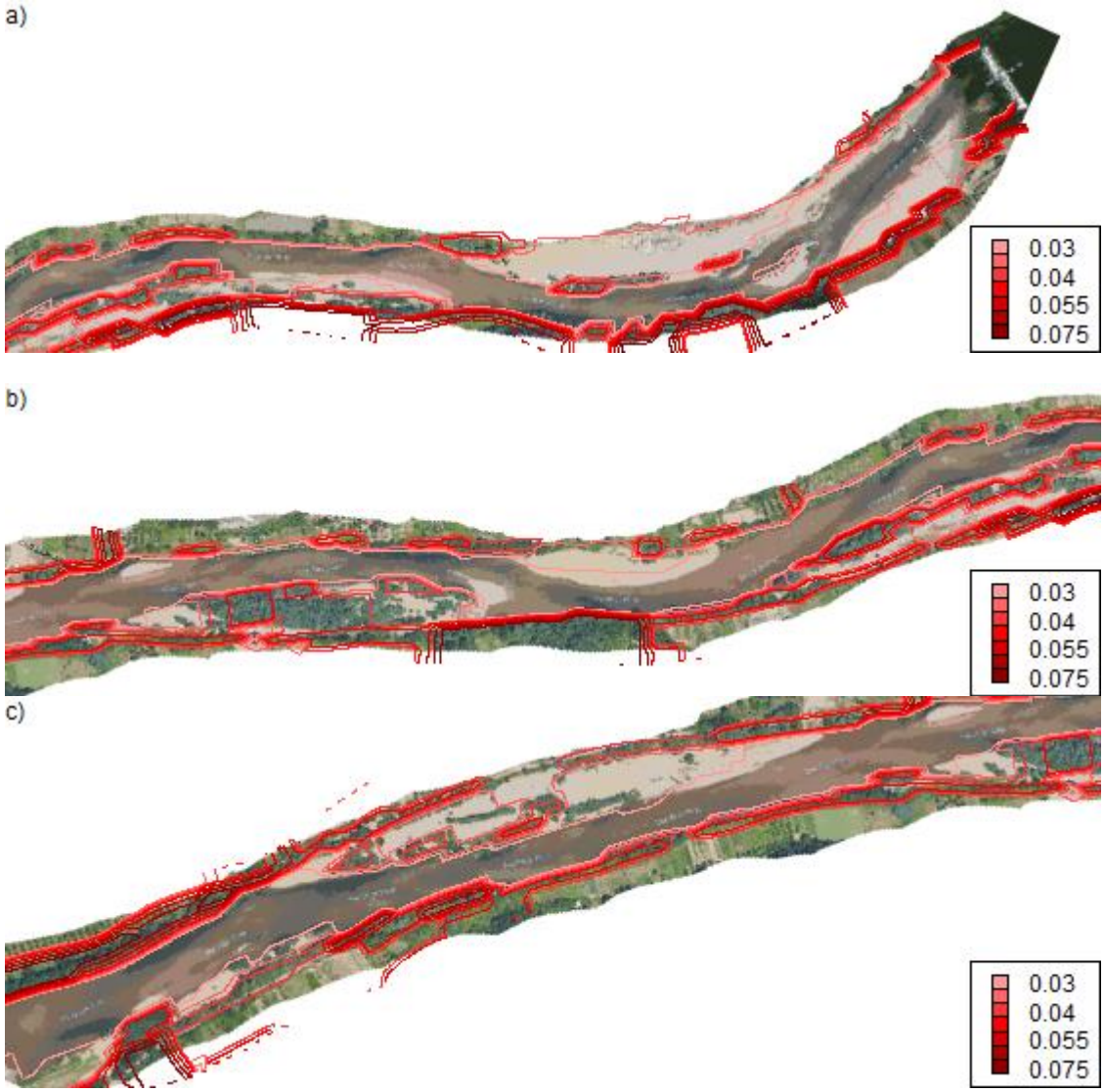

Figure 31 – Rotated graphical overlap of the aerial map of the study reach and the spatial distribution of bed roughness values along the river reach (where the letters a, b and c coincide with the areas a, b and c of the study reach, delimited in Figure 24).

The bed roughness values attributed to the channel bed range from 0.025 (for the river bed) to 0.075 (for the areas with densely packed shrubbery and trees), with various intermediate values for the dry areas as a proportion of the vegetation density.

Further information, particularly regarding the simulation parameters and the values adopted for the variables/parameters of the numerical HM models' variables for each simulation in this study, can be found in section 5.

4.2. STYLIZED CHANNEL

The present study analyzed the behavior and sensitivities of morphodynamics based on a stylized/simplified representation of the Mondego Case Study's channel, created using data from in-situ measurements and historical data. Using a simplified representation of this channel will help in producing clearer, straightforward and representative results of potential real river conditions.

The Stylized Case Study corresponds to a stylized straight, longitudinally-symmetric channel. The shape and other geometrical characteristics of the study channel were simplified and averaged in order to define the desired stylized channel. The resulting channel shape consists of a simplified cross section (defined in Figure 32), with an overall geometrical shape virtually identical to the river's mean cross section. A mean thalweg slope of 0.066% was adopted for the stylized channel, equal to the slope of the Mondego case study.

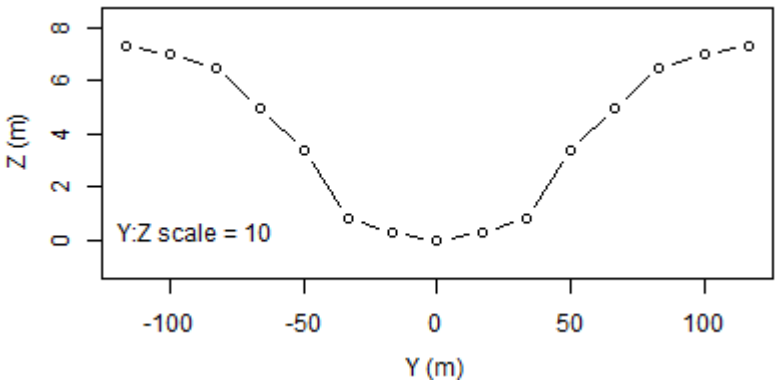

Figure 32 – Stylized channel cross section.

Similarly to the Mondego Case Study, the uncertainty in the D_{50}, n and Q variables was simulated, with the Q being represented by a simplified parameter Q^* (defined below). In addition, due the simplified nature of the channel (which considered a longitudinally uniform cross-section), the ΔQ_s variable (i.e., the uncertainty in the definition of the sediment input of the model) was also included in the uncertainty modelling of the Stylized Case Study.

As a matter of simplicity, both D_{50} and n were simulated as uniform/constant parameters along the entire channel within each simulation. Whilst, in real river situations, D_{50} (and particularly n) are rarely uniform, the representation of the effects of its complexity in a stylized channel could be, to some extent, unrealistic and therefore more appropriately estimated by adjusting the corresponding variability ranges.

The D_{50}'s variability range was based on the granulometric data for the Mondego river, presented in section 4.1.2. Based on the measured D_{50}, a range of 1.5 to 30 mm was adopted for the D_{50}'s variability range.

The values of n were estimated based on the available literature (Schall, et al., 2008; Arcement & Schneider, 1984; Chow, 1959) for the mean n values in a river channel. Given that the stylized channel is intended to represent a river channel, and that the large number of factors which define n in a river channel is so large (e.g., vegetation, granulometry, bed forms, slope, etc.), the channel's mean n was assumed to be independent of the grain size and to have values between 0.03 and 0.04, which are common reference values (in the literature) for a natural river channel. A uniform distribution was assumed for representing the PDF of n.

The streamflow data which was available consisted of the previously mentioned four and a half year long hourly streamflow series measured at the reservoirs upstream from the selected reach of the Mondego river and corrected for the channel's hysteresis. As the exact shape of flood events is very hard to qualify from this quantity of data, several different sets of characteristic hydrograph shapes were experimented with along with different definitions for the flood parameter which is intended to characterize flood intensity. Regarding the flood hydrograph, a standardized flood hydrograph, based on a Fréchet distribution for its shape, was adopted. The relative proportion of the stylized hydrograph's temporal and flow scale was adjusted to match that of the available data. The adopted reference flood event is of around 600 m3/s, which was observed (in the data presented in Figure 29), on average, for a duration of around 100 hours, to have a flow magnitude above 140 m3/s. The selected flood magnitude parameter corresponds to a scaling parameter for the simulated stylized hydrograph, identical to the maximum flow magnitude of the hydrograph. Each simulated hydrograph therefore corresponds to that standardized hydrograph (presented in Figure 33 for a unitary value of Q^*) multiplied by the Q^* parameter (in terms of its flow magnitude and temporal scale). The standardized hydrograph is intended to represent the overall conceptual shape of a real flood event while the Q^* parameter is intended to represent the corresponding flood event's intensity and is defined based on the flow's PDF, as estimated based on the recorded data.

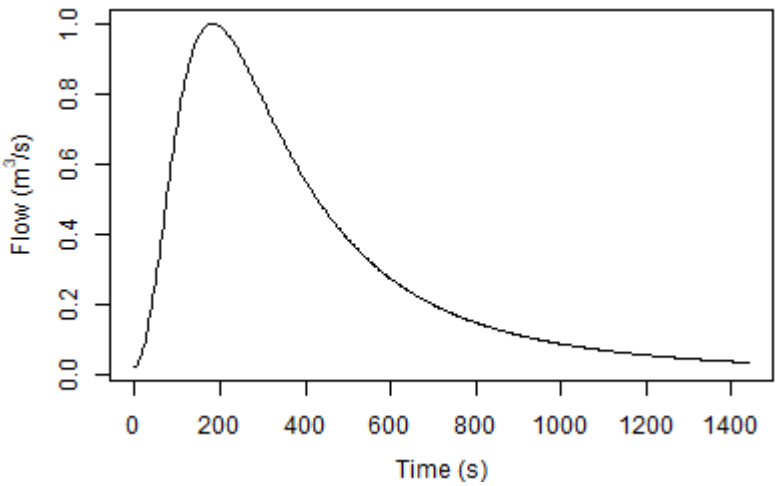

Figure 33 - Stylized hydrograph over time for a unitary value of the flood magnitude parameter Q^*.

Further information (particularly regarding the simulation parameters and the values adopted for the variables/parameters of the numerical HM models' variables for each simulation in this study) can be found in section 5.

5
SIMULATION OF FLUVIAL MORPHODYNAMICS

As mentioned in the Case Study Data section of this Thesis, two sets of data from two case studies were used in the development of this PhD study. These case studies are based on (1) field and historical data from the Mondego river (i.e., a real life situation) and (2) a simplified/stylized representation of a river channel (whose data is therefore estimated based on a simplification of the data from the Mondego river and the available literature).

The simulations (i.e., the HM modelling) performed as part of this study are intended to provide a statistical representation of the overall behaviour of fluvial morphodynamics (particularly for the Mondego Case Study). These simulations were based on the data presented in section 4 and were performed with the aid of the stochastic streamflow series generation methodology presented in section 3.

The process of simulating and representing the morphodynamical change of both case studies as a function of their respective hydrodynamics and the selected, morphodynamically-relevant variables was accomplished by applying the selected numerical HM model for the data presented in the previous section. For each application of the model, the geometrical data of the channel, along with sampled values of the different variables, was used to simulate the morphodynamical uncertainty resulting from these variables. The entire group of simulations jointly represents the uncertainty and the probability distribution of fluvial morphodynamical change, as a function of the different variables. Given their respective natures, there are however some disparities between the issues to be considered in the definition of each case study. The Mondego Case Study, given that it is based on observed/recorded data, has inherent complexities which are more difficult to represent, particularly for the intended applications of the simulations' results (viz., the sensitivity analysis, the statistical characterization of fluvial morphodynamics and a risk analysis application). The Stylized Case Study, on the other hand, given its conceptual nature, has a much simpler and complete definition. The different aspects, parameters and assumptions relating to the simulation of these case studies are detailed in the present section.

As was referred in the section 1.1, the simulations' setup and output was performed using an interface developed specifically for this study in the R language. The HM modelling itself was performed using the CCHE2D model, the CCHE_GUI 3.29 and the CCHE_MESH 3, all of which are available at the

website for the National Center for Computational Hydroscience and Engineering of the University of Mississippi (NCCHE, 2017). In both case studies, the Wu et al. formula (Wu, et al., 2000) was used to represent the flow's sediment transport capacity and the adaptation length for bed load (a parameter used in the CCHE2D model which corresponds to the distance along which the sediment transport is considered to be non-conservative) was set to the average grid length. The specific sediment gravity was set to 2.65 (relative to the water density).

Finally, an optimization approach for the numerical HM models, directed at improving the quality of the results of stochastic morphodynamical modelling and reducing its computational requirements, and developed in parallel with the numerical simulations and validated and applied based on the data and model of the Mondego river, is also presented and systematized in section 5.3.

5.1. MONDEGO RIVER CASE STUDY

The Mondego River was used as the main case study in this work. Its simulation provided a realistic representation of fluvial morphodynamics for the analyses envisioned as part of this PhD study. Nonetheless, the appropriate representation of fluvial morphodynamics, particularly in what regards the simulation of real life situations, requires a well-founded definition of the river's boundary and initial conditions (amongst other aspects). Accordingly, the (stochastic) simulation process involved (due to being based on the use of field/historical data) is significantly complex. This and other aspects are presented and systematized in the following sections of this Thesis. While stochastic modelling was already possible in the past, a corresponding methodology had yet to have been refined, particularly one which encompasses the issues and limitations which result from its application in a real fluvial environment. This section is meant to cover a lot of the main issues involved in this process.

Albeit some of the analysis later executed in this study (namely, the sensitivity analysis of morphodynamics) primarily focus on just a segment of the Mondego Case Study's reach (designated as the Study Segment), all of the simulations performed in the context of this study were based on and applied to the entire study reach.

5.1.1. MODEL SETUP

The study reach, previously represented in Figure 23, was simulated (using the numerical HM model CCHE2D) for multiple sets of values of the variables. Each simulation is intended to represent the morphodynamical change in the channel over the period of one year, for a given set of values of the streamflow (Q), bed roughness (n) and granulometry (D) variables. The modelling grid used to represent the terrain is reproduced in Figure 34. The modelling grid is a structured grid with a variable size (averaging 16.71 meters in the longitudinal direction and 9.68 meters in the transversal direction), composed of 200 nodes in the longitudinal direction and 20 nodes in the transversal direction for a total of 4000 grid nodes.

The bed level data along the grid was first obtained by directly interpolating (by way of linear triangular interpolation) from the bathymetric and topographic data obtained for the Mondego Case Study (graphically represented in the previous Figure 26). In a second step, the bed level data obtained by direct interpolation was corrected by applying the pre-modelling approach to numerical HM models systematized in section 5.3 of this Thesis. This approach essentially consists of simulating a warm-up period in the hydro-morphodynamic modelling. Topographical/Bathymetrical uncertainty has a large spatial variability which cannot be easily quantified As an alternative, this technique has helped in reducing the uncertainty in bed level data itself. The final bed level data along the modelling grid (obtained from interpolating the bathymetric and topographic measurements and corrected with the pre-modelling approach) was, therefore, deemed to be accurate for the purposes of uncertainty modelling.

The numerical HM modelling was performed using the CCHE2D's unsteady flow simulation, coupled with the mixing length model for turbulence closure. The Wu et al. formula (Wu, et al., 2000) was used to estimate the sediment transport capacity. The simulations' adopted time step (26 seconds) was estimated by experimenting with different values of it until reaching the most stable result in terms of morphodynamical change, i.e., using a time step significantly distant from that value was observed to result in the potential production of small numerical instabilities in the bed levels. The adopted time step is often larger than the time step provided by the CFL (Courant-Friedrichs-Lewy (Courant, et al., 1928)). However, given that CCHE2D is based on a implicit scheme for solving the RANS equations, this option was not deemed to significantly affect the work which has been developed.

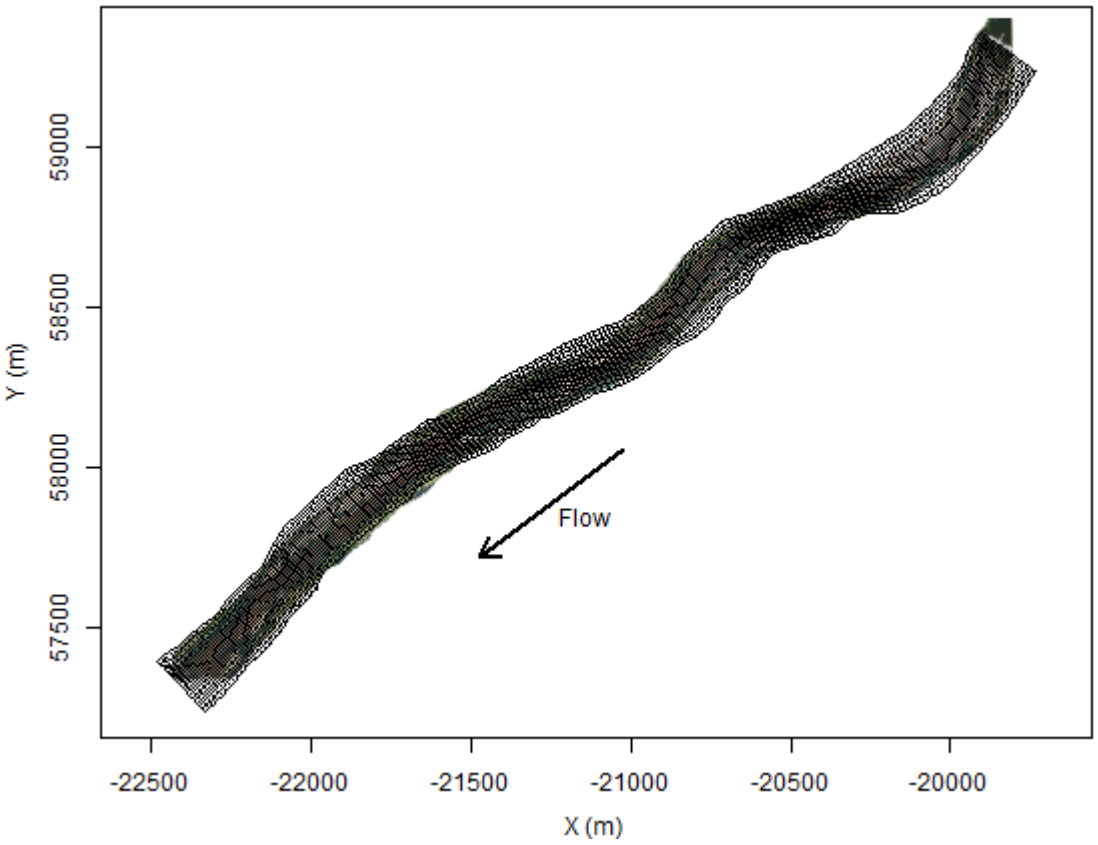

Figure 34 – Numerical modelling grid used to simulated the fluvial morphodynamics in the Mondego Case Study's study reach.

The boundary conditions for the numerical models are:

- On the upstream end: A streamflow time series, taken or generated from the historical records. As a solution to speed-up the simulations, only a period of three months was simulated at a time; this representative time span is intended to represent the wetter period of each hydrological year where the vast majority of morphodynamic changes are known to occur (Phillips & Sutherland, 1989). The definition of the streamflow series is described in section 5.1.2 of this Thesis.
- On the downstream end: A rating curve, estimated based on the assumption of uniform flow at the downstream boundary of the study reach (represented in Figure 35). The rating curve was obtained from the flow-to-water depth ratio provided by the Manning-Strickler equation (Eq. 6, where R is the hydraulic radius and i is the average longitudinal slope). A larger scale factor would produce larger changes in the downstream end of the reach (comparatively to the overall reach's dH) and vice-versa.

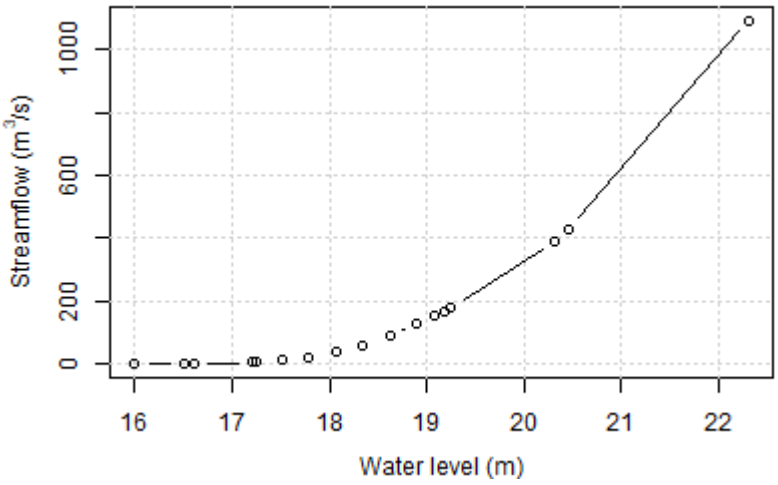

Figure 35 – Downstream boundary's rating curve for the Mondego Case Study.

$$Q_{downstream} = \frac{1}{n} \times A \times R^{2/3} \times \sqrt{i} \times f \qquad \text{Eq. 6}$$

Some consideration must be made in this case study regarding the definition of sediment input at the upstream boundary. Based on observations of the water in this area during flood events, sediment transport through suspended load was assumed, for the purposes of this study, to be null at this boundary. On the other hand, while some magnitude of bed load may be passing through the upstream boundary's levee under high or very high flow conditions, most of the time, bed load should not be capable of surpassing the levee. The definition of the bed load in these conditions is very hard to accomplish, as the levee has a very large effect on sediment transport, causing a significant (but hard to quantify) reduction in sediment transport. Without a long term measurement campaign (which was not performed in this instance), existing sediment transport laws are not applicable in this situation. The characterization of the uncertainty in sediment input is also, therefore, virtually impossible to define (as is in fact the case for most real case studies). In a long term analysis (e.g., for 5 to 10 years – or more), this (reduced) sediment input may have a significant effect on *dH*. However, for the relatively short (time-wise, in the context of fluvial morphodynamics and of the entire stretch of simulated river) simulations performed in this study (three months), the sediment input at the boundary was deemed to be immaterial and, for the purposes of the simulations, as null.

The initial conditions for all simulations were set at clear-water steady flow conditions with a streamflow magnitude of 10 m^3/s.

The simulations for this case study were based on the bathymetry data presented in Figure 28 and, for each simulation, the variables of *Q* (streamflow), *n* (bed roughness) and *D* (granulometry) were adjusted in order to represent their respective statistical variabilities. Amongst the many different possibilities, these variables were chosen to represent (by way of their statistical variabilities) the variability of morphodynamics because:

- They have been identified as being important for morphodynamic variability (as is stated in (Visconti, et al., 2010; van Vuren, 2005; Kasvi, et al., 2015));
- Their uncertainty pertains exclusively to fluvial morphodynamics itself (unlike, for example, the Shields parameter or the von Kárman coefficient which are numerical parameters of the theoretical models' representations of the mechanisms in real river sediment dynamics). While there is uncertainty in the definition of these types of variables in numerical model, there is not evidence that such variables are uncertain in real life. These types of variables were therefore excluded from the selection.

The variables selected to represent the natural uncertainty of fluvial morphodynamics (*Q*, *n* and *D*) were defined as follows:

- *Q* was defined as a time series of streamflow inputs at the upstream boundary of the study reach. The variability of *Q* was represented by using different time series (taken from the historical records or generated based on the historical records) for different simulations.
- *n* corresponds to the (non-uniform) spatial distribution of bed roughness along the study reach's channel bed. The variability of bed roughness was represented considering a uniformly distributed variability range around its mean values (represented in Figure 31). The variability range was adjusted as a function of the bed roughness value itself, being smaller for smaller values of *n*, peaking (in range) at 0.04 s/m$^{1/3}$ (where bed roughness is generally associated with vegetation and therefore the uncertainty is the highest) and becoming null for a bed roughness of 0.075 s/m$^{1/3}$ (deemed as the maximum potential value of *n*). This formulation of uncertainty works as a partial uncertainty, in the sense that the initial estimate of bed roughness is deemed to be reasonably accurate and the uncertainty is defined as change factors around this initial estimate. The adopted variability range (defined based on a general assessment of the potential values prescribed in the literature) is represented in Figure 36 (expressed as a function of bed roughness itself).

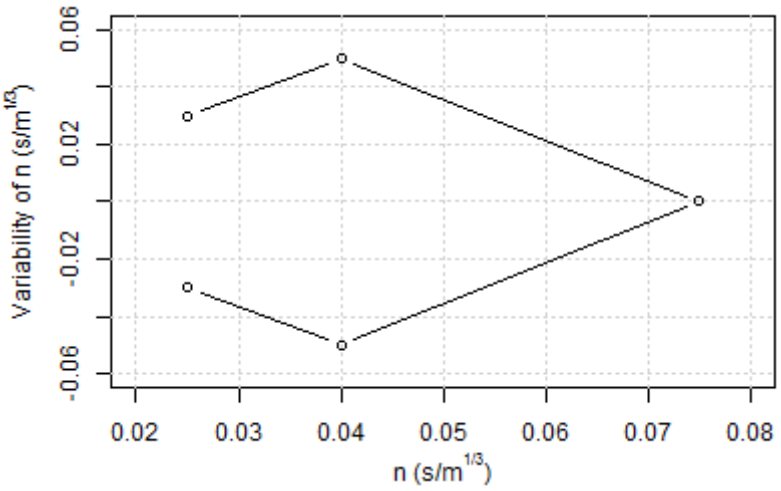

Figure 36 – Variability range of *n* as a function of its own value for the Mondego Case Study.

- *D* was simulated by adjusting the (non-uniform) granulometric curves which represent the channel bed's particles' sizes. Within each simulation, a single granulometric was used to represent the entire reach. The variability of *D* was represented by using different granulometric curves (taken from in-situ measurements or generated based on these measurements) for each simulation.

While, generally speaking, the magnitude of *n* is associated with the magnitude of *D*, their respective variability ranges were deemed as independent. This is because of the large, mostly non-*D*-related uncertainty which surrounds the values of bed roughness along a river channel. While the most commonly used quantile of *D* for representing granulometry is the median (D_{50}), other authors have also suggested the use of the quantiles 65 (D_{65} (Einstein, 1942)), 84 (D_{84} (Limerinos, 1970)), 90 (D_{90} (Meyer-Peter & Müller, 1948)) and 3.5 times the quantile 84 (supposedly equivalent to the quantile D_{99} (Hey, 1979)). Table 5 presents a comparison of the bed roughness values estimated using some of the different formulas in the literature. Looking at the *n* values for each of six available profiles, the selection of the empirical formula produces a level of uncertainty in the bed roughness values similar (if not larger) than the choice of granulometric curve. In simple terms, the variation of bed roughness with the choice of the empirical relation is more than twice the variation which results from the choice of the granulometric curve. In additions, other factors such as bed forms, the banks' vegetative cover (Ricardo, et al., 2013) (which is itself dependent on the seasons) and even the *Q*'s magnitude can affect bed roughness (Noordam, et al., 2006). For these reasons, the uncertainty surrounding bed roughness has been deemed as largely independent on the uncertainty surrounding granulometry.

While all of the variables considered in this study were deemed independent, dependent variables may be reasonably considered for uncertainty modelling. To do this, the generation/selection of the variables' representative values must, however, take into consideration this dependency. This is done by defining either a joint probability distribution for the variables involved or by defining the condition probability of one variable as a function of the other. As long as this dependency can be statistically represented, then the dependency itself can also be integrated into the stochastic modelling.

Table 4 – Comparison of the different bed roughness values (*n*, in s/m$^{1/3}$) estimated using different empirical relations.

(Reference)	Profile						
	P9	P20	P26	P30	P35	P42	Range of *n*
(Limerinos, 1970)	0.017	0.021	0.025	0.018	0.026	0.025	0.009
(Bray, 1979)	0.018	0.022	0.026	0.019	0.028	0.026	0.010
(Anderson, et al., 1970)	0.043	0.053	0.068	0.047	0.069	0.065	0.026
(Blodgett, 1986)	0.020	0.023	0.029	0.021	0.030	0.028	0.010
(Strickler, 1923)	0.051	0.063	0.082	0.056	0.083	0.078	0.032
(Meyer-Peter & Müller, 1948)	0.015	0.020	0.023	0.016	0.024	0.023	0.009
(Lane & Carlson, 1953)	0.017	0.022	0.027	0.019	0.029	0.027	0.012
(FHWA, 2000)	0.028	0.028	0.028	0.028	0.028	0.028	0.028
Range of *n*	0.036	0.043	0.059	0.040	0.059	0.055	---

Regarding this case study, no sediment input was considered as coming in from upstream. However, based on experiments, it was observed that this sediment input did not have any significant effect on the results of the simulations. This was observed by simulating different magnitudes of sediment input for different lengths of time. As a result, it was concluded that, within the one year simulations performed in this thesis, the maximums length of the reach affected by this variables was the first 150 meters of the reach.

In this study, based on the recorded median particle diameters (presented in Table 3) and on in-situ observations (which indicate a visible lack of suspended sediments in the water, even during the winter months), suspended sediment was considered to be virtually absent from the river. Concurrently, only bed load was simulated as part of the numerical modelling.

5.1.2. SIMULATION PROCESS

The stochastic simulation of fluvial morphodynamics, similarly to any MCS, can be generally described as the repeated simulation of fluvial morphodynamics for different sets of parameters'/variables' values, defined according to their respective variability ranges and probability distributions. However, the modelling of a river's morphodynamical behaviour requires the application of numerical HM models, which in turn require significant computational resources. In order to reduce the computational requirements in this study, some different solutions were considered when preparing the simulations, namely:

- The choice of numerical model (viz., CCHE2D is an implicit morphodynamics-centred numerical model, allowing for faster simulations of fluvial morphodynamics in comparison with many of the available programs);
- The use of parallel processing, i.e., the performed simulations were spread out over 24 Central Processing Units (CPUs);
- The use of a representative time span (three months) of streamflow series to represent the hydrodynamic forcings over a period of one year. Given that the vast majority of morphodynamical changes is known to occur during the wetter seasons of the year (van Vuren, 2005), these series were deemed to provide a good representation of the effects of the hydrodynamic forcings on morphodynamical change (despite not representing the entire year's seasonal hydrodynamic variability).

Finally, the correct definition of the numerical HM models is inextricably linked with the credibility of the corresponding study. Accordingly, given the spatially and temporally complex nature of the variables whose uncertainty is to be simulated (i.e., Q, D and n), the definition of the variables' representative values (which are to be simulated) needs to be correctly justified. In a real life situation, this can be a particularly complex process. An additional limitation can be found in the large computational requirements of numerical HM models, which do not allow for the application of crude MCS (were a very large number of model input values would be directly sampled and simulated).

Stochastic HM modelling therefore requires a careful selection of the variables' values which are to be simulated. In this study, a version of stratified sampling (Neyman, 1934) (where each variable is independently defined) was used to define the variables and the combinations of the variables' values which should be simulated in order to properly reflect their individual uncertainties in the morphodynamical uncertainty. In order to select the representative values of the variables, each variable had to undergo two stages of processing before the stochastic modelling itself. The sequence of the stages of the stochastic modelling of fluvial morphodynamics are as follows:

1. Direct Simulation (DS): In this first stage, the variables' relationship with fluvial morphodynamics is studied by individually (i.e., for one variable at a time) simulating the estimated, historical or recorded values of the variables using the numerical HM model. The objective of the DS stage is to determine whether these initial estimates of the variables' values provide (or not) a proper representation of the variability range induced in morphodynamics by the uncertainty of this variable. For each variable, if this relationship is strongly non-linear, or if there are significant gaps in the representation of morphodynamics (i.e., if there are large disparities between the values of dH for different consecutive values of the variable), this variable should continue to the second stage of this process. If, on the other hand, the relationship between a variable and morphodynamics is relatively simple (i.e., close to a linear relationship) and the evolution of dH as a function of that variable is fairly continuous, then only the application of the DS stage is required before the third stage of the selection process. This is because, generally speaking, it can be stated that an approximately linear relationship between two variables is indicative of a match between their respective quantiles. Accordingly, if this variable can be directly correlated with morphodynamics, then a suitable number of representative values (e.g., quantiles) can be directly sampled for that particular variable from the estimated, historical or recorded values in order to represent its' effect on morphodynamical uncertainty;
2. Complete Simulations (CS): The CS stage consist of, for the variables whose effect on morphodynamics could not be properly represented just based on the historical/recorded data, using an appropriate generation technique (i.e., in accordance with the variables' characteristics) and generating a large number of new, potential values of each variable. By simulating each of the variables' new values (independently from other variables), a new, more comprehensive and representative set of potential dH values is produced, clarifying the relationship between each variable and morphodynamics. The variables' values to be selected in this stage correspond to the values which produce representative values of dH (e.g., quantiles).
3. Final Simulations (FS): In this final stage, all of the potential combinations of the representative values of the different variables (selected in the previous two stages) are to be simulated. This stage essentially consists of the stochastic modelling of fluvial morphodynamics *per se*.

Considering the possibility of the existence of non-linearity of many (if not all) variables in relation to morphodynamics, the quantile sampling of the representative variables' values should be based on the

quantiles of the bed level change statistic and not on the quantiles of the variable's values themselves. In this manner, the selected values will properly represent the variables' range of potential effects on morphodynamics, as opposed to the range of its own potential values.

Given the complexity of both the nature of the variables involved and of the morphodynamics itself, the representation of the morphology and the selected variables for the purpose of analysing their respective relation requires the selection of suitable statistics. These statistics will be the reference point for defining the representative values of each values as it regards to their effects on *dH*. In this case, in order to select the variables' representative values, a set of four statistics should be determined for representing (1) *dH*, (2) *Q*, (3) *D* and (4) *n*. Starting at the DS stage, the relationship between the variables and morphodynamics should be analysed using different statistics for both (such as means, medians, standard deviations, etc.) in order to determine which particular statistic is more appropriate for them. Both correlation and error statistics, as well as graphical analysis can be used to assess the quality of the statistics. The criteria for selecting the optimal statistics is that they should provide a clear description of the relationship between the variables' magnitude/intensity and the magnitude of *dH*. The application of this criteria can be observed in sections 5.1.2.1 to 5.1.2.2 of this Thesis.

The use of the numerical HM models in this study was very extensive. Therefore, it required, for the purposes of facilitating the input and output of data, the creation of an interface with the CCHE2D model. Further details on this model regarding its basic mathematics, numerical techniques, hydraulics and sediment transport approaches can be found in the corresponding manual (Jia & Wang, 2001). This interface was constructed in the R language. The interface was responsible for creating the simulations' files (for all of the possible combinations of the variables' values) and for reading and compiling the data from all of the simulations, thereby minimizing human error and the use of the GUI of the CCHE2D model and speeding-up the stochastic modelling process.

Given the statistical nature of the simulations performed in this study, it should be noted that none of the simulations are significant in and of themselves but should instead be looked at as an element of a whole. The different simulations represent the different equally-probable potential evolution paths of bed level and therefore have no individual meaning and must be interpreted together.

5.1.2.1. Direct Simulations (DS)

In the DS stage, the simulations for each variable (i.e., *Q*, *D* or *n*) were based solely on the data available for that variable (which was presented in section 4.1.2). When simulating one of the variables, the remaining two variables are set to their (selected) intermediate values, namely, the 2010's streamflow series, the P20 profile for granulometry and the bed roughness was set to its mean value (i.e., without any variation from its original spatial distribution, represented in Figure 31). This corresponds to performing the following number of simulations for each variable (for a total of 17 simulations):

- Five simulations, one for each 3-month streamflow series available in the historical records (presented in Figure 29);

- Six simulations, one for each of the granulometric curves available in the historical records;
- Six simulations, one for each of the equally-spaced six quantiles of proportional bed roughness change. Taking advantage of the continuous definition of bed roughness, the simulated values of bed roughness can be directly sampled from the uniformly distributed uncertainty range defined in Figure 31. For the purposes of this study, six values of bed roughness (corresponding to the 0^{th}, 20^{th}, 40^{th}, 60^{th}, 80^{th} and 100^{th} percentiles) were considered in order to represent the corresponding uncertainty range.

As an example of the results obtained in the DS stage, Figure 37 represents the relationship between the variables' values and the corresponding mean absolute *dH* (obtained from the numerical HM model). In this example, the variables' values were represented by the maximum flow, mean granulometry and mean bed roughness statistics, respectively for the *Q*, the *D* and the *n* variables. Each point in Figure 37 represents one simulation from each of the previous referred three sets of simulations which took part in the DS stage.

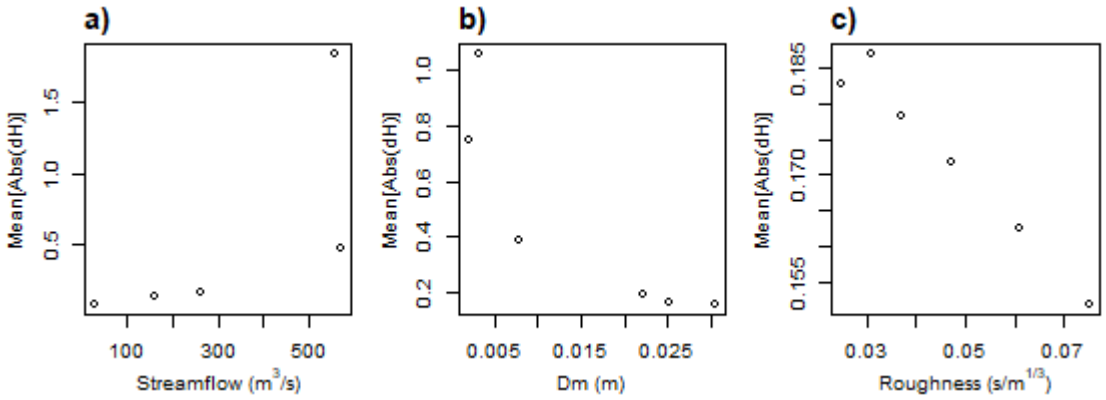

Figure 37 – Comparison between the different variables (*Q* in a, *D* in b and *n* in c) and their effect on the mean absolute *dH* in the channel.

As can be observed, while some semblance of a relation between morphodynamics and the different variables can be observed in Figure 37, there are significant inconsistencies in the results. In the cases of both *Q* and *D* the relationship with *dH* is clearly complex/non-linear. Given the discontinuous/discrete nature of the variables values, this behaviour was to be expected for the *Q* and *D*. In the case of *n*, while the variable appears to be linearly relatable with *dH*, there are again some inconsistencies in the behaviour of this relationship, as can be observed in the leftmost points of Figure 37c. Nonetheless, looking at the Empirical Cumulative Density Function (ECDF) of *dH* along the entire channel for the different values of bed roughness (represented in a logarithmic scale in Figure 38), the results indicate a clear increase in the absolute *dH* with a reduction in bed roughness. This behaviour can be seen in the regular/continuous change of colours for most of Figure 38. Taking this fact into consideration, there is a clear necessity for statistics better suited for the purpose of providing a clearer description of the relationship between the *dH* and the selected variables.

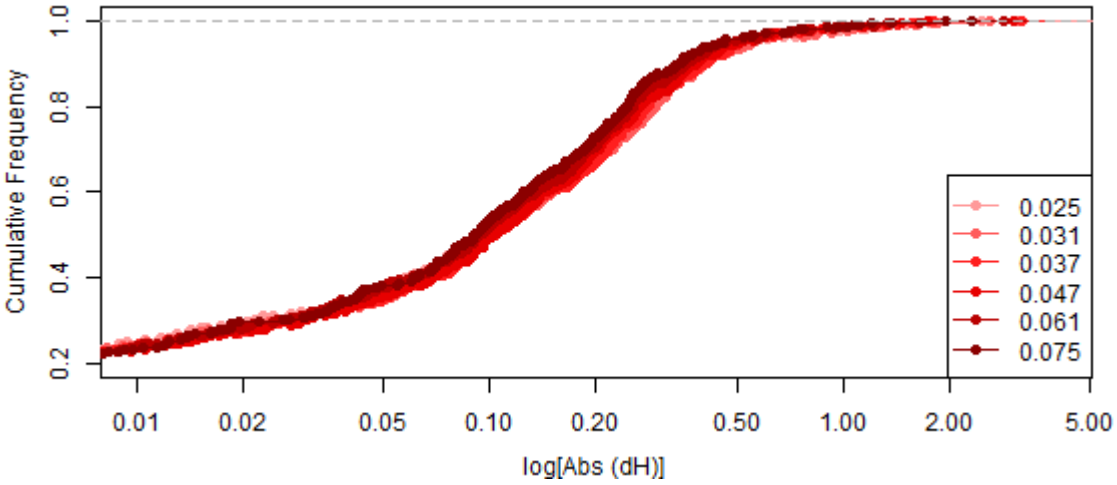

Figure 38 – ECDF of the absolute *dH* (in the logarithmic scale) for the simulations with different values of bed roughness.

Regarding the selection of suitable statistics, the overall behaviour of morphodynamics was studied based on three different statistics of *dH* for each simulation, namely the overall mean *dH*, the overall mean absolute *dH* and the *dH*'s PDF ranking. While the first two statistics are relatively well-known and self-explanatory, the last statistic was created based on the results of the observation of Figure 38, where the ECDFs were observed to provide a clear relation between the *dH* and the corresponding variable's values. The PDF ranking of a simulation consists of the most common/mode rank (in terms of absolute *dH*) for the corresponding simulations *dH*'s ECDF. Additionally, in order to represent the variables' values, a few different statistics were experimented with, namely:

- For *Q*: the maximum flow value in a series, the mean flow value in a series and a quantile-based location estimate (optimized, by trial and error, to be the difference between the series 25^{th} and 95^{th} quantiles);
- For *D*: the median, mean and standard deviation of the distribution of sediment grain sizes;
- For *n*: the mean and standard deviation of the bed roughness distribution along the channel.

By comparing the different combinations of statistics for *dH* and each of the different variables, the optimal combination of statistics was selected. The selected statistics should provide the best possible description of the relationship between morphodynamics and each of the variables. Mainly, these statistics should, as much as possible, demonstrate a correspondence between the hierarchical order of the *dH* for each simulation and the corresponding variables' values used. Accordingly, the statistics selected to represent the physical quantities of *dH*, *Q*, *D* and *n* were, respectively, the PDF rankings, the 25^{th} to 95^{th} quantile difference, the mean grain size and the mean bed roughness. Of the statistics analysed in this study, these statistics consistently provided the best description of the variables values, at least in terms of their relationship with *dH*. While, unlike the other statistics, the PDF ranking is a partially qualitative statistic (because of its discrete nature), it was observed to provide the clearest relationship between the variables and *dH*. Figure 39 presents a graphical comparison between the statistics which represent the different variables and the PDF rankings (which were used to represent the

corresponding simulation's *dH*). As can be observed, the relationship between morphodynamics and the different variables is significantly clearer using the selected statistics. Both *Q* and *D* display much less irregularity in their behaviour (despite their discrete/discontinuous nature of their values) and *n* shows an even clear relationship with *dH*.

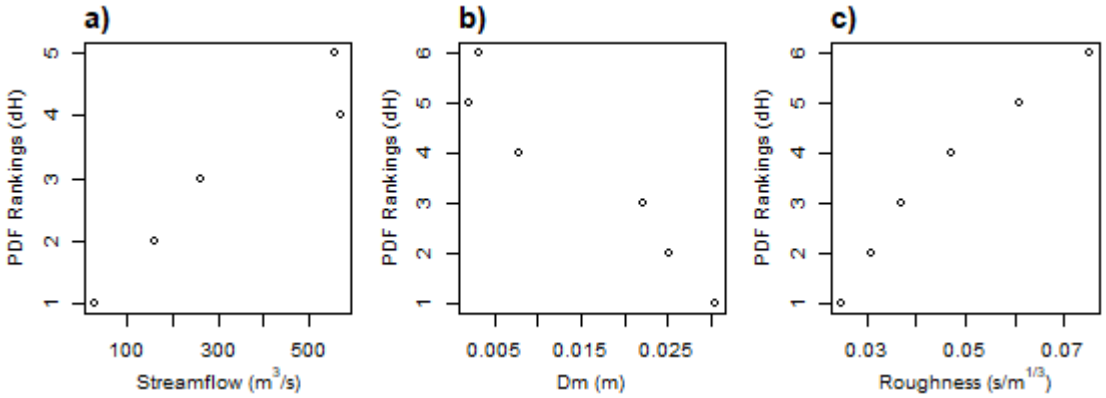

Figure 39 – Comparison between the different variables representative statistics and the *dH*'s PDF rankings.

According to the results of the DS stage, it can therefore be concluded that variations in bed roughness can be directly related to the corresponding change in *dH* (as there is an observable monotonic relationship between the two). Concurrently, the sampling of the quantiles of bed roughness is most likely sufficient to represent the effect of bed roughness on fluvial morphodynamics. This relatively simple and monotonic relationship between bed roughness and *dH* can be observed for both the selected statistics as well as for other statistics (as can be observed in Figure 37 and Figure 39). As a result, the quantile values of the bed roughness can be used to represent this variable's uncertainty (for the purposes of stochastic modelling) and can be directly applied in the FS stage.

However, the same cannot be said for the other two variables. The simulation of both the *Q*'s and the *D*'s effect on fluvial morphodynamics using the historical records was observed to produce a non-monotonic and non-linear relationship with *dH*. Additionally, the gaps/discontinuity between consecutive simulated values of *dH* for these two variables are irregular, indicating that, using historical records to represent the *Q*'s and the *D*'s variability is likely to result in a statistical misrepresentation of the corresponding variable's effect on morphology (this is particularly true in Figure 37a, where there is clearly a part of the potential *dH* variation which is not represented between the values of 0.5 and 1.8). Accordingly, these two variables should pass proceed to the CS stage.

As can be understood from the results of the DS stage, directly using historical records to represent a variable may not always be the best solution as it compromises the statistical representativeness of the variable's effect on morphodynamics. Additionally, its discontinuous nature will greatly complicate the interpretation of results, particularly in the context of sensitivity analysis (whose complexity grows in accordance with the complexity of the variables and relationships under analysis). The CS stage is meant to compensate for this discontinuous nature by generating and sampling the variables' representative

values from a larger selection of potential series/curves, providing a much clearer continuum of points relating *dH* and each variable from which to choose from.

5.1.2.2. Complete Simulations (CS)

In the CS stage, variables whose estimated, historical or recorded values were observed to not be sufficient to provide a continuous/detailed representation of those variables' effects on morphodynamics are treated in order to facilitate their application in the stochastic modelling of fluvial morphodynamics. This treatment process consists of, firstly, the generation of new values, series or curves for the variables (in accordance with the nature of the individual variables) and, secondly, the statistical analysis of the simulation's results. This statistical analysis is intended to both validate the choice of the variables' statistics (first selected in the DS stage) and to choose the best representative values for the variables for the implementation of the FS stage (i.e., the stochastic modelling of fluvial morphodynamics).

The concept behind the CS stage is that, by generating and simulating fluvial morphodynamics for a large number of potential values of a variable, the ensemble of the results will provide a better overall description of the effect of that variable's uncertainty on morphodynamics. More importantly, the large number of generated values has the potential to produce a much more continuous medium from which to sample the variables' representative values (in comparison with the historical records which have a highly discrete nature). This method of selecting the variables' representative values provides some assurance of the continuity of the relationship between these variables and fluvial morphodynamics. A significant effort was made to apply the most suitable generation tools for reproducing the historical/observed nature of the selected variables.

For bounded variables, as long as a suitable generation technique is applied, the generated values can be assumed to fully represent the range of potential values of those variables. For unbounded variables, specific quantiles of the generated series can be utilized to represent that variable in the stochastic modelling of fluvial morphodynamics. By using this approach to provide an estimate of the potential range of *dH* produced by the generated values of the variables, it is possible to sample the variables' values according to the quantiles of *dH*. Accordingly, obtaining this continuum of values is the main objective of this stage because they can provide a description of the probability distribution of the variables' effects on fluvial morphodynamics. This effect is produced by way of the hierarchical classification of each variable's value's effect on morphodynamics. The values sampled based on the *dH*'s quantiles provide a complete statistical representation the variables' effects for the purpose of the stochastic modelling of fluvial morphodynamics.

For the purposes of this study, the data available from the historical records was assumed to provide a good description of both the *Q*'s and the *D*'s overall probability distribution, specifically when supported by the application of a suitable series/curve generation technique.

In order to produce new values of a variable, it is very important to understand the nature of that variable. Specifically regarding *Q*, its characteristics and potential generation techniques have already been

thoroughly systematized and presented in section 3 of this Thesis. The methodology proposed in this section was used in order to produce new streamflow series for the CS stage, taking into consideration the statistical characteristics of the available data. The joint PDF of the streamflow's behaviour (which is the main tool of the proposed methodology) was represented using a combination of a Markov Chain model (to represent the different stages of flow discharge from the reservoirs) and of different conditional PDFs to generate streamflow series based on the available data for the Mondego Case Study.

For reference purposes, Markov Chain models consist of models for generating the different states which compose a series (Gilks, et al., 1995). In this particular instance, the different states correspond to different levels of discharge from the dams. For example, one state corresponds to only the ecological flow being discharged, while another state may correspond to the discharge from one of the turbines and another to the discharge of two turbines. By analysing the data, a set of five different states (and the behaviour of streamflow in each state) were defined and characterized. Table 5 displays the Markov Chain model's states and the corresponding conditional PDFs used to generate the new streamflow series. The mean value and upper and lower threshold are characteristics of the selected generation process. The Markov Chain model is itself applied by, starting from a randomly generated state (from the data), randomly sampling the next state based on the empirical transition probabilities between the previous and the next state (estimated from the data). Table 6 presents the corresponding transition probabilities of the adopted 5-state Markov Chain model. These elements were derived based on the data from the 3-month long wettest periods of each year of data (based on the considerations made in section 4.1.2).

Table 5 – Markov Chain model's states and transition probabilities used to describe the Mondego Case Study's streamflow series.

State	Mean Value (m^3/s)	Lower Threshold (m^3/s)	Upper Threshold (m^3/s)	Generation Process
1	10	-	-	Fixed value
2	-	10	60	Shot noise model
3	140	-	-	Oscillating around mean
4	190	-	-	Oscillating around mean
5	-	225	-	Conditional joint PDF based on the data

Table 6 – Adopted Markov Chain model's state transition probabilities.

State (to\from)	1	2	3	4	5
1	0	0.907	0.009	0.009	0.075
2	0.369	0	0.578	0.01	0.042
3	0.005	0.874	0	0.105	0.016
4	0	0.104	0.458	0	0.438
5	0	0.409	0.045	0.545	0

A total of 50 *streamflow* series were generated which, in addition to the 5 historical series, were simulated in order to represent the relationship between *Q* and *dH* for the CS stage. Figure 40 presents some random examples of streamflow series generated using the methodology proposed in section 3 of this Thesis, based on the available data for the Mondego Case Study.

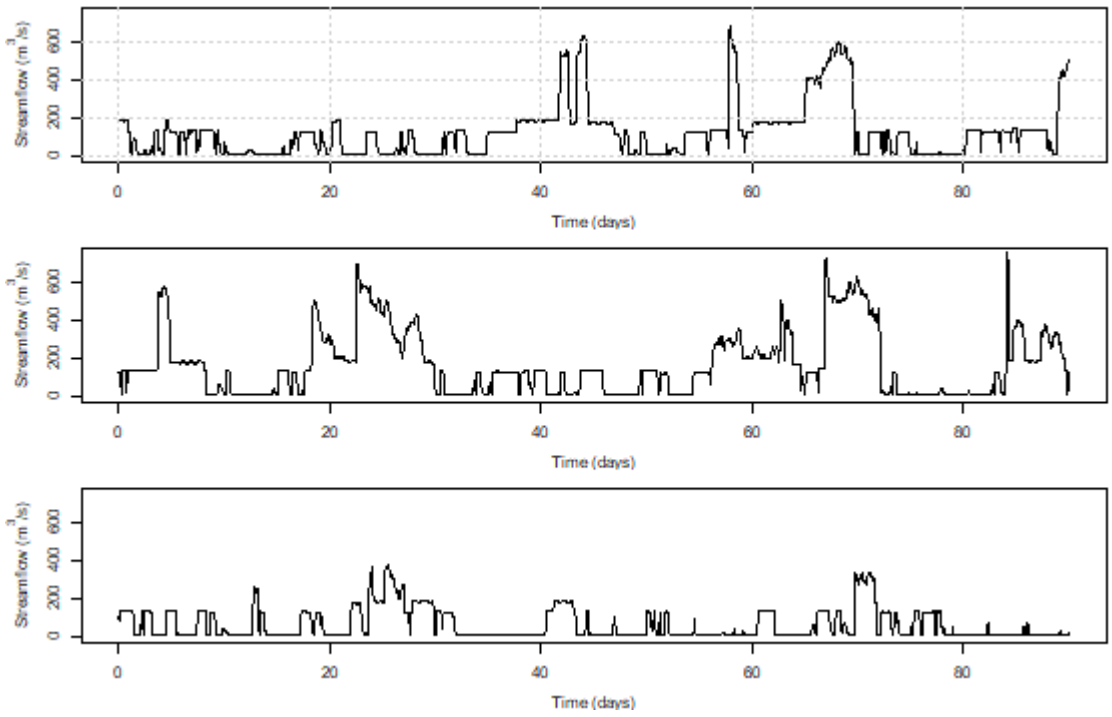

Figure 40 – Examples of the streamflow series generated for the CS stage using the methodology proposed in section 3.

Regarding the granulometry as a variable, the generation technique applied largely consisted of assuming the variable's overall variability to be bounded by the variability range provided by historical data, with each of the recorded granulometric curves being equally probable (in accordance with the maximum entropy principle). Under the assumption that the recorded granulometric curves properly represent the empirical PDF of the river's granulometry, the corresponding generation process consisted of a weighted mean (i.e., a linear combination) between these recorded curves. This weighted mean was applied to every combination possible of two granulometric curves (out of the six on record) with weights of 1/3 and 2/3, generating 30 new potential granulometric curves from the linear combination of the different recorded curves. While a simple mean between granulometric curves could also be a potential solution to produce new potential curves, this approach was observed to over-smooth the generated curves' shape. The [1/3; 2/3] weights allow for the linear combination technique to generate more granulometric curves while maintaining more of the curves' characteristics and respecting the likely empirical PDF of granulometry (as represented by historical data). For the purposes of the CS stage, both the historical and the generated granulometric curves were simulated in order to represent the relationship between the granulometry as a variable and fluvial morphodynamics. Figure 41 presents all of the granulometric curves simulated during the CS stage.

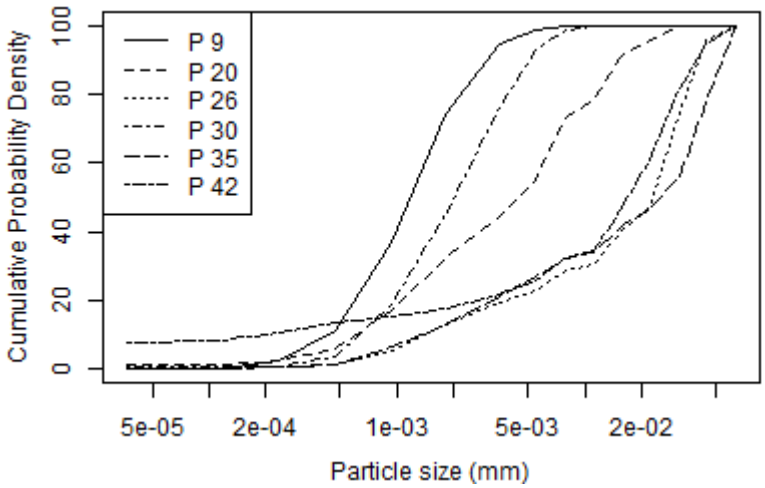

Figure 41 – Granulometric curves simulated in the CS stage (including both the curves generated from the observed data and the observed granulometric curves themselves).

In accordance with the generation process described, two sets of simulations were performed in the CS stage, namely:

- 55 simulations for each of the historical and generated streamflow series (5 historical + 50 generated series);
- 36 simulations for each of the historical and generated granulometric curves (6 historical + 30 generated series);

Finally, the statistics representative of *dH* and of the two variables under analysis (first determined in the DS stage) were reassessed in the CS stage. This choice of statistics remains very important because it is the means by which the relationship between these variables and morphodynamics is represented. Accordingly, these statistics determine the hierarchy of the simulated values (in terms of their effects on *dH*) and, consequently, the representative values of each variable (for the purpose of the stochastic modelling of fluvial morphodynamics).

Figure 42a and Figure 42b compare the PDF rankings (determined to be the best statistic for *dH* in the DS stage – section 5.1.2.1) with the rankings of the mean relative and absolute *dH* for the *Q* and *D* variables, respectively, where each point representing one application of the numerical HM models. As can be observed, the rankings of the different statistics produce relatively similar results regarding the classification of the simulations' hierarchy (as can be observed by the concentration of points around the 45°/optimal fit line). Concomitantly, as a matter of consistency, the PDF rankings were once again adopted to represent the value of each simulation's overall *dH*.

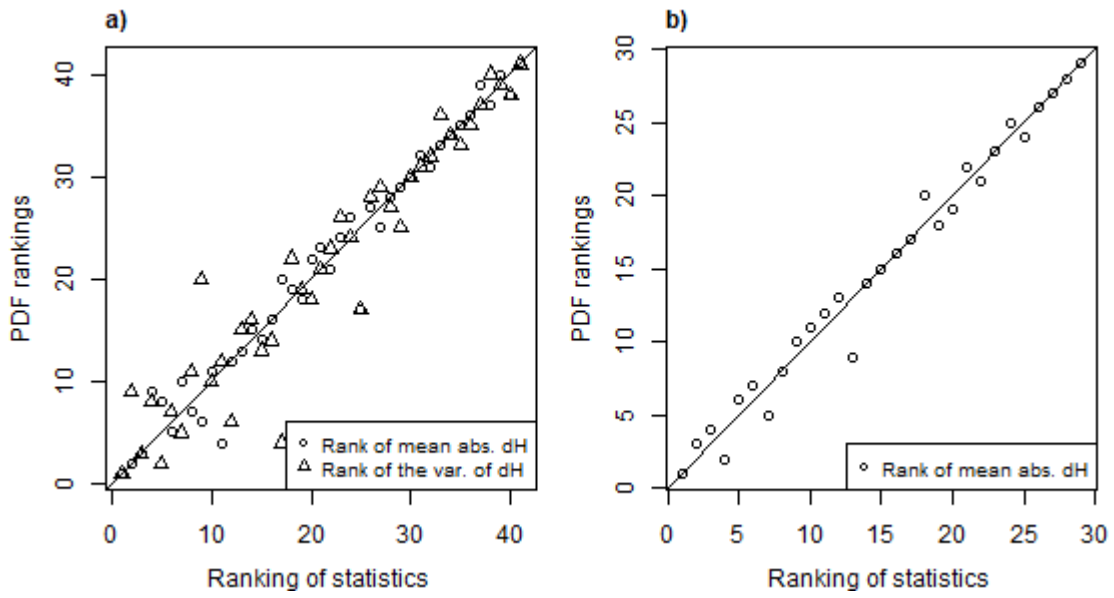

Figure 42 – Comparison of the different statistics in terms of their rankings for the two sets of simulations performed in the CS stage, namely for a) the generated streamflow series and b) the granulometric curves.

Regarding the representation of the two variables in question, the statistics derived in the DS stage were again observed to produce the best results. The 25th to 95th quantile difference and the mean grain size, respectively for the *Q* and the *D* variables, were observed to produce the clearest relationship with the PDF rankings. Figure 43a and Figure 43b provide a visual comparison between the PDF rankings and the two statistics representative of the two variables under analysis. As can be observed, while some uncertainty in the relationship between the variables and *dH* is present, overall, there is a visible trend in both of these relationships. Relatively speaking, the relationship of *dH* with *Q* is more uncertain and irregular then that of *D*. Nonetheless, as was the intention of this CS stage, there is a clear continuum in the relationship of these variables with *dH*, allowing for an appropriate sampling of the *dH*'s quantiles.

In similarity with the bed roughness variable, for the purposes of the stochastic modelling of fluvial morphodynamics, a total of six series/curves for each variable was used to represent them. This number of representative variables values/series/curves was assumed to provide a good middle ground between correctly representing the effects of the variables' uncertainty (which improves with the number of representative values) and the computational requirements of numerical HM modelling (which increase geometrically with the number of values used to represent the variables). While this choice can affect the quality of the results of the stochastic modelling, if the process of defining the variables' representative values (which was the purpose of the DS and CS stages) is well defined, the representation of a variables' effects on morphodynamics should not require a larger number of values. The previous application of the DS and CS stages is sufficient to guarantee (from a statistical standpoint) that the range of *dH* produced by each variable is well represented. In order to fully represent the variable's range of effects on *dH*, the sampled values of the variables should generally correspond to equally spaced quantiles of the *dH* simulated in this stage. Figure 43 represents (in the form of black dots) the two variables' statistics regarding each of the six selected representative values. The selected values

were chosen because they describe a continuous relationship between the variables and provide a complete representation of the *dH* variability (i.e., very close to its 0^{th}, 20^{th}, 40^{th}, 60^{th}, 80^{th} and 100^{th} quantiles).

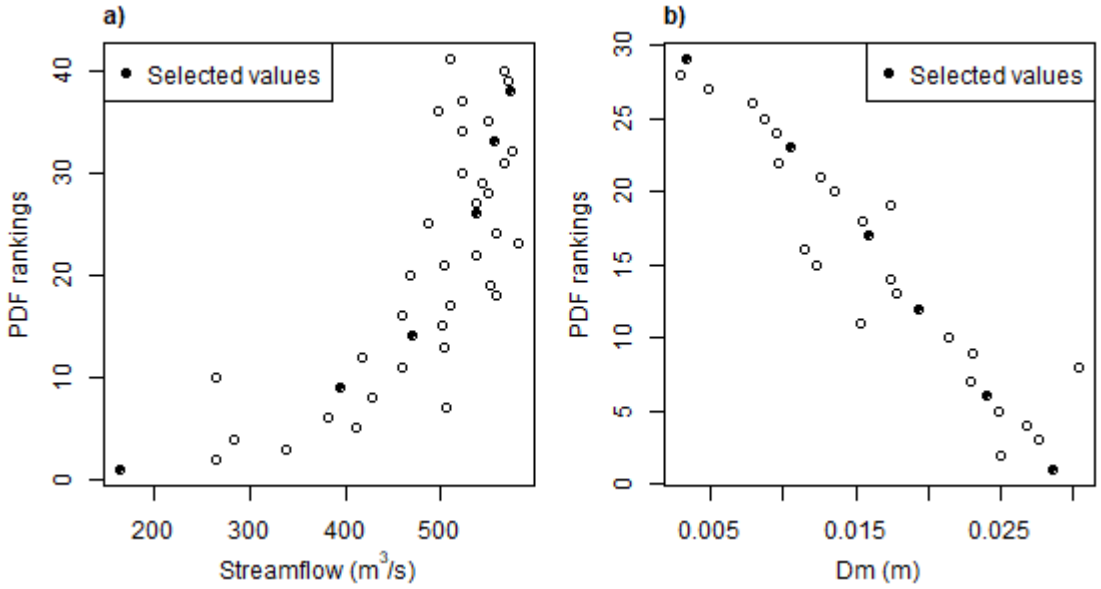

Figure 43 – Comparison of the simulated statistics regarding *dH*'s and the two variables for each set of simulations performed in the CS stage, namely for a) the generated streamflow series and b) the granulometric curves. The black dots in the plots represent the variables' values selected to represent those same values in future stochastic simulations.

Figure 44 and Figure 45 present, respectively, the six streamflow series and the six granulometric curves selected based on the corresponding simulations performed in the CS stage. These two sets of six series/curves, along with the six values of bed roughness (chosen in the DS stage) were used to represent the effects of the variables' uncertainty in the stochastic modelling of fluvial morphodynamics.

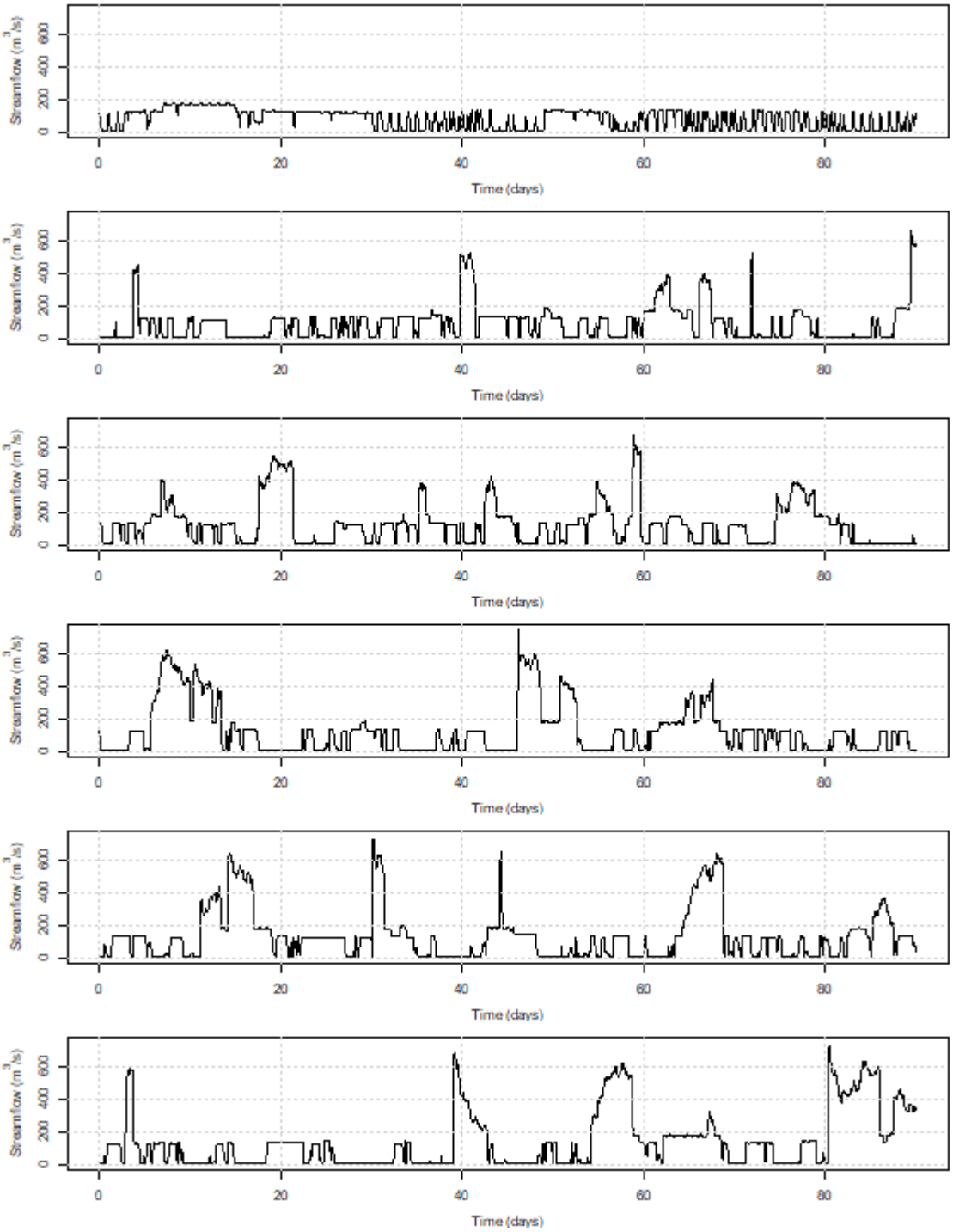

Figure 44 – Streamflow series selected from the set of historical and generated series, in accordance with the corresponding simulations' *dH*'s rankings.

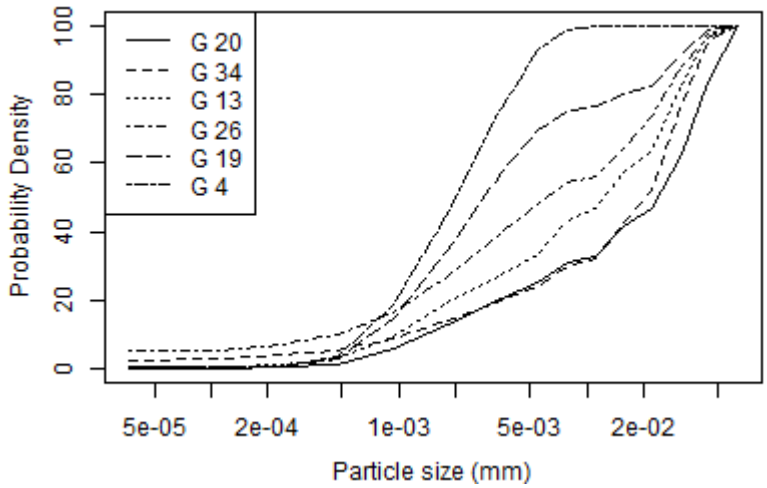

Figure 45 – Granulometric curves selected from the set of historical and generated curves, in accordance with the corresponding simulations' *dH*'s rankings.

5.1.2.3. Final Simulations (FS)

The FS stage conceptually corresponds to the stochastic modelling of fluvial morphodynamics. In this stage, every combination of the three variables' (i.e., *Q*, *D* and *n*) representative values (selected in the previous DS and CS stages) was simulated with the CCHE2D model so as to represent the effect of the variables' uncertainty on fluvial morphodynamics in the Mondego Case Study.

The total number of simulations performed was 216 (equal to six times six times six). While other combinations of the variables representative values may have been more efficient, in this case, this option was necessary to guarantee a full representation of the uncertainty involved. In fact, based on this large number of simulations, it was possible, in chapter 7, to evaluate other, less extensive combinations of the variables values.

The setup of these simulations was performed using the R interface developed for the CCHE2D model. Figure 46 displays an aerial map of the entire study area (divided into areas a, b and c) simulated with the numerical HM models, along with the mean simulated bed level (over all of the simulations), along the study reach. Figure 47 also displays the mean and the standard deviation of the *dH* along the specific study segment of the Mondego Case Study. Overall, the results indicate a strong tendency of the entire study reach's behaviour to lean towards an increase in sedimentation. The global maximums and minimums of *dH* (respectively, the maximum sedimentation and the maximum erosion) in the channel throughout all of the simulations were of 5.99 meters and -5.06 meters. These results are in accordance with other studies on the behaviour of the Mondego river in this area (Rocha & Freitas, 1998; ARH Centro, 2011).

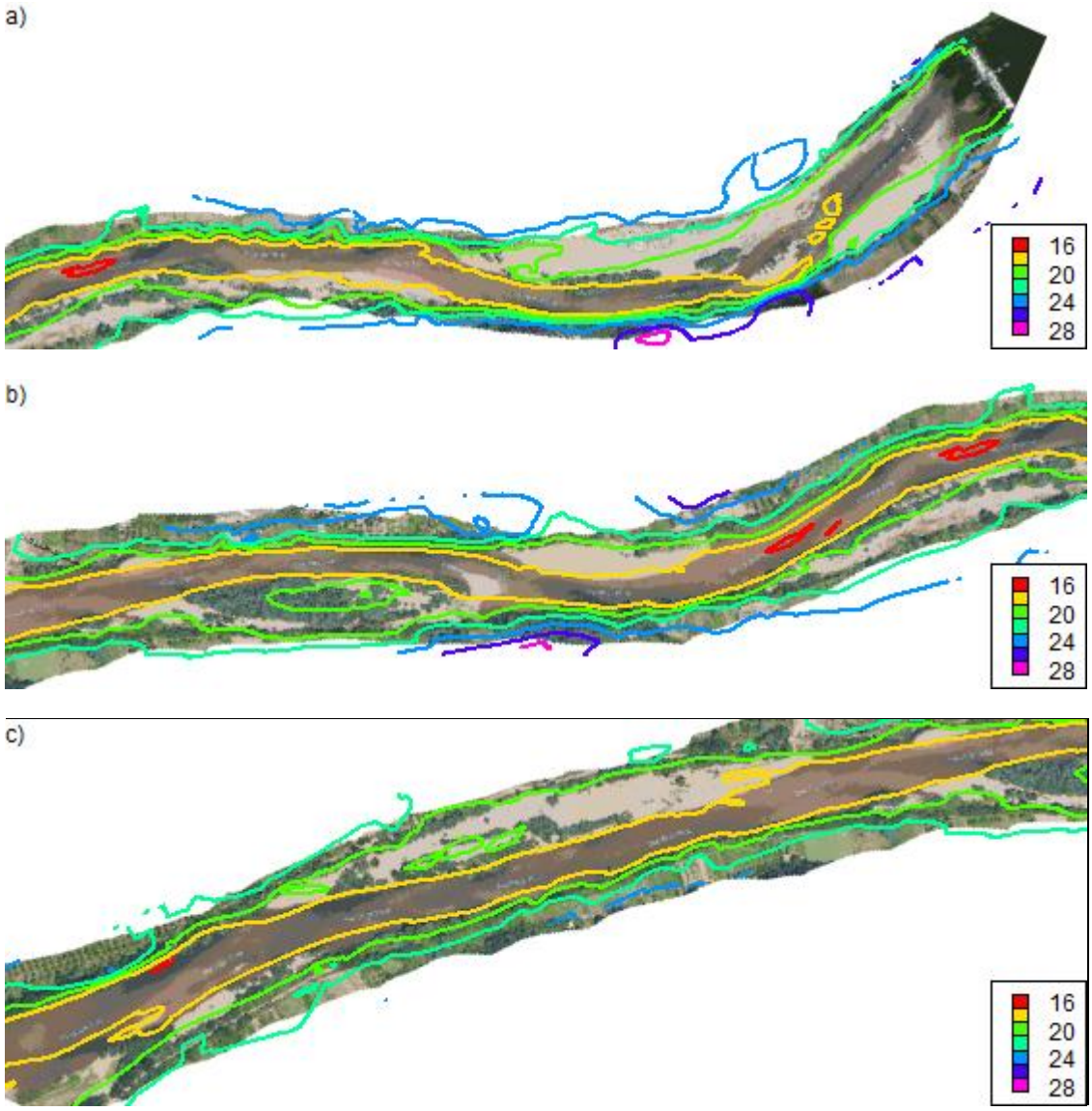

Figure 46 – Rotated graphical overlap of an aerial map of the study reach and the simulated mean *dH* in the study segment of the Mondego river for the three areas of the reach, respectively.

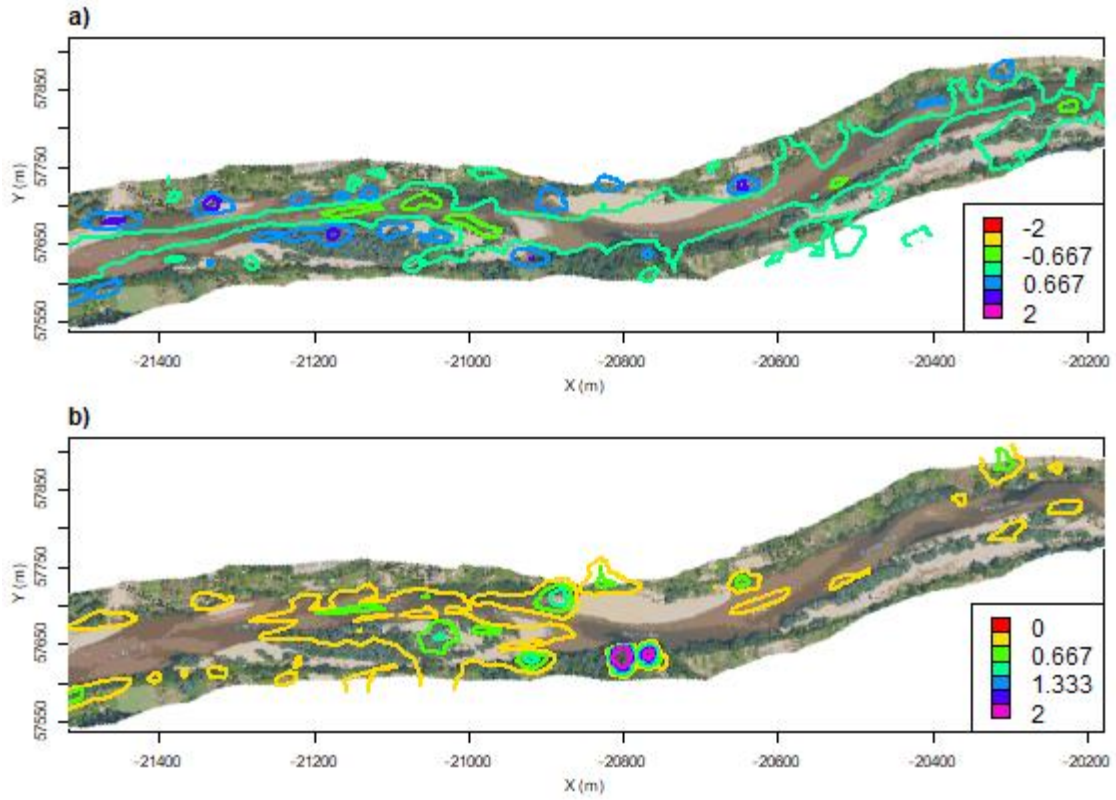

Figure 47 – Rotated graphical overlap of aerial map of the study segment and the mean (in plot a) and the standard deviation (in plot b) of the simulated *dH* (over all of the simulations).

As referred in section 5.1.1, the choice of the variables representative values was based on a number of representative quantiles of the *dH* variability produced by each variable (i.e., its 0th, 20th, 40th, 60th, 80th and 100th quantiles). These quantiles-based values are not representative of portions of the *dH*'s PDF but representative of the corresponding quantiles. This choice is particularly appropriate for the purposes of sensitivity and extreme analysis, as it portraits the PDF up to its extreme values. However, for the purposes of probabilistic and risk analyses (where individual simulations represent independent samples of the morphodynamical change), this choice results in an over-representation of the variables' extreme values. However, as some level of uncertainty in the definition of the range of the variables' probability distribution is admissible and one of the variables (*Q*) is only semi-bounded, this choice of representative values was also used for the probabilistic and risk analyses performed in this study. At the same time, this choice allows one to avoid duplicating the amount of simulations to be performed. The alternative would be to also simulate (i.e., apart from the 0th, 20th, 40th, 60th, 80th and 100th quantiles) the 8th, 25th, 42th, 58th, 75th, and 92nd quantiles (corresponding to the centre values of 6 equally-sized quantile spaces).

5.2. Stylized Channel Case Study

In this portion of the study, a stylized straight channel with an initial well-defined cross sectional shape and constant longitudinal slope was simulated under varying combinations of variables' values and flood events (i.e., in unsteady flow conditions). The uncertainty in fluvial morphodynamics was modelled with respect to the channel's granulometry (represented by its median diameter D_{50}), the channel's bed

roughness (represented by the Manning's roughness parameter n), a flood magnitude parameter Q^* (which defines the intensity of the flood event simulated) and the uncertainty in the sediment input at the upstream boundary (represented by its deviation ΔQ_s from its value as estimated with the Wu et al. formula (Wu, et al., 2000)).

These variables were selected (as is described in previous section of this Thesis) because they have been shown to have a very significant influence in morphodynamics (van Vuren, 2005; Visconti, et al., 2010; Kasyi, et al., 2015) and because these are variables which specifically influence morphodynamics and not just the modelling of fluvial morphodynamics itself.

The advantage of this Stylized Case Study is that it is less impacted by the complexity of fluvial morphodynamics (in particular its natural tendencies in terms of bed level evolution), thereby producing a clearer description of the relation and sensitivities between the variables and morphodynamics itself. Additionally, the clearer nature of the results also favours the application of more informative sensitivity analysis tools, as opposed to the standard morphodynamic variability range-based analysis that is most commonly used (which is a highly discrete and therefore unstable measurement of sensitivity). This case study can therefore serve as a good term of comparison for the Mondego Case Study. The results of the numerical HM modelling for this Stylized Case Study were used as a control-case in the analysis of the morphodynamical sensitivities, allowing for a more in-depth understanding of the mechanisms behind fluvial morphodynamics.

The setup, simulation and statistical analysis of this case study are part of one of the journal articles developed in the context of this work (Oliveira, et al., s.d.).

5.2.1. Model Setup

The initial conditions for the numerical simulations correspond to a steady flow of 10 m^3/s along the channel. The boundary conditions used to represent the limits of the numerical model (in terms of hydrodynamics) in the simulations were as follows:

- For the upstream boundary: a flow hydrograph time series defined for a given return period. The exact definition of the flow hydrographs simulated (which was based on recorded streamflow data) is presented in section 4.2 of this document.
- For the downstream boundary: a stage-flow curve corresponding (an example of which is presented in Figure 48) to uniform flow conditions (adjusted as a function of the simulation's value of n), as taken from the Manning-Strickler equation.

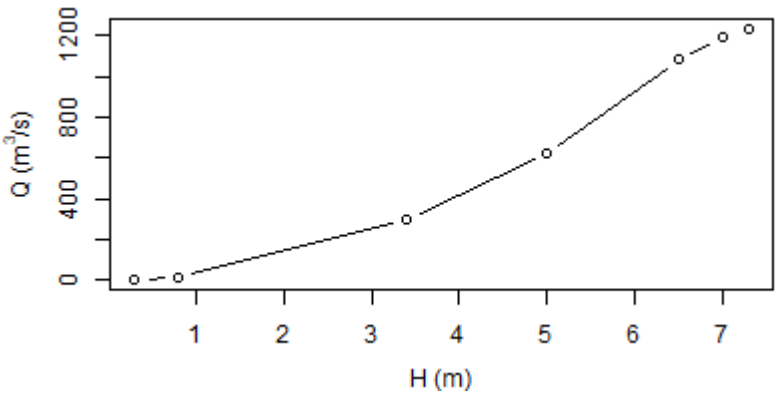

Figure 48 – Example stage-flow curve for the downstream boundary of the model.

The numerical HM modelling was performed using the CCHE2D's unsteady flow simulation, coupled with the mixing length model for turbulence closure. Only bed load was considered in the numerical hydro-morphodynamic simulations (i.e., suspended load was not considered relevant to the channel's morphodynamic behavior). The Wu et al. formula (Wu, et al., 2000) was used to represent the flow's sediment transport capacity throughout the channel. Considering that this case study consists of a uniform channel, some influx of sediments at the upstream boundary was considered, as this has a significant potential to alter the overall results The uncertainty in this sediment influx is one of the variables in this study. The same Wu et al. formula was used to define the sediment input at the upstream boundary, as a function of the corresponding flow hydrograph. On the other hand, uniform, steady flow conditions (i.e., defined using the Manning-Strickler formula) had to be assumed in order to define the sediment input at the upstream boundary and the stage-flow curve for the downstream boundary. Due to that, a disparity exists between the sediment transport at the boundary (defined for uniform flow conditions) and in the channel (defined for unsteady flow conditions directly by the CCHE2D model). Such approximations at the boundaries are however virtually inevitable. Considering that the HM model represents a river channel (and not of an idealized/conceptual channel), this imperfect representation of the boundaries is unlikely to significantly detract from the goals of the related sensitivity analysis and is therefore deemed sufficient.

The Δ_{Qs} variable itself, i.e., the uncertainty surrounding the sediment input in a reach, while being known to be relevant for fluvial morphodynamics, is hard to be characterized. Its uncertainty can change greatly from case to case depending on a multiplicity of factors, such as the channel slope, the flow regime, the granulometry and the characteristics of the sediments themselves (both locally at the boundary and significantly upstream from the boundary). For the lack of a more detailed alternative in the literature, the Δ_{Qs} variable was expressed as a constant percentage deviation (within each simulation) of the sediment input at the upstream boundary. Concretely, for each simulation, the sediment input at the boundary (estimated using a semi-empirical formula, under uniform flow conditions, as a function of the corresponding flow hydrograph) was adjusted by a fixed factor of Δ_{Qs} in order to represent the sediment input's uncertainty. Across simulations, a uniform distribution was assumed for the Δ_{Qs}'s

uncertainty. The range of this uncertainty was set to 10% of its estimated value, as suggested by Topping, et al. (Topping, et al., 2000) for a large river.

The channel was simulated using a symmetrical horizontal two-dimensional (2DH) numerical modeling grid defined by a longitudinal spacing of 2 meters over a length of 1000 meters (totaling 51 cross sections) and a transversal spacing which coincides with the 15 defining points of the channel's cross section (presented in Figure 49), for a total of 765 grid cells. In addition to the 2DH numerical modeling grid used in this study, the location of the channel's upstream and downstream boundaries is also presented in Figure 49.

The adaptation length for bed load (a parameter used in the CCHE2D model which corresponds to the distance along which the sediment transport is considered to be non-conservative due to inertia effects) was set to the grid cell length (in accordance with (Wu, 2007)). The specific sediment gravity was set to 2.65 (relative to the water density) and curvature effects were disregarded.

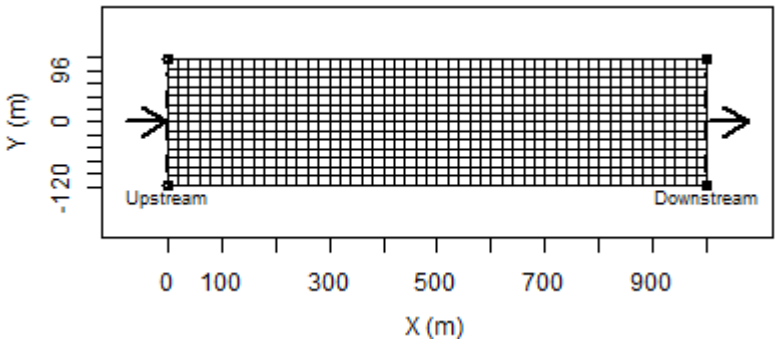

Figure 49 – 2DH modeling grid used in the present study. The dashed lines represent the locations of the upstream and downstream boundaries.

5.2.2. SIMULATIONS

The magnitude of most sensitivity statistics is generally directly proportional to the variability ranges of the different variables involved. Because of this, the appropriate definition of the variability ranges is important for the correct representation of realistic morphodynamical sensitivities and must be taken into consideration when comparing morphodynamical sensitivities across different cases. In this instance, the definition of the variability ranges was essentially based on the available literature and the information from these variables' values, as taken from the data of the Mondego river.

The D_{50}'s variability range was based on granulometric data from the selected reach of the Mondego river. The median diameters of the granulometric measurements (summarized in Table 3) range between 1.64 and 29.65 mm. As the exact probability distribution is not quantifiable from the measurements and a significant spread of values is observable, an uniform distribution of D_{50} values throughout the channel was adopted.

The n values along the river bed were estimated based on the available literature (Schall, et al., 2008; Arcement & Schneider, 1984; Chow, 1959) for mean n values in a river channel. Given that the stylized

channel is intended to represent a river channel, the large number of factors which define *n* in a river channel is so large (e.g., vegetation, granulometry, bed forms, slope, etc.), the channel's mean *n* was assumed to be independent from the other variables and to be situated between values of 0.03 and 0.04, common reference values (in the literature) for a natural river channel. A uniform distribution was assumed for representing the PDF of the *n*. The stage flow curve which determines the outflow at the downstream boundary was adjusted in conformity with the value of the *n*.

The streamflow data which was available consisted of a four and a half year long hourly streamflow series. Figure 50 represents the estimated PDF of the streamflow data's peak flood magnitudes (obtained based on the corresponding data) and, therefore, by extension, the PDF of the Q^* parameter for this case study.

Regarding the ΔQ_s variable, while it is a variable with a significant and recognized level of uncertainty, the definition of its uncertainty can be very complex. As virtually no studies have attempted to quantify this uncertainty in terms of its relative magnitude and probability distribution, the uncertainty in ΔQ_s was defined, for each simulation, as a constant percentage deviation from its estimated value (as provided by the Wu et al. formula). Across simulations, a uniform distribution was assumed for the ΔQ_s's uncertainty. The range of this uncertainty was set to 10% of its mean value, as suggested by Topping, et al. (Topping, et al., 2000) for a large river.

Figure 50 represents the final choices for the uncertainty distributions for all variables. As said, uniform distributions were assumed for the granulometry (D_{50}=1.5→30 mm), roughness (n=0.03→0.04 s/m$^{1/3}$) and sediment input (Δ_{Qs} =-10%→+10%); for the water discharge, its variability was defined by fitting a Weibull distribution to the recorded values of peak flood magnitude.

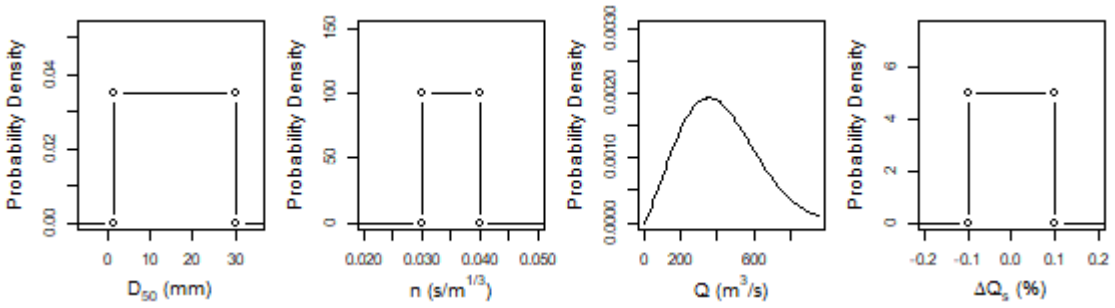

Figure 50 - Probability density functions for each of the simulated variables considered in the study.

For the purposes of these simulations, the referred variability ranges were assumed as adequate. Nevertheless, while other values could possibly be assumed, given the exemplificative nature of this case, it is considered that there is no added value in further postulating on their distribution.

As a reference, the resulting distribution of simulated mobility parameters (defined as the effective shear stress divided by the critical shear stress calculated using the Shields diagram), for the maximum flow in each simulation, and assuming uniform (i.e., unidimensional), steady flow conditions (i.e., estimated

using the Manning-Strickler formula) is presented in Figure 51. Each point represents one simulation's maximum mobility parameter, calculated under the uniform, steady flow assumption.

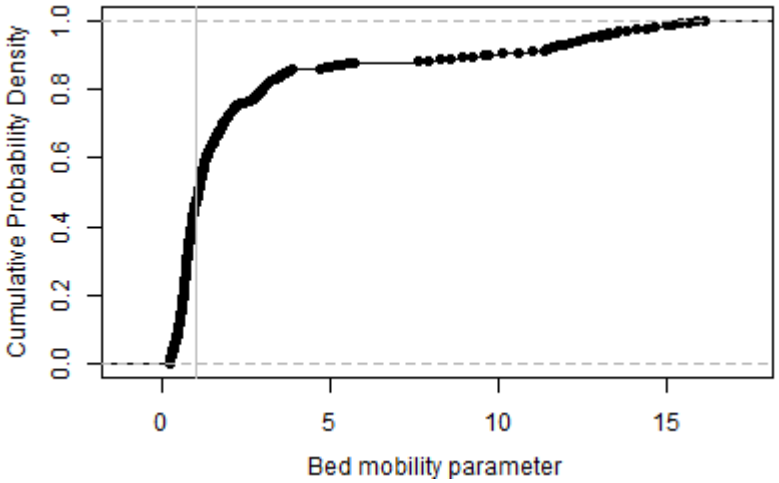

Figure 51 – Probability distribution of simulated mobility parameters for all of the simulations (defined as the ratio between the effective shear stress and the critical shear stress).

Given the large computational capacity required by the numerical HM model, a crude Monte Carlo to stochastic modelling is not viable. The values of the variables which are to be simulated cannot therefore be randomly sampled. In this study, specific quantile values of each variable were selected to represent their respective PDFs. For simulation purposes, the entirety of both the D_{50}'s, the n's and the Δ_{Qs}'s variability ranges were sampled. Concerning parameter Q^*, since the corresponding PDF is unbounded, the more extreme values of the variability range are not realistic (such as a null valued or a virtually infinite parameter). Accordingly, the variability of Q^* was represented by the corresponding PDF's 5^{th} to 95^{th} quantiles. For each of the variables, a set of seven values was used to represent their respective PDF, matching the 0^{th}, 17^{th}, 33th, 50^{th}, 67^{th}, 83^{th} and 100^{th} quantiles for the D_{50}, n and Δ_{Qs} variables and the 5^{th}, 20^{th}, 35^{th}, 50^{th}, 65^{th}, 80^{th} and 95^{th} quantiles for Q^*. The modelling of all of the potential combinations of these values results in a total of $7^4 = 2401$ simulations (the number of combinations of the seven values for each of the four variables). When necessary, these simulations have been individually identified by the ranking of their respective quantiles, for example, the 0^{th} (1^{st} value), 17^{th} (2^{nd} value), 65^{th} (5^{th} value) and 100^{th} (6^{th} value) quantiles of the D_{50}, n, Q^* and Δ_{Qs} are symbolized as {1, 2, 5, 7}.

5.3. PRE-MODELLING

As part of this study's objectives, and given the extensiveness of the HM (hydro-morphodynamic) simulations which are to be performed, a variety of solutions for imroving the speed and quality of the simulations (and their respective results) were adopted. One such solution was the application of a hot-start approach to numerical HM modelling, specifically aimed at improving the quality of the bed level data used in numerical modelling. The criteria for applying this approach, hereby designated as a pre-

modelling approach, is condensed and presented. Originally, the study of this hot-start/model optimization approach was compiled in one of the journal articles developed in the context of this study (Oliveira & Maia, 2019). The extensive validation of this approach presented in this section of the Thesis was necessary given the lack of other significant references about this application of hot-start approaches.

5.3.1. CONCEPT

The proposed hot-start approach was validated for general application in numerical hydro-morphodynamic (HM) modelling and is specifically aimed at improving the quality of the bed level data used in numerical modelling. Accordingly, the criteria for applying this approach, hereby designated as a pre-modelling approach, is condensed and presented throughout this section.

Many examples of hot-start approaches can be found in the literature, particularly when the modelling of geophysical processes is involved. The most common applications include the hot-start of fluvial hydrodynamics models (Nelson, et al., 2016; Tritthart, et al., 2011) or hydrological models (Moser & Gallus Jr., 2015; Ortiz, et al., 2016) and they are most commonly applied with the purpose of reducing simulation run times. Additionally, some applications have been performed with the purpose of improving the results of sensitivity analysis in the field of hydrology (e.g., Cloke, et al., 2008). Applications of pre-modelling/hot-start approaches specifically to the numerical modelling of morphodynamics are, however, comparatively rare (French & Clifford, 2000). Nonetheless, as will be demonstrated in this section, the application of a pre-modelling approach in this context has very significant benefits for the quality of the simulated topography (both the model's initial conditions and its final results). This is likely to be especially relevant for real case studies, where the topographical uncertainty involved is the highest.

Specifically regarding numerical hydrodynamic and morphodynamic (HM) models, a significant amount of uncertainty and small scale errors will almost always be present in the model's gridded bed level (mostly due to measurement and interpolation errors). As an example, triangular interpolation (the most commonly used approach for interpolating topographical data) quite commonly produces errors and instabilities in the continuity of bed level. All that it is necessary for this to happen is a disparity between the magnitude of the spacing of the bed level measurements and the grids nodes to occur (as it does frequently). These errors can only be completely removed if the spatial scale of the bathymetric survey used to define a numerical model's initial bed level data is relatively similar (in terms of distribution and spacing of the measurements) to the spatial scale of the model's grid. The proposed (and applied) pre-modelling approach is intended to be a universally-applicable approach for reducing the influence of these small scale systematic errors in the bed level data in the overall results of the models.

Pre-modelling consists on performing an initial simulation of a river's morphodynamics (using an HM model), using criteriously defined boundary conditions (i.e., flow and associated sediment influx at the

boundaries), and analysing the changes that this simulation produces in terms of the bed level. Naturally, small values of flow should not produce significant changes to a mostly stable river (Throne, et al., 1996). Therefore, when changes are observed in the simulated morphology for small flows conditions, they are likely to reflect some small scale natural errors in the definition of the bed level itself. By applying pre-modelling, it is possible to reduce these small scale systematic errors while maintaining the large scale components of fluvial morphodynamics and the natural overall behaviour of the river. The definition of the boundary conditions used for pre-modelling is based on a mostly qualitative comparative analysis of a range of potential scenarios. While the application process has a mostly qualitative nature, it can produce quantifiable improvements to the quality results of numerical simulations.

In fluvial environments, the primary forcings which affect a river's morphology are (1) the water flow (and the sediment transport associated with it), (2) the vegetation – or the lack of it – and (3) artificial (man-made) interventions in the river bed (Nones & Di Silvio, 2016). While the last two are hard to predict without a significant amount of data, the forcing produced by the flow of water in the river can be understood and reproduced by way of HM numerical modelling (using information on flow records and a characterization of the river's morphology). This general application pre-modelling method is meant to mimic the forcing produced by the water flow, thereby serving as a tool for, using a scientifically based approach, removing a portion of the small scale systemic errors which affect the outcome of the fluvial morphodynamics modelling. The mimicking of this forcing is to be performed by applying the numerical HM models under specific conditions. The proposed approach is not intended as a filter (which is generally context-blind by nature) but as a scientific approach to improve on the interpolated bed level data, respecting the large scale trends of the channel and (per the user's prerogative) the raw/uninterpolated bed level measurements.

By eliminating these errors in the results of numerical HM models, the proposed method can produce improvements in terms of:

- The accuracy of the gridded bed level data (which results from the interpolation of bed level measurements onto a numerical model's grid), both regarding the model's initial conditions and its final results;
- The intelligibility of the numerical models' results (allowing for a better representation of the overall trends regarding erosion and sedimentation along the river);

These benefits of the pre-modelling are particularly useful for studies involving the comparison of scenarios, such as, potential solutions for river rehabilitation or hydraulic structure design (e.g., Pender, et al., 2016). The improved representation of the overall trends of morphodynamics can provide a much clearer distinction between the results of the corresponding numerical simulations.

In section 5.3.2, the principles and criteria involved in the application of the proposed pre-modelling approach are systematized and presented. The limitations and the choices involved in its application are

discussed. An application example of the proposed pre-modelling approach was developed and its effects in the overall model outputs were demonstrated. The case study data used in the HM modelling for this study corresponds to a reach of the Mondego river in Portugal. The model's results with and without the use of pre-modelling for each intervention are compared for each potential river intervention and the effect of pre-modelling is quantified.

The HM modelling was performed using the CCHE2D model, the CCHE_GUI 3.29 and the CCHE_MESH 3, all of which are available at the website for the National Center for Computational Hydroscience and Engineering of the University of Mississippi (NCCHE, 2017).

5.3.2. PRE-MODELLING

In a common hot-start approach, the input variables of a model are "pre-simulated" in order to define a more appropriate starting point for the model simulations, specifically with the objective of improving the quality and realism of the model's results. Accordingly, pre-modelling conceptually consists of simulating the effect of fluvial morphodynamics in the temporal evolution of bed level (i.e., by applying the numerical HM models) in order to improve the quality of the HM model's own starting conditions, i.e., the initial bed level data (interpolated onto the modelling grid). The corrected bed level data resulting from the pre-modelling's application then serves as more appropriate start-up bathymetry for the desired model run/study.

Just like any hot-start approach, the pre-modelling's application usually comes associated with an envisaged numerical HM study (such as, for example, morphodynamical modelling and comparison of solutions for river rehabilitation) for which the referred improvements in the initial conditions will be useful. The pre-modelling approach therefore consists of running an additional/initial numerical HM simulation with a set of criteriously defined boundary conditions and starting from the same initial conditions as the intended study would otherwise use. The boundary conditions and the time period of the simulation are the components of the models which determine the magnitude of the corrections introduced in the bed level data by the pre-modelling. The concept of the pre-modelling approach is expressed in Figure 52.

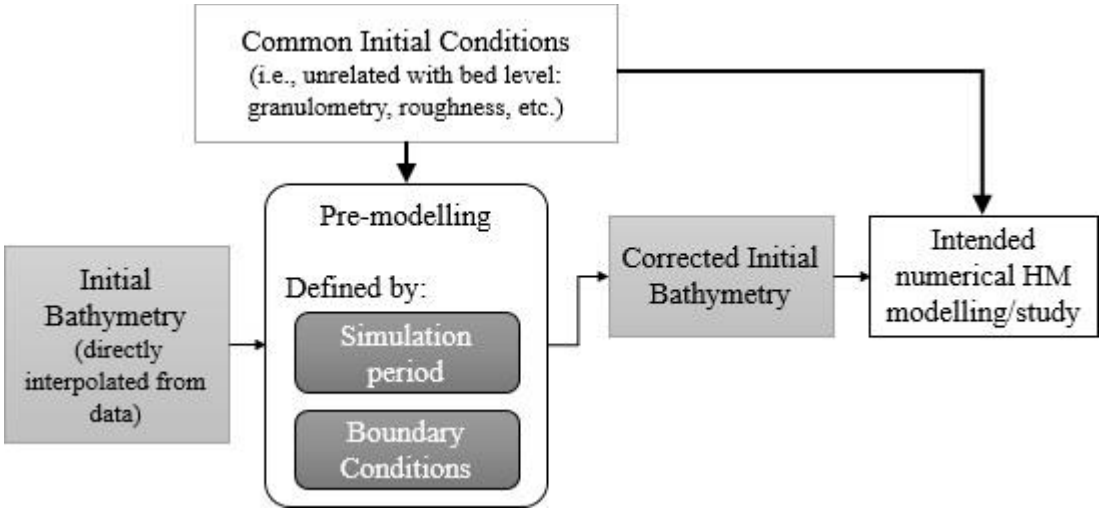

Figure 52 – Schematic representation of the context of the pre-modelling approach's application.

Generally speaking, the pre-modelling itself is no different from any other HM simulation for a given channel. The only distinguishing feature is the definition of the magnitude of the corrections introduced by the pre-modelling, which is the primary aspect in the correct implementation of the pre-modelling itself. As a general criteria, the boundary conditions and the simulations' time period should be defined in such a manner that the bed level changes produced are relatively small in order to conserve the vast majority of the river's overall trends and morphology while producing changes at smaller spatial scales. This section focuses on establishing criteria for the correct definition of effects to be introduced by the pre-modelling (and, inherently, of its simulation period and boundary conditions).

As a matter of simplicity, the pre-modelling's simulation time period was set to a large enough value to ensure the stabilization of bed level change during the pre-modelling's simulations. Concerning sediment transport and downstream boundary conditions, those are most often defined in accordance with local conditions and the corresponding range of flow values. Concurrently, in most cases, the variable which can be used to regulate the changes introduced by the pre-modelling is the inflow at the upstream boundary. For the prescribed application of the pre-modelling the definition of the boundary conditions used in the application of pre-modelling can be accomplished by way of a comparative qualitative approach, whose guidelines are expressed in section 5.3.3.

Following that, and depending on the user's degree of confidence on the available bed level measurements, the pre-modelling's simulations may be performed according to two hypothesis:

- A freely moving bed, where a significant uncertainty is assumed to exist in those measurements. The entire grid is therefore adjusted (by HM modelling) in accordance with the hydrodynamic forcings;
- A partially fixed bed, where bed level measurements are assumed to be virtually correct. The nodes of the grid which coincide with the locations of the measurements are therefore fixed during the pre-modelling's simulations. From another perspective, only grid nodes whose bed level data is interpolated are allowed to change freely during the HM modelling. This particular hypothesis, due

to conserving some of the correct initial information on bed level, should provide a more realistic representation of bed level (albeit removing less of the fluvial morphodynamics small scale evolutionary trends, given the partial restraining of the *dH* during the pre-modelling).

5.3.2.1. Boundary Condition Definition

As previously referred, the improvement of the numerical model's bed level data with the pre-modelling approach is produced by introducing a certain magnitude of corrections with a criteriously defined HM simulation. The initial conditions (bed level, bed roughness, granulometry, etc.) for the pre-modelling's simulations are the same as those which would be naturally used for simulating the river's morphodynamics (i.e., as provided by in-situ data). The main difference between a regular HM simulation and the simulations performed in the context of pre-modelling is that the boundary conditions and the simulations' time period used in the corresponding HM modelling are defined in order to produce a specific level of morphodynamical correction/change in the bed level data.

As previously mentioned, the flow at the upstream boundary is generally the critical variable in terms of defining the bed level change introduced by the pre-modelling. Concordantly, this study analysed the potential of using a constant flow series at the upstream boundary (with the sediment input at the upstream boundary and outflow conditions being dictated by the corresponding local transport capacities) and a long simulation period (i.e., until stabilization/until bed level change becomes null) to apply this hot-start concept in morphodynamic modelling. In order to produce an adequate/desired level of change in the bed level data via pre-modelling, an optimal flow value must be defined at the upstream boundary. This optimal flow can be understood as the flow which removes only the small spatial scale errors which obfuscate the numerical HM models' results while maintaining the large scale components of the morphodynamics' behaviour.

The definition of the boundary conditions/optimal flow can be accomplished by way of the application of a comparative qualitative approach. The criterion for the selection of an optimal flow is based on the random nature of the targeted small scale errors. Specifically, the base criteria is that the optimal flow *Q'* should induce only sporadic changes along the bed level, i.e., if a value of flow produces either generalized erosion or sedimentation then it is likely to be inappropriate for pre-modelling purposes. Additionally, if the bed level changes introduced by a given *Q'* flow in pre-modelling include only sporadic/occasional (i.e., small and wide spaced) occurrences of erosion and sedimentation, the overall behaviour of the river's morphodynamics can be deemed to have been maintained. Figure 53 presents an example of a comparison of different potential values of *Q'* for a schematic U bend channel.

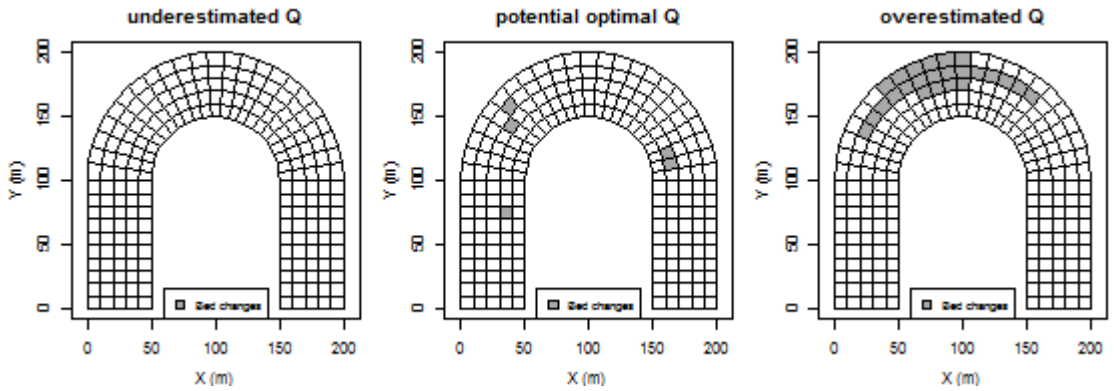

Figure 53 –Examples of the locations of bed change produced by different values of *Q'* along a schematic U bend channel (with *Q'* increasing from the case on the left to the right). The plot on the left corresponds to a low *Q'* value (underestimated since it does not produce bed changes). The middle plot corresponds to a potentially optimal *Q'* value (since it only produces occasional bed changes). The plot on the right corresponds to an excessive *Q'* value (overestimated since the bed level changes are too continuous along the river bed.

The optimal flow can be defined by experimenting with multiple potential *Q'* values, i.e., running the HM models with multiple potential *Q'* values at the boundary until bed stability is reached. The lowest potential value of *Q'* which should be considered in pre-modelling is the flow value which initiates the river's morphodynamical evolution (i.e., the incipient flow, $Q_{min} \leq Q'$). Above this Q_{min}, different quantiles of the streamflow's probability distribution should be experimented with (in an iterative process) until an optimal *Q'* value is found. The selection of the optimal *Q'* value is then performed by comparing the different simulations in terms of the spread and distribution of erosion and sedimentation along the bed, in accordance with the criteria presented in this section.

The optimal *Q'* value (i.e., the *Q'* value adopted in the pre-modelling) can be considered as a redefined, virtual incipient flow, namely, because the pre-modelling's simulations are run until bed level stability under that *Q'* flow is achieved. The adopted *Q'* flow can therefore be used to limit the range of the streamflow series to be modelled, thereby speeding-up the simulations themselves (i.e., the simulations only need to be run when the channel is morphodynamically active, namely when the flow is above the *Q'* value used in pre-modelling).

Section 5.3.5 presents an example of the application of this criteria for selecting the optimal flow value *Q'*.

5.3.3. Model Setup

In a previous study (FEUP, et al., 2016) focused on this specific study reach, the right bank of the river in the study segment was observed to be suffering significant erosion. In that study, in order to lessen the magnitude of the erosion in the study segment (part of area b of the study reach), two different river rehabilitation solutions were considered for reinforcing the stability of the study segment of the river channel. In order to quantify the improvements introduced by the application of the pre-modelling approach, the two river rehabilitation solutions (designated as Solution 1 and Solution 2, described below) were simulated in this study. For comparison, a baseline considering no intervention on the

channel case (hereafter referred as Solution 0) was also considered. In accordance, the solutions considered for the present study are as follows:

- Solution 0: No intervention is performed in the river channel;
- Solution 1: The alignment of the right (eroded) river bank is straightened (thereby diminishing the current channel's width by up to 5 meters). Overall, this solution should increase the erosion of the channel bed in comparison with solution 0 (by increasing the overall flow velocity);
- Solution 2: Removal of 20 meters of the sand bank (transversally to the river's flow) on the left side of the channel. Overall, this solution should increase the sedimentation in the channel bed in comparison with Solution 0 (by reducing the overall flow velocity).

The prescribed river rehabilitation solutions were simulated in the present study with and without the application of pre-modelling and the corresponding results were analysed and compared.

Figure 55a and Figure 55b represent, respectively, the locations and the extension of the interventions involved in Solutions 1 and 2.

Figure 54 – Location of and extension of the intervention in Solution 1 (a) and 2 (b).

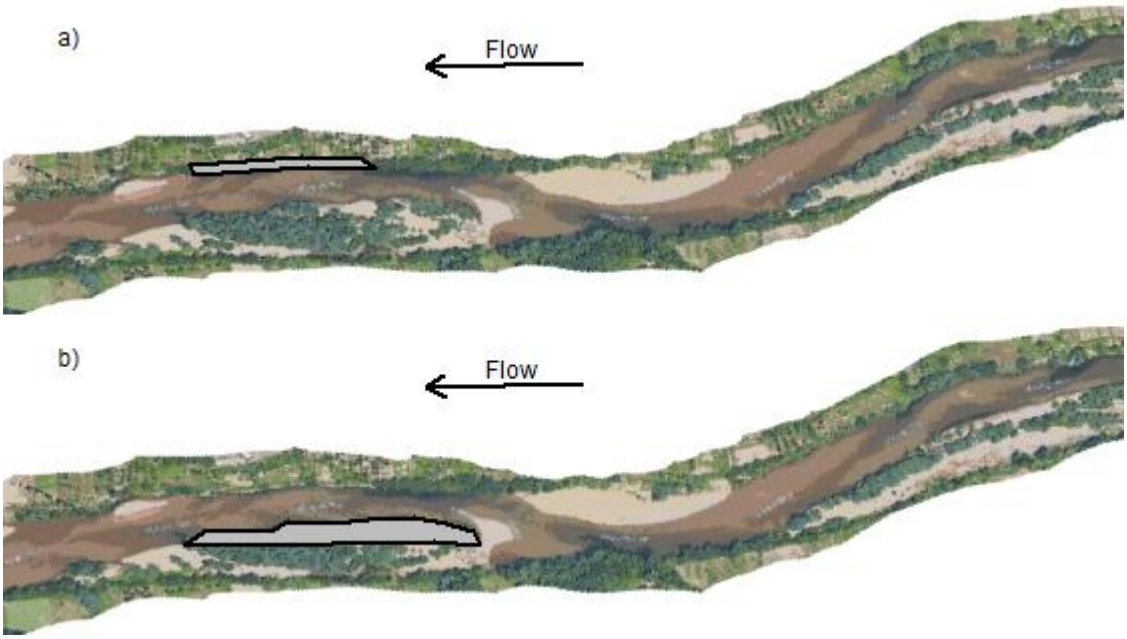

Figure 55 – Location of and extension of the interventions planned for the study segment in a) Solution 1 and b) Solution 2.

The three potential river rehabilitation solutions (including no river rehabilitation and the two solutions previously referred) were simulated considering different scenarios regarding the possible degrees of bed level corrections introduced by pre-modelling (as previously referred in this section). The combinations of the different solutions for river rehabilitation and the different scenarios for pre-modelling were simulated in order to analyse the sensitivity of the simulations with and without the application of pre-modelling.

For the Mondego Case Study, the flow magnitudes considered correspond to the 70th, 75th and 90th percentile of streamflow's hourly values. These flows correspond to 50, 90 and 150 m^3/s. These flows were chosen as examples of potential, demonstrative values of the optimal *Q''* value. Q_{min} was determined (via HM modelling) to be approximately 40 m^3/s. The downstream boundary was simulated using the appropriate flow-to-depth ratio function (defined for uniform flow conditions at the boundary). In the present study, given the presence of a levee on the upstream boundary and the relatively small flow values which are simulated during the pre-modelling's application, the sediment transport at the upstream boundary was considered as insignificant. Naturally, in other, different situations, the sediment transport at the boundaries should be defined according to the corresponding local conditions. Options (in situations where a significant and relevant sediment input may be present) may include calibrated sediment flow-to-water flow curves, where such data is available, or theoretical sediment transport capacity functions otherwise.

In order to demonstrate the relevance of the pre-modelling approach in improving the numerical models' representation of the overall behaviour of fluvial morphodynamics, the 3 potential river rehabilitation solutions were simulated for different magnitudes of bed level correction as introduced by pre-modelling. The combinations of the different solutions for river rehabilitation and the different applications of pre-modelling were simulated in order to analyse the sensitivity of the simulations with and without the application of pre-modelling.

The number of pre-modelling scenarios (*i*) in this study totals 4, including no pre-modelling (1 scenario) and pre-modelling (3 scenarios with values of *Q'* of 50, 90 and 150 m^3/s) (numbered as *i* = 0 to 3), with *Q'* as the flow value at the upstream boundary

Regarding the uncertainty/accuracy (or lack thereof) of bed level measurements, both hypothesis (suggested in section 5.3.2) were analysed, namely, (1) allowing for the bed level to change freely, in accordance with the flow's morphological forcing and (2) allowing for the bed level to change freely except at the locations where the model's grid's nodes coincide with in-situ bed level measurement locations, which essentially corresponds to partially restraining the bed level during the HM simulations. This second option is intended as a way to maintain the information from the available bathymetric measurements. In accordance, the hypothesis (*j*) for the pre-modelling procedure are 3, including: no pre-modelling, freely changing bed and partially fixed bed (numbered as j = 0 to 2).

Each of the 7 pairs of scenarios and hypothesis (represented in Table 7) corresponds to one application of the pre-modelling approach, specifically performed by applying the numerical HM models using the corresponding *Q'* flow from its respective scenario *i* and hypothesis *j* (represented by acronym *j*-*i*).

Table 7 – Pairs of scenarios and hypothesis simulated in the pre-modelling.

Pair (*j-i*)	0-0	1-1	1-2	1-3	2-1	2-2	2-3
Scenario (Pre-modelling Flow)	N	Y (50)*	Y (90)	Y (150)	Y (50)	Y (90)	Y (150)
Hypothesis (Partially Fixed Grid Nodes)	–	N	N	N	Y	Y	Y

Y/N: YES/NO; (Q)*: (Flow)

The number of solutions for river rehabilitation (*k*) analysed in this study are 3 (numbered as *k* = 0 to 2, as previously presented). A total of 21 combinations of scenarios and hypothesis (7, Pairs *j-i*) and solutions (3, *k*) was simulated. Each combination (designated as *k-j-i*) corresponds to the application of the pre-modelling scenario and hypothesis *j-i* in the analysis of Solution *k*, i.e., the resulting bed level data (as produced by the pre-modelling's simulations) being used as the initial bathymetry for the numerical HM models to simulate the river's morphodynamics after the implementation of the referred solution. These combinations are represented in Table 8.

Table 8 – Combinations of scenarios and solutions simulated in this study.

	Combination Acronym	Solution		
	Pair Acronym	No intervention	Solution 1	Solution 2
		0	1	2
Without pre-modelling	0-0	0-0-0	1-0-0	2-0-0
With pre-modelling	1-1	0-1-1	1-1-1	2-1-1
	1-2	0-1-2	1-1-2	2-1-2
	1-3	0-1-3	1-1-3	2-1-3
	2-1	0-2-1	1-2-1	2-2-1
	2-2	0-2-2	1-2-2	2-2-2
	2-3	0-2-3	1-2-3	2-2-3

5.3.4. APPLICATION OF THE METHODOLOGY

All the previously referred combinations of scenarios and solutions were simulated using the numerical HM model CCHE2D. The resulting bathymetries produced by the 7 pairs of scenarios and hypothesis for pre-modelling (Table 7) were analysed and the criteria for the definition of the optimal *Q'* flow (referred in section 5.3.2.1) was applied.

In accordance with the criteria previously established, the selection of the best pair of hypothesis and scenarios for pre-modelling was based on the changes in bed level introduced by the pre-modelling. The changes introduced by each pair of hypothesis *j* and scenario *i* (respectively numbered as j-i) in the bed level were analysed using maps of the morphodynamical evolution of the channel. The maps representing bed level change along the study segment are presented in Figure 56. All of the numerical simulations in this study were performed in the standard PT-TM06/ETRS89 coordinate system and are presented as such.

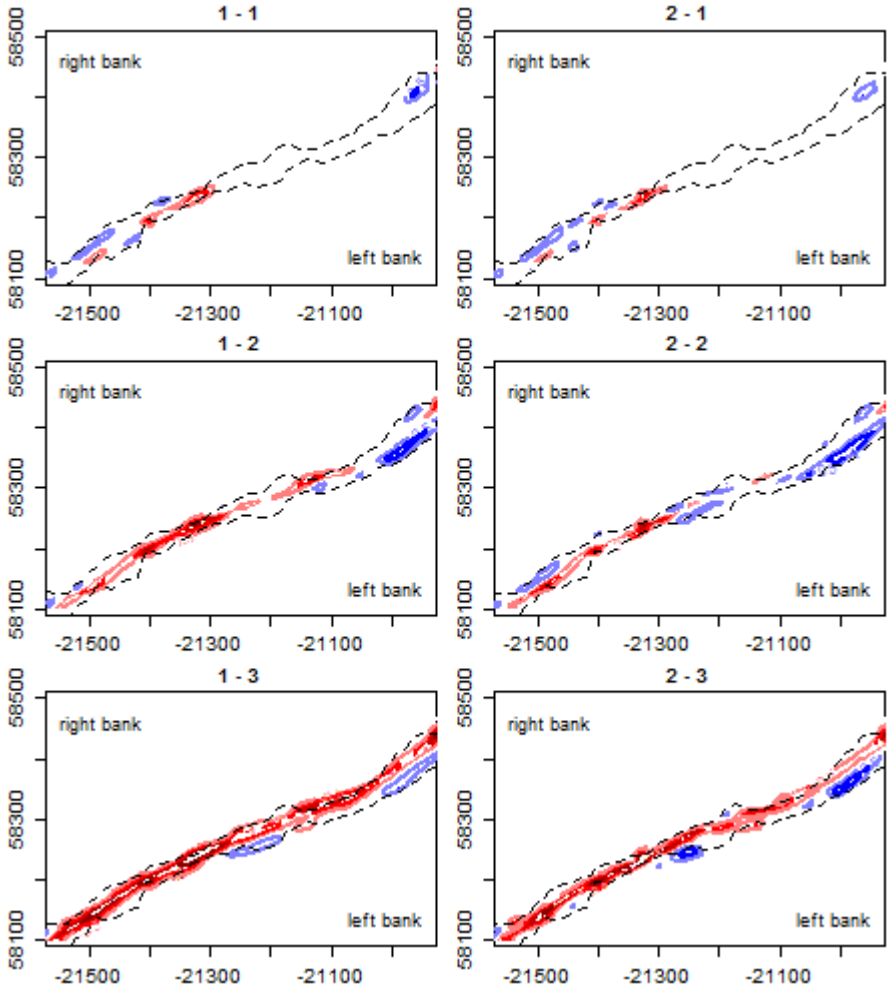

Figure 56 – Channel bathymetry along the study segment after the pre-modelling (the change between lines is 0.5 meters; the red colours indicate erosion and the blue colours indicate sedimentation and the dashed lines indicate the limit of the normal river channel).

Additionally, in order to provide an assessment to the overall magnitude of bed change, boxplots of the absolute non-null bed change for each scenario were calculated and are represented in Figure 57.

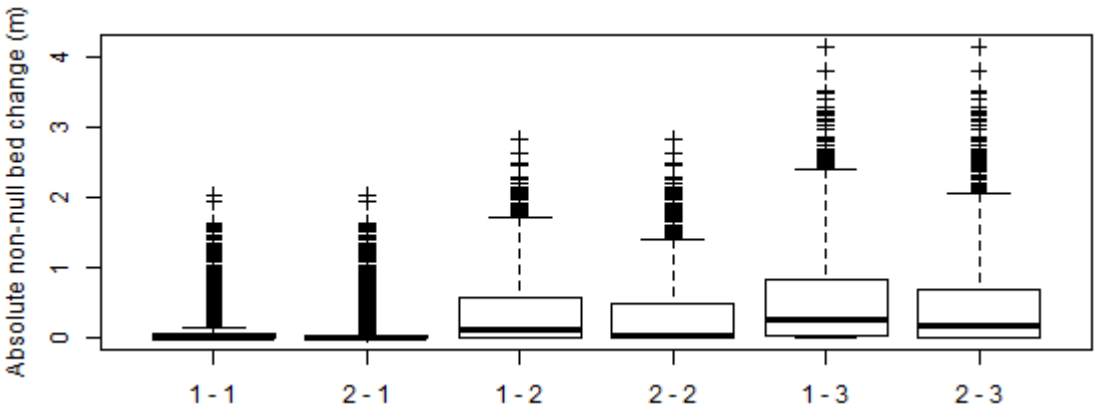

Figure 57 – Boxplots of the absolute non-null bed change for each pair.

Pair 1-3 produces the strongest alteration of the bed level for all the scenarios. This is understandable given that the bed level was allowed to change freely (i.e., hypothesis 1) and the value of *Q'* at the

upstream boundary is the maximum considered (i.e., scenario 3, for $Q' = 150 m^3/s$). The resulting change can be considered too extreme (according to the previously established qualitative criteria), as it mostly produces erosion of the channel bed (as can be seen by the widespread predominance of red coloured lines, which denote erosion, in the corresponding graphic in Figure 56). The regularity and continuity of the bed change observed in Figure 56 are indicative of an excessive alteration of the river bed in the pre-modelling process (as referred in section 5.3.2.1). The changes produced by pre-modelling with 1-3 are therefore inconsistent with what could be designated as small scale systematic errors which may exist in the study reach. For the same reasons, Pair 2-3 can also be considered to produce an excessive magnitude of bed level changes.

Comparatively, Pairs 1-1 and 2-1 produce small but relevant changes in the bed level, providing a good first indication of the locations where small scale components (be they natural trends in the morphodynamics or errors in the bed level data) of the channel's morphodynamics are more present. It should be noted that Pairs 1-1 and 2-1 appear to produce more sedimentation than erosion in the river channel, as can be understood from the comparatively larger concentration of blue lines (which denote sedimentation) in the corresponding graphic in Figure 56. Given the convex shape of most river channels' transversal sections (demonstrated, for example, by Li, et al., 2014) and the commonly discontinuous nature of bed level measurements, in most rivers, it is more likely for the sediment volume and distribution along any transversal river profile to be estimated in excess when obtained by interpolating from bed level measurements into the numerical HM models' grid (as is exemplified in Figure 58). Accordingly, this effect potentiates excess erosion in HM modelling based on the direct interpolation of bed level measurements, which has not been observed in scenarios 1-1 and 2-1. While this does not mean that scenarios 1-1 and 2-1 are incorrect per se, it does imply that the corresponding Q' value used in these instances of pre-modelling (Scenario 1, with $Q' = 50\ m^3/s$) could reasonably have been higher.

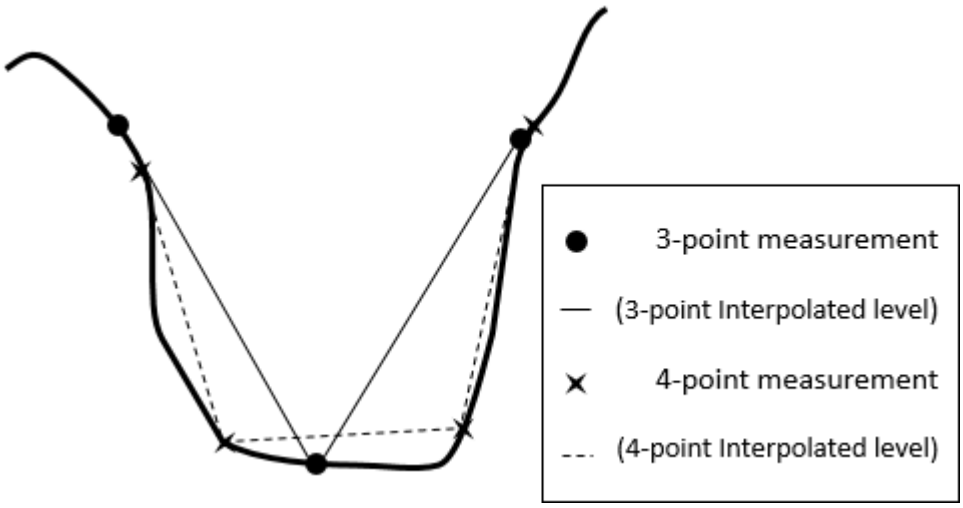

Figure 58 – Example of the likely error that interpolation generally induces in bed level data.

Overall, while significant, the majority of the bed changes introduced by the pre-modelling approach are relatively moderate (mostly staying below 0.5 meters), with only 1-3 and 2-3 producing larger changes to the river bed (as can be seen in Figure 57).

Using the criteria summed up in section 5.3.2.1, the potential pairs of optimal *Q'* values and modelling hypothesis are relatively clear. The Pairs 1-2 and 2-2 present a clearer overall balance between erosion and sedimentation along the entire study segment (as is observable in the corresponding graphics in Figure 56) and are therefore more likely to produce a more accurate representation of the channel's bathymetry. Their respective *Q'* values (of 90 m^3/s) can therefore be considered the optimal *Q'* (in the context of the different values experimented). The choice of the corresponding hypothesis is up to the user. For the purposes of the validation that is to be performed, the 2-2 pair was deemed as the most appropriate for the application of pre-modelling.

5.3.5. VALIDATION

In this section, the benefits introduced by the application of the pre-modelling approach, be it in terms of the bed level's accuracy or the quality of the bed level data's intended purpose, are reckoned.

Each of the 3 solutions (*k*) for river rehabilitation previously presented were simulated and analysed under the optimal pre-modelling Pair of *Q'* flow and hypothesis (Pair 2-2, determined in the previous section) and without the application of pre-modelling (Pair 0-0). The resulting bed level change along the study segment (simulated for each Solution *k* over a representative period of one year of flow records, corresponding to the recorded year of 2010) is presented in Figure 59 (combination *k-j-i*, where *j-i* refers to the corresponding pre-modelling pair used to define the simulation's initial conditions).

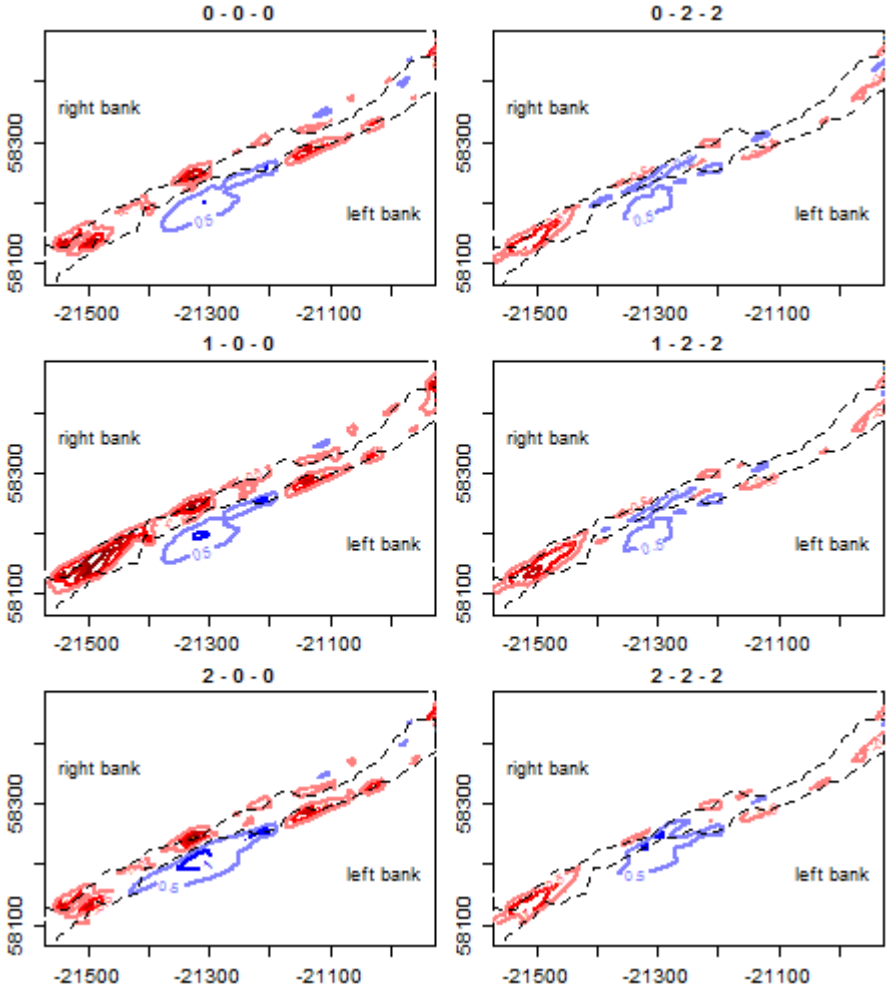

Figure 59 – Resulting change in channel bathymetry along the study segment over a year for each combination (the change between lines is 0.5 meters; red lines indicate erosion and blue lines indicate sedimentation and the dashed lines indicate the limit of the normal river channel) (in the standard PT-TM06/ETRS89 coordinate system).

From in-situ observations, and as has been referred in section 5.3.3, the right bank of the river has been observed to be suffering generalized erosion in the downstream half of the study segment. However, looking at the results from Combination 0-0-0 (in Figure 59), the areas of the river bank which are exposed to significant erosion cannot be immediately determined from the results (i.e., the simulation does not indicate any significant or continuous concentration of erosion in the right bank). The simulations resulting from the application of pre-modelling (with Pair 2-2) provide a significantly more accurate portrayal of the areas prone to erosion (i.e., which matches with observations).

Nevertheless, even looking solely at Combination 0-2-1 (which is based on the modelling pair which introduces the least amount of changes in bed level, namely, a partially fixed bed and a *Q'* value of 50 m^3/s), it is much easier to determine the areas of the river bank which are subject to erosion than in Combination 0-0-0. The bed level changes obtained in these two combinations are presented on a larger scale in Figure 60. From these results it is possible to deduce that even a minimal amount of bed level correction (using the pre-modelling approach) can produce visible improvements in terms of the intelligibility of the channel's morphodynamics.

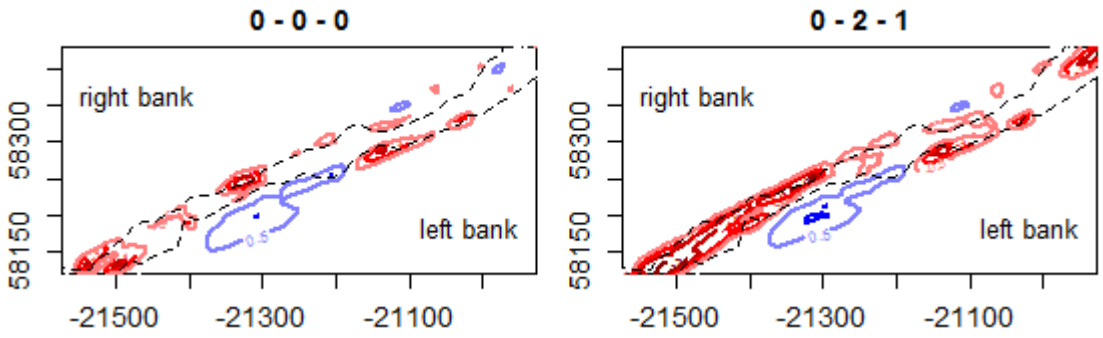

Figure 60 – Comparison between the bed level changes obtained in combinations 0-0-0 and 0-2-1.

In sub-sections 5.3.5.1 and 5.3.5.2, the potential of the pre-modelling approach for improving the quality of bed level data is quantified and validated. In addition, a quantitative assessment of the improvements produced by the pre-modelling in the context of the comparison of solutions is also presented (in section 5.3.5.2).

5.3.5.1. Improvement of Bed Level Accuracy

By altering the shape of the river bed using water flow as a forcing/source of information (i.e., applying the pre-modelling approach), it becomes possible to improve (to a certain extent) the quality of the bed level data along the modelling grid, particularly in comparison with bed level values directly interpolated from bed level measurements. However, it should be noted that the efficiency of this option is highly dependent on a variety of factors. The sources of error in the bed level data are dependent not just on the measurements data (i.e., their magnitude and distribution) themselves but also on the interpolation method used. Therefore, the improvement of the quality of bed level data along the model's grid is dependent on the relative spatial distribution of bathymetric measurement points and of grid nodes (i.e., the spacing and locations of the measurement points relative to the grid nodes), and the proper representation of relevant relief points in the river bed (such as the river thalweg and local maxima and minima of bathymetry).

The potential of the pre-modelling approach for improving gridded bed level data was assessed and validated in this study. This validation process consisted of four steps, namely: (1) removing 50% of the bathymetric measurements, (2) interpolating the remaining bed level measurements into gridded bed level data (using triangular interpolation), (3) applying the pre-modelling approach to correct the gridded bed level data and (4) compare the corresponding corrected bathymetry with the bed level measurements removed by means of step 1. The points removed total over 16500 in evenly spaced sets of 100 points taken from the otherwise, virtually continuous sonar-based bathymetric measurements. The number of points to be removed was defined by experimentation in order to introduce a small but significant difference (i.e., error) between the interpolated versus the measured gridded bed level data. The locations of the measurement points removed for validation purposes are represented in Figure 61.

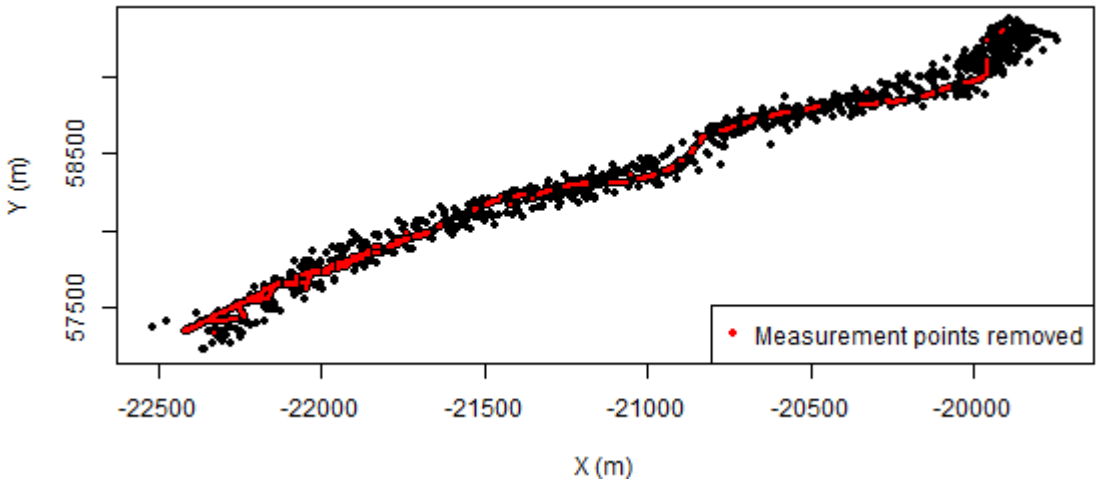

Figure 61 – Location of the bed level measurement points removed from the channel bed (in the PT-TM06/ETRS89 coordinate system).

Overall, the best improvement that could be obtained in terms of the quality of the gridded bed level data (by adjusting the *Q'* flow used in pre-modelling) was of 5% in terms of the overall mean error in bed level. The mean error in bed level was defined by the average difference between the bed level measurements (at the points removed) and the interpolated bed level (defined at the same locations by directly interpolation from the remaining points) or considering the interpolated bed level corrected by the pre-modelling. The error in considering the directly interpolated bed level was of 0.375, which is significantly larger than the error obtained from the interpolated and corrected (by means of the pre-modelling) bed level of 0.36.

The results of this assessment imply that the pre-modelling's application does not necessarily involve a reduction in the accuracy of the bed level data (for reasonable values of *Q'*) and may instead significantly improve upon the purely interpolated bed level data.

5.3.5.2. Efficacy in Comparison of Solutions

The entropy/spatial regularity/variability of erosion and sedimentation was measured in order to assess the regularity of morphodynamical changes, and, thereby, the clarity of the results. Larger information entropy implies faster, more discontinuous changes between sedimentation and erosion along the river bed and thereby less clear results (such as those referred in section 5.3.5 for Combination 0-0-0). The spatial variability of morphodynamics was assessed based on the mean spatial variation of bed level change and corresponding standard deviation (SD) for each combination (measured along the entire study segment), represented in Figure 62. Purely for comparative purposes, the effects of the other pre-modelling pairs (described in Table 7) were also simulated and their results presented (albeit Pair 2-2 having been previously determined as the optimal application of pre-modelling). This consideration is intended to allow for a better understanding of the importance of a proper selection of the optimal Pair in pre-modelling.

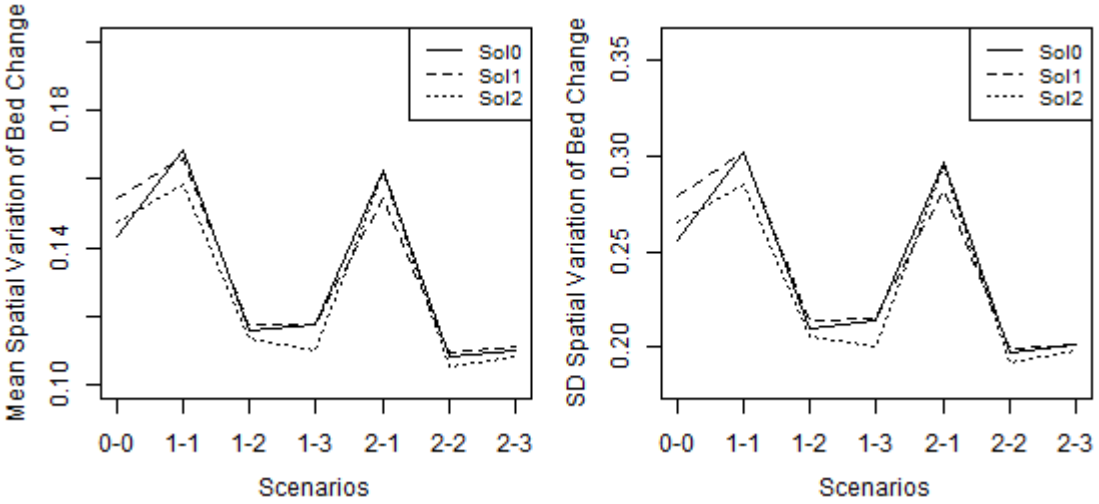

Figure 62 – Mean and Standard Deviation (SD) of the spatial variation of bed level change (along the entire study segment) observed for each pre-modelling pair and solution analysed.

As can be observed, the mean (and SD) spatial variation of bed change drops very significantly by applying the pre-modelling approach (by 15 to 20%), specifically for combinations based on Pairs 1-2, 1-3, 2-2 and 2-3, as compared with Pair 0-0. These results demonstrate the pre-modelling's capacity for removing the small scale components of the morphodynamics, improving on the intelligibility of the HM models' results. Pairs 1-1 and 2-1 on the other hand led to an increase in information entropy, indicating that they were unsuitable for pre-modelling (as was determined in section 5.3.4).

Given the improved intelligibility of the results (obtained by pre-modelling, as opposed to the simulations without pre-modelling: 0-0-0, 1-0-0, 2-0-0), the numerical simulations should be more sensitive to the effects of the different solutions tested on the river's morphodynamics and, therefore, the distinction between solutions should be clearer from a graphical and numerical point-of-view. In order to assess this aspect, the differences between the bed changes produced by Solutions 1 and 2 (relative to Solution 0) were compared to their conceptual/theoretical qualitative effects on bed level change. In fact, considering the nature of the solutions, Solutions 1 and 2 should promote, respectively, an increase in the erosion and in the sedimentation of the river channel in comparison with Solution 0. In addition, based on the concept of cause and effect, the differences in bed level change between Solutions 1 and 2 and Solution 0 should be limited to the areas surrounding the implementation of the solutions themselves. Disparities between, on the one hand, the simulated and theoretical effects of the solutions and, on the other hand the location of each solution and the location of the changes introduced by the solution in the simulated bed level change indicate a reduced accuracy and applicability of the simulations' results.

The sensitivity of the simulations was assessed in terms of:

- The percentage of change in terms of increase in erosion and in sedimentation, respectively, for Solutions 1 and 2 relative to Solution 0 (presented in Table 9) and measured for the entire study segment. The percentage of grid nodes in the study segment which are in accordance with the

solutions' theoretical effects is directly proportional to the morphodynamics' sensitivity to the different solutions;

- The relative location of the grid nodes where Solutions 1 and 2 produce changes in bed level, relative to Solution 0, measured as the longitudinal distance between each grid node and the areas were each solution was implemented, i.e., the spatial spread of the change introduced by each solution (presented in Figure 63).

Table 9 – Percentage of cells whose behaviour is in agreement with the corresponding Solutions' conceptual/theoretical effects (relative to Solution 0).

	Percentage cells in agreement with the Solutions' theoretical behaviour						
Pre-modelling pair	0-0	1-1	1-2	1-3	2-1	2-2	2-3
Erosion (Solution 1)	98%	74%	88%	100%	8%	97%	82%
Sedimentation (Solution 2)	40%	74%	95%	88%	95%	64%	83%

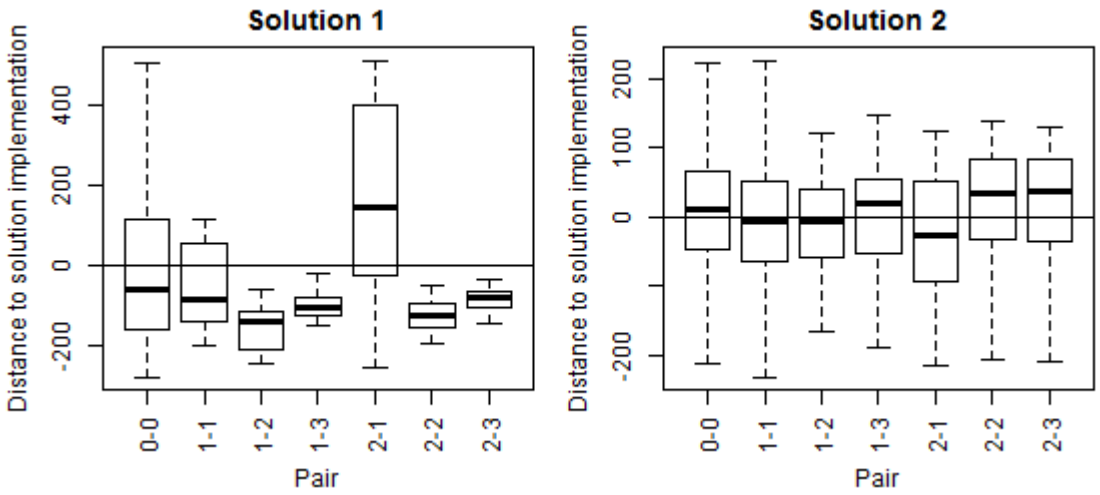

Figure 63 – Relative location of grid nodes with differences in bed level change between Solution 1 and 0 (on the left) and Solution 2 and 0 (on the right), for each combination of pre-modelling pair and hypothesis.

Considering the theoretical effects of the solutions, i.e., an increase of erosion and sedimentation in Solutions 1 and 2, respectively, Table 9 shows that the simulations based on Pairs 1-2, 2-2, 1-3 and 2-3 produce a significantly improved representation of the erosion/deposition effect of the river rehabilitation solutions analysed. The results indicate a clear increase in the agreement between the conceptual/theoretical and the simulated morphodynamical response of the river channel to the implementation of Solutions 1 and 2. Particularly for Solution 2, there is a minimum improvement of around 50% in the agreement between the theoretical and simulated behaviour of the channel for these pairs, evidencing the improved realism of the simulated results (from 40% in Pair 0-0 to a minimum of 64% in Pair 2-2). The difference in improvement between Solutions is possibly due to the characteristics of the likely effect of interpolation errors (which tends to produce an excess of sediment in the channel, as discussed in section 5.3.4).

As can be observed in Figure 63, the Pairs 1-2, 1-3, 2-2 and 2-3 produce a significantly clearer physical and spatial relationship/dependency between the implementation of the solutions and the alterations to the bed level change pattern produced by each solution, particularly regarding Solution 1. The nature of Solution 1 (which involves the tightening of the river channel) dictates that its incrementing erosive effect on the channel bed should be mostly felt in the immediate vicinity and downstream from its location (over a relatively short period of time on a morphological scale), which is in agreement with the four pairs referred above.

Finally, it should be noted that, unlike the analyses on the quality of the gridded bed level data itself, the comparison of solutions for river rehabilitation is not particularly impaired by adopting a larger *Q'* values for pre-modelling as the distinction between solutions is equally (if not more) clear. This is because adopting *Q'* values above its optimal value (as defined by the criterion in section 5.3.2.1) removes some portion of the small scale spatial trends of morphodynamical change, thereby giving prominence to the channel's overall behaviour. However, adopting higher *Q'* values in pre-modelling may cause some (potentially small) reductions in the accuracy of the results of HM modelling. Applications of pre-modelling using *Q'* values above its optimal value for pre-modelling should be aware of this factor.

From these results (namely from Figure 62), it can be concluded that, in comparative terms, when simulating the effects of the different solutions for river rehabilitation, Pair 0-0 produces a great deal of spatial noise (regarding bed level change) in comparison with other scenarios (reducing the intelligibility of the results). Additionally, without using the application of the pre-modelling (cases *k*-0-0), the changes in bed level produced by each solution may sometimes not be consistent with the solution in question (Table 9 and Figure 63). Therefore, pre-modelling was observed to provide an important improvement in the quality of this analysis, particularly in terms of the intelligibility of the results, with reduced entropy and an increased sensitivity of the simulations' results to the different solutions.

5.4. SUMMARY

The application methodology for the stochastic modelling of fluvial morphodynamics in both case studies has been summarized and presented. The underlying complexities/hindrances in this methodology's application, mostly related to the generation of new values of the variables and selecting the representative values for said variables for the purposes of stochastic modelling, are presented along with the corresponding solutions. The results of this stochastic modelling (summarily represented in sections 5.1.2.3 and 5.2.2) constitute a representation of morphodynamical uncertainty and will be applied as such in sections 7 (in the statistical characterization of fluvial morphodynamics) and 8 (in the risk analysis of near-bank infrastructure).

In addition to the application of the methodology itself, a pre-modelling/hot-start approach, which was applied in parallel with the stochastic modelling, is also presented. This approach (designed primarily to improve the quality of the output of numerical HM models) was proven to produce quantifiably more

intelligible results regarding the representation of the natural large-scale trends of fluvial morphodynamics. By suppressing the effect of some small scale errors in the channel's morphodynamical behaviour, the bed change results of the numerical simulations show a much reduced spatial information entropy of morphodynamics (by over 15%, as shown in Figure 62) and a much stronger agreement between the theoretical and the simulated behaviour of the channel morphological changes for each of the two solutions tested in this context (with increases of up to 50% in the match between the referred behaviours, defined relative to Solution 0, expressed in Table 9).

For the purposes of this PhD study, considering the results observed in section 5.3.4 of this Thesis, and, as was previously mentioned in section 4.1.1, the base bathymetry of the Mondego Case Study (i.e., the bathymetry as was provided by interpolating from the bed measurements to the modelling grid) was corrected using a steady Q' value of 90 m^3/s, under the partially fixed bed hypothesis.

6
SENSITIVITY ANALYSIS OF FLUVIAL MORPHODYNAMICS

Sensitivity analysis is a type of statistical analysis which consists of the quantification of a model's/system's sensitivity to a given set of relevant variables, or, from a different perspective, it consists of the quantification of the relative importance of each variables' uncertainty towards the overall uncertainty of that same model's/system's. While this definition corresponds to the most basic application of sensitivity analysis, it can also be useful to the validation of the stochastic applications of numerical models (van Vliet, et al., 2016; Kleijnen, 1999; Sargent, et al., 2016). By analysing the results of stochastic modelling, sensitivity analysis can not only characterize a model's/system's sensitivities but also, by way of a comprehensive understanding and analysis of the variables' behaviour, provide a tool for their validation. As part of the stochastic application of numerical HM models developed as part of this PhD study, both of these applications have been realised.

In the vast majority of the situations, the individual simulations which are a part of stochastic modelling hold no inherent value, unless understood in the context of all of the simulations. The validation of applications of stochastic modelling is therefore most often based on the validation of certain characteristic behaviours of the underlying processes (in turn represented by the corresponding models) which are deemed to be virtually universal across case studies. Concordantly, the potential for the validation of stochastic modelling by way of sensitivity analysis is directly tied with the potential generalization of the results of sensitivity analysis. From a different perspective, the validation of stochastic modelling application requires the existence of behavioural patterns in the morphodynamical processes and/or the bed level change.

In order to assess the generalizability of the results of sensitivity analysis, both a review on existing studies on this subject in the context of bed morphodynamics (presented in section 2) and a reference/comparison case (i.e., a term of comparison regarding sensitivity analysis) to the Mondego Case Study were developed. That reference was created by applying the sensitivity analysis to a stylized straight channel (defined based on a simplification of the Mondego Case Study) and simulated using a HM model. The literature's results regarding the magnitudes of the morphodynamical sensitivities, as well as the variables' hierarchy of importance relative to morphodynamical change and the methods used in quantifying the sensitivities in the literature have been considered and compared with the case

studies' results. Based on this comparison, results of sensitivity analysis were assessed in terms of the generalization potential of the sensitivities' magnitudes and of other characteristics of the stochastic simulations.

The most commonly used measurement (in the available literature) for sensitivity in the context of the stochastic modelling of fluvial morphodynamics is the variability range. Using this statistic, the measurement of a variable's importance corresponds to the relative change in the variability range of bed level change (*dH*) which results from considering that variable's uncertainty. However, this type of measurement is both highly discrete (as it only measures the extreme values of the *dH*) and incapable of reflecting the complexities and inter-dependencies inherent to the different variables relevant for fluvial morphodynamics. For the purposes of the sensitivity analysis, each simulation's morphodynamical change was therefore summarized by a set of statistics (described below) and the variables' effects on each of these statistics was analyzed by either Independent Sensitivity Analysis (ISA) or Joint Sensitivity Analysis (JSA). Multiple statistics were used to capture and represent the complexities of fluvial morphodynamics in both ISA and JSA. Variance-based Global Sensitivity Analysis (Saltelli, et al., 2008) was used to quantify the morphodynamical joint sensitivities to the different variables (in terms of different morphodynamically-representative statistics). In addition, some other personalized techniques (such as the graphical comparisons between pairs of variables) were used to quantify other aspects of the morphodynamical sensitivities, such as the interdependencies between variables and the importance of the rivers' natural trends in comparison with its overall uncertainty.

This study on sensitivity analysis was based on data from the simulations of two case studies (described in sections 4 and 5 of this Thesis), namely, the Mondego Case Study (constructed from real-life data) and the Stylized Case Study (consisting of simplified example of a straight channel, defined based on the data from the Mondego Case Study). The purpose of the Stylized Case Study was to provide a term of comparison (i.e., a control-case) for the results of the sensitivity analysis obtained for the Mondego Case Study. The analysis of a simplified/stylized case study is intended to reduce the effects of the complexity of fluvial morphodynamics (in particular its natural tendencies in terms of bed level evolution), thereby producing a clearer description of the relationships between the variables and morphodynamics, as well as, the corresponding morphodynamical sensitivities. Additionally, the clearer nature of the results also lends itself to the production of more informative analyses using appropriate sensitivity analysis tools. This is because, in more intricate case studies, the superposition of morphodynamical effects can obscure the results of sensitivity analysis.

6.1. MONDEGO RIVER

The purposes of the application of sensitivity analysis to the Mondego Case Study were two-fold, namely, to study the relationship between fluvial morphodynamics and the simulated variables and to validate the results of the stochastic modelling performed as part of this work. The sensitivity analysis of the Mondego Case Study was based on the simulations' results for the study reach of the river. Based

on in-situ observations, the study reach is known to be very active (from a morphodynamical point-of-view), providing therefore a good foundation for the sensitivity analysis of fluvial morphodynamics.

The sensitivity analyses was based on two main principles, namely:

- Using both ISA and JSA to outline each variable's individual relative importance and to represent the variables' respective interdependencies pertaining to their effects on morphodynamics;
- Computing multiple statistics in order to fully characterise morphodynamical change (i.e., *dH*), thereby developing a more complete description of the complexities involved in morphological processes.

The variables considered in this analysis were the streamflow (*Q*), bed roughness (*n*) and granulometry (*D*) variables. In most cases, a variable's importance to a given process can generally be estimated based on the part of that processes' uncertainty which is due to that variable's uncertainty. However, this does not imply that a processes' variability can be entirely described by a collective representation of all of the process-relevant variables. This same fact holds true for fluvial morphodynamics. Due to the strong time-dependency of morphological processes, a river's natural morphodynamical tendencies also play an important role in the definition of morphodynamical variability. Accordingly, in this study, as part of the ISA, some measurement statistics were developed in order to represent the influence of the natural tendencies of the Mondego river in the channel's overall morphodynamical change as a proportion of the simulated variables' importance.

Aside from *dH* (which, as previously referred, was decomposed into multiple statistics), the three variables' values/series/curves were represented by the same three statistics selected in section 5.1.2 (as part of the DS and CS stages of the stochastic modelling). These statistics have already been observed to produce a good representation of their respective variables' characteristics in the context of fluvial morphodynamical modelling and can therefore be used in the graphical JSA analysis.

In order for the extensive information on simulated bed level change (*dH*) across the channel (which results from the stochastic modelling) to be usable for sensitivity analysis, it must be summarized using a series of statistics. Each of these statistics is meant to represent a quantification of a feature of the morphodynamical behavior for each simulation (each simulation would therefore have one value for each individual statistics). While a single general statistic (such as the mean *dH*) may be able to capture the overall behaviour of morphodynamics, it is possible for different variables to affect different aspects of morphology differently, at which point the use of multiple statistics is necessary. In order to compensate for this fact, a variety of different statistics was used. The statistics used to represent the different aspects of *dH* (defined for an *n* number of grid nodes, in this case equal to 4000) are:

- Overall mean absolute *dH* (OMAC, corresponding to the mean value of the absolute dH measured over/along the entire channel – Eq. 7);

$$\text{OMAC} = \frac{1}{n}\sum_{i=1}^{n}|dH_i|, for\ n\ grid\ nodes \quad \text{Eq. 7}$$

- Overall mean *dH* (OMC, similar to OMAC but in relative terms, corresponding to the mean value of the *dH* measured over/along the entire channel – Eq. 8);

$$\text{OMC} = \frac{1}{n}\sum_{i=1}^{n} dH_i, for\ n\ grid\ nodes \quad \text{Eq. 8}$$

- Percentage of channel area flooded (PFA). The percentage of the simulated area (measured as projected in a horizontal plane) wetted during the flood events, represented in Eq. 9;

$$\text{PFA} = \frac{1}{n}\sum_{i=1}^{n}\begin{cases}0\ , if\ dH_i = 0\\ 1\ , if\ dH_i \neq 0\end{cases} \quad \text{Eq. 9}$$

- Harmonic mean absolute *dH* (HMAC, similar to OMAC but measured with a harmonic mean instead of an arithmetic mean, corresponding to the harmonic mean value of *dH* measured over/along the entire channel – Eq. 10);

$$\text{HMAC} = \frac{n}{\sum_{i=1}^{n}\frac{1}{dH_i}}\ , for\ n\ grid\ nodes \quad \text{Eq. 10}$$

- Localized mean absolute *dH* (LMAC, similar to OMAC but measured solely in areas where the *dH* is non-null, consisting of the mean absolute *dH* in the channel, measured where $dH \neq 0$ – Eq. 11);

$$\text{LMAC} = \frac{1}{\sum_{i=1}^{n}\begin{cases}0\ , if\ dH_i = 0\\ 1\ , if\ dH_i \neq 0\end{cases}}\sum_{i=1}^{n}|dH_i|, for\ n\ grid\ nodes \quad \text{Eq. 11}$$

- Localized mean *dH* (LMC, similar to LMAC by in relative terms, consisting of the mean *dH* in the channel, measured where $dH \neq 0$ – Eq. 12). This statistic serves as an indication of the average tendency of *dH* (i.e., towards erosion or sedimentation);

$$\text{LMC} = \frac{1}{\sum_{i=1}^{n}\begin{cases}0\ , if\ dH_i = 0\\ 1\ , if\ dH_i \neq 0\end{cases}}\sum_{i=1}^{n} dH_i, for\ n\ grid\ nodes \quad \text{Eq. 12}$$

- Spatial variability of morphodynamics (a measurement of the spatial irregularity of *dH*, as defined by the 2nd order variability/derivate of *dH* in the longitudinal and transversal direction – MASV – Eq. 13): corresponds to the average 2nd order differentiated dH along the grid (designated as $\Delta^2 dH_{i,j}$, for grid node *i*, *j*, corresponding to the curvature of *dH*), standardized by the *dH*'s variance (i.e., $\text{Var}(dH)$, thereby being adimensional). Larger values of this statistic indicate that the discontinuity

of *dH* (represented by elevated curvatures in *dH*), relative to the overall variability of *dH*, is larger and vice-versa;

$$\mathrm{MASV} = \left(\frac{1}{n'} \times \sum_{i=2}^{n^t-1} \sum_{j=2}^{n^l-1} \left(\Delta^2 dH_{i,j} \right)^2 \right) \Big/ \mathrm{Var}(dH) \qquad \text{Eq. 13}$$

where n^l and n^t refer to the number of grid nodes in the longitudinal and transversal direction and n' corresponds to the number of nodes where the $\Delta^2 dH$ can be calculated (viz., which have other grid nodes around them).

- PDF rankings of *dH* (PDFR, identical to the statistic adopted in section 5.1.2 in order to represent the variability of *dH*).

Examples of the values of these values for specific simulations can be found in section 6.2. Aside from the previously enumerated statistics, other statistics were also experimented with, such as a mean spatial variability of morphodynamics or a standardized *dH*. However, no other statistics was found to both be important for the representation of fluvial morphodynamics and to provide additional information regarding the variables' hierarchy. Generally speaking, non-absolute statistics (such as the OMC and LMC statistics) were deemed to provide less reliable representations of morphodynamical change, as measured by their correlation with the morphodynamically representative variables, both in the previous section 5.1.2 and in this sensitivity analysis.

6.1.1. Independent Sensitivity Analysis

In this section, the individual effects of the three selected morphodynamically-relevant variables on the Mondego Case Study's study reach were characterized and quantified. This particular goal was accomplished by way of the visual analysis of the relationship between the different variables' representative statistics (determined in section 5 of this Thesis) and the different morphodynamically representative statistics (presented in section 6.1). These graphical comparisons, describing the mean overall effect of each variable in the morphodynamical statistics (obtained by averaging the statistics for the simulations with identical variable's values), are presented in Figure 64 through to Figure 71. While an overall assessment of the variability range induced in each morphodynamical statistic (summarized in Table 10) can already provide some information on the morphodynamical sensitivities, visual analysis of these plots can provide additional information. Oftentimes, the relationships between the pairs of statistics/variables can be less clear, be it because of the statistics' or the variables' nature. Nonetheless, some relevant conclusions can be drawn from this analysis:

- Generally speaking, *Q* has a positive correlation with the overall morphodynamical change, as can be observed for the vast majority of the statistics (with the exception of HMAC). On the other hand, the other two variables (i.e., *D* and *n*) have negative correlations with most morphodynamically representative statistics;

- *D* and *n* displayed the most irregular/non-monotonic behaviour in terms of the different morphodynamical statistics analysed. This is most likely a result of the natural complexity of *D* as a variable and of the spatial variability of *n*. Nonetheless, the statistics selected to represent these two variables in this study still performed well for multiple statistics;
- *Q* was observed to be, by a large margin, the main determining factor for the PFA indicator. This result implies that the streamflow is virtually the only variable which influences the maximum water level (with a small contribution from *n*) reached during the simulations, thereby determining the area of the river which is exposed to morphodynamical change;
- The HMAC statistic in particular (and, to a significantly lesser extent, also the OMC and LMC statistics) is the morphodynamic statistics which produces the least visible relationship with the selected variables. This may a result of the complexity of the statistic or an indication of the statistics' unsuitability for representing morphodynamical change in the context of the stochastic modelling of fluvial morphodynamics;
- The PDFR statistic exhibits the clearest relationship with the morphodynamically-relevant variables, particularly regarding the *Q* and *D* variables. This was to be expected, given that this statistic was selected in section 5.1.2 to represent morphodynamical change and as a criteria for selecting the variables' representative values in the stochastic simulations performed in this study.
- Looking at the variability ranges of the different statistics (induced by each of the variables; presented in Table 10), the results generally attribute a larger relative importance to the *Q* variable (in comparative terms). Simultaneously, *n* was observed to produce the smallest impact in the statistics, with *D* displaying an intermediate effect.

Table 10 – Summary of each variables' effects on the morphodynamical statistic, measured by the corresponding induced variability ranges and standard deviations.

		OMAC	OMC	PFA	HMAC	LMAC	LMC	MASV	PDFR
Q	Range	0.234	0.121	0.163	0.0034	0.219	0.113	0.16	138.1
	SD	0.089	0.046	0.064	0.0013	0.085	0.043	0.06	53
D_m	Range	0.196	0.034	0.0046	0.0028	0.235	0.042	0.13	82.1
	SD	0.07	0.012	0.0019	0.001	0.084	0.015	0.047	29.3
n	Range	0.025	0.013	0.016	0.0013	0.034	0.017	0.017	23.7
	SD	0.0096	0.0048	0.0063	0.0005	0.013	0.0064	0.0062	8.9
Ranking of importance (SD & Range)	Most I.	*Q*	*Q*	*Q*	*Q*	D_m	*Q*	*Q*	*Q*
	...	D_m	D_m	*n*	D_m	*Q*	D_m	D_m	D_m
	Least I.	*n*	*n*	D_m	*n*	*n*	*n*	*n*	*n*

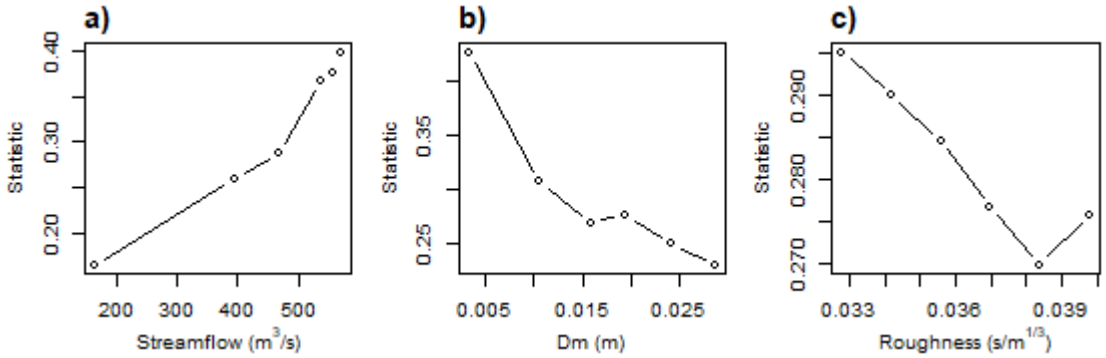

Figure 64 – Relationship between the OMAC statistic and the different variables, namely, *Q* in plot a, *D* in b and *n* in c.

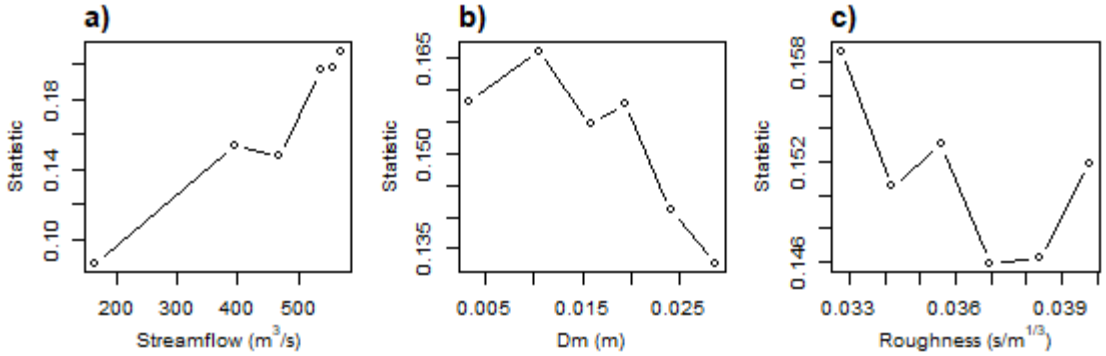

Figure 65 – Relationship between the OMC statistic and the different variables, namely, *Q* in plot a, *D* in b and *n* in c.

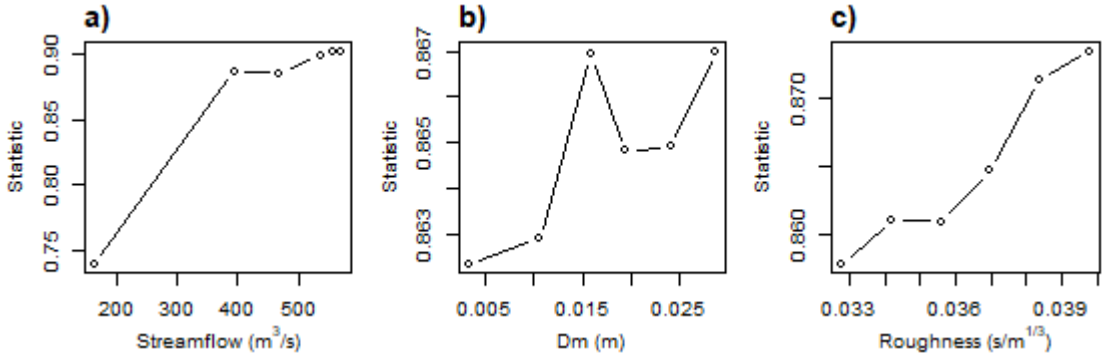

Figure 66 – Relationship between the PFA statistic and the different variables, namely, *Q* in plot a, *D* in b and *n* in c.

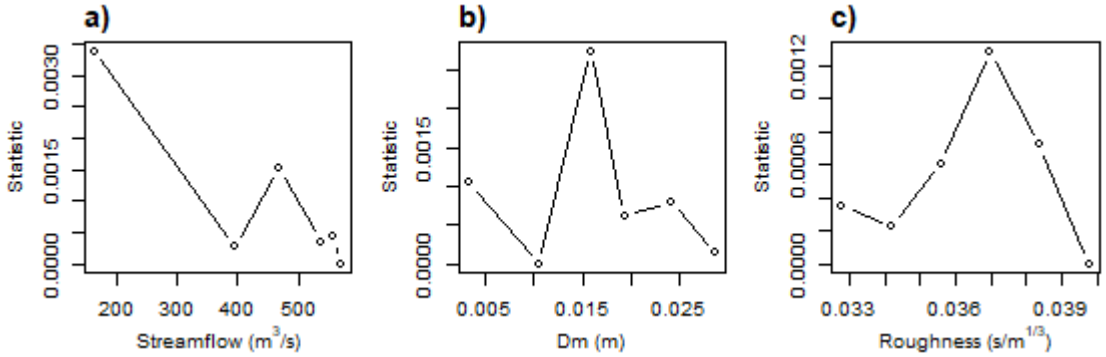

Figure 67 – Relationship between the HMAC statistic and the different variables, namely, *Q* in plot a, *D* in b and *n* in c.

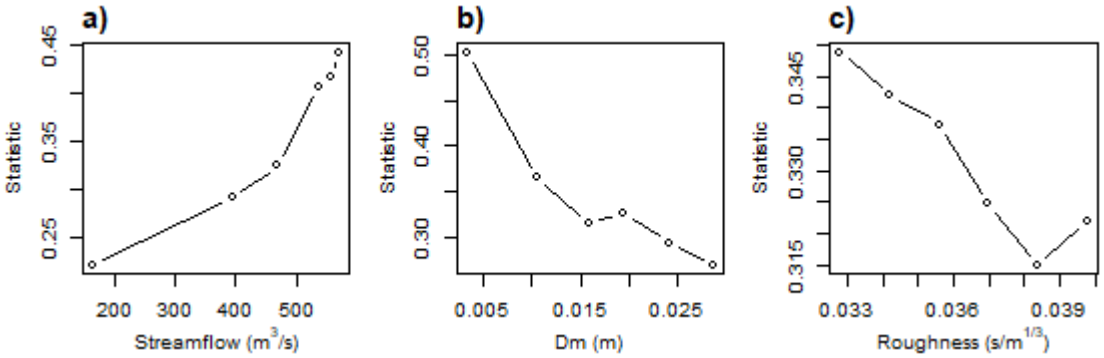

Figure 68 – Relationship between the LMAC statistic and the different variables, namely, *Q* in plot a, *D* in b and *n* in c.

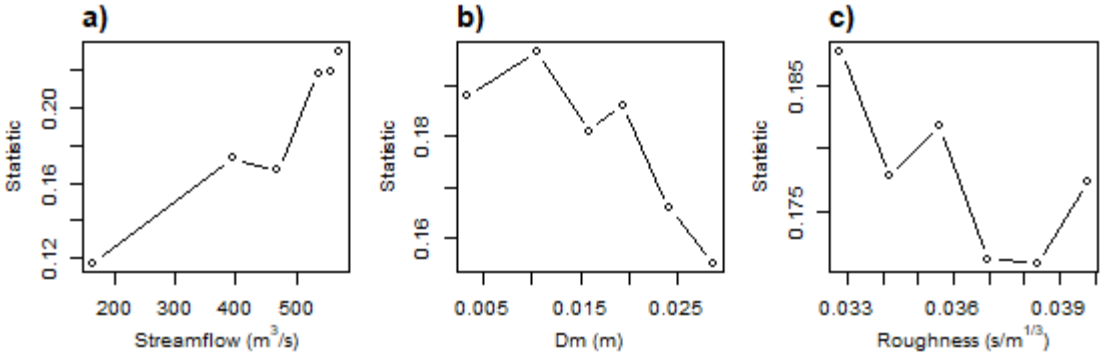

Figure 69 – Relationship between the LMC statistic and the different variables, namely, *Q* in plot a, *D* in b and *n* in c.

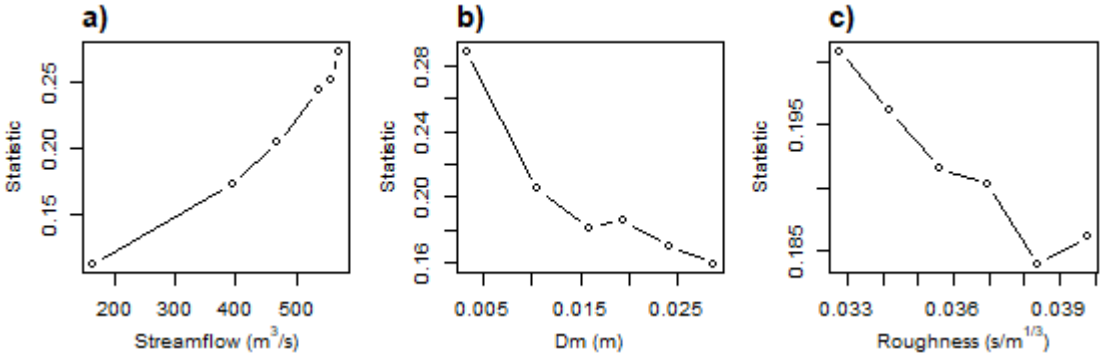

Figure 70 – Relationship between the MASV statistic and the different variables, namely, *Q* in plot a, *D* in b and *n* in c.

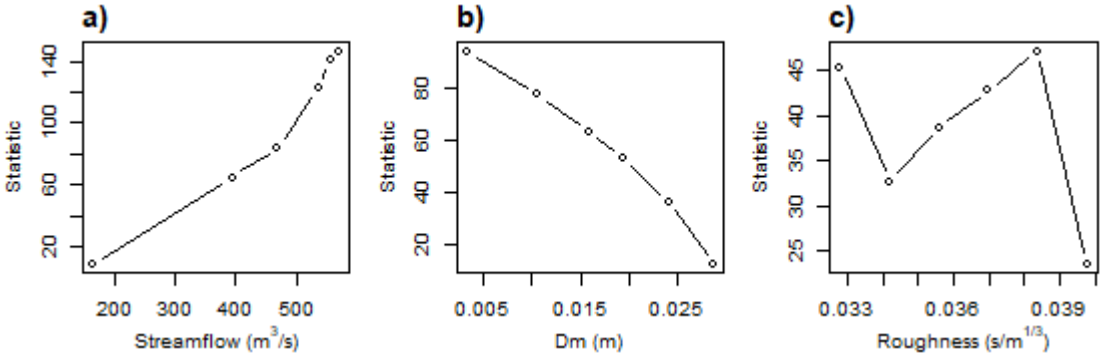

Figure 71 – Relationship between the PDFR statistic and the different variables, namely, *Q* in plot a, *D* in b and *n* in c.

As part of the ISA, a few different approaches were tested in order to assess the variables' overall importance in comparison with the river's natural tendencies. The objective was to estimate which

proportion of the study reach's overall *dH* is due to the selected variables' values and which proportion of that *dH* is due to the river's natural evolutionary tendencies, i.e., the temporal dependency of morphodynamical processes and morphodynamical *dH*. The natural tendencies of a channel's evolution can be simply understood as its mean evolution over time. Naturally, deviations from this mean evolution can be assumed to be a result of the selected variables' influence. Based on these concepts, the following approaches were adopted to define the relative importance of the variables and the channel's natural tendencies:

- Using function fitting: For each grid cell, the *dH* values obtained from the 216 simulations (defined in section 5.1.2.3) were fitted by a multi-linear model (with a form similar to Eq. 14) in order to determine each variables' fitting coefficients. The variables' resulting three coefficients (a, b and in Eq. 14) and the constant parameter (d in Eq. 14 representative of the channel's natural tendencies) were averaged out over all of the grid nodes and their normalized value represents their relative importance. While this estimate disregards the non-linear relationships between the different variables and morphodynamics, it does provide an approximate description of the morphodynamical sensitivities to the variables and its evolutionary dependency.

$$dH_i = a \times Q + b \times D_m + c \times n + d, for\ grid\ cell\ i\ \&\ parameters\ a, b, c\ and\ d \quad \text{Eq. 14}$$

- Using variance-based statistics: For each grid cell, the First Order Indexes (FOIs) of *dH* were calculated for each of the variables. The FOIs can be calculated using the formula in Eq. 1. The comparative importance of the channel's natural tendencies in each cell was defined by the inverse of the coefficient of variation (which is also a variance-based measurement, like the FOI). Averaging these statistics over all of the simulations and normalizing their values (the FOIs and the inverse coefficient of variation) produces the relative magnitudes of the importances of the variables and the natural tendencies of the river.
- Using range-based statistics: The importance of the individual variables corresponds to, for each simulation, the mean variability ranges induced by each variable on *dH* (calculated for each grid cell and then averaged along the grid), normalized by the variability range of the mean *dH* over all of the simulations. The importance of the channel's natural tendencies is calculated by the average of the mean *dH* for each simulation divided by the corresponding variability range. Averaging these statistics over all of the simulations and normalizing their values produces the corresponding relative importances. Given that this measurement is based on the variability ranges (which are defined by the most extreme scenarios of the variables' influence on morphodynamics), this range-based estimate will naturally attribute the smallest importance to the channel's natural tendencies, in comparison with the other two approaches.

The results of these approaches are displayed in Figure 72. As can be observed, the importance of the natural tendencies of this study reach's morphodynamical behaviour can vary between 20 and 25%, representing a sizable proportion of the channel's morphodynamical forcings. None of the approaches

can be directly excluded from the results as their respective estimates are valid from the perspective of their respective criteria. The hierarchy of the variables' importance remained approximately the same for all of the selected approaches.

The relative importances of the different variables, and, particularly, their relationship with morphodynamics may well remain unchanged for different simulations periods. Nevertheless, over time (i.e., for longer or shorter simulation periods), the relative importance of the channel's natural tendencies for the morphodynamical change is likely to vary. Further studies on the convergence or divergence of stochastic morphodynamics (performed, to some extent, in section 7.4) may provide some insight on whether this relative importance is likely to increase or decrease.

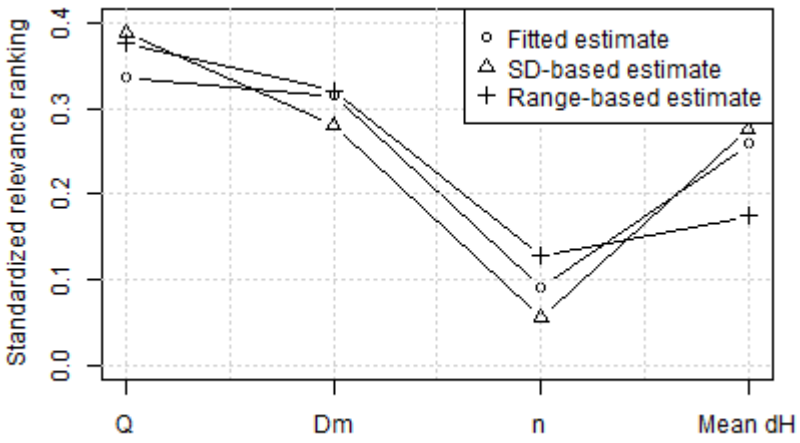

Figure 72 – Comparison of the different estimates of the relative variable importance as a proportion of the natural tendencies of the study reach's morphodynamics.

6.1.2. Joint Sensitivity Analysis

The purpose of the JSA is to estimate the selected variables' importance (i.e., relative to one another), while taking into consideration their interdependencies and correlations in the context of fluvial morphodynamics. The JSA was based on the calculation of the Total Effect Indexes (TEIs) (Saltelli, et al., 2008) and the graphical pairwise comparisons of the variables' mean effects on *dH*.

The TEIs can be calculated using the formula in Eq. 2 and corresponds to a variance-based measurement of the effect (on morphodynamical sensitivities) of removing the uncertainty of a specific variable, indirectly providing an estimate of that variable's importance for morphodynamics. The TEIs' values for the different variables, calculated for the study reach and for the study segment, are presented, respectively, in Figure 73 and in Figure 74. Given the stochastic nature of the sensitivity analysis, only when there are significant differences between the values of TEIs for the different variables, can a proper hierarchy be deduced between them.

The pairwise graphical comparisons of the variables' effects on morphodynamics represent the effects of the two variables on the corresponding statistic by averaging the *dH* along the third variable (as is mathematically represented in Eq. 15). Accordingly, while these comparisons are only capable of

providing a qualitative analysis of sensitivities, they are capable of capturing more complex relationships between the variables (i.e., their interactions/interdependencies in the context of morphodynamics). The TEIs can be understood as providing a summary of the global behaviour displayed in the graphical comparisons. These pairwise graphical comparisons are presented in Figure 75 to Figure 78.

$$Y_{i,j} = E\left[Y \mid \mathbf{X_{k,l}}\right], where\ i,\ j,\ k,l\ \in \{D_{50}, n, Q, \Delta Q_s\} \quad \text{Eq. 15}$$

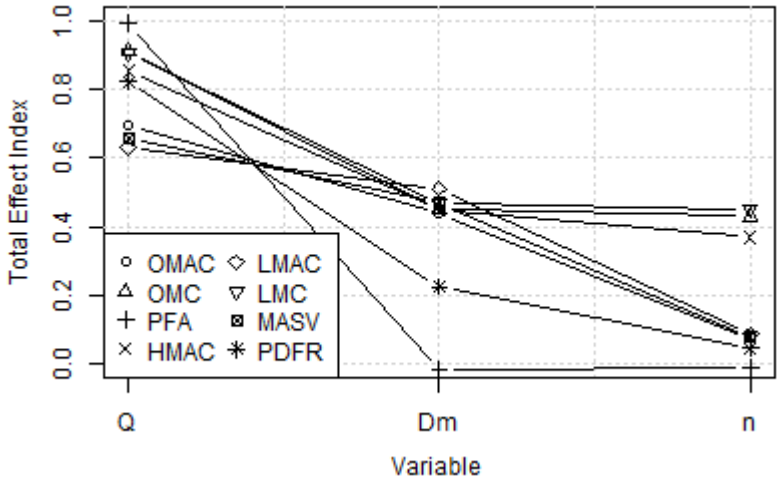

Figure 73 – TEI values for each of the different variables (in the x-axis) and for each of the statistics (defined for the entire study reach).

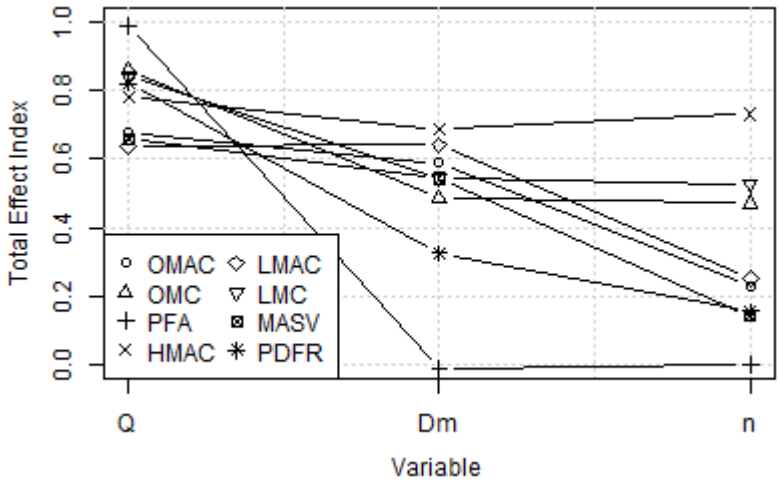

Figure 74 – TEI values for each of the different variables (in the x-axis) and for each of the statistics (defined solely for the study segment).

Regarding the results of the TEIs, *Q* was generally observed to be the most important variable for the definition of the morphodynamical uncertainty, oftentimes displaying twice the magnitude of the importance (measured in terms of TEI) as the other variables. In a smaller scale analysis (i.e., of the study segment), *Q* was observed to have a smaller overall importance. This indicates that the selection of the area of the reach is important for the results of the sensitivity analysis. As an example, given that, for the study segment, the *Q*'s importance is comparatively less, it is likely that for other areas of the study reach (i.e., outside the study segment) it allocates an even larger importance to the *Q*'s uncertainty.

Regarding the *D* and *n* variables, the results are very similar between the study reach and the study segment. In terms of the OMC, PFA, HMAC and LMC statistics, the variables possess virtually identical importances. Regarding the OMAC, LMAC, MSAV and PDFR statistics, *D* displays a larger importance than *n*. These results demonstrate the importance of considering multiple statistics when analysing fluvial morphodynamics, as different variables can impact different aspects of morphology differently.

For reference purposes, the main criteria for interpreting the information represented in the pairwise graphical comparisons of Figure 75 to Figure 78 is as follows:

- The more perpendicular the contour lines are to a given axis, the more important the corresponding variable is to the morphodynamical statistic under analysis;
- Very irregular contour lines are strong indicators of an independence between the variables' effects regarding that particular morphodynamical statistic. Generally speaking, situations like this occur when the inherent complexity and aleatory nature of morphodynamical change is more significant than the variables' relationship in determining the statistics' values;
- Continuous contour lines (i.e., where a clear pattern can be observed in their progression as a function of the variables) are indicative of an observable, potentially replicable and structured relationship between the variables' effects.

The natural uncertainty of the stochastic processes which were evaluated with sensitivity analysis is also present in the pairwise graphical comparisons. Consequently, if some variables have a (very) weak relationship between them, this uncertainty will still cause their relationship to be displayed as independent (corresponding to the second criteria for interpreting the pairwise graphical comparisons previously referred). Nevertheless, for the purposes of this sensitivity analysis, this type of relationship will still be counted as independent.

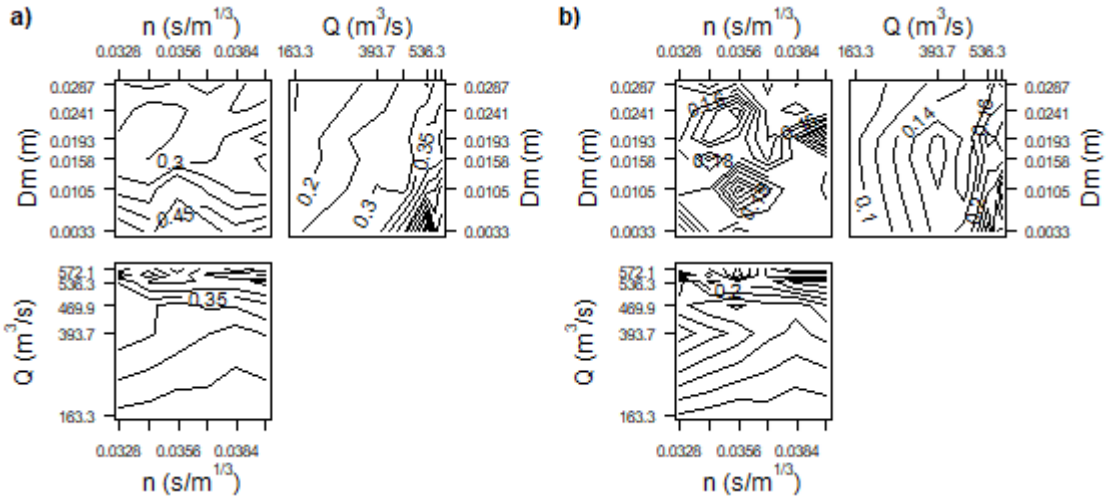

Figure 75 – Pairwise comparison of the variables effects on the OMAC (in plot a) and OMC (in plot b) statistics.

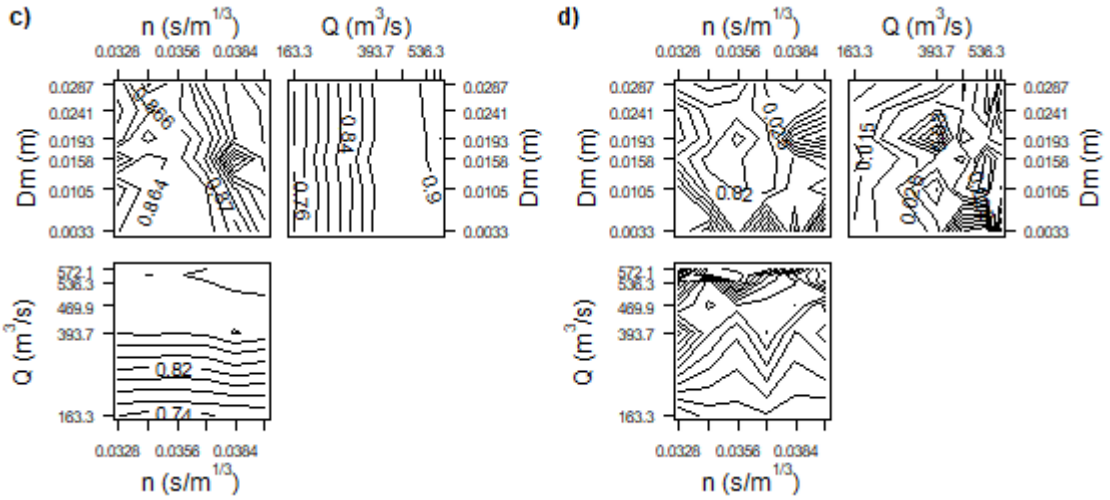

Figure 76 – Pairwise comparison of the variables effects on the PFA (in plot a) and HMAC (in plot b) statistics.

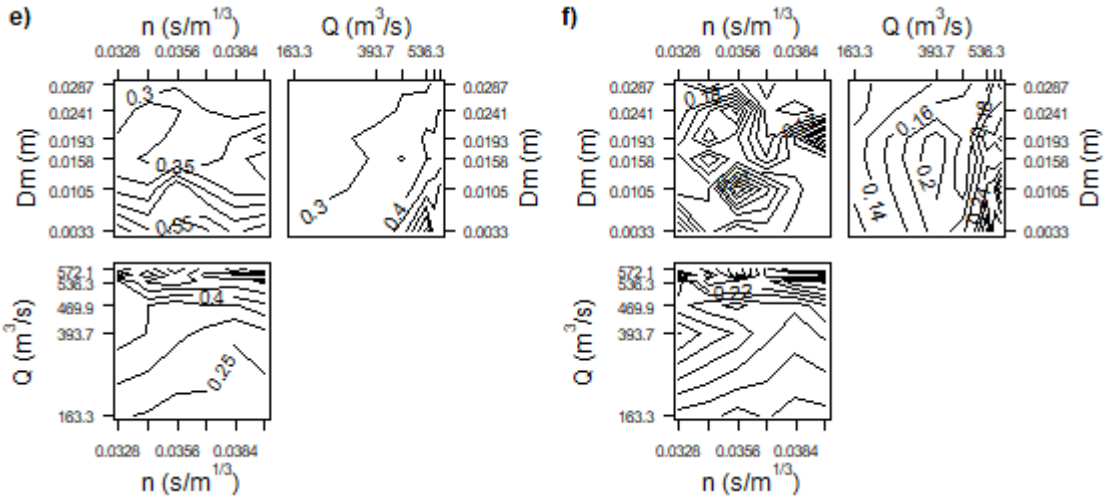

Figure 77 – Pairwise comparison of the variables effects on the LMAC (in plot a) and LMC (in plot b) statistics.

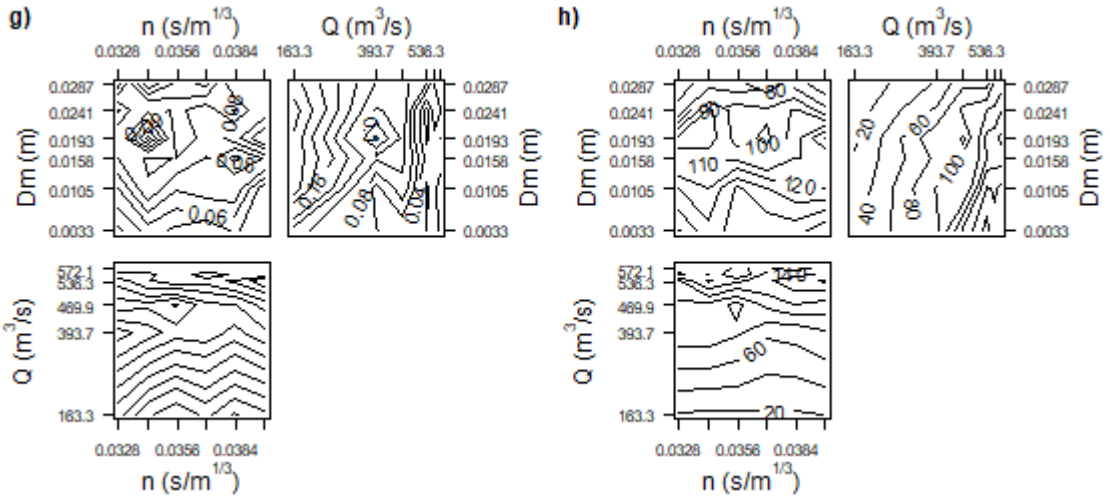

Figure 78 – Pairwise comparison of the variables effects on the MASV (in plot a) and PDFR (in plot b) statistics.

While some of the relationships demonstrated in the plots are relatively less clear than others, this is likely to be a natural consequence of the uncertainty in JSA and the complexity of the morphodynamical processes (which is likely to be even more relevant in a real fluvial environment).

The results of the pairwise graphical comparisons approximately confirm the results of the TEIs regarding the relative importance of the variables. Nonetheless, the results indicate, for several statistics (such as OMAC, LMAC, MASV and PDFR), a significant non-linear dependency between Q and D regarding their effect on fluvial morphodynamics. Furthermore, regarding certain aspects of morphodynamics (represented by the OMC, HMAC and LMC statistics), granulometry and bed roughness appear to be virtually independent.

Finally, it should be noted that while two variables may always be, to some extent, interdependent (regarding their respective effects on morphodynamics), these results clearly indicate that one variable's effects can overcome another variable's effects. After a variable's magnitude goes beyond a certain level, the other variables can lose importance in the global description of morphodynamics. Examples of this behaviour can be observed in the comparisons of the D and Q variables regarding the OMAC, LMAC and MASV statistics (Figure 75a, Figure 77a and Figure 78a). In these cases, after the Q rises above $\approx 500\ m^3/s$, the D variable virtually loses its effect on morphodynamics (relatively speaking).

6.2. STYLIZED CHANNEL

Similar to the sensitivity analysis performed based on the Mondego Case Study, the analysis of the simulations performed with the Stylized Case Study were separated into an independent sensitivity analysis (ISA) and a joint sensitivity analysis (JSA). The sensitivity analysis of the Stylized Case Study is, first and foremost, meant to provide a term of comparison for the sensitivity analysis of the Mondego Case Study. The comparison of the two case study's results, as well as, the comparison with other examples of the sensitivity analysis of morphodynamics available in literature (presented in section 2), is intended to both provide an understanding on the variables' interactions with morphodynamics and provide a reference point for the validation potential of the results of the stochastic modelling of fluvial morphodynamics. In addition, the simplified nature of the Stylized Case Study (in terms of the definition of the related variables and of the simulations themselves) should help to clarify the relationships between the variables and their impact on fluvial morphodynamics and reduce the effects of the stochastic uncertainty in sensitivity analysis. This application of sensitivity analysis was first systematized and discussed in one of the journal articles prepared in the context of this study (Oliveira, et al., s.d.).

Based on the criteria described in section 2.2, the most morphodynamically-relevant variables were selected. Accordingly, the uncertainty in fluvial morphodynamics was represented by taking into consideration the uncertainties from the channel's granulometry (represented by its median diameter D_{50}), the channel's bed roughness (represented by the Manning's roughness parameter n), a flood magnitude parameter Q^* (which defines the intensity of the flood event simulated) and the uncertainty

in the sediment input at the upstream boundary (represented by its deviation ΔQ_s from its value as estimated with the Wu et al. formula (Wu, et al., 2000)).

The ISA focused on describing the relationship between the channel's morphodynamics and each of the different variables, namely, the characteristics of the relationship (e.g., linear/non-linear) and the respective magnitudes (in terms of bed change) of the variables' individual effects in the channel's morphodynamics. The individual effects of each variable, as it pertains to morphodynamical change, were analyzed along the corresponding variability ranges (as estimated from the Mondego river's data) so as to represent the relationship between the variables and morphodynamics.

Regarding the JSA, the objective was to assess the relative sensitivities and respective inter-dependencies for the different variables regarding a variety of different aspects (based on variance based global sensitivity analysis (Saltelli, et al., 2008)). Multiple combinations of values of the different variables (selected from the distributions presented in Figure 50 from section 5.2.2) were simulated in order to represent not only their relative importance for fluvial morphodynamics but also to take into account the variables and respective sensitivities' inter-dependencies. The statistics analysed in the JSA were:

- Overall mean absolute *dH* (OMAC, corresponding to the mean value of the absolute *dH* measured over/along the entire channel – Eq. 7);
- Localized mean absolute *dH* (LMAC, similar to OMAC but measured solely in areas where the *dH* is non-null, consisting of the mean absolute *dH* in the channel, measured where $dH \neq 0$ – Eq. 11);
- Mean absolute *dH* in the central channel (CMAC) and in the banks (BMAC): similar to OMAC but measured solely in the centre and banks of the channel, respectively corresponding to the central 7 nodes and the outermost 8 grid nodes;
- Percentage of channel area flooded (PFA). The percentage of the simulated area (measured as projected in a horizontal plane) where the water reached during the flood events, represented in Eq. 9. This value is measured as the percentage of the channel area where *dH* is non-null (because, computationally, any area which is flooded is subject to, even if only to a very small degree, erosion);
- Spatial variability of morphodynamics (a measurement of homogeneity/entropy of bed change, defined by the absolute mean spatial alteration of *dH* – MASV – Eq. 13): corresponds to the mean difference between the *dH* magnitude of consecutive nodes

The formulas presented describe the method for calculating the each of the statistics for each of the individual simulations. All of these statistics were analyzed in the context of the JSA. The ISA, on the other hand, was performed based solely on the LMAC and LMC statistics. Other statistics considered (such as the standardized *dH*) were also calculated but they were observed to not provide any additional, useful information for the classification of the different variables regarding their relative importance for fluvial morphodynamics.

As an example of the results obtained, Figure 79 displays three random examples of simulations with parameters {3, 2, 2, 1}, {4, 5, 7, 3} and {5, 7, 7, 5} (according to the notation defined in section 5.2.2, where each of the numbers corresponds, respectively, to the D_{50}, n, Q^* and Δ_{Qs} values, in rising order of magnitude of the corresponding induced dH). The corresponding OMAC, LMAC, CMAC, BMAC, PFA and MASV statistics are presented in Table 11.

Table 11 –Values of the statistics for the {3, 2, 2, 1}, {4, 5, 7, 3} and {5, 7, 7, 5} simulations performed in this study.

Simulations	OMAC (m)	LMAC (m)	LMC (m)	CMAC (m)	BMAC (m)	PFA (---)	MASV (---)
{3, 2, 2, 1}	0.0012	0.0025	-0.0022	0.0025	0	0.464	0.955
{4, 5, 7, 3}	0.0020	0.0028	0.0002	0.0044	2.67×10^{-5}	0.723	0.707
{5, 7, 7, 5}	0.0008	0.0011	0.0011	0.0017	1.13×10^{-5}	0.731	0.486

On average over all of the simulations, dH in the channel tends towards erosion. While both generalized erosion and generalized sedimentation cases are present, simulations involving erosion have generally higher magnitudes of dH. In addition, a significant portion of dH tends to concentrate in the vicinity of the model's boundaries. Both of these effects are likely a result of the previously referred (in section 5.2.1) imperfections in the definition of the model's boundary conditions. However, because the purpose of these simulations is the simplified representation of a real channel (and not of an idealized channel), these imperfections do not affect the satisfaction of the goals for this Stylized Case Study. The existence of underlying trends is to be expected in any natural river channel, such as the one which the Stylized Case Study is intended to represent.

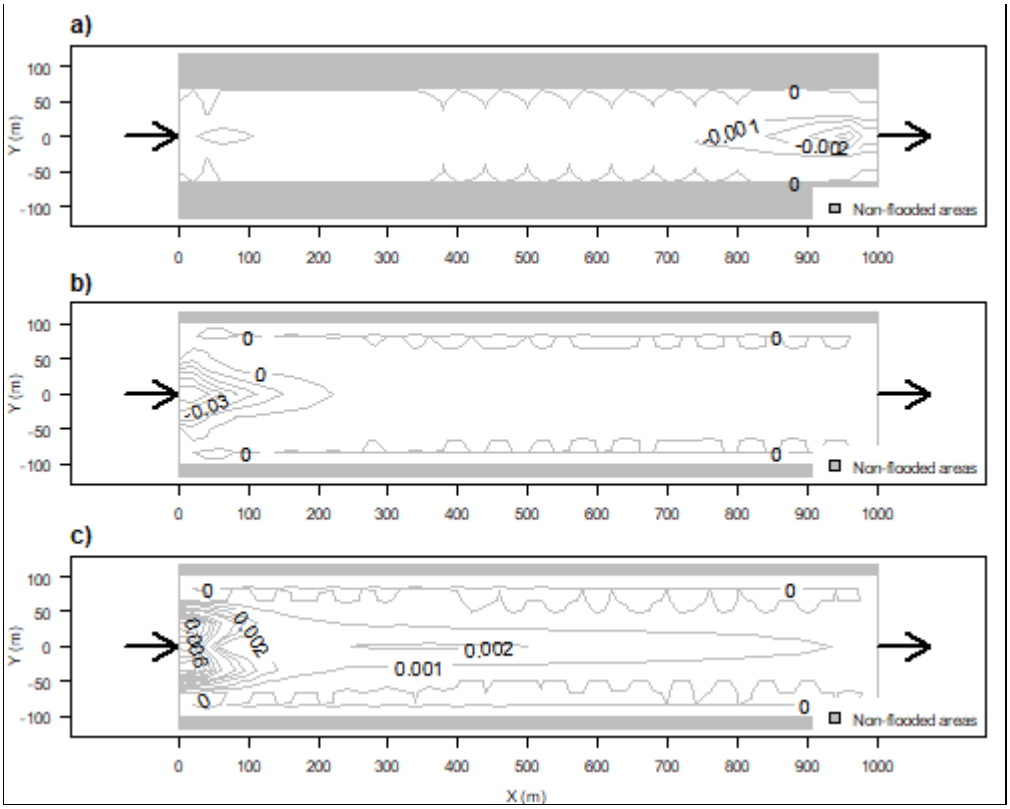

Figure 79 – Bed level change for parameters {3, 2, 2, 1} in plot a, {4, 5, 7, 3} in plot b and {5, 7, 7, 5} in plot c.

As can be observed, the first and second examples (for parameters {3, 2, 2, 1} and {4, 5, 7, 3}) have very similar LMACs but very different OMACs. This is a result of the smaller *Q* and *n* values from the second example, which reduce the area affected by *dH* (with a smaller PFA in the former relative to the latter), resulting in the same average magnitude of *dH* but different average *dH* channel-wide. The CMAC and BMAC statistics confirm a concentration of morphodynamical change in the center of the channel in the first example relative to the second. The MASV decreases successively from the first to the last case, as the *dH* shifts from a more intense and concentrated (and thereby irregular) distribution in the first case ({3, 2, 2, 1}) to a more widespread and continuous distribution in the last example ({5, 7, 7, 5}). The choice of statistics performed in this study is meant to capture these different aspects of morphodynamics for the evaluation of morphodynamical sensitivities.

Across the simulations, the values of the selected statistics can vary significantly. Table 12 summarizes the range of values of these statistics for the 2401 simulations performed.

Table 12 –Range of potential values of the statistics for the simulations performed in this study.

	OMAC (m)	LMAC (m)	LMC (m)	CMAC (m)	BMAC (m)	PFA (---)	MASV (---)
Minimum	2.03E-05	4.38E-05	-0.113	4.35E-05	0.0000	0.46	0.433
Maximum	7.56E-02	1.20E-01	0.003	1.61E-01	0.0015	0.73	2.099

The sensitivity analysis of the simulations performed in this study was separated into an ISA and a JSA.

While the values of these statistics are relatively small, this is to be expected considering that they pertain to the effects of single flood events (which are naturally limited in terms of their morphodynamical capacity). In addition, these are average statistics, meant to characterize the reach as a whole and not the more extreme values of *dH*. Further discussion on these results can be found in section 6.3.

6.2.1. Independent Sensitivity Analysis

The individual effects produced by the different variables were assessed in terms of the localized mean absolute *dH* and the localized mean *dH* (LMAC and LMC, respectively). The independent sensitivity to each variable was measured by setting the remaining three variables to their median value (e.g., the representative LMAC and LMC values for the granulometry {1, x, x, x} is obtained by setting the values of the *n*, *Q*, and Δ_{Qs} variables to the 50th quantile of their PDFs, i.e., to values {x, 4, 4, 4). Figure 80 presents the relationship between the simulated *dH* and each of the different variables.

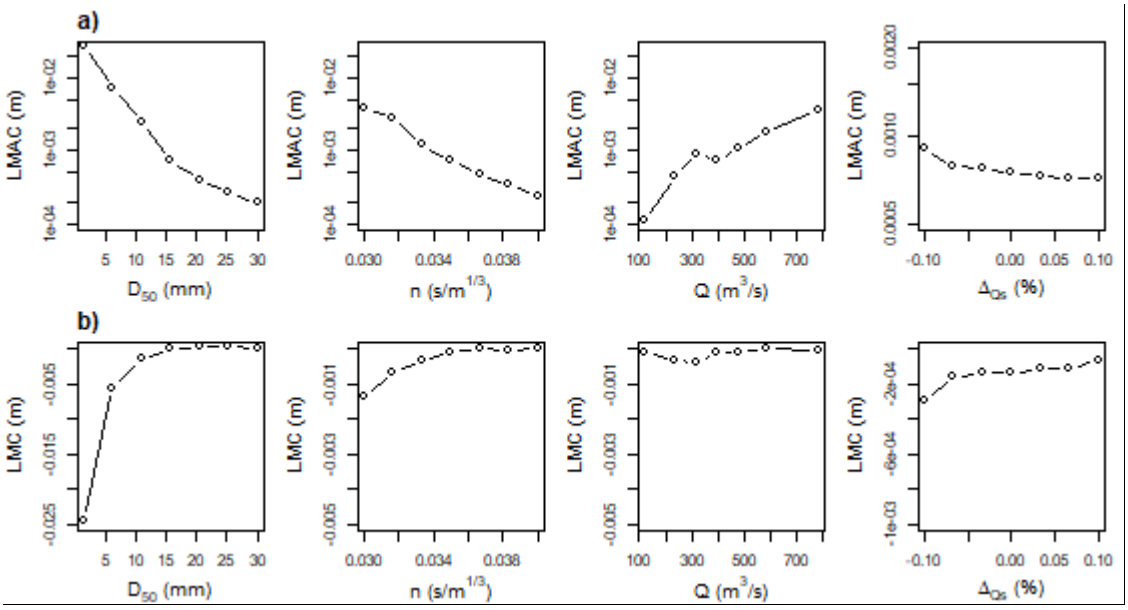

Figure 80 - Comparison of the individual effects exerted by the variables in the channel's *dH* (measured in terms of the LMAC statistic, in plot a, and the LMC statistic, in plot b). In order to facilitate the reading of the data, the y-axis in plot a was defined in log scale and the y-axis in plot b has a varying size scale.

The relationships between the morphodynamics and the selected variables can be clearly observed in Figure 80. It is clearly non-linear (potentially following an exponential/power decay for most cases except the *n*'s relative to LMAC and the *Q*'s relative to LMC), albeit its shape for the Δ_{Qs} variable is only observable on a smaller scale. Considering that the channel's natural tendency leans towards erosion, the D_{50}, *n* and Δ_{Qs} variables are inversely correlated with the LMAC statistic, while the *Q** variable is directly correlated with LMAC. If the channel's *dH* tendency was towards sedimentation, the relationship between *dH* and *Q** would most likely be reversed. In terms of the LMC statistic, the effects of the *Q** variable in particular grow more complicated and the variable itself clearly loses a significant amount of importance, relative to the other variables.

In terms of the morphodynamical sensitivities, the variables' hierarchy regarding LMAC is not entirely clear: the D_{50} is always the most important variable (with a ΔLMAC = 0.027 m and a ΔLMC = 0.024 m, according to Figure 80) and the Δ_{Qs} variable produces the least impact on the statistics (with a ΔLMAC = 0.0002 m and a ΔLMC = 0.0002 m). The Q^* and n variables however, while having a very similar importance regarding the LMAC statistic (with ΔLMACs of 0.00351 m and 0.00352 m, respectively), have very different effects regarding the LMC statistic (with ΔLMCs of 0.0014 m and 0.0004 m, respectively). These results clearly evidentiate the importance of using multiple statistics to capture the different aspects which characterize morphodynamical change.

6.2.2. Joint Sensitivity Analysis

The JSA was applied based on the results of the numerical HM simulations of the previously described stylized channel, performed for different values of the variables under analysis, as described in the 5.2 section. The JSA was based on the calculation of the Total Effect Indexes (TEIs) (Saltelli, et al., 2008) and the graphical pairwise comparisons of the variables' mean effects on dH (as described in section 6.1.2.

This sensitivity analysis was detailed in terms of all of the different statistics (referred at the start of section 6.2), thereby analyzing different aspects and underlying characteristics of the channel's morphodynamics. Figure 81 displays the values of the TEI calculated for the different statistics (normalized so that each statistics' TEIs sum up to unity).

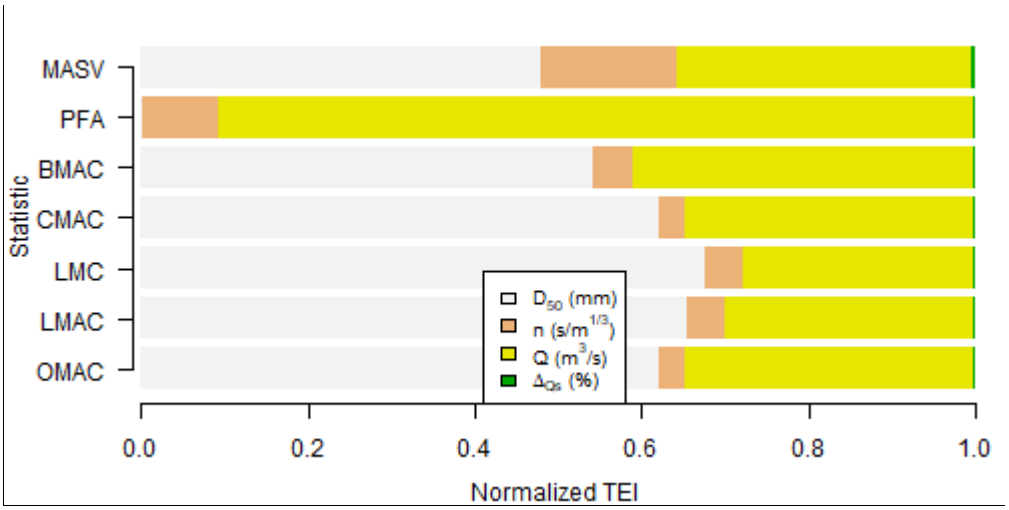

Figure 81 – Total Effect Index TEI values for the different variables in relation to each statistic.

As can be observed in this section, the different statistics (with the exception of the PFA) are generally in agreement regarding the variables' hierarchy. However, while the hierarchy itself is identical, the relative importance of the variables changes very significantly. In terms of the TEIs, in decreasing order of importance, the D_{50}'s, the Q^*'s, the n's and the Δ_{Qs}'s importances fluctuate between 43 and 66%, 30 and 40%, 3 and 18% and 0 and 2%. The choice of statistic in particular, can have a very significant

impact in the variables' relative importances. For example, the relative importance of Q^* relative to n can change between two times higher in the MASV statistic to ten times higher in the CMAC statistic.

Figure 82 to Figure 84 represent the pairwise comparison between the effects of the four variables under analysis for the LMAC, LMC and MASV statistics. The remaining statistics were not represented as they produced very similar results to the LMAC, LMC statistics and do not provide additional information. These graphical representations provide a qualitative description of the relative importance of the different variables (much in the same way as the TEI) and (in comparison with statistics-based approaches) a much more complete description of the relationships between the variables and their respective influences on fluvial morphodynamics. For reference purposes, the main criteria for interpreting the information represented in these figures is identical to the criteria presented in section 6.1.2.

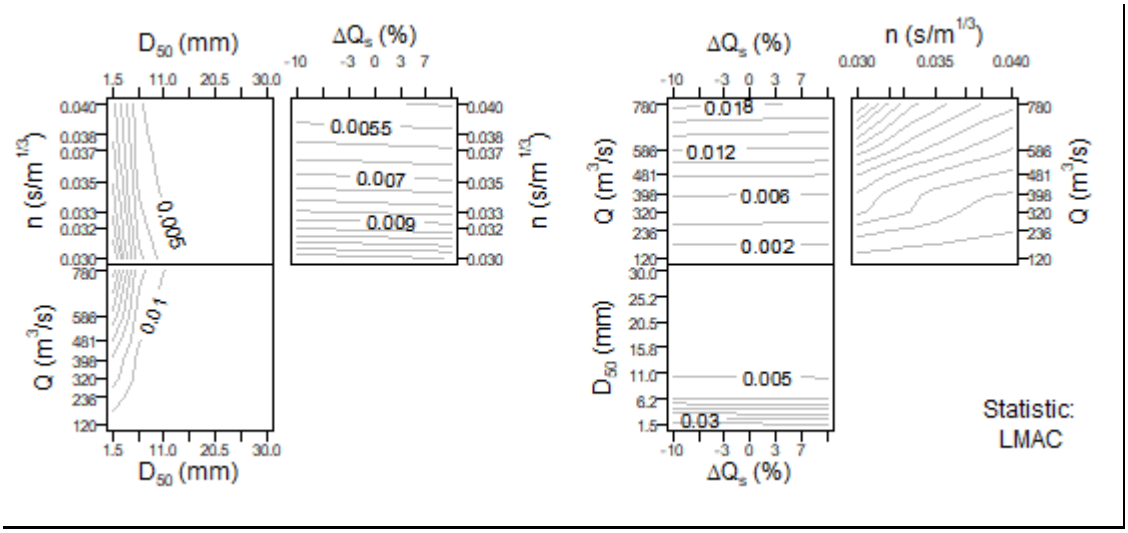

Figure 82 – Pairwise comparison of the LMAC statistic between the different variables.

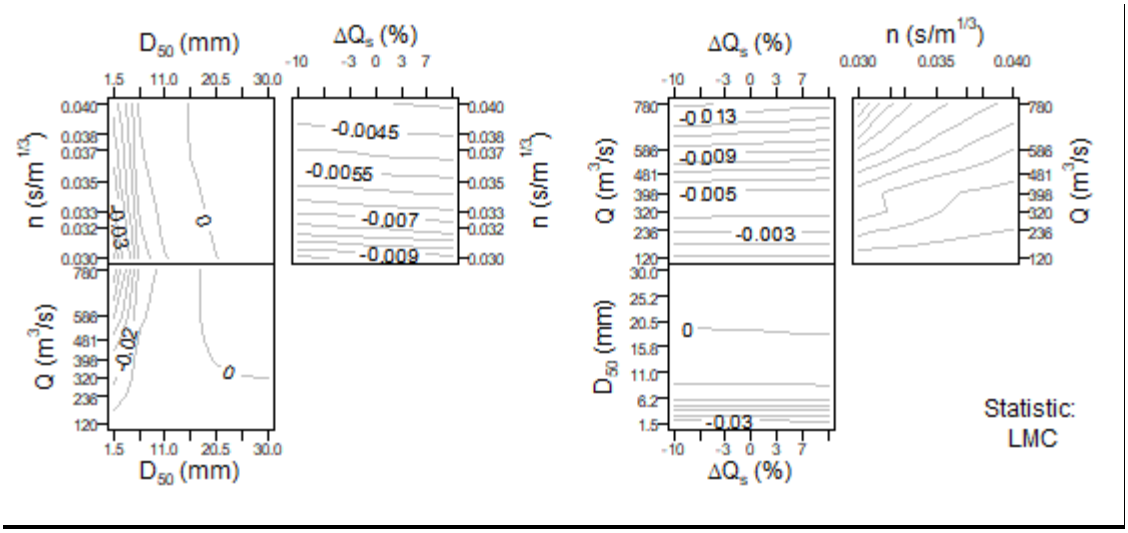

Figure 83 – Pairwise comparison of the LMC statistic between the different variables.

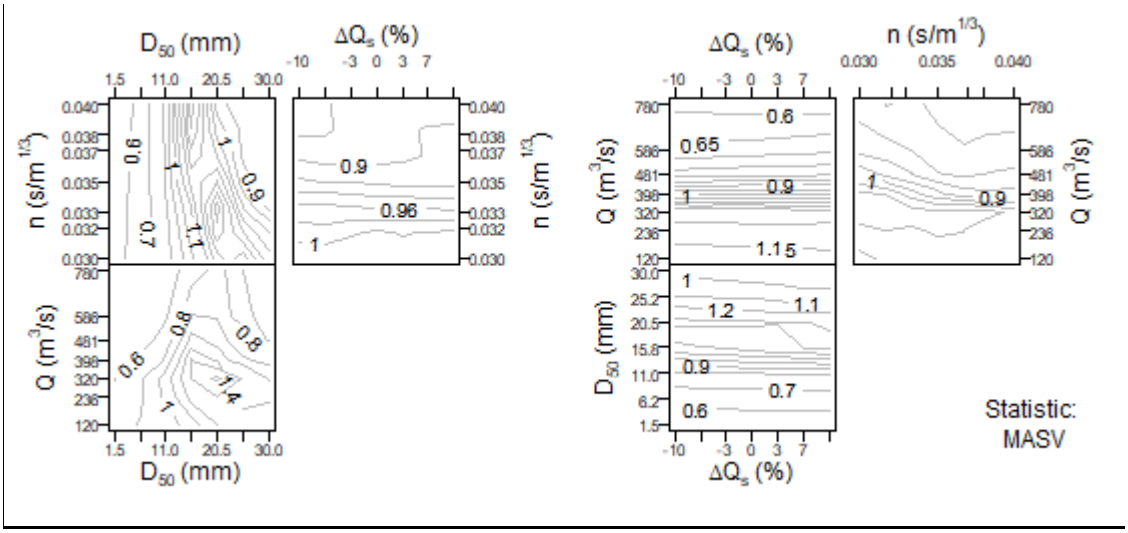

Figure 84 – Pairwise comparison of the MASV statistic between the different variables.

Analyzing multiple statistics is not only important in the analysis of the TEIs but also in the pairwise comparisons. While significant similarities can be found between different statistics, the LMC statistic for example, captures inflexion points in the channel's morphodynamical behavior which are not present in the other statistics (namely in the relationship between the Q^* and the D_{50} variables, portrayed in Figure 83 by the diversion of the contour lines as a function of the value of D_{50} – approximately around the 11 mm value – where the simulations' dH trend changes from erosion to sedimentation). In this particular case study, no clear example of an independence between the variables' effects was observed. With varying degrees of intensity, an organized structure has been observed to relate the different variables' effects on the statistics.

For the purposes of better understanding the variables' interactions, the exact nature of the structured relationships between the variables' effects may be determined by way of additional sensitivity studies. Determining whether these relationships are the result of a superposition of effects (and therefore the effects of the variables on the statistics are statistically independent) or if there is a dependency between the variables' effects can be better-founded by looking into case studies with different characteristics and variable definitions (regarding their nature and magnitude). Nonetheless, in a complex system, as is the case of fluvial morphodynamics, where strong spatial and temporal dependencies are present, a complete independence between any two variables is not likely.

The full analysis of these results and their likely causes and consequences is detailed in section 6.3 of this study.

6.3. DISCUSSION

In the available literature, only two examples of studies cold be found were two or more of the selected variables are analyzed and a quantitative description of morphodynamical sensitivities is calculated. Table 13 summarizes the normalized sensitivities obtained in these studies. As can be observed, there is

no agreement between these results and the results obtained in this study. The variables determined to be the most important were Q and n, respectively in each of the two examples whereas, in the case study, it was the Q. This disparity, along with the highly variable importance hierarchy which has been determined in some other studies on the subject (referred in Table 2), shows that the morphodynamical sensitivities are significantly case dependent and cannot be readily generalized. The scientific relevance of any set of individual sensitivities can therefore be concluded to be virtually limited to the corresponding case study. While these values may be useful for comprehending a specific situation, they are clearly not extendable to other situations. The highly complex and compounding effects of the spatial and temporal dependencies of morphodynamics (also observed by van Vuren (2005)), along with the strong case-specificity of the variability ranges of the variables are likely to render most comparisons across case studies ineffective.

Table 13 –Sensitivities estimated in the literature.

Statistic	Uncertainty Simulation	Normalized sensitivity				Reference
		D_{50}	n	Q	Δ_{Qs}	
Variance-based	FOSM	N/A	23.8%	76.2%	N/A	(Villaret, et al., 2016)
	MC	N/A	28.6%	71.4%	N/A	
Correlation-based	MC	0-5%	5-61%	0-25%	4-53%	(van Vuren, 2005)
Variance-based	MC	1-12%	8-77%	5-62%	7-82%	

While the results of this study regarding the interdependencies between the variables and morphodynamics are similar across case studies (e.g., regarding the variables' effects on morphodynamics in ISA or the dependency between these effects in JSA), the same cannot be said for the variables' hierarchy of importance for fluvial morphodynamics. While the results both attribute a smaller importance to the n variable, there is no consensus between case studies on the remaining positions. On the other hand, a parallel study developed on the subject of sensitivity analysis for the Mondego Case Study using unidimensional (1D) numerical HM models produced similar (in terms of their relative proportions) sensitivity magnitudes for the same selected variables and corresponding statistics (presented in Table 14) (Santos, 2018). The differences which exist between the two studies are very likely due to the two-dimensional (2D) nature of the present study, which is capable of capturing more complex aspects of fluvial morphodynamics which are not present in a 1D analysis. This fact suggests that the sensitivity analysis results for the Mondego Case Study are a proper representation of the study reach's morphodynamical behaviour and morphodynamical processes.

Table 14 – TEIs obtained in the sensitivity analysis of fluvial morphodynamics for the Mondego Case Study using a 1D numerical HM model (Santos, 2018) and the TEIs obtained for this study.

Reference		Q	D_{50}	n
(Santos, 2018)	OMAC	0.756	0.655	0.020
	LMAC	0.718	0.284	-0.095

Reference		Q	D_{50}	n
Present Study	OMAC	0.70	0.45	0.09
	LMAC	0.62	0.51	0.10

In the Mondego Case Study, the variables' decreasing hierarchy of importance is Q, D and n. As for the Stylized Case Study, this same hierarchy is D, Q*and n (ignoring the ΔQ_s variables which was not part of the Mondego Case Study). These results provide a strong indication of the fleeting nature of morphodynamical sensitivities. For many common applications of sensitivity analysis, the uncertainty around the corresponding relevant variables is, to some extent, restricted by the nature of variables and/or the system, allowing for the generalization of the results across case studies. However, in the case of fluvial morphology, the results (of both case studies and the available literature) indicate that the large entropy in the related morphodynamical processes renders impossible the direct comparison of sensitivities across case studies. Studies on sensitivity analysis of morphodynamics cannot therefore be easily generalized to other situations or case studies.

The simulation of the Stylized Case study considered only single event floods, a fact which is potentially responsible for the low importance of the Δ_{Qs} variable. Observations indicate that this variable's importance for morphodynamics should increase with the time span of the simulations. In this case study, that possibility is strengthened by the morphodynamical sensitivities to this variable, which were observed to be seven times larger at the start of the channel (defined in terms of the OMAC statistic for the first three sections of the river) than for the channel as a whole (according to the normal definition of OMAC). This possibility requires, however, further validation.

As can be concluded, the magnitudes of individual sensitivities are very unlikely to be comparable across significantly different cases. This fact, for the purposes of the validation of stochastic modelling, is undesirable. As was previously stated, the validation of stochastic modelling is linked to the potential existence of a common, generalizable behavior across case studies. The only remaining alternative solution is to identify replicable, relative characteristics of the stochastic modelling's results. Examples of these relative characteristics may be the relationships between the different variables and morphodynamics (represented in Figure 64 to Figure 71 and Figure 80 of the ISA) and the relationships (or lack thereof) between the variables' effects on morphodynamics (represented in Figure 75 to Figure 78 and Figure 82 to Figure 84of the JSA). Characteristics such as the direct or inverse correlation of the curves or contour lines and the features of their respective curvatures should be, from a theoretical point-of-view, a consequence of the morphodynamical processes inherent to the HM modelling and not of the variables themselves. In these figures the following behaviors were observed:

- Relative to the LMAC in Figure 68 and Figure 80, the Granulometry variable displays an inverse (at least 2nd order) correlation with LMAC with an upwards-facing curvature. Streamflow and Bed Roughness display positive and negative correlations with LMAC, albeit their individual curvatures are harder to define from these two examples (most likely due to their different definitions in each of the two case studies);

- Relative to the LMC in Figure 69 and Figure 80, the Granulometry and Bed Roughness variables display negative and positive correlations with the LMC for sedimentation and erosion -prone channels, respectively.
- In relationship between Streamflow and Granulometry, the pairwise comparisons show a 2nd order correlation between their effects (possibly with a negative-facing curvature). Other relationships could not be conclusively estimated from the two case studies, most likely to the inherent disparity between their levels of complexity in the variables' and the bathymetry's' definition.

In order that they may be conclusively used for validating the stochastic modelling of fluvial morphodynamics, these characteristics still require further validation from other case studies with different characteristics, most likely requiring a dedicated study. Nevertheless, sensitivity analysis is still a meritorious tool for understanding and representing the variables' impact and relevance for fluvial morphodynamics, as well as to validate, to a certain degree, the stochastic modelling of fluvial morphodynamics in the context of a specific case study.

Regarding sensitivity analysis specifically, even within the same type of environment, numerical model and uncertainty simulation, the choice of morphodynamical and sensitivity statistics can have a great impact in the results. This much was observed in this study, when comparing the results of the ISA and the JSA, which used, respectively, a range-based statistic and a variance statistic to quantify morphodynamical sensitivities. In this instance, the hierarchy of the importance of the Q and n variables changed depending on the choice. In addition, the relative importance of the D_{50} variable changes from nearly ten times larger than any other variable in the range statistics to a maximum of two and half times in the variance statistic. In the work by van Vuren (2005), the sensitivity of Q in particular more than doubled when switching from a correlation statistic to a variance statistic. While a definitive answer on what is the optimal statistic cannot be forcefully stated, from a conceptual point of view, the variance statistic should be a more appropriate choice because it is less unstable than the range-based values used to assess dH statistics in ISA (i.e., the ΔLMAC and ΔLMC values, which are discrete/calculated based on the extreme values of the dH produced by each of the corresponding variables). In addition, the variance statistic also does not assume a linear relationship between the variables and morphodynamics (as does the correlation statistic).

The use of multiple morphodynamical statistics (OMAC, LMAC, LMC, etc.) was observed to be relevant in capturing different aspects of morphodynamics, producing different magnitudes of sensitivities (and even a different hierarchical order in the ISA). In order to fully understand a fluvial system, these statistics can help in producing a much clearer picture of the variables' effects and interactions with fluvial morphodynamics. The results show that future studies involving sensitivity analysis in a fluvial context should make use of multiple morphodynamical variance-based statistics in order to provide a more stable and complete description of morphodynamics.

On the other hand, the relationships presented using the pairwise graphical comparisons proved very consistent in this study. For both case studies, Q (or Q^*) was observed to be dependent on n and on the

D variables, specifically regarding their respective impacts on the morphodynamical statistics. In all likelihood, the reason behind this common behaviour is that it is a natural characteristic of morphodynamical processes. Further validation regarding the variables dependencies (such as a potential independence between the *D* and *n* variables, visible in the Mondego Case Study) were unconfirmed due to the simplified nature of the Stylized Case Study.

The interdependency between *Q* (or *Q**) and each of the other two variables is most likely a result of the *Q* being largely responsible for the definition of the flood area (represented by the PFA statistic). Because the PFA determines the ratio between the flooded surface and the flood volume (represented transversally by the hydraulic radius), it very likely to influence the relative importance of the *n* and *D* variables in comparison with the other hydraulic forcings, probably constituting the driving force behind the *Q*'s interdependency with these variables. In opposition, the independency observed between *n* and *D* is most likely a result from the two variables pertaining to two different ends of the morphodynamical modelling (namely, to the actions and resistances, respectively).

The differences between the variables' interdependencies in each case study are most likely a result of the added complexity of the Mondego Case Study in comparison with the Stylized Case Study. In the Mondego Case Study, the selected variables possess a much more complex nature (being represented by a complex and hard to summarize set of series or curves of values) and the simulation of a year's worth of morphodynamical change adds a significant temporal dependency to the results (potentially exacerbating or averaging out some morphodynamical effects). This factor greatly adds to the difficulty in generalizing sensitivity analysis results in this context. The effects of the variables' definitions is particularly evident in this case considering that the Stylized Case Study was constructed based on a simplification of the Mondego Case Study Plausibly, most likely, only in cases with similar characteristics regarding these aspects can there be a direct comparison of morphodynamical sensitivities.

While the PFA may not appear to directly be a morphodynamical statistic, it was determined based on the percentage of the grid area where morphodynamical change occurs. In both studies, the results point towards *Q* (or *Q**) being the only variable with a very significant effect on the definition of PFA (with only a minor contribution from *n*).

Finally, regarding the validation of the results of the stochastic modelling of fluvial morphodynamics on the Mondego Case Study, within the natural limitations of sensitivity analysis applications in the context of fluvial morphodynamics, the simulations can be deemed to be validated. *Per se*, a model cannot be "proven true" but it can be corroborated, which was the purpose of this part of the work. The validity of the stochastic modelling can be stated because:

- The fluvial morphodynamics' sensitivities (expressed in terms of the TEI) are very similar in magnitude to the corresponding values obtained in a parallel study (Santos, 2018) also developed for the Mondego Case Study;

- The calculated sensitivities using the numerical HM modelling are in accordance with the variables' natures (i.e., infinite, semi-infinite or bounded) and variability ranges (i.e., their respective widths). Streamflow, which is semi-infinite in terms of its range of variability was observed to have the highest impact in the morphodynamics overall uncertainty. Concurrently, granulometry (which was deemed to be uniformly variable over the entire range of historical measurements) and bed roughness (which was represented as a partial uncertainty around its estimated mean spatial distribution – and therefore possessed only a relatively small level of uncertainty) displayed the second least and the least impact on morphodynamical uncertainty, respectively.

7
STATISTICAL ANALYSIS OF MORPHOLOGICAL EVOLUTION

The statistical analysis of morphological evolution is intended to provide a general description of fluvial morphodynamics in terms of its magnitude, spatial distribution and local patterns of bed level change (*dH*). These results are intended to provide an understanding of morphodynamics processes (represented by the previously developed 216 simulations) which may come to be useful in the application of the statistical description of *dH* produced in previous chapters. Additionally, the statistical distribution of different aspects of fluvial morphology and morphodynamics was fitted to several theoretical statistical distributions in order to assess which of those is the most suitable.

The steps/intermediate stages required in order to apply the results of this statistical analysis (or of the stochastic modelling of fluvial morphodynamics in general) are presented and applied in this section. The analyses developed were based on the results of the stochastic morphodynamical simulations (i.e., each simulations' *dH* magnitude along the grid), detailed in section 5. The characterization of fluvial morphodynamics was based on the data for the entire study reach.

Finally, the possibility of applying stochastic modelling of fluvial morphodynamics in a multi-year setting (i.e., for periods of time longer than two years or more) was studied and presented at the end of this section.

7.1. STATISTICAL CHARACTERIZATION

In this section, the statistical nature and distribution of fluvial morphodynamics was studied based on the results of the stochastic modelling of fluvial morphodynamics. The characteristics of the probability distribution of *dH* were analysed in terms of the characteristical shapes of their PDFs and CDFs, their skewness/symmetricity and the theoretical probability density functions which are most suitable for the representation of the *dH*'s uncertainty. The uncertainty in morphodynamics was represented individually (i.e., independently for each grid cell) by means of the corresponding *dH* magnitude for all of the 216 simulations performed and summarized as part of section 5 of this Thesis regarding the full study reach of the Mondego Case Study.

Figure 85 presents the overlapped plots of all of the ECDFs obtained from the stochastic modelling, both for the relative (i.e., the simulated) and absolute (i.e., the absolute simulated) *dH* magnitude (with transparency in order to represent the intensity of the concentration of probability lines). As can be observed, there is no visible, distinctive pattern in the ECDFs, as their overlapped shapes simply constitute an indistinguishable smudge. The only distinguishable characteristic is a tendency of the relative *dH*'s ECDFs towards positive values (i.e., sedimentation), otherwise in agreement with the observations made in section 5.1.2.3 regarding the overall behaviour of the study reach (which was shown to produce more sedimentation than erosion). Nonetheless, looking at individual probability distributions, there is a significant pattern regarding the shapes of the grid nodes' histograms: The individual nodes' histograms' shapes differ as a function of the cell's transversal position on the reach. Nodes over the or closer to the river bank tendentially have exponential distributions while nodes in the centre of the river channel approximately follow a normal distribution (centred on its mean values). Intermediate nodes (situated close to the edge of the main channel) can be better approximated by a gamma distribution. This tendency is also present (and often more prevalent) in terms of absolute *dH* magnitudes. An example of this effect can be seen in Figure 86.

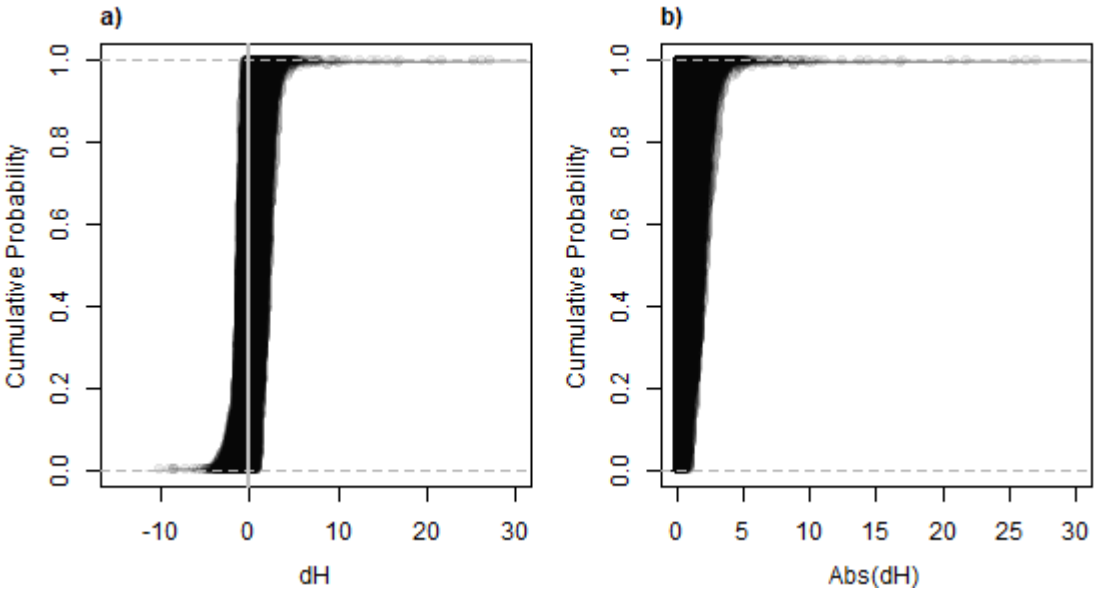

Figure 85 – Overlapped plot of the ECDFs (defined over the course of the 216 simulations) of the relative (in plot a) and absolute (in plot b) *dH* (in meters) for each individual grid cell.

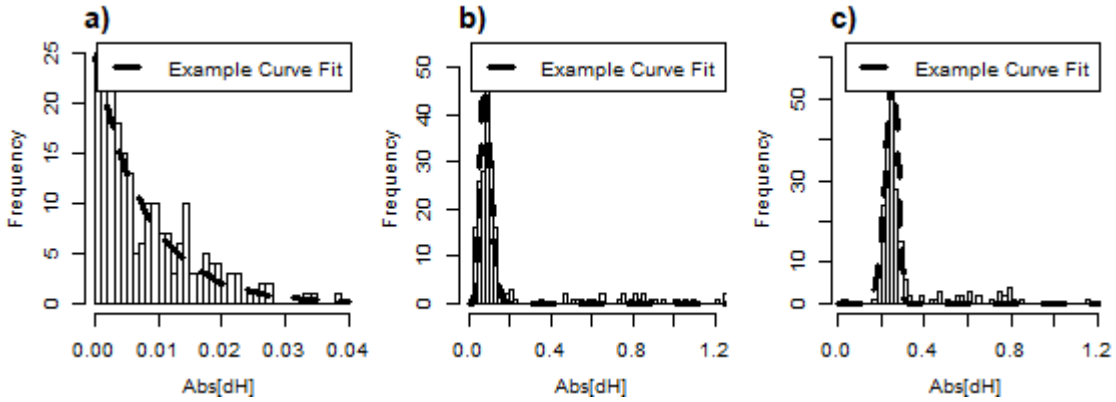

Figure 86 – Example of different histograms of *dH* (and potential theoretical PDF curve fits, in meters) depending on the corresponding grid nodes' transversal position on the reach. From a to c, the plots show the corresponding histogram of nodes on the river bank, at the edge of the river channel and in the centre of the river channel.

Figure 87 displays the histograms of the grid nodes' skewness coefficient (calculated for the corresponding grid cell's relative and absolute *dH* values). The skewness of *dH* along the grid nodes is mostly always positive, with a mean value of 1.35 and 2.8, respectively for the simulated relative and absolute *dH*. Over 78% of grid nodes have a positive skewness for the relative *dH* and over 93% of the nodes have a positive skewness for the absolute *dH*. Figure 88 provides a discretization of each grid nodes' skewness coefficient as a function of the corresponding mean *dH* value.

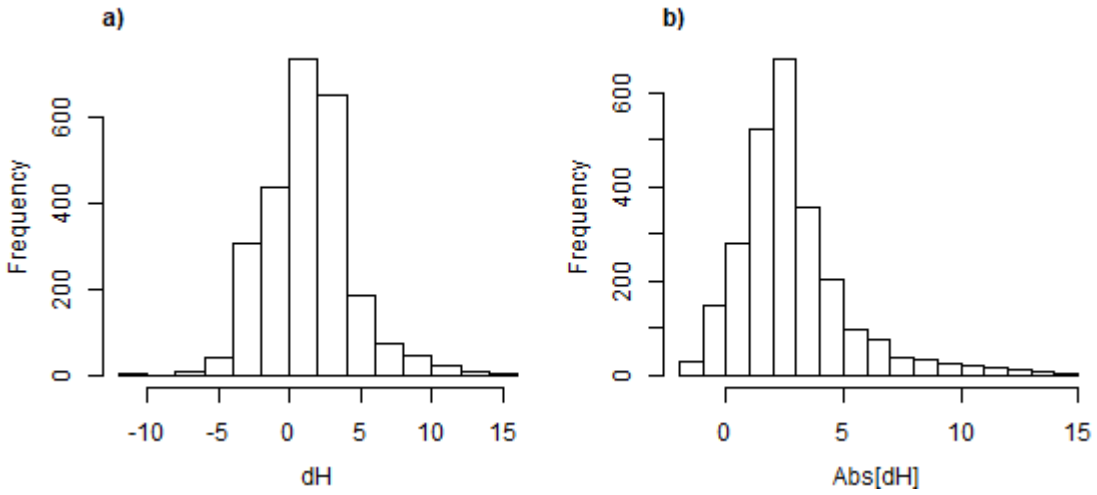

Figure 87 – Histogram of the grid nodes' skewness coefficient for both relative (in plot a) and absolute (in plot b) *dH*.

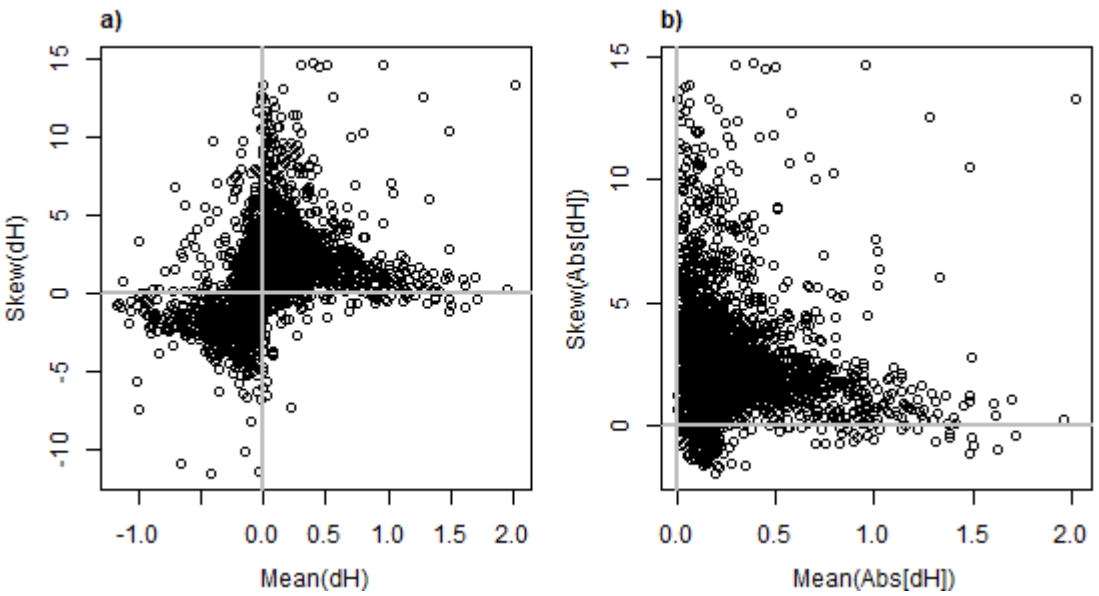

Figure 88 – Comparison between each cell's skewness coefficient and mean value for the relative (in plot a) and absolute (in plot b) *dH*.

The results of Figure 88a are particularly interesting: skewness appears to be directly correlated with the grid nodes mean value, with positive mean *dH* values generally implying a positive skewness value and negative mean *dH* values generally implying a negative skewness value. These two effects are possibly the cause for the mostly positive skewness of the stochastic modelling's results – observed in Figure 87. These results indicate that the skewness coefficient may be used as a statistic/measurement of the stochastic modelling's morphodynamical change. Additionally, both plots in Figure 88 show that asymmetry (expressed by the high skewness values) in the probability distribution of *dH* is generally only present for small values of *dH*, or, concomitantly, nodes with larger *dH* magnitudes produce more symmetrical PDFs.

The grid nodes' PDFs were additionally fitted by several different sets of theoretical probability distributions in order to determine the distribution best suited to represent the probability density of localized fluvial morphodynamics. The selected distributions were chosen based on whether (1) they are applicable in the mathematical real space or the positive real space, (2) they are unimodal and (3) they are flexible enough to encompass the range of potential distribution shapes (previously represented in Figure 86). The theoretical distributions selected for fitting with the relative *dH* were the Normal, Cauchy, Logistic, Asymmetric Laplacian, Skewed Normal and Gumbel distributions. The theoretical distributions selected for fitting the absolute *dH* were the Gamma, Weibull, F (also known as Fisher-Snedecor), Chi-Square, and Folded Normal distribution. Figure 89 presents the mean and SD of the fitting error for the different selected probability distributions.

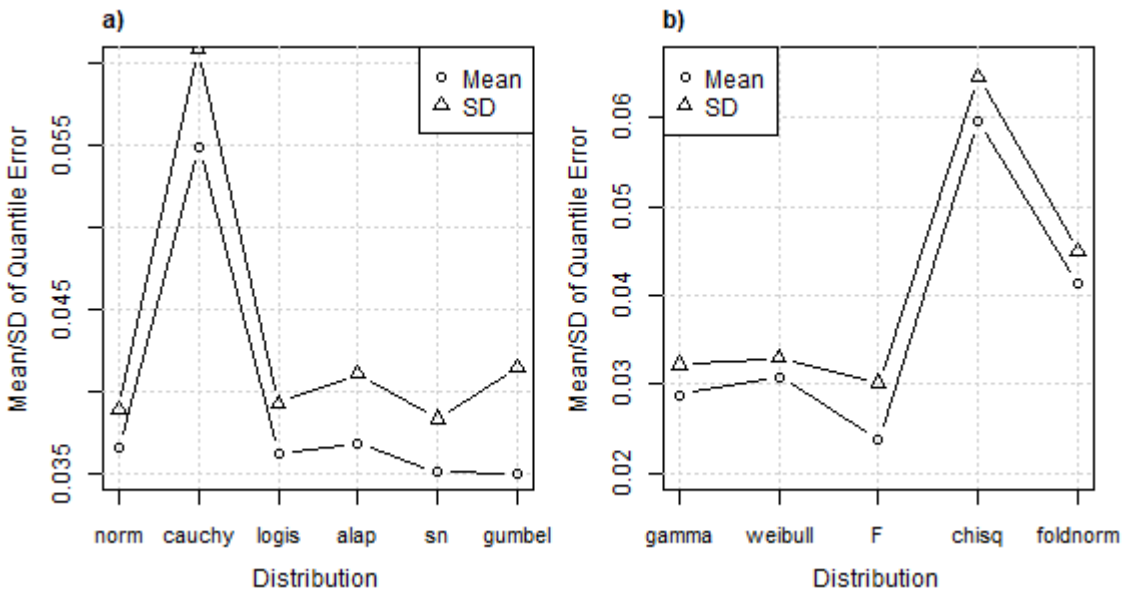

Figure 89 – Mean and SD of the error of the theoretical PDF fits for both relative (in plot a) and absolute (in plot b) *dH*.

The results of the distribution fitting showed that the Gumbel and F distributions are the most suitable probability distributions for the grid nodes' relative and absolute *dH* values. In addition, for the relative *dH* values, the Skewed Normal distribution also appears to produce good results (while it has a slightly larger mean error, the corresponding SD is much smaller). These distributions can therefore be applied to represent different aspect of morphodynamical change, as was accomplished in section 7.3.

Finally, a common measurement for statistically characterizing stochastic modelling applications is the confidence interval. However, both the *D* and the *n* variables were deemed to be bounded and therefore, their probability spaces are fully represented in the simulations. On the other hand, while the *Q* (or *Q**) is a semi-unbounded variable, the large number of series used to represent its probability distribution implies that the part of its probability space which is not represented by these series is only a small percentage of the whole. Accordingly, in this particular study, the results of the simulations were deemed to single-handedly represent the (virtual) entirety of the fluvial morphodynamics probability space. The concept of confidence interval is therefore not relevant for this study.

7.2. Directional Effects

In order to better understand the study reach's morphological processes and to facilitate the application of the results of the stochastic modelling, several different, statistical aspects of morphodynamical change were analysed separately in the longitudinal and transversal direction of the channel. This directional statistical analysis was performed both in terms of the overall *dH* values along the entire grid and around the morphodynamics' peak values (i.e., its local and global maxima and minima). This analysis was based on the entire study reach of the Mondego Case Study.

The discretization of the results of the stochastic modelling in its longitudinal and transversal direction is meant to facilitate the description of local patterns of *dH*. By analysing the directional statistical

characteristics of consecutive values of *dH*, it becomes possible to estimate the likely shape of the morphodynamical patterns. The stochastically-generated morphodynamical patterns can afterwards be translated into a PDFs or PDF-like description of the likely morphodynamical evolution of the study reach (a point later discussed in section 7.3). The understanding of the inherent spatial patterns of fluvial morphodynamics is essential to application of the stochastic modelling's results and therefore, to the rest of this PhD study's tasks.

The directional analysis of fluvial morphodynamics was performed in terms of:

- Serial (Pearson) correlation coefficients calculated between stochastic values of *dH* of consecutive grid nodes along the longitudinal and transversal direction (represented in Figure 90), measured for all the simulations performed. As the spacing between longitudinal grid nodes is approximately 1.73 times the corresponding transversal spacing, the 1st order longitudinal serial correlation (i.e., the correlation between each pair of consecutive grid nodes in the longitudinal direction, e.g., the $X_{i,j}$ and $X_{i+1,j}$ grid nodes) is more closely comparable in terms of spatial representativeness with the 2nd order transversal serial correlation (i.e., the correlation between the end values of each set of 3 consecutive values, e.g., the $X_{i,j}$ and $X_{i,j+2}$ grid nodes). The longitudinal correlation has a mean value of 0.67, while the 1st and 2nd order transversal correlations have a value of 0.76 and 0.25, respectively. As can be observed in Figure 90, the longitudinal correlation is much higher for the same spacing between grid nodes (i.e., 1st order longitudinal correlation vs. 2nd order transversal correlation). This is most likely a result of the hydrodynamic forcing, which should orient the bed channel's large scale shape in the direction of the flow (producing aerodynamic forms).

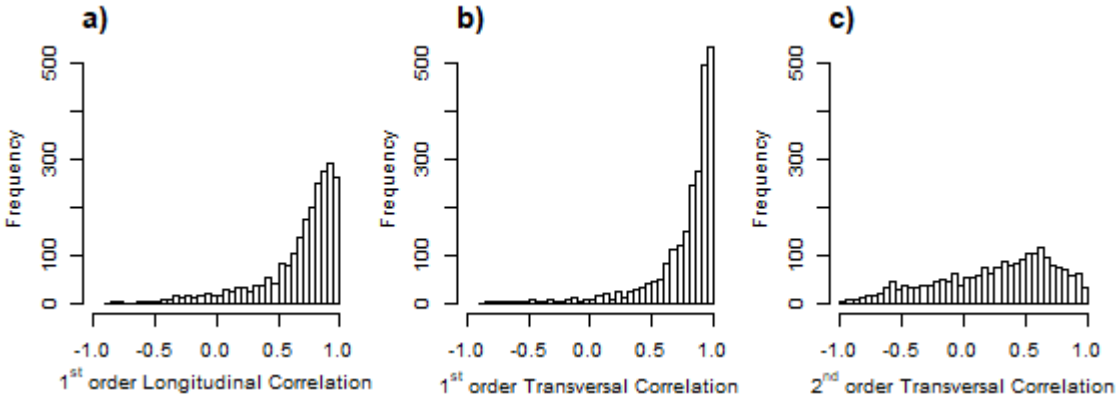

Figure 90 – Longitudinal (1st order in plot a) and transversal (1st order in plot b and 2nd order in plot c) serial correlation between the stochastically simulated *dH* values of consecutive grid nodes.

- The graphical comparison between consecutive *dH* values (in the longitudinal and transversal direction) across all of the simulations. In Figure 91, the consecutive 1st order (in the longitudinal and transversal direction) and 2nd order (in the transversal direction) pairs of *dH* values are presented. Generally speaking, the *dH* values in the longitudinal direction present a much stronger orientation along the 45º line, representative of the strong longitudinal serial correlation identified in Figure 90. On the other hand, and particularly for the 2nd order transversal comparison, the transversal

comparison is mostly a random point cloud without significant meaning, also representing the lack of a significant transversal serial correlation identified in Figure 90. Finally, the 1st order longitudinal comparison shows that the serial correlation observed is stronger when erosion is present (i.e., the area of Figure 91a below the -45º line, where the points line up considerably more along the 45º line). These results indicate that, while the longitudinal correlation is significant, the main responsible for this behaviour is the erosion-prone areas of the reach (or, from another perspective, the areas of the reach prone to sedimentation have a much smaller Pearson correlation coefficient).

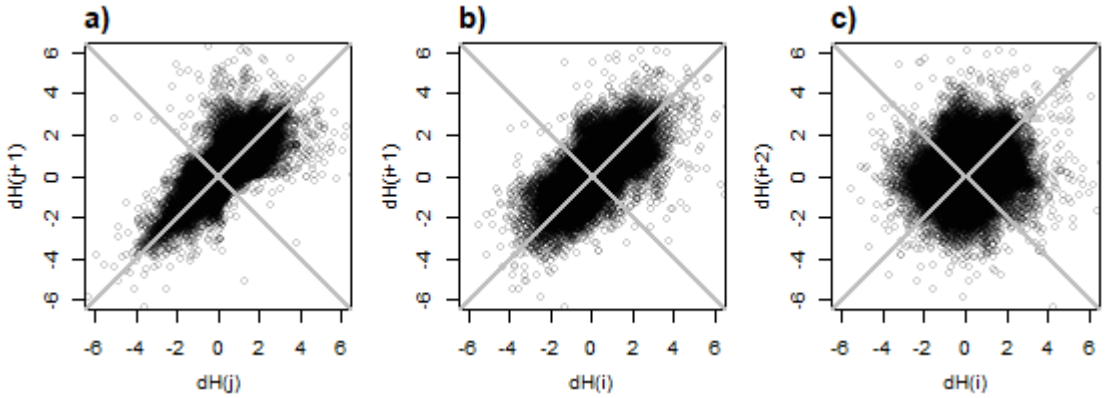

Figure 91 – Comparison between the *dH*'s magnitude for consecutive grid nodes in the longitudinal (1st order in plot a) and transversal (1st order in plot b and 2nd order in plot c) direction.

- The symmetricity/skewness of morphodynamical change, determined relative to the study reach's local maxima and minima of *dH* (i.e., the symmetricity of the peak erosion and sedimentation forms in the channel). This symmetricity was analysed by comparing the simulated values of *dH* closest to the *dH* local maxima and minima (i.e., the near-peak values) in the two directions (represented in Figure 92). Generally speaking, the results show that *dH* is relatively symmetric in both directions. While relatively small (presenting a mean value of 1.06), the skewness of *dH* is more significant in the longitudinal direction, where it determines the shape of large scale profiles of morphodynamical change.

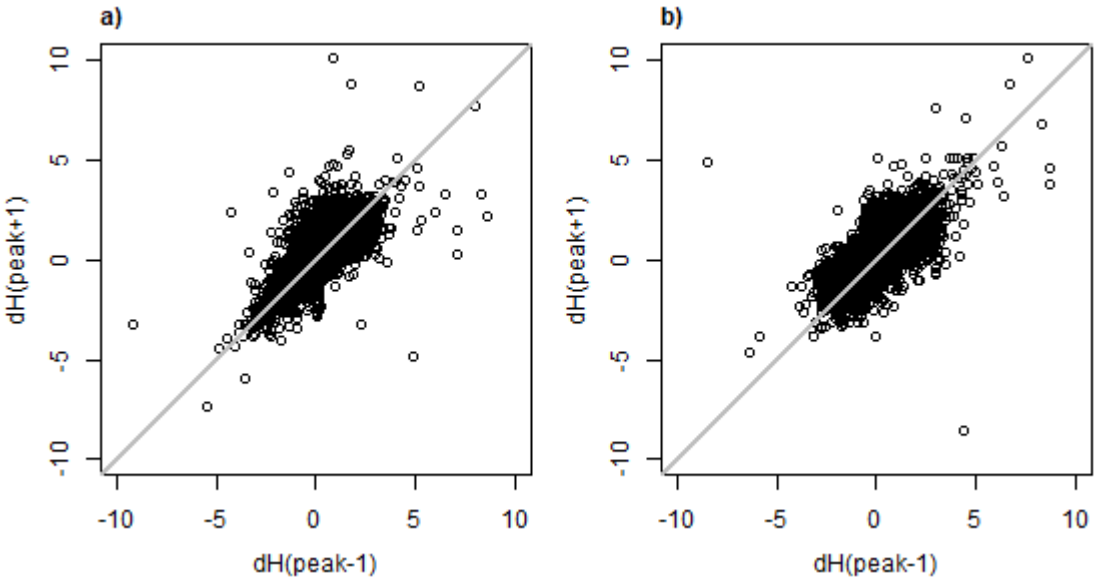

Figure 92 – Comparison between near-peak values in both the longitudinal (in plot a) and transversal (in plot b) direction.

- The peakdness of morphodynamical change, determined relative to the study reach's local maxima and minima of *dH* (i.e., how distinctive the peak *dH* values are from its neighbouring grid nodes' *dH* in both the longitudinal and transversal direction). Figure 93 presents the comparison between the peak values of *dH* (i.e., the local maxima and minima in the each direction) and the mean *dH* magnitude around the peak *dH* (discretized in terms erosion and sedimentation *dH*s). As can be observed, particularly for larger values of erosion, the near-peak values tend to be relatively similar to the corresponding peak values (i.e., in Figure 93a and Figure 93c they are close to the 45º line). In the case of sedimentation, there is mostly only similarity between peak and near-peak values in the transversal direction (although only to a smaller extent – Figure 93d). While an exact cause for this behaviour was not determined, it is quite possibly related to the conditions required for the erosion and deposition processes to occur. These results indicate that, at least regarding erosion-prone areas, there is likely to be some similarity between peak and near-peak values. For smaller peak values, there is a much more significant disparity between peak and near-peak values (visible in the significant distance between these values and the 45º line), probably due to the sporadic and random nature of these peaks (as opposed to larger magnitudes of *dH* which are more commonly the result of a significant coherent structure in the behaviour of morphodynamics).

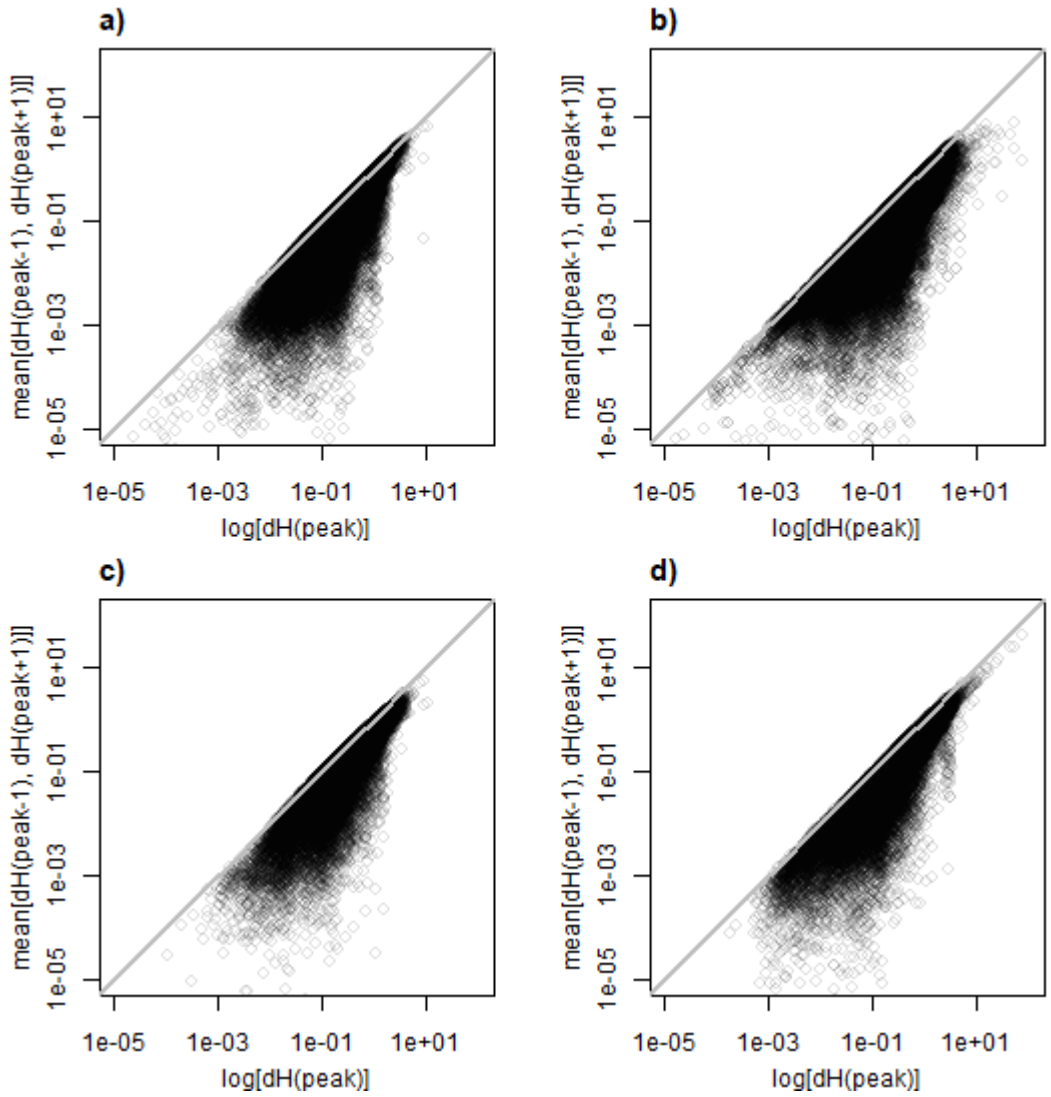

Figure 93 – Comparison (in logarithmic scale for a better interpretation) between peak erosion and sedimentation values and the mean near-peak values in both the longitudinal (erosion in plot a and sedimentation in plot b) and transversal (erosion in plot c and sedimentation in plot d) direction.

In conclusion, the results of the directional characterization of fluvial morphodynamics indicate that (1) the longitudinal serial correlation is very significant and much stronger than the transversal serial correlation, (2) the correlation between consecutive grid nodes (particularly in longitudinal direction) is much stronger in the presence of erosion than sedimentation (i.e., sedimentation does not appear to have a significant serial correlation), (3) the profiles of morphodynamical change around peak values display a significant symmetricity and (4) the grid nodes closest to larger peak/maximum values of erosion display generally similar (albeit naturally smaller) *dH* magnitude as those peak/maximum values (i.e., the peakdness of grid nodes prone to high levels of erosion is not very significant/accentuated).

These results have significant implications regarding the application of the stochastic modelling's results, particularly where local patterns may be concerned. When the study or application considering morphodynamical uncertainty focuses on small areas of the river, the results of the directional analysis provide insight on potential simplifications and considerations which are important when taking into

consideration this morphodynamical uncertainty. The directional analysis described the existence of a large spatial uncertainty (due to lack of serial correlation and/or a strong peakdness of higher *dH* values) in the transversal direction and/or in areas prone to the occurrence of sedimentation.

This knowledge on the spatial patterns of fluvial morphodynamics can be of significant use in fluvial engineering. As an example, the results clearly indicate that, for studies focusing on small sectors of the study reach (e.g., at least around two longitudinal sections of distance ≈ 30 meters), using a 2D cross-sectional profile (i.e., longitudinally infinite) to describe the behaviour of erosion-prone areas provides a reasonable description of the localized morphodynamical change in the vicinity of these areas. Simultaneously, the same cannot be said for longitudinal descriptions of *dH* profiles or any simplified description of areas prone to sedimentation, because both these situations suffer from a significant spatial uncertainty/entropy). Areas with significant spatial uncertainty should be described using the full 3D description of the corresponding *dH*.

The results of the directional characterization of fluvial morphodynamics are likely generalizable to other case studies as the effects here reproduced are seemingly a result of the very nature of morphological processes.

7.3. EROSION PROFILES

The definition of erosion profiles is commonly a necessary step for the use of the results of the stochastic modelling in the many different applications, particularly those related to the stability/reliability analysis of infrastructures situated in a river's bank. The results of section 7.2 showed that, while logically both cross-sectional and longitudinal profiles can be defined, only cross-sectional profiles of erosion-prone areas are likely to provide a good representation of the morphodynamical behaviour and uncertainty of the surrounding area. The alternative (i.e., longitudinal profiles or sediment-prone areas) suffers from a significant level of spatial uncertainty which reduces their accuracy and representativeness.

In this section, the characterization of erosion was split into two alternatives, namely:

1. A general description of the process of defining/generating erosion profiles for a given section of a river (with an example from the Mondego Case Study) and;
2. An application of this process adjusted for the use of the erosion profiles in the analysis of an infrastructure with significant longitudinal development (i.e., parallel to the river channel).

Additionally, some considerations are made towards the potential generalization/simplification of future applications of the stochastic modelling of fluvial morphodynamics by way of a well-designed generation process for the erosion profiles.

7.3.1. GENERAL DEFINITION

The application of the results of the stochastic modelling of fluvial morphodynamics can be performed in three dimensions (3D, namely, by directly using the results of the stochastic modelling) or in two

dimensions (2D, by simplifying the otherwise three-dimensional reality into a representative 2D profile). While the 3D application is more realistic, it is very often far more complex to perform. Conversely, the 2D application of the results, while still remaining a simplification, is appropriate for many different applications, for example, where the system(s) involved has(ve) a significant longitudinal development. Additionally, the 3D structure of a channel's morphodynamics is generally so complex that its generalization (i.e., the simplified representation of its probability distribution) is generally impossible, most likely requiring the simulation of the full range of possible channel morphologies (the equivalent of simulating the full 216 simulations in this study).

This study therefore focused on the analysis and generalization of 2D/cross-sectional erosion profiles, with the purpose of facilitating future studies aiming to represent the uncertainty of fluvial morphodynamics and apply it in the analysis of near-bank/near-channel case studies.

In order to analyse the natural patterns of erosion profiles in fluvial morphodynamics, this study focused on profile 115 of the study reach of the Mondego Case Study (which is also a part of the study segment). This particular profile was selected because it is situated in an area which is known (based on in-situ observations) to be prone to the occurrence of erosion. The location of this profile relative to the study segment (part of area b of the reach, as defined in Figure 24) is presented in Figure 94. The overlap of the corresponding *dH* profiles for profile 115 is presented in Figure 95, along with the initial bathymetry.

Figure 94 – Representation of the location of profile 115 in the study segment (indicated by the black line).

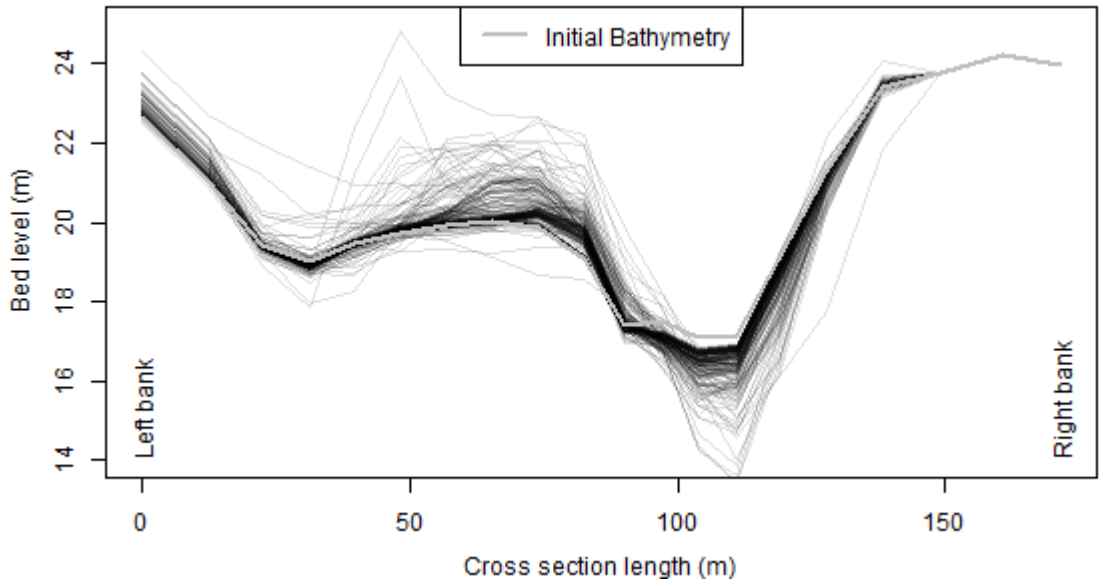

Figure 95 – Overlapped plots of all of the simulated bathymetric *dH* in profile 115 of the study reach.

The intended generalization of 2D erosion profiles consists of analysing the patterns of erosion behaviour and summarizing the probability distribution of the *dH* profiles (produced by the stochastic modelling) into a set of characteristics/parameters and representative *dH* profiles shapes. The summarizing of the probability distribution of the *dH* profiles is intended to allow for the generation of new, realistic *dH* profiles based on the simulated data. Using this generalization, it should be possible to use a smaller number of simulations (i.e., less than the 216 simulations used in this study) to correctly represent, with the same accuracy, the probability distribution of the *dH* profiles. On the other hand, the lack of a strong spatial pattern to sedimentation-prone areas means that this type of generalization is most likely not possible. In fact, for the same reason, such areas should be simulated using their complete 3D definition because their simplifications into 2D profiles is likely to misrepresent the corresponding morphodynamical uncertainty. Accordingly, the generalization process which was here developed is only intended for areas of the river where erosion is the most predominant process.

The generalization of erosion profiles was initiated with the determination of a characteristic erosion pattern of the river channel (or, from another perspective, the erosion decay profile, i.e., the profile of the reduction of the *dH* from the river channel to the river bank). The section of profile 115 which is generalizable corresponds to the area of it which is prone to erosion. The erosion profiles in this area are situated between the location with the highest erosion magnitude in the main channel (on the left, approximately situated in the centre of the channel) and the location where the *dH* is null for all of the simulations (on the right, over the right bank). In order to determine the characteristic shape of these erosion profiles, profile 115's *dH* in this area was vertically standardized (made to vary between 0 and 1) and horizontally adjusted/linearly displaced in order to match each profiles' median *dH* values. For the purposes of validating the generalization process, the example of profile 115 was analysed in this study.

The corrected (i.e., standardized and adjusted) erosion profiles are presented in Figure 96. Based on the resulting corrected erosion profiles, the characteristic shape of the erosion profiles was determined and approximated using a hyperbolic tangent function (also presented in Figure 96). This approximated representation of the erosion's characteristic shape (i.e, hyperbolic tangent function) produced a good match with the overall behaviour of the corrected erosion profiles. Aside from this characteristic shape, the profile 115's erosion profiles can therefore be summarized by the two characteristic values/parameters which were used to convert the simulated erosion profiles into the corrected erosion profiles, namely: the maximum erosion (used to standardize the erosion depth) and the relative displacement (used to equalize the profiles' medians). For the purpose of generalizing these results, the statistical characteristics of these two selected parameters were analysed.

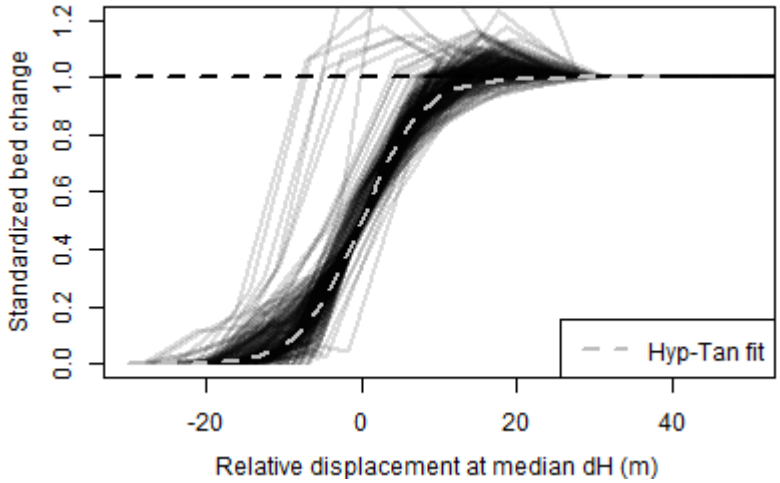

Figure 96 – Standardized erosion/erosion decay profile for the right bank of profile 115 of the study reach. The dashed grey line represents the best fit line of the hyperbolic tangent function.

The two parameters (maximum erosion and relative displacement) were found to be virtually independent, displaying a correlation coefficient of -0.33. Therefore, the two variables were assumed to be independently samplable. The two parameters' probability distributions are represented in Figure 97 by their respective histograms. Concurrently, the bounded and unbounded theoretical PDFs previously applied in section 7.1 were fitted to the erosion depth and relative displacement parameters, respectively. The best fit distributions for the maximum erosion and relative displacement parameters were the F and Gumbel distributions, respectively (with corresponding fitting mean quantile errors of 0.043 and 0.184).

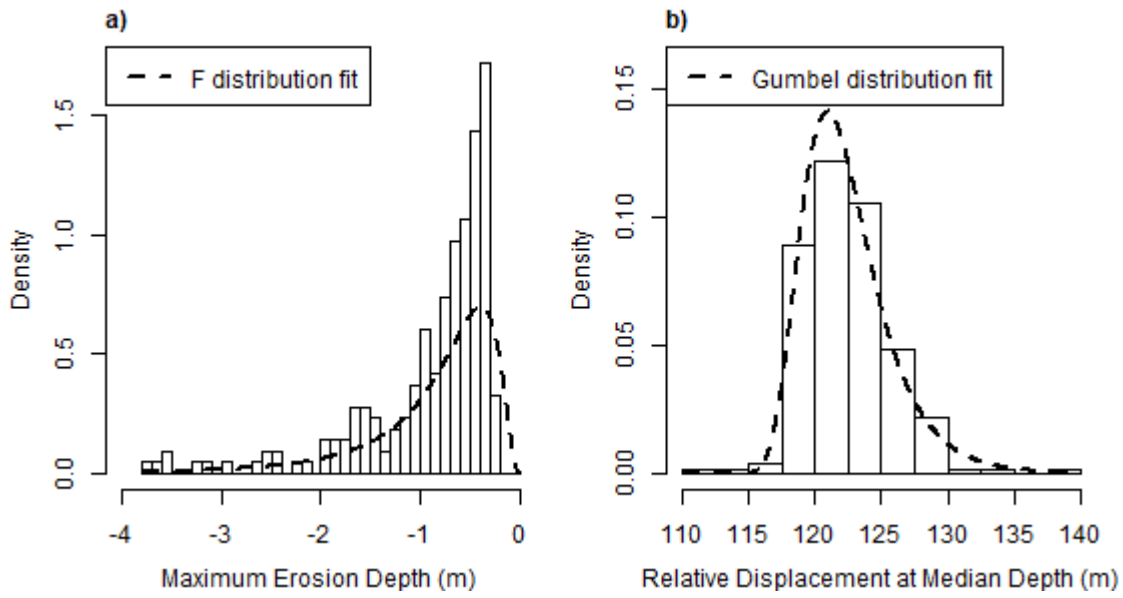

Figure 97 – Histograms of the two selected parameters of the generalization process and corresponding optimal fit theoretical PDFs (represented by the dashed lines).

As the purpose of the generalization process is for it to be applicable to other case studies, its validation is therefore essential to its application. The validation of the generalization process was performed by generating and analysing new sets of 216 erosion profiles (the same number of profiles produced by the stochastic modelling) based on the erosion's characteristic shape (approximated by a hyperbolic tangent function) and:

- The generalization parameters PDFs fitted to the 216 simulations performed in section 5 (i.e., by generating a large number of parameter values from the PDFs presented in Figure 97);
- New PDFs fitted to only 6 representative simulations (taken from the total of 216 simulations). These representative simulations correspond to the simulations performed using the variables with matching *dH* quantiles, e.g., the most erosive variables' values, the second most erosive variables' values, etc..

The erosion profiles produced by the stochastic modelling, the erosion profiles generated using the full 216 simulations and the erosion profiles generated using solely the 6 representative simulations are presented in Figure 98.

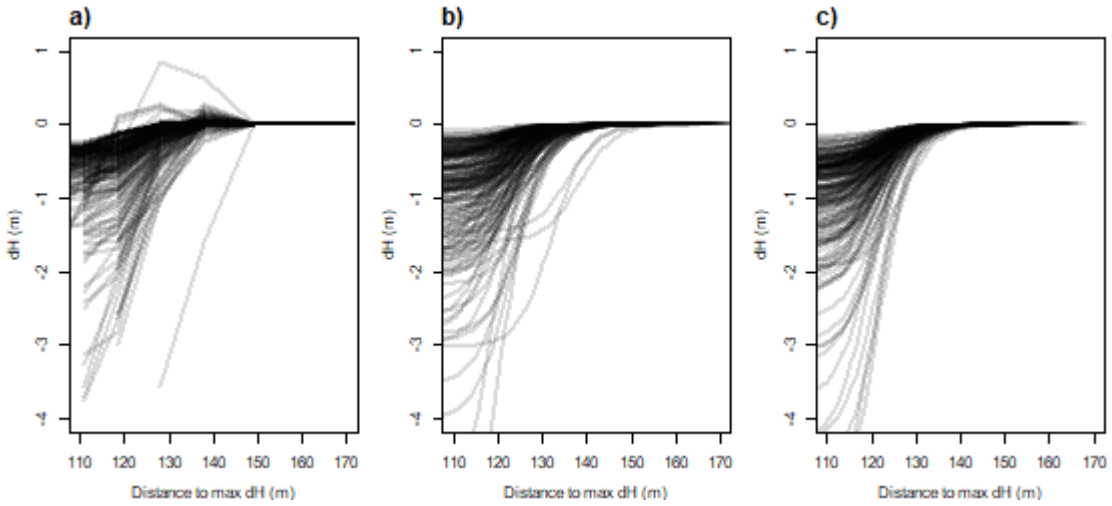

Figure 98 – Representation of the erosion profiles for the right bank of profile 115 produced by a) the stochastic modelling of fluvial morphodynamics, b) randomly sampling the generalization parameters (estimated from the 216 simulations) and c) randomly sampling the generalization parameters (estimated from the 6 representative simulations).

Based on the results presented in Figure 98, it can be observed that the product of the generalization process possesses a significant similarity with the simulated erosion profiles. Graphically speaking, using a representative set of simulations was also observed to produce only small differences in terms of the generalization parameters' PDFs of the generated erosion profiles. Accordingly, it is likely that, in future applications of stochastic modelling (specifically, when its purpose is the representation or study of the erosive processes in a given area), the use of a small number of quantile-matched simulations (e.g., 5, 10 or 20 simulations) can provide a speedy alternative to the full MCS (i.e., the approach which was adopted in this study).

Despite these positive results, the generalization of erosion profiles for application purposes still requires further validation from more case studies in order to confirm the characteristic shape of the erosion (here represented as a hyperbolic tangent function) and, in particular, the theoretical probability distributions which best fit the erosion profiles' characteristic values. Given the characteristics of the morphodynamical processes delineated in the previous sections of this study, case studies regarding areas prone to erosion are naturally preferred. Nevertheless, the work developed in this PhD study will greatly aid future studies in the finalization of the generalization process and in the application of the results of the stochastic modelling of fluvial morphodynamics.

7.3.2. Definition for Risk Analysis Application

While the stochastic modelling of fluvial morphodynamics can provide a good indication on the areas of a river which are prone to erosion or sedimentation, the exact definition of the prevailing morphological trends in an area should take into consideration in-situ observations. Naturally, numerical HM models, independently of their respective accuracy, are incapable of taking into consideration all of the aspects which determine morphodynamical change. For example, the effects of vegetation and artificial (man-made) interventions are very difficult to represent. This aspect of uncertainty in numerical modelling is inescapable and logically will affects the results of any study.

In-situ observations indicate the presence of a concentration of erosion in front of the risk analysis case study's location, which in turn is approximately centred around profile 121. Although variable across simulations, the results of the stochastic modelling of the Mondego Case Study also showed a concentration of erosion occurrences in the right bank of the study segment, albeit more commonly concentrated around profile 115. The distance between the two locations is not very large, being under 100 meters. In-situ conditions suggest a probable cause for this difference: in the area of the study segment where the stochastic modelling indicates the presence of erosion (profile 115), there is a significant presence of resilient vegetation, reducing bed erodibility (an effect which is unaccounted for in the numerical modelling). As the risk analysis case study (further detailed in section 8 of this study) has a significant longitudinal development parallel to the river channel, the effects of this type of uncertainty for the application of the risk analysis were mostly disregarded. Accordingly, the maximum erosion/*dH* profiles in the right bank for each simulation along the study segment (all situated in the direct vicinity of the risk analysis case study's area) were adopted as the representative erosion profiles for this case study.

The methodology for defining the representative erosion profiles for the each of the 216 simulations consisted of selecting, along the initial spatial limits of the right bank of the river (i.e., the right borderline of the main channel, presented in Figure 99), the transversal erosion profile with the highest eroded volume to the right (i.e., on the right river bank) of those limits. The transversal erosion profile producing the highest eroded volume on the right bank of the longitudinal extent defined in Figure 99 was considered to be the corresponding simulation's representative, maximum erosion/*dH* profile for the right bank.

The application of this method for determining the simulations' representative, maximum erosion profiles essentially consists of a reorientation of the generalization process offered in section 7.3.1 in consonance with the longitudinal development of the intended application of the stochastic modelling (in this case, an infrastructure with a significant longitudinal development). Figure 100 presents the corresponding maximum transversal bank erosion profiles obtained using this approach. In consonance with the characteristics of the risk analysis case study, these erosion profiles (each of which pertain to a different simulation of the stochastic modelling) were used in the risk analysis application developed in this study. The maximum erosion depth reached 3.7 meters.

Figure 99 – Location of the limit of the right bank defined along the study segment (represented in the context of the area b of the study reach).

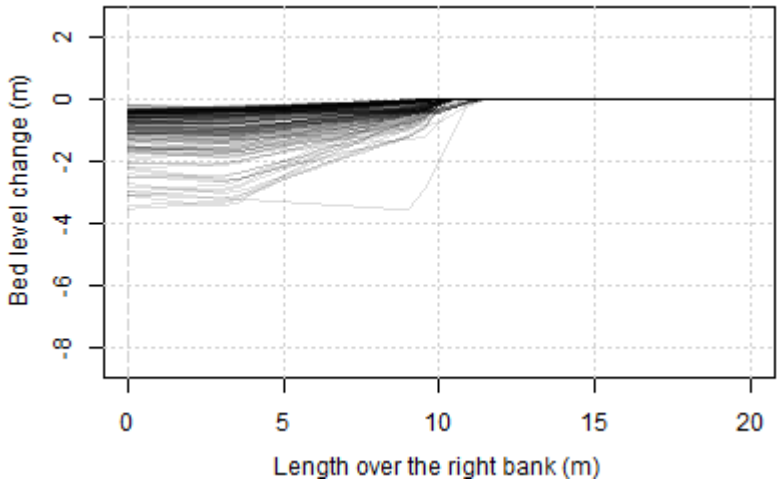

Figure 100 – Overlap of the simulated transversal maximum bank erosion profiles.

For consistency purposes, the simulated values of maximum erosion depth (one of the generalization parameters adopted in section 7.3.1) were also fitted to the semi-unbounded theoretical PDFs referred in section 7.1. The best fit PDF was (matching the results of section 7.3.1) the F distribution.

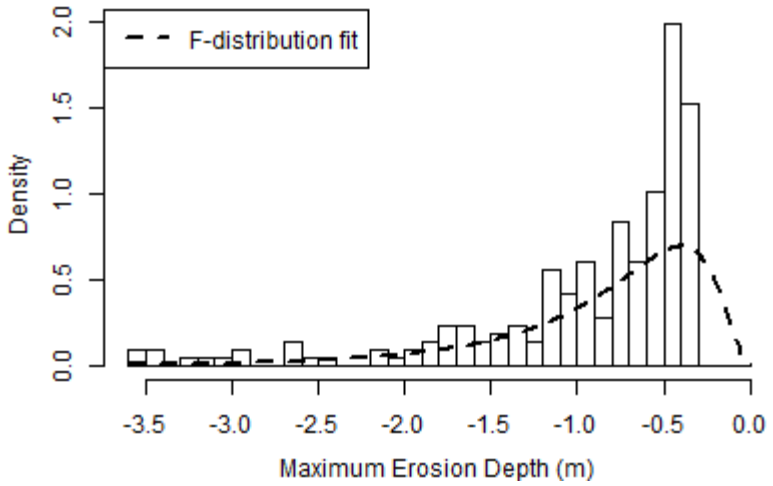

Figure 101 – Histogram of the maximum erosion depth in the right bank of the study segment. The dashed line represents the histogram's fitted F distribution.

7.4. MULTI-YEAR ANALYSIS

In an effort to establish the foundations for a multi-year application of stochastic modelling of fluvial morphodynamics (in terms of the simulations' time period), a new set of simulations was performed for the Mondego Case Study. Specifically, these simulations analysed the morphodynamical change produced by streamflow series representative of two years' worth of hydrodynamic forcings, simulated, according to the criteria presented in section 5, with six months-long streamflow series (twice the regular yearly wet period, three months, as referred in section 5.1.1), with a small transition period of 10 days in between (in order to guarantee independence between the series effects). In total, 36 new simulations were performed corresponding to all of the potential combinations of the 6 streamflow series selected

in section 5.1.2. The objective of this analysis is to (at least on a preliminary basis) assess the potential for convoluting/transforming the results of the single-year stochastic modelling into a multi-year stochastic modelling via the adaptation of the stochastic modelling's results.

This application of stochastic modelling of fluvial morphodynamics in a multi-year setting is meant to be an example application, presenting the main steps necessary to the understanding (and, in the future, representation) of the uncertainty in the compounded nature of hydrodynamic forcings. As the *Q* variable is virtually the only time-dependent variable, it was also the only variable analysed in this study. For this particular multi-year application, for all of the 36 simulations, the remaining two variables (D_m and n) were set to the same representative values used in the DS stage of the simulation process (described in section 5.1.2, viz., the P20 profile for granulometry and the mean spatial distribution of bed roughness, represented in Figure 31). Since the order of the simulations does not possess any significance, for the purposes of the analysis of their results, the simulations were identified by the rankings of the streamflow series' produced *dH* (from lower to higher, as defined in section 5.1.2.2) used in the simulations (in their respective order). For example, the simulation [1, 6] was performed with a 2-year composite streamflow series, the first year of which being the 3-month streamflow series which produces the least *dH* (with rank 1) and the second year of which being the 3-month streamflow series which produces the highest *dH* (with rank 6).

Figure 102 shows the PDF rankings for the *dH* of each of the 36 simulations performed in this multi-year (i.e., with two-years' worth of hydrodynamic forcings) stochastic modelling of fluvial morphodynamics, organized in two dimensions (respectively, the 1st series and 2nd series of the composite series in the x and y axes) so as to represent each of the potential combinations of series. The interpretation of the results presented in Figure 102 is identical to that of the pairwise graphical comparisons presented in section 6. As can be clearly observed, the relationship between the series is clearly not linear, albeit apparently simple and well-defined.

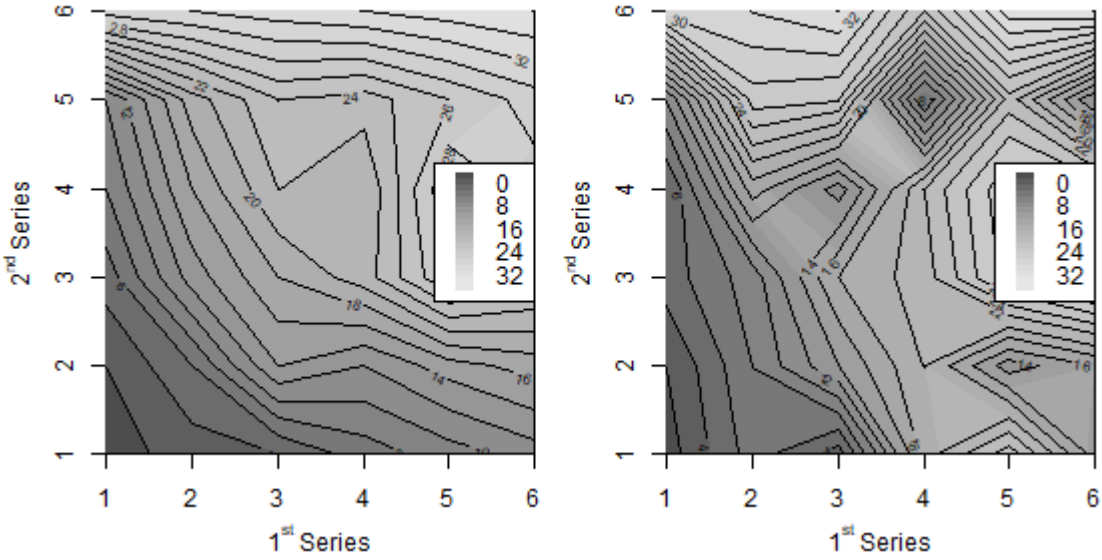

Figure 102 – Pairwise graphical comparison of the 36 combinations' rankings in terms of the corresponding mean absolute (in plot a) and mean relative (in plot b) *dH* for the 1st and 2nd series.

In consonance with what has been observed in previous sections of this study, the absolute value of *dH* once again appears to be a more reliable description of the *dH* in comparison with the relative value of *dH*. Concurrently, for the rest of this multi-year analysis, while an assessment of the relative value of *dH* is still performed, it is no longer presented as an indicator of morphodynamical change as no added information could be obtained from its analysis.

One of the aspects which is important to clarify is whether the order of the streamflow series is relevant for the characterization of the fluvial morphodynamics. In order to assess this facet of multi-year analysis, a comparison was established between the pairs of simulations with opposite first and second streamflow series, for example, the pair [1, 2]; [2, 1] or the pair [3, 5]; [5, 3]. This comparison is presented in Figure 103. Overall, aside from the pairs of simulations involving higher rankings, the differences between the order of the series does not appear to be an extremely important factor in the characterization of the fluvial morphodynamics, given that the pairs' points generally present only small deviations from the "optimal match" 45º line. On the other hand, particularly in terms of the mean absolute *dH*, there appears to be an increase in the dispersion of the points for more highly ranked simulations. These results are a further indication of the non-linearity of the *Q*'s effect on morphodynamics. In addition, they appear to indicate that the complexity of the *Q*'s relationship with morphodynamics (relative to a same initial bathymetry) increases with *dH* itself and therefore with the accumulation of the *Q*'s effects. Accordingly, the importance of the order of the streamflow series is likely to increase with the number of streamflow series (from single-events to multiple consecutive events and from single years to multiple years). The corresponding convolution of effects must logically take this into account.

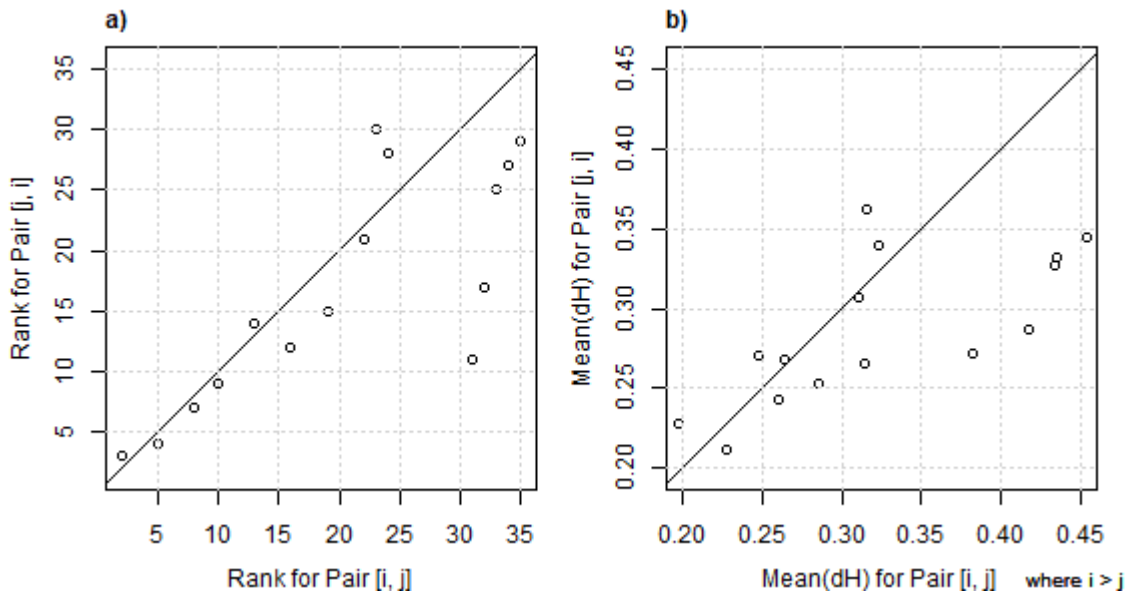

Figure 103 – Comparison of simulations with opposing pairs of streamflow series, namely in terms of the corresponding PDF rankings (in plot a) and the mean absolute *dH* (in plot b).

In addition, the relative importance of the streamflow series used in the simulation is also a relevant indication of the statistical characteristics of the compound effect of streamflow series on fluvial morphodynamics. This analysis provides information important to understanding the effects of multiple years-worth of hydrodynamic forcings, which in turn is essential to the assessment of the potential for convoluting the effects of singular years into multiple years. The relative importance of the 1st and 2nd streamflow series for the overall morphodynamical change (or, from another perspective, the fluvial morphology's sensitivity to the two series) was therefore assessed. First of all, the pairwise graphical comparisons of the 1st and 2nd series were produced and are presented in Figure 104. Using the same criteria presented in section 6 for the pairwise graphical comparisons, regarding the *dH*'s PDF ranking (PDFR) and overall mean absolute *dH* (OMAC) statistic, the results of Figure 104 clearly show a non-linearity in the relationship between the series effects and a significantly larger importance of the 1st series versus the 2nd series.

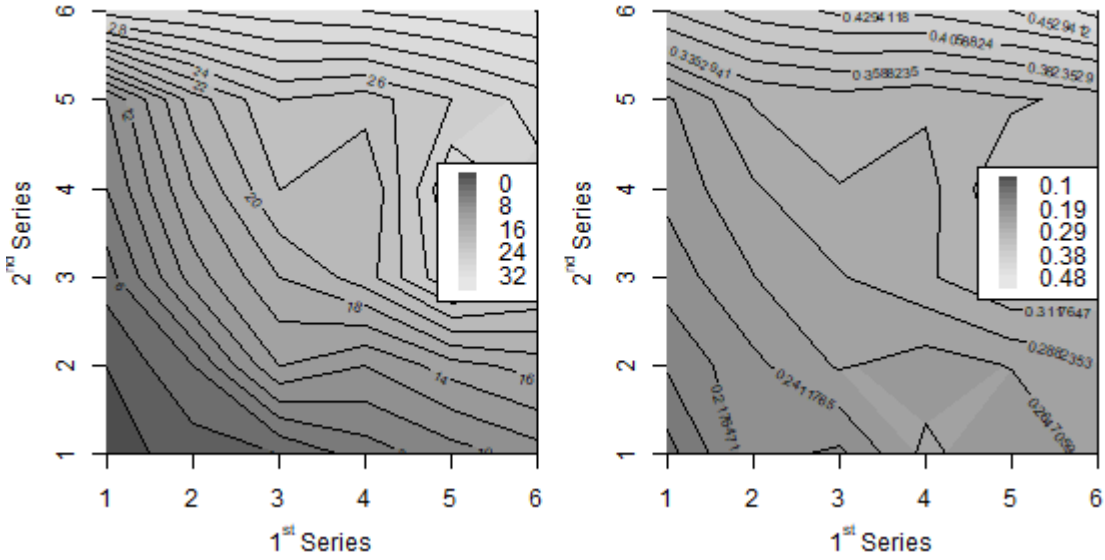

Figure 104 – Pairwise graphical comparison of 1st and 2nd series in terms of the PDF rankings (in plot a) and the mean absolute *dH* (in plot b).

As an initial attempt to convolute the effects of multiple streamflow series, a multi-linear fitting of the *dH*'s values as a function of 1st and 2nd series was performed (with the form indicated in Eq. 16). Additionally, in order to represent the different possible ways in which the streamflow series can affect morphodynamics, several statistics were used to represent morphodynamical change, namely: the OMAC and PDFR statistics, the minimum *dH* in the right bank of the study segment (selected in accordance with the approach presented in section 7.3.2) and the maximum and minimum *dH* in profile 115. The results (i.e., their respective fitted coefficients and squared Pearson correlation coefficient) of this multi-linear fitting are presented in Table 15. The results of the multi-linear fitting are clear: the 1st series has a significantly higher importance for the resulting *dH* over a period two years, often displaying nearly twice the importance of the 2nd series for the overall result. The 1st and 2nd series corresponding FOIs are 0.823 and 0.281 for the absolute *dH* and 0.488 and 0.314 for the relative *dH*.

$$dH_{i,j}^{2Y} = a \times dH_i^{1Y} + b \times dH_j^{1Y}, for\ parameters\ a\ and\ b \qquad \text{Eq. 16}$$

Some very high correlation coefficients were produced, decreasing in magnitude from reach-wide statistics (such as the PDFR and OMAC, with R^2 of over 0.8) to local statistics (such as minimum and maximum *dH* in profile 115, with R^2 of around 0.6) and to complex local measurements (such as the minimum *dH* in the right bank of the study segment, with an R^2 of 0.2). These results show that the convolution of the effects from single years into multiple years using a multi-linear fitting is feasible. However, for more specific aspects of fluvial morphology, the multi-linear fitting's accuracy is unsound.

As far as convolution processes, in addition to the multi-linear fitting, an independent convolution of the streamflow's effects was attempted (i.e., a convolution based on the principle that the *dH* produced by the individual flow series can be directly superimposed to produce the corresponding 2Y simulations). Figure 105 summarizes, for the morphodynamically representative statistics presented in

Table 15 (with the exception of the PDFR), the ECDFs for the one year long (1Y) simulations and the two years long (2Y) simulations and the estimated ECDFs using an independent convolution and a multi-linear fitting-based convolution. A visual comparison of the simulated and generated ECDFs shows that the independent convolution consistently fails to reproduce the 2Y simulations, while the multi-linear fitting-based convolution actually generally produces a relatively good solution for the convolution of the morphodynamical ECDFs. The results produced by the multi-linear fitting-based convolution (i.e., the "Fitted 2Y *dH*") largely align with the simulated 2Y ECDFs (i.e., the "Simul. 2Y *dH*"), with only some deviations closer to the more extreme values of the corresponding distributions.

Table 15 – Multi-linear fitting coefficients and R^2 coefficient for the different morphodynamically representative statistics defined as a function of the 1st and 2nd series.

	1st Series	2nd Series	Intercept	R^2
PDF Rankings (Abs[*dH*])	4.943	2.876	-8.867	0.884
Mean (Abs[*dH*])	1.234	0.648	-0.021	0.810
Minimum *dH* in right bank	0.776	0.102	-0.465	0.199
Maximum *dH* in P115	0.631	0.273	-0.442	0.628
Minimum *dH* in P115	0. 738	0. 396	0.139	0.522

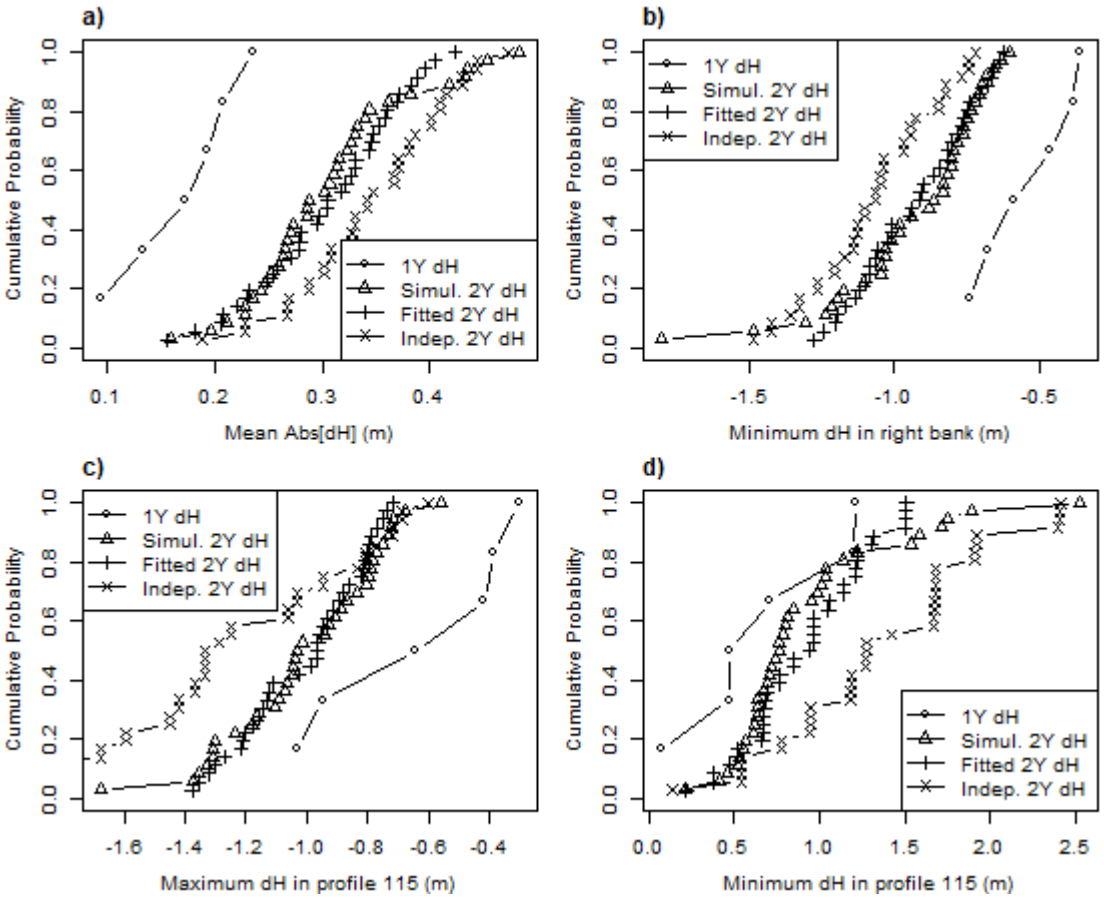

Figure 105 – Comparison of the simulated/generated ECDFs for the different statistics (mean absolute *dH* in plot a, minimum *dH*/maximum erosion in right bank of study segment in plot b, maximum *dH*/maximum sedimentation in profile 115 in plot c and minimum *dH*/maximum erosion in profile 115 in plot d), estimated for the 1-year and 2-year long simulations and the corresponding estimates for the 2-year fitted and 2-year independent CDFs.

The corresponding simulated maximum erosion profiles for the right bank of the study segment (defined according to the approach used in section 7.3.2) for the 1Y and 2Y long simulations are presented in Figure 106. As can be observed, at least on a local scale, no significant convergence of the simulations can be observed, given that the simulated magnitudes of *dH* for the 1Y simulations are often less than half of those of the 2Y simulations. Nonetheless, theoretically, based on the observed reduced importance of consecutive streamflow series compared with prior series (deducible, for example, from Table 15), the overall magnitude of morphodynamical change should reduce and/or stabilize over time.

The results here obtained seemingly indicate that, on a local level (and, most likely, in the proximity of locations with relatively extreme levels of *dH*), the convolution of *dH* is generally very hard to accomplish (due to its inherent unpredictability). However, on a global scale, given its significant overall predictability (particularly demonstrated by the high correlation coefficient obtained with the multi-linear fitting), estimating the by-product of compounding the effect of streamflow series should be, at least to some extent, feasible.

Geometrically speaking, no significant increase in the eroded width of the right bank was observed for the 2Y simulations. While no lateral expansion of the affected area was observed, for longer simulations, it is quite possible for this width to increase.

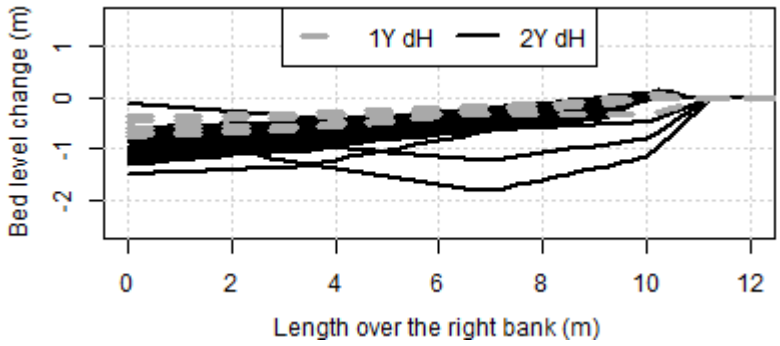

Figure 106 – Overlapped transversal maximum erosion profiles for the 1Y and 2Y simulations.

In summary, from the observations produced in this section, it was concluded that:

- The temporal order of the streamflow series (in what pertains to their respective effects on fluvial morphodynamics) is a relevant factor in determining the streamflow series compounded effect on *dH*;
- The 1st streamflow series is more important in determining the series compounded effect on *dH* than the 2nd series (often displaying twice the overall relevance for the final result);
- The convolution of the streamflow series effects on a global scale (i.e., in terms of the series overall effects on *dH*) from one year into multiple years can be performed, for the most part, by way of a simple multi-linear fitting. Moving from the global to the local scale, the feasibility of the convolution of effects decreases in accuracy and would most likely require a more complex (potentially stochastic) solution.

In accordance with the deductions drawn from the analysis of the multi-year simulations, for exploratory purposes, a simplified approach was adopted to transform the erosion profiles selected from the 1Y simulations (in section 7.3.2) to 2Y simulations. This simplified approach is based on the fact that, at least in global terms, it is possible to transform the results of the 1Y simulations into 2Y simulations. The approach consists of (1) defining a mean change factor (from 1Y to 2Y) for each of the streamflow series used and (2) applying that factor to the erosion profiles produced in the 1Y simulations as a function of the corresponding streamflow series used. By applying this approach, it is assumed that the representative erosion profiles for the 2Y simulations (which were only performed with *Q* as a variable) would differ from the erosion profiles of the 1Y simulations in equal proportion to the mean overall change in the study reach. The definition of the mean change factor was implemented based on a bias-correction/quantile-matching approach (visually described in Figure 107). The corresponding change factors are equal to the proportion between the 1Y simulations' *dH* (taken from the corresponding 6 simulations with *Q* as a variable) and the 2Y simulations' *dH* (the 36 simulations performed for the purpose of the multi-year analysis).

The adopted approach ignores potential lateral erosion expansion effects (by considering only a global *dH* change factor). However, as was observed in Figure 106, at least for the period of two years, no such lateral expansion was observed. Nonetheless, for larger time periods, it is very likely that the complexity of the applied convolution approach would have to greatly increase.

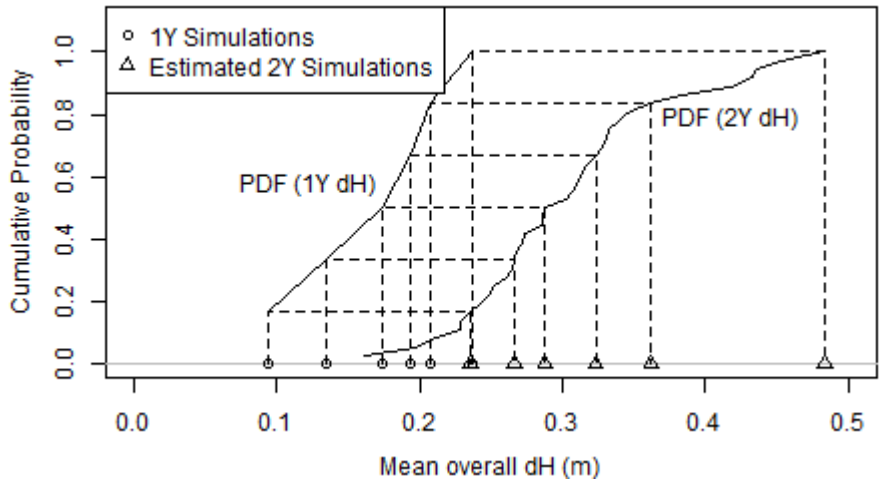

Figure 107 – Example application of bias correction procedure applied in order to transform the 1Y simulations into 2Y-corresponding results.

The resulting/updated *dH* profiles for the 2Y simulations obtained using the proposed approach are presented in Figure 108. The maximum erosion depth for the updated erosion profiles for the 2Y horizon reached 5.8 meters.

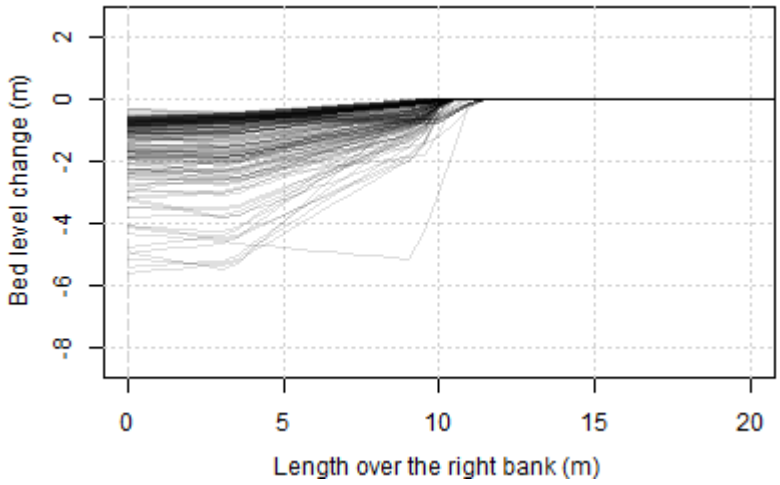

Figure 108 – Updated bank erosion profiles considering the estimated mean effects of the *Q*'s uncertainty in *dH* over a period of 2 years.

Based on the results presented in this section, it is clear that the convolution of the study reach's overall tendencies is a possibility. Strong evidence of this is the high values of R^2 obtained in the multi-linear fitting, which essentially consists of a convolution approach itself. For research purposes, the updated bank erosion profiles defined in this section will nonetheless be used as a simplified solution to represent the potential effects of morphodynamical uncertainty in this study's risk analysis case study.

The importance of the multi-year analysis of fluvial morphodynamics is undeniable. Its complete systematization will inevitably require a specific and exhaustive application of stochastic modelling (which goes behind the main purposes of this PhD study). For example, the application of the mean change factors to transform the erosion profiles produced in section 5 (which take into consideration the uncertainty of multiple variables) naturally disregards potential compound effects between variables in this context. However, analysing and taking into consideration this effect would require a large number of simulations representing the different variables' uncertainties and the uncertainty in the streamflows' compounded effects (which again fall outside the established objectives of this PhD study). The work developed in this section can hopefully provide some insight on the nature of the composite effect of the consecutive years of hydrodynamic forcings on fluvial morphology. Nonetheless, the systematization and generalization of multi-year applications will still require further studies in order to guarantee its applicability. For example, the compounded effect of streamflow series is likely to have an effect on the variables' respective sensitivities (and even the natural trends of morphological change), an effect which is important to clarify in order to validate future applications of stochastic modelling of fluvial morphodynamics.

7.5. SUMMARY

In this section, an extensive analysis of the statistical characteristics of fluvial morphodynamics (represented by the previously developed 216 simulations) is performed, namely with the purpose of

facilitating the application of the statistical description of fluvial morphodynamics (summarized in section 5.1.2.3) in a risk analysis case study relative to a near-bank infrastructure (in section 8).

While a direct application of the results of the stochastic modelling of fluvial morphodynamics in a risk analysis is conceptually executable, the aspects assessed in this section can significantly facilitate and improve the application of these results by taking advantage of their underlying characteristics. Aspects such as a potential simplification of the representation of *dH* (in the transversal direction and in areas prone to erosion, as concluded in section 7.2) and the potential generalization and extrapolation/convolution of the variables' effects on *dH* have the potential to greatly diminish the computational requirements of the stochastic modelling of fluvial morphodynamics, as well as, of its subsequent application in risk analysis. While some future developments are still necessary (particularly regarding the potential generalization and extrapolation of the stochastic outputs of the models), this statistical characterization of fluvial morphodynamics should significantly improve the viability and usefulness of this stochastic modelling, benefitting future applications.

8
RISK ANALYSIS

The development of risk analysis in this context is meant to provide an application example of the results of the stochastic modelling (performed in section 5) while establishing the foundation and defining the steps necessary for the application of risk analysis in a fluvial environment.

Generally speaking, it must be affirmed that, in the context of fluvial morphodynamics, the generally assumed concept of risk (often involving a given structure's collapse) is rarely present. This is because, morphodynamical change mostly occurs at a relatively slow pace, compared to the geometry of the terrain and structures involved. In most cases, as long as sufficient maintenance is performed, there will be no structural collapse (potentially, some light damage may occur but only requiring a reduced level of intervention). After all, most often, when visible damage to the structure or terrain is present, either the people in charge of maintenance, or potential bystanders will evenly inform the authorities responsible for this maintenance. Nevertheless, the costs associated with all potential interventions (maintenance or otherwise) are quantifiable as a function of uncertainty.

The case study used to apply the risk analysis in this study was an embankment (and the surrounding terrain) which was implemented in the vicinity of the Mondego river's main channel, namely in the right bank of the study segment. This support structure is situated in the proximity of an area of the main channel which has been previously observed to suffer from a significant level of erosion. Accordingly, the support structure itself may be subjected to collapse or damage from the effects of fluvial morphodynamics, a factor which will be analysed in this section.

8.1. APPLICATION EXAMPLE

The risk analysis developed in the context of this PhD study constitutes an application example of the results of the stochastic modelling of fluvial morphodynamics. Accordingly, this instance of risk analysis is intended to take into consideration the uncertainty inherent to fluvial morphodynamics (i.e., the bed level change – dH – over time) in the quantification of the risk associated with the corresponding case study. The system which composes this case study is constituted by an embankment/landfill (supported at the bottom by a retention wall) which was implemented in the vicinity of the Mondego river's main channel, as well as the right bank of the river in between the two. The embankment (which

is presently supporting a main road) is situated mid-length in the study segment (about three quarters of the way through area b of the study reach), in an area known to be prone to the occurrence of erosion (due to hydrodynamic forcings). In this application of risk analysis, the main goal will be to quantify the risk associated with the system's stability (defined in section 8.2) and to assess possible, illustrative intervention scenarios with the potential to minimize this risk. As this analysis focuses on the effects of morphodynamical uncertainty, only terrain-related failures were considered (where the change in the local morphology affects the safety factor of the system). The location of this risk analysis' case study is represented in Figure 109.

Figure 109 – Location of the case study for risk analysis (defined by the black box) within the area b of the reach.

The landfill/embankment supports an elevated platform, relative to the original terrain, upon which the N110 national road was built. The base of the slope stands upon a relatively flat agricultural terrain situated between the national road and the river. The shape and composition of the different elements of the embankment and its base retention wall was estimated based on in-situ observations and measurements. The base wall was observed as being composed of a vertical gabion wall. The embankment presents a high slope (41º) and loose rock protection. The resulting, average cross-section of the system is presented in Figure 110. The longitudinal extension of the embankment is of approximately 37 meters.

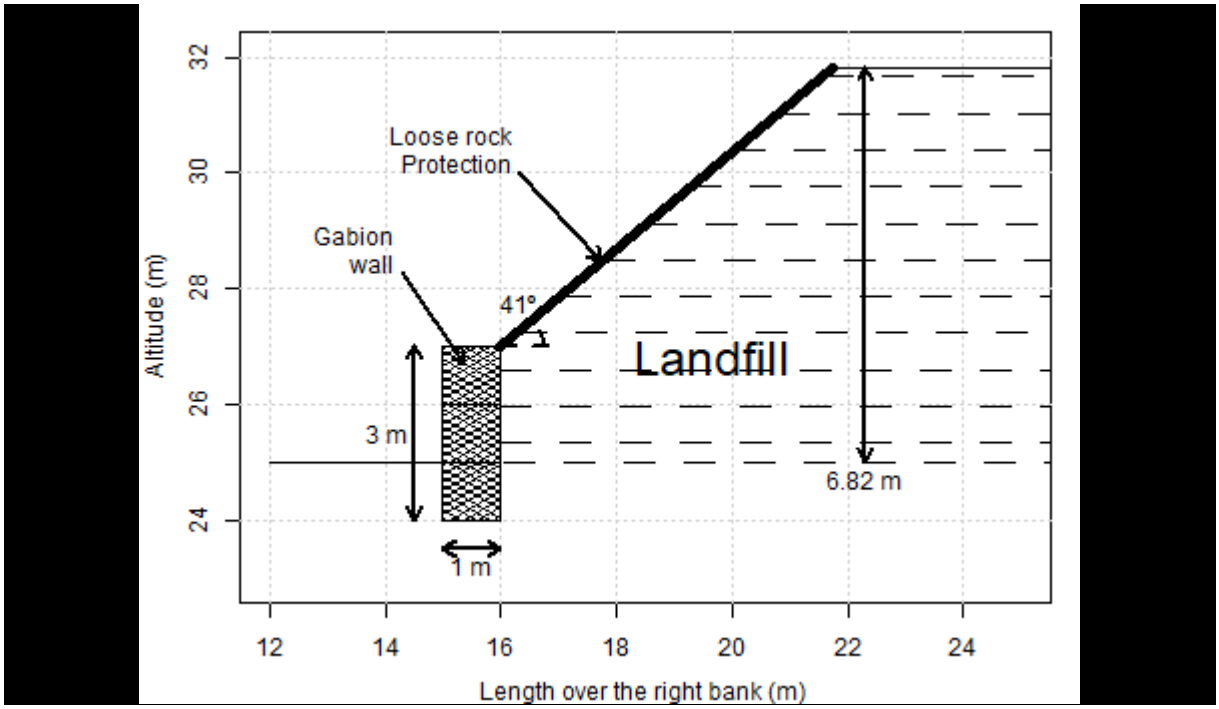

Figure 110 – Schematic cross-section of the retention wall and the embankment.

The average distance between the main channel and the base of the retention wall is of approximately 25 meters. For the 1Y horizon of the simulations, the transversal extension of the erosion profiles (which is generally of about 12 meters, as can be observed in Figure 100) was deemed insufficient to produce a significant impact on the system's stability. Although this is unlikely to remain true for longer temporal horizons, for the demonstrative purposes of this application of reliability and risk analysis, the distance between the main channel and the base of the retention wall was reduced to 15 meters (by 40%), thereby providing a more clear representation of the potential effects of bed morphodynamics in this situation. The adjusted location of the retention wall and embankment is presented in Figure 111. Photographs of this area can be found in the annex of this Thesis.

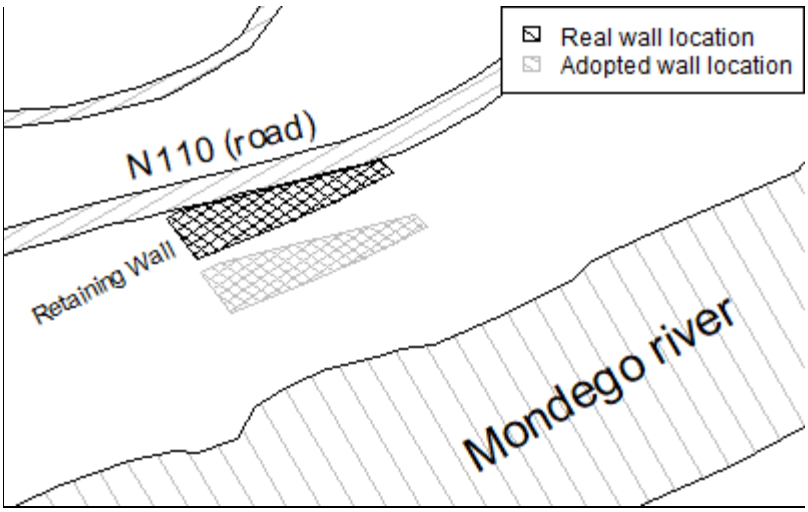

Figure 111 – Scaled schematic map of the terrain in the proximity of the case study for risk analysis.

Apart from the morphodynamical change (whose uncertainty was defined by the stochastic modelling), three other variables were considered in this risk analysis, namely, the sediment's critical/shear angle (deemed to be virtually identical for both the natural terrain and the embankment), the volumetric density of the natural soil and the volumetric density of the retention wall's and embankment's material. Further details on the definition of the variables can be found in section 8.2.

The schematic cross-section of the system, represented alongside the selected variables (i.e., the variables whose uncertainty was deemed to be relevant for the retention wall's stability), defined for the 1Y horizon is presented in Figure 112.

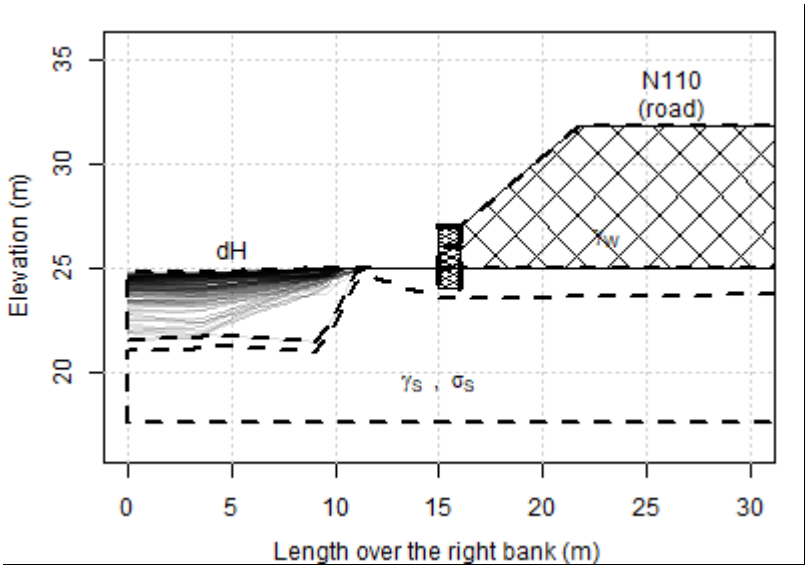

Figure 112 – Schematic cross-sectional representation of the case study and the variables whose uncertainty was deemed to be relevant for the purposes of the risk analysis, defined for the 1Y horizon.

The system (along with the morphodynamical change) was represented using a 2D model of the average transversal section (relative to the river). Its application assumes that this representation provides an appropriate description of the corresponding mechanisms. Regarding morphodynamical change, the conclusions derived in sections 7.1 and 7.2 provide strong indication of a longitudinal coherency/structure to morphodynamical change. These same observations also imply that a 2D representation of an eroded area can provide a correct representation of the system. In what concerns the embankment, as the terrain behind it curves away from the river, a 2D (infinitely developed) representation of the cross section of the case study indeed produces a reasonable (on the safe side in terms of structural stability) description of the system's behaviour. As was previously stated, the location of the channel profile with the highest erosion magnitude (for which the erosion profiles were defined) is not precisely known. At the same time, the geometry of the slope is not constant along the longitudinal direction. Accordingly, although considering an averaged 2D representation of the case study does introduce some measure of approximation (by disregarding some magnitude of 3D effects), given the demonstrative nature of this risk analysis application and the relative characteristics of the surrounding terrain, these effects have been considered as being virtually irrelevant.

In order to construct the model of the system's stability, the following assumptions were adopted:

- The natural soil was assumed to be saturated due to being relatively flat and only slightly above the water level. The embankment on the other hand, having been constructed on top of the ordinary terrain, was assumed to be virtually dry;
- The embankment's material/landfill itself and the retention wall (as well as the loose rock placed on top of the embankment) were deemed to have approximately the same physical characteristics (weight, etc.) and were therefore simulated as one individual element;
- For the purpose of this analysis, the terrain in the vicinity of the risk analysis' case study was deemed to be approximately homogenous in terms of all of its characteristics, such as, granulometry, shear angle, shear stress resistance and volumetric density;
- The gabion wall and loose rock protection were assumed to have been properly designed from conception (in that their design falls outside of the purview of this Thesis). Therefore, all potential failure surfaces which cross through their surfaces were inherently disregarded.

Conceptually, the quantification of risk for any given system/structure consists of determining (1) the different failure types which may occur, as well as (2) their respective likelihoods of occurrence and (3) the costs associated with each failure type. The product of the costs with the corresponding likelihoods describes the expected costs, i.e., risk. Risk analysis itself essentially consists of a comparative probabilistic cost-benefit analysis of the risk associated with different scenarios, where each scenario is considered to have inherent costs and to affect the relevant failure types, likelihoods and costs.

Generally, in most analyses of terrain stability, the types of terrain failure considered include slide failure (where the shear stress resistance of the soil is exceeded on a steep slope), block failure (where a directional orientation of the terrain's properties leads to an instability in a portion of the terrain) and rotational failure (where an excessive imbalance/loading of the terrain leads to the formation of – usually circular – failure surface) (Matos Fernandes, 2011). However, for the purposes of this work, only rotational failure was considered.

The definition of the failures' likelihoods requires a definition of the uncertainty of the underlying variables. Stochastic modelling, which was the main focus of this study, was used as tool to define the uncertainty surrounding morphodynamical change. This uncertainty, along with the uncertainty from other relevant variables, helps to determine the system's resistance relative to rotational failure (expressed by its safety factor). The quantification of the system's stability (to the rotational failure mode) was performed using the simplified Bishop method (Bishop, 1955) to estimate the safety factor for each potential failure surface. The safety factor of a given rotational failure surface corresponds to the ratio between the resisting and the active forces in the system (represented in Figure 113). The definition of the representative safety factor for each potential configuration of the system (i.e., the terrain and the wall/embankment) and set of variables' values is accomplished by iteratively determining the failure surface with the smallest safety factor. The implementation of this approach (which is the

standard approach for analysing rotational failure) was performed by implementing and applying the simplified Bishop method and the iterative approach for estimating the optimal failure surface (i.e., the failure surface with the lowest safety factor) in the R programming language.

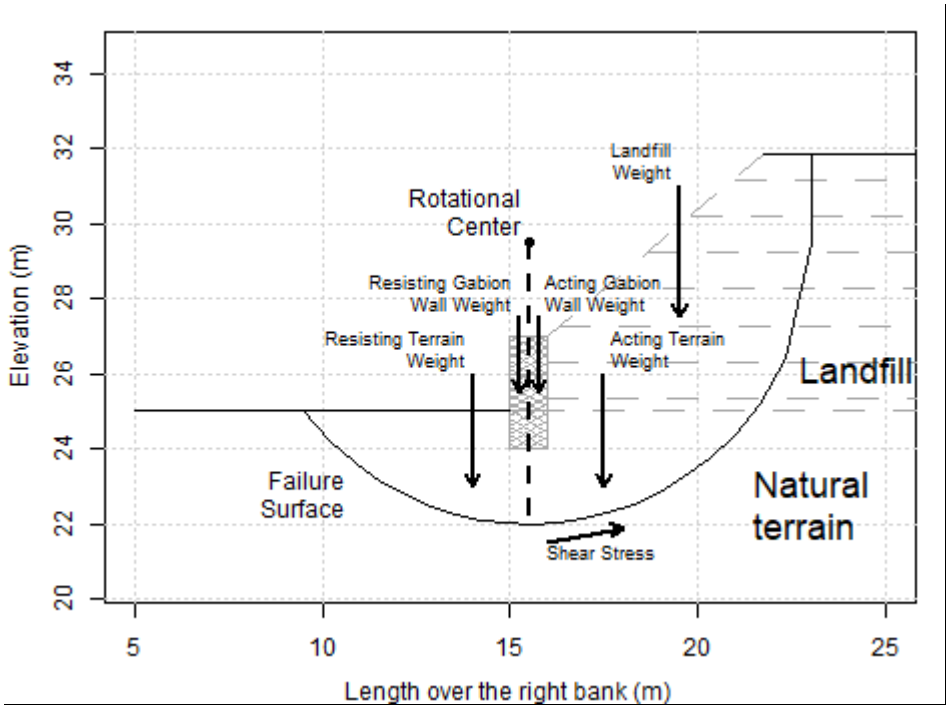

Figure 113 – Schematic representation of a rotational failure surface and the forces which determine the failure surfaces' corresponding safety factor.

While other (more complete) methods for estimating a failure surface's safety factor exist (such as the Fellenius Method and the Spencer Method), the simplified Bishop method has been found to still produce a very good representation of the safety factors for a large range of the variables values (Matos Fernandes, 2011).

8.2. VARIABLE DEFINITION AND STABILITY SIMULATIONS

As previously referred, aside from the morphodynamical change itself, the three variables whose uncertainty was analysed in this risk analysis were the shear angle (assumed to be identical for both the natural soil and the embankment's material), the volumetric density of the soil and the volumetric density of the wall's and embankment's materials. The uncertainty associated with the first three variables was estimated based on the physical characteristics of the soil's particles (particularly granulometry) and suggested values from the literature (Matos Fernandes, 2011). For the purposes of this analysis, the variables were additionally assumed to be approximately independent. Table 16 summarizes the assumed statistical parameters of the three variables whose uncertainty was simulated (alongside the uncertainty in morphodynamical change) as part of the risk analysis.

Table 16 – Theoretical probability distributions and statistical parameters of these distributions of the shear angle, soil density and wall density variables.

Variable	Symbol	Distribution	Parameters		Units
			a	b	
Shear Angle	Φ_r	Uniform	34	38	^{o} (degrees)
Dry Density of the soil	γ_s	Uniform	20	22	KN/m^3
Dry Density of the embankment's materials	γ_{wall}	Uniform	21	23	KN/m^3

The definition of the uncertainty of the morphodynamical change was estimated based on the approach developed in section 7.3.2 of this Thesis, namely assuming that each stability simulation's representative erosion profile corresponds to the highest erosion volume profile for the right bank of the river (in the vicinity of the risk analysis case study). The mean embankment cross-section and the maximum erosion profiles were used in the analysis of the system's stability in this study. The entire set of simulated profiles was assumed to be equally probable and to jointly provide a complete representation of the statistical distribution of *dH*.

The representation of the four variables' uncertainties in the risk analysis was performed by assessing the system's stability for each of the 216 representative erosion profiles combined with all potential combinations of 5 equidistant quantile values (i.e., the 0th, 25th, 50th, 75th and 100th quantiles) of the remaining three variables (the shear angle and volumetric density of the soil and the volumetric density of the wall/embankment's materials). The number of stability simulations therefore sums up to 27000 (= 216 × 5 × 5 × 5). The analysis of the system's stability was performed with the simplified Bishop method applied with these selected/sampled values/profiles of the selected variables.

The representation of morphodynamical uncertainty was performed for the 1Y horizon (using the results of the HM simulations performed in section 5) and for the 2Y horizon (estimated using the simplified approach presented in section 7.4). Figure 114 presents the schematic cross-section of the system, with a representation of the selected variables and of the updated erosion profiles for the 2Y horizon.

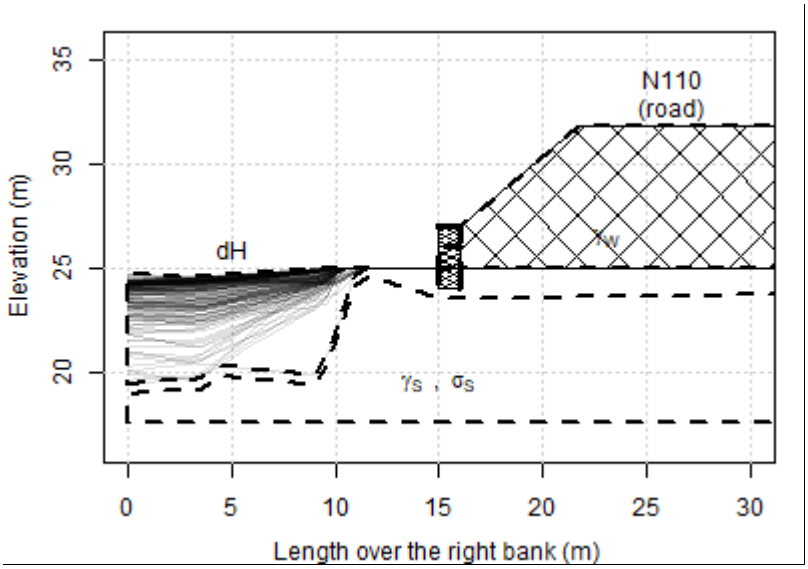

Figure 114 – Updated cross-sectional representation of the case study and the selected variables (considering the estimated effects of the morphodynamical uncertainties in *dH* for the 2Y horizon).

8.3. RESULTS AND DISCUSSION

The analysis of the system's stability was split into three independent stages, namely:

1. The analysis of the stability without the effect of fluvial morphodynamics (i.e., considering only the uncertainty from the remaining three variables);
2. The analysis of the stability for the 1Y horizon, namely, using the representative erosion profiles for each of the 216 simulations performed in section 5 to represent morphodynamical uncertainty;
3. The analysis of the stability for the 2Y horizon. Making use of the simplified approach used to extrapolate the potential erosion profiles for a 2Y horizon (presented in section 7.4), an estimate of the system's stability was produced considering the projected effects of morphodynamical change over a period of two years.

Naturally, there is always some measure of uncertainty that cannot be taken into account when performing reliability/uncertainty/risk analysis. Depending on whether the resisting forces were overestimated or the active forces were underestimated (or vice-versa), the actual safety factor of the system will change. If a harmful uncertainty has not been considered then the safety factor which may cause system collapse will generally be larger than one. However, on the other hand, if the shear resistance of the terrain is larger than anticipated, a safety factor below one does not necessarily imply system collapse. The effects of this uncertainty was considered by studying failure likelihood as a function of the system's safety factor, providing a representation of the implications of the variability of the safety factor on the overall uncertainty of the system's stability.

The risk analysis, which analysed a few potential, representative scenarios of fluvial interventions (meant to reduce the overall costs associated with morphodynamical change), was based on the results

of the system stability analysis performed for each of these phases. For the purposes of expanding on the potential applications of risk analysis (purely from an exploratory perspective), the results of the 1Y and 2Y analyses (regarding the system's stability) were also extrapolated/extended up to a 10 year horizon by fitting a geometrical decay curve to the safety factor curves (i.e., considering that the river bank' morphodynamics are likely to stabilize as time progresses).

8.3.1. System Stability Analysis

Figure 115 presents the optimal (i.e., which produce the smallest safety factor) rotational failure surfaces and the corresponding rotation centres (around which the momentum of the different forces produced by the components of the system are calculated). The definition of the rotational failure surfaces and rotation centres was determined using the R code previously described in section 8.1 and which implements the simplified Bishop method and an iterative approach for determining the optimal failure surface.

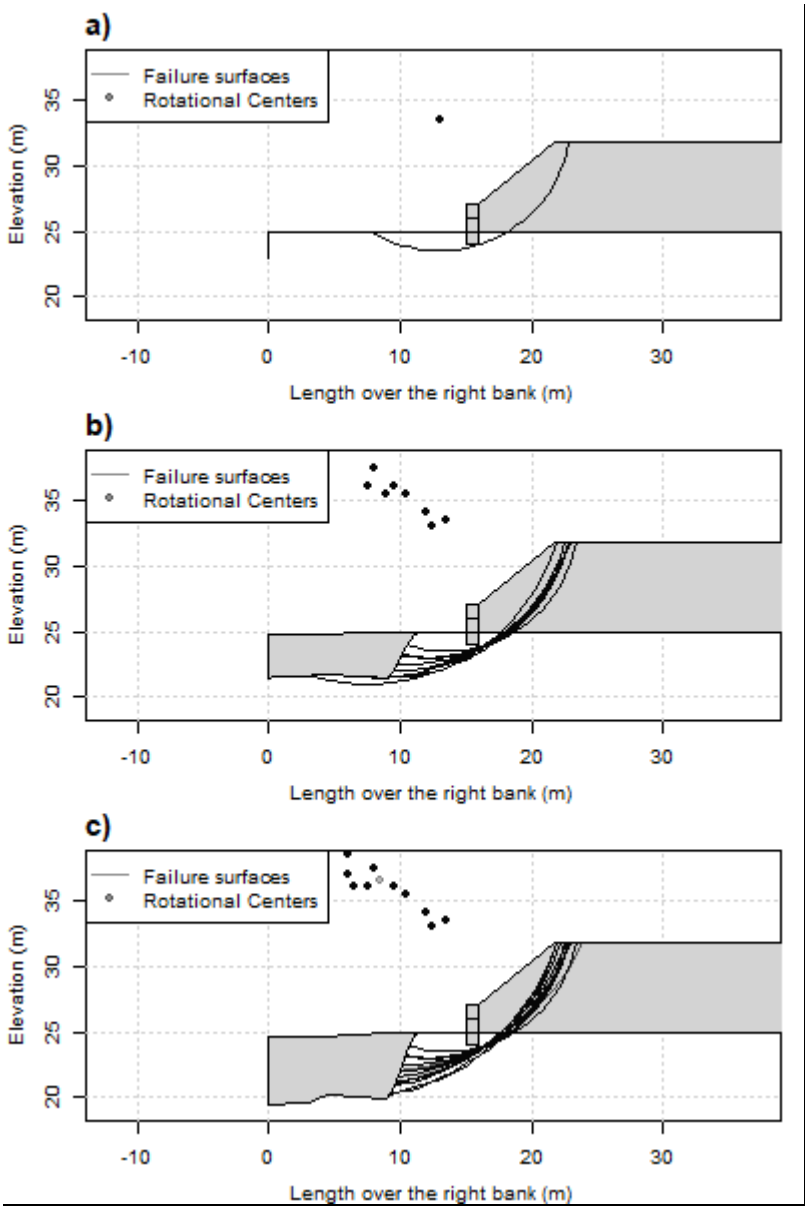

Figure 115 – Representation of the geometrical location of the estimated rotational failure surfaces and the corresponding rotational centres for stage 1 (i.e., without considering the effects of morphodynamical change, in plot a), stage 2 (considering the *dH* at the 1Y horizon) and stage 3 (considering the *dH* at the 2Y horizon). Transparency was used to accentuate the concentration of rotational centres and rotational surfaces.

As can be observed in Figure 115, in stage 1 (where the effects of fluvial morphodynamics are disregarded in the stability analysis) the rotational centres and surfaces are virtually always situated in the same spatial location.

Each of the simulations performed regarding the system's stability (represented by one rotational surface and one rotational centre in Figure 115) has its own safety factor. The histograms representing the variability of these stability simulations' safety factors are displayed in Figure 116, along with the different stages' mean safety factors.

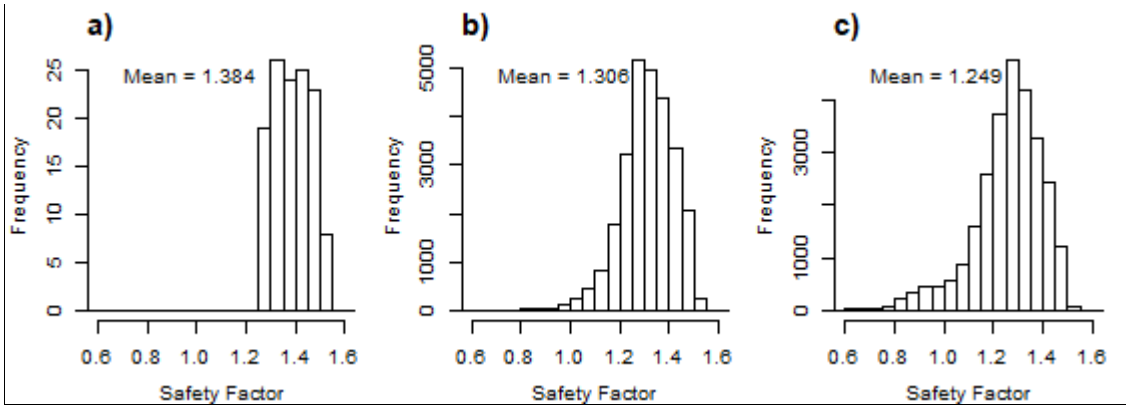

Figure 116 – Histograms of the safety factors for the three stages of the system's stability analysis (stage 1 in plot a, stage 2 in plot b and stage 3 in plot c).

The effects/magnitude of *dH* can consequently be stated to be an important aspect of the structural stability of near-river infrastructures. The mean failure likelihood (which corresponds to the percentage of stability simulations with a safety factor below one) for each of the 216 simulated/selected erosion profiles was calculated and is shown in Figure 117. As can be observed, the change in the failure likelihood between erosion profiles is relatively gradual. The fact that there are failure occurrences in more than one erosion profile, suggests that there is no single profile responsible for the potential failure (which could have signified the presence of a bias in the results).

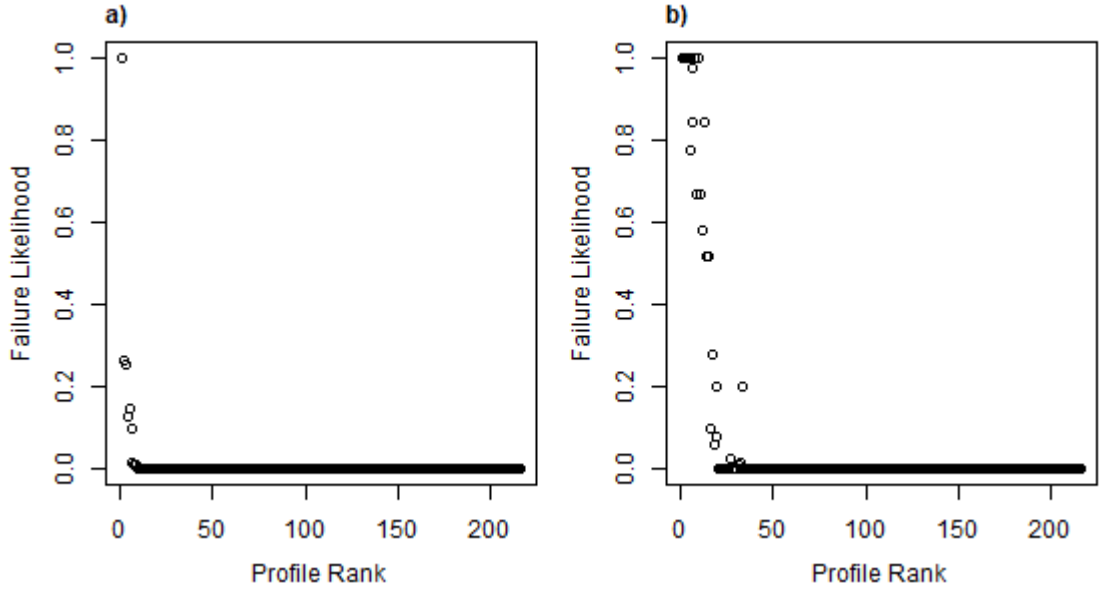

Figure 117 – Mean system failure probability (for an admissible safety factor of 1) for each of the 216 simulated bank erosion profiles, ordered in terms of *dH* PDF rank. Plot a and b respectively show the results produced with the 1Y (stage 2) and 2Y (stage 3) representative erosion profiles.

Even in the context of the stochastic modelling of fluvial morphodynamics (as well as the other variables' uncertainties), certain aspects of the case studies cannot be completely represented. Apart from the natural epistemic uncertainty which is ever-present in all forms of numerical/computational modelling, simplifications must be made in order to possibilitate the implementation of stochastic modelling. Such simplifications include the use of a reduced (albeit carefully selected) number of

variables' values to represent the variables' variability or the 2D representation of the terrain's and the embankment's behaviour. Accordingly, the safety factor which leads to the failure of the simulated system may not be always below one (which generally corresponds to the situation where the active and resisting forces are equal). Figure 118 shows the relation between the critical safety factor (the value of the safety factor below which structural collapse is likely to occur) and the corresponding cumulative probability density (i.e., the system's failure probability).

The increase in the failure likelihoods due to the inclusion of the uncertainty in morphodynamical change in the system's stability analysis is clearly significant. As a term of comparison, in the area of structural design, an acceptable failure probability for most common buildings is of around 0.0001 or 0.01%, decreasing even further for more important buildings and infrastructures. Considering only the 1Y horizon for morphodynamical change, the failure probability for a safety factor of one is of 0.89%, a much higher probability than most generally admissible values in terrain/structural stability design approaches.

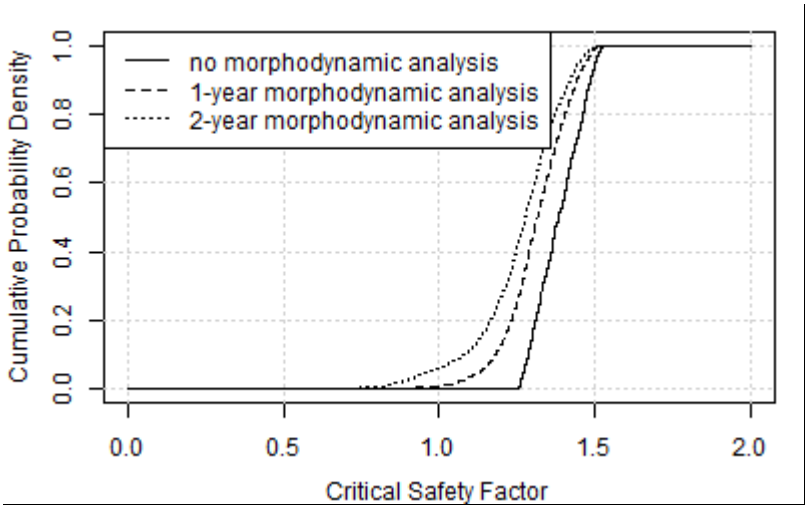

Figure 118 – Variation of the system's failure probability as a function of the corresponding admissible safety factor for the three stages of the system's stability analysis.

The results clearly show that the fluvial morphodynamics can have a very significant impact in the system's stability. A simple comparison between the different stages of the stability analysis shows that the influence of the choice of erosion profiles is a decisive factor in the occurrence of safety factors below one. Conceptually speaking, this information indicates that the system's failure can occur only by way of the influence of the *dH* in the nearby river. It is therefore important for future studies involving a system's stability in erosion prone areas to take into consideration the potential evolution of the surrounding terrain by way of the hydrodynamic forcings.

The results presented in Figure 118 translate, as a function of the admissible safety factor, the failure likelihoods (equal to the inverse of the cumulative probability density) which can be used in risk analysis to quantify the expected costs associated with failure events.

8.3.2. RISK ANALYSIS

The risk analysis application developed in this work is intended to be an exploratory example of the application of the results of the stochastic modelling of fluvial morphodynamics. This example is meant to both illustrate the potential importance of considering morphological uncertainty in the structural stability analysis of near-river infrastructures and to establish the methodology necessary for its addition in uncertainty, reliability and risk analysis.

Risk assessment can be defined as the probabilistic analysis of a set of events/failures in terms of their respective, expected costs (usually defined in monetary terms). Concurrently, risk analysis most often consists of analysing (i.e., performing risk assessment for) different scenarios in terms of the overall risk of the system. The analysis of a system's risk is generally developed in the context of a particular time period or temporal/spatial horizon. In this section, three different exemplificative scenarios of fluvial interventions (intended to reduce/mitigate the effects of morphodynamical change in the system's stability) were analysed, namely:

a) Not intervening in the area until the system's collapse occurs (i.e., the situation described in section 8.1, designated as Bank & Wall Repair solution). This scenarios involves no amount of initial investment but will eventually (upon the system's collapse) imply a significant cost associated with the system's rehabilitation and the potential (human and material) consequences;

b) Implementing a river bank protection (such as riprap, gabion walls, etc.) which renders impossible the occurrence of *dH* (designated as Y0 Bank Protection solution). This option, to be implemented in year zero of the risk analysis, while virtually removing the possibility of system destabilization by morphodynamical change, often involves a significant initial investment;

c) Actively monitoring the system's conditions and performing partial rehabilitations as needed in order to minimize the risk of system collapse (designated as Active Monit./Rehab. solution). Essentially it is assumed that, in this scenario, the soil's conditions will be kept the same as in year zero.

The assessment of the risks associated with a given scenario is generally divided into two sections, namely (1) the definition of probability distribution of the related events and failure modes and (2) the estimation of the costs associated with these same events and failure modes.

The probability distributions of the different variables involved in this risk analysis (which is often the hardest component to calculate) have already been defined in the previous sections of this Thesis. In order to provide a better description and comparison of the long term effects of the different solutions, the probability distributions of failure likelihood for the 1Y and 2Y horizons were extrapolated up to 10 years, assuming a constant decay (i.e., assuming that, for any given failure likelihood, the reduction in the corresponding safety factor is directly proportional to the previous yearly reductions by a factor *p*, calibrated based on the 0Y (zero-year horizon) to 2Y failure rates, as presented in Eq. 17). This extrapolation is purely exemplificative as the definition of the exact yearly statistical progression of *dH*

(or the most appropriate decay curve) would require a more profound study of the compounded/multi-year effects of streamflow and morphodynamics. Figure 119 shows the relationship between the system's safety factor and the corresponding failure likelihood extrapolated for the three to ten years horizon assuming a geometrical decay of the *dH* effects.

$$SF\left(F_{lik.}^{iY}\right) = \frac{SF\left(F_{lik.}^{(i-1)Y}\right) \times (p-1) - SF\left(F_{lik.}^{(i-2)Y}\right)}{p}, for\ i = 0, \ldots, n \qquad \text{Eq. 17}$$

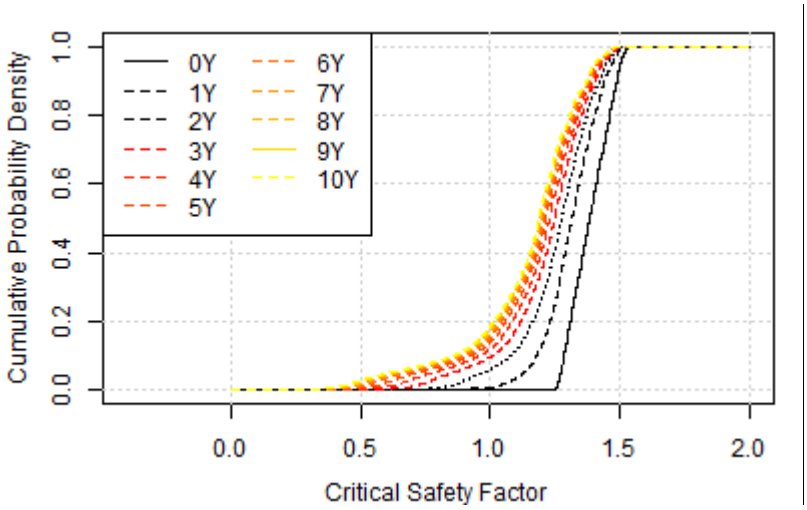

Figure 119 – Extrapolated decay of the system's failure probability as a function of the system's admissible safety factor considering a geometrical decay of the failure rate.

The second portion of the risk analysis, i.e., the definition of the costs associated with the system, is generally easier to implement (albeit sometimes suffering from some level of inaccuracy). For this section, the costs associated with the system were defined as the sum of the initial investment and the long term costs associated with the different scenarios of fluvial interventions. The quantification of the costs, while still grounded on a simplification of the reality, was estimated based on the characteristics of the solutions. The costs associated with the different, previously listed scenarios are as follows:

a) Bank & Wall Repair: In this scenario, the associated consequences correspond to the cost of reconstructing the retaining wall (assumed to be of approximately 120,000 euros) and the costs associated with the potential loss of human lives (considering an average of two people involved in the collapse). The costs associated with the loss of human lives were estimated based on the Life-Quality Index (LQI) (Nathwani, et al., 1997), in accordance with Eq. 18, where g represents the Gross Domestic Product (GDP) per capita of a country (in the case of Portugal, in 2017, it was set at 21,136 €, according to the World Bank (World Bank, 2017)), e represents the average life expectancy of individuals (set to 81.2 years, in accordance with the OECD (Organization for Economic Co-operation and Development, 2017)) and w is the proportion of the individuals' time which is invested in economic activities (set to 0.8, a common value for developed countries). The total cost of this scenario was therefore set to 160,000€ (120,000€ + 2×20,000€);

$$LQI = g^{w} \times e^{1-w} \quad \text{Eq. 18}$$

b) Y0 Bank Protection: The implementation of the bank protection itself was assumed to come at a cost of 40,000 euros. Given that there is no significant risk of erosion (and therefore of added system collapse likelihood) after the implementation of the bank protection at year zero, no other costs were considered in this scenario;

c) Active Monit./Rehab.: This solution's costs consist of a fixed component for monitoring expenses (set at 3,000 euros per year) as well as probabilistic component for potential bank repairs (with an estimated cost of 15,000 euros but only occurring in scenarios where the safety factor is below 1.0). Considering that active monitoring is implemented, the maximum progression for erosion at any given year was considered to be limited to the dH of the Y1 horizon.

These costs are summarized in Table 17. The expected costs/risks associated with a given solution for a given temporal horizon correspond to the summation of: (1) the initial costs of the solution, (2) the recurrent/maintenance/periodical costs of the solution (often defined as cost per year) up to the temporal horizon (e.g., the number of years) and (3) the morphodynamics/failure-dependent expected costs, which are defined by multiplying the failure likelihood (determined in section 8.3.1) by the failure costs.

Table 17 – Costs associated with the different types of solutions considered in this risk analysis.

Solution	Solution costs		Failure costs
	Fixed	Periodical	Fixed
Y0 Bank Protection	40,000.00 €	- €	- €
Bank & Wall Repair	- €	- €	160,000.00 €
Active Monit./Rehab.	3,000.00 €	3,000.00 €	15,000.00 €

The results of risk analysis applied using these elements (i.e., the probability space of the system's failure likelihood and the corresponding scenarios and costs) produces a comparison of the costs/benefits associated with the different scenarios over time. This comparison is presented in Figure 120, where the expected risk of each scenario is calculated by multiplying its respective costs (expressed in the previous bullet points) by their likelihoods for the different critical safety factors (presented in Figure 119).

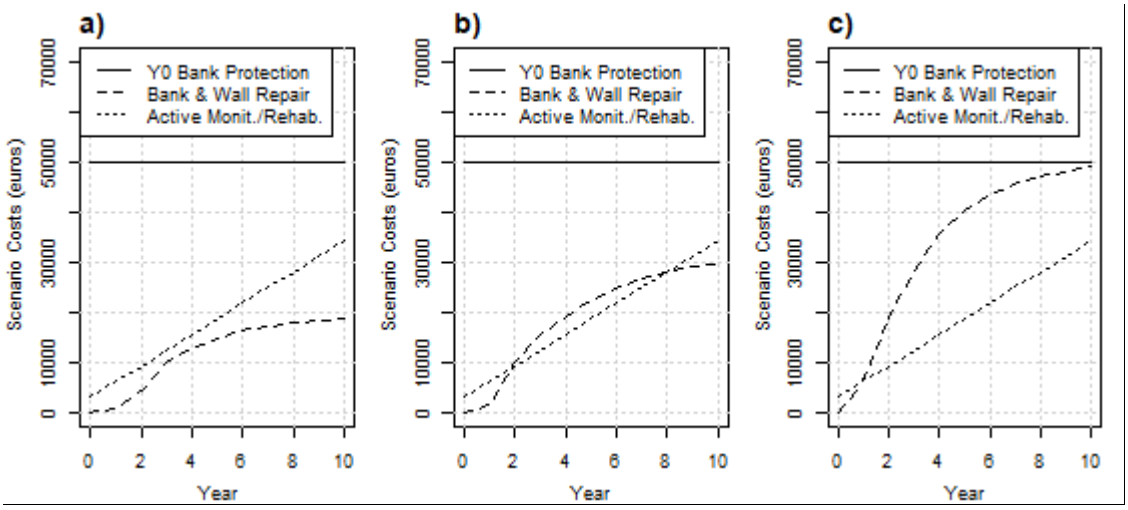

Figure 120 – Total overall costs associated with the system's failure for the three potential scenarios of fluvial interventions and calculated for an critical safety factor (above which there is no system collapse) of 0.9 (in plot a), 1 (in plot b) and 1.1 (in plot c).

The results of risk analysis provide a comparison between the costs of the different scenarios based on the ten year horizon. These results show that the choice of the optimal scenario (i.e., the one with the smallest expected overall cost can greatly change depending on the selection criteria. The selection of the optimal scenario can be performed by selecting the appropriate safety factor and comparing the scenarios expected costs for the system's desired life expectancy.

Depending on the failure criteria (i.e., the admissible safety factor below which system collapse may occur), the significance of the different scenarios can change. As an example, the optimal scenario changes between Bank & Wall Repair for a safety factor of 0.9 to Active Monit./Rehab. for a safety factor of 1.1. In the case of a safety factor of 1.1, the Bank & Wall Repair and the Y0 Bank Protection scenarios approximately reach the same expected cost after a period of 10 years. This time period essentially corresponds to the time necessary for recovering the expenses associated with the bank protection intervention (the minimum time during which the bank protection must remain functional in order for this scenario to be more cost-effective than not intervening in the channel). The application of this type of risk analysis provides a much more complete understanding of the design criteria itself (e.g., the safety factors), whilst delivering a scientific basis for cost-benefit comparison of scenarios. In addition, for analyses spanning longer periods of time, other aspects of the different scenarios could be included, for example, the expected maintenance costs of the bank protection intervention.

8.4. SUMMARY

The risk analysis developed in the context of this PhD study is intended to provide an example of how the results of the stochastic modelling of fluvial morphodynamics (i.e., the statistical description of *dH* along the river, produced in section 5) can be integrated into the risk analysis of a real life system's stability, including all of the related complexities and assumptions necessary for its inclusion. While, in the 2Y horizon of the stochastic HM simulations performed in this study, the case study's system

analysed in this section may not be significantly affected by the progression of morphodynamical change (due to its distance to the river bank), the results provide a clear demonstration of the potential of fluvial morphodynamics to affect the stability of near-bank infrastructures.

In terms of the morphodynamics' effects on the system's stability, the results of the stability analysis (section 8.3.1) for the 1Y horizon alone (which were obtained solely based on the stochastic modelling described in section 5.1 of this Thesis) indicate a failure likelihood of 0.89%, a value which would be ultimately unacceptable in the vast majority of terrain/structural design applications. The importance of fluvial morphodynamics observed in this context is itself demonstrative of the effects of morphodynamical change and of their potential importance in stability analysis.

9
CONCLUSIONS

The present study produced a complete application of stochastic modelling of fluvial morphodynamics (i.e., its main objective), designed and implemented all the way from the data to the modelling itself and its potential applications (e.g., uncertainty, reliability and risk analysis). While stochastic fluvial modelling was already possible in the past, a corresponding methodology had yet to have been refined, particularly one which encompasses the issues and limitations which result from its application in a real fluvial environment. For this purpose, a series of methodologies and tools were created (when necessary) or systematized (when feasible) in order to render possible the different stages of the stochastic modelling of fluvial morphodynamics itself. These methodologies, provide an up-to-now non-existent, systematic and scientific approach to representing the uncertainty inherent in fluvial morphodynamics. This representation of the uncertainty may then be used in other studies/analysis as necessary and as a function of their individual specificities.

In general terms, the work developed in this study involved the following tasks:

- The collection of in-situ and historical data for the Mondego Case Study (on bathymetry and topography, granulometry, streamflow, etc.);
- The creation of a stochastic streamflow time series generation technique (which was observed to produce significantly more accurate and realistic series than existing approaches);
- The development and application of a methodology for the stochastic modelling of fluvial morphodynamics;
- The sensitivity analysis of fluvial morphodynamics, intended to characterize morphodynamical sensitivities but also to validate the stochastic modelling performed;
- The statistical characterization of fluvial morphodynamics, necessary to understand how to translate the stochastic modelling's results into usable information for its application;
- A risk analysis application of the stochastic modelling's results.

Three different variables were selected for the purpose of the stochastic modelling and the representation of the natural uncertainties in fluvial morphodynamics. These variables were the streamflow (or simply the bulk flow per time interval in the channel), the granulometry of the sediment particles which

compose the channel bed (represented as a median diameter or as complex set of granulometric sizes) and the channel's bed roughness (represented as a mean, uniform value or by its spatial distribution along the channel). These variables were chosen based on the criteria (developed in section 9.1) of being relevant to fluvial morphodynamics (as opposed to being relevant only for the numerical modelling tools themselves), having a well-defined (or at least definable) uncertainty probability space and being linearly independent (in order to avoid interdependencies or overlaps between their respective uncertainties).

The stochastic streamflow time series generation technique was successfully systematized, validated and applied in this PhD study, with satisfying results (for the generation of the streamflow variable). Its' output was used as a tool for the application of the stochastic modelling of fluvial morphodynamics in a real fluvial environment.

The results of the stochastic modelling were applied in three separate tasks intended to establish and/or validate the methodology for the stochastic modelling and the potential applications of its results. These tasks were the (1) characterization of the sensitivities of the morphodynamics in relation to the selected variables, (2) the definition of a complete statistical description of fluvial morphodynamics and (3) the implementation of a risk analysis application of the stochastic morphology. The summary of the results produced in these different tasks is presented in the following subsections. Additionally, a methodology for the implementation and application of the stochastic modelling of fluvial morphodynamics (defined and optimized during the course of this study) is also presented.

While a simplified/stylized case study was also analysed in this PhD study, the focus of the developments here created is the application of the stochastic modelling in the context of a real life situation (using as an example a case study from the Mondego river), namely bearing in mind and solving all of the inherent complexities and difficulties associated with this procedure in this context. The new approaches and/or methodologies developed in this study in order to circumvent and overcome these difficulties have allowed for the implementation of the stochastic modelling of fluvial morphodynamics, as well as for the statistical characterization of fluvial morphodynamics (both individually and as a function of the simulated variables) and the application of the corresponding stochastic results.

9.1. APPLICATION METHODOLOGY FOR THE STOCHASTIC MODELLING OF FLUVIAL MORPHODYNAMICS

In this study, a methodology for performing the stochastic modelling of fluvial morphodynamics in a real fluvial environment was created, systematized and optimized. The following application methodology summarizes the different tasks, complexities and difficulties which must be taken into consideration when attempting to perform stochastic modelling for a given set of variables (whose uncertainty is to be simulated) and modelling conditions (regarding the corresponding case study's characteristics and available data).

The main tasks involved in the implementation of the stochastic modelling of fluvial morphodynamics (represented graphically in Figure 121) are as follows:

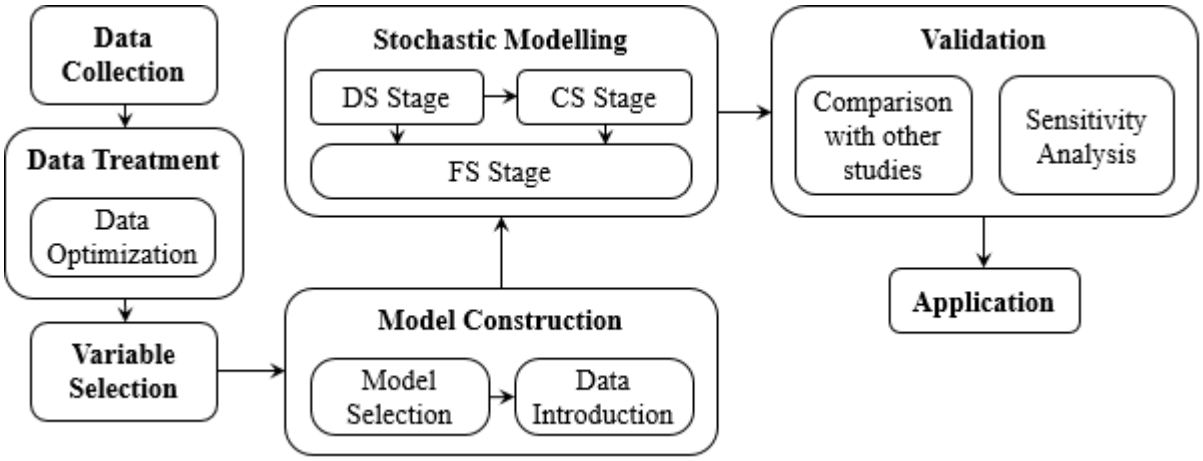

Figure 121 – Application process of the stochastic modelling of fluvial morphodynamics starting at the data collection up to the application of the corresponding results.

1. Data collection: The first task is naturally the collection of information from historical records or in-situ measurements. A complete definition of each variables' probability distributions is essential in order to correctly characterize the variables' corresponding variability ranges as, depending on the nature of the variables, the data can represent the entire range of potential values. Naturally, some knowledge on the most important variables for fluvial morphodynamics (obtainable, for example, from this and other sensitivity analyses) is important to know which information is truly necessary for the representation of uncertainty in the case study;
2. Data treatment: Through analysis of the data collected in task 1 and treatment, if necessary. As part of this task, the pre-modelling approach developed in section 5 can be an useful tool to optimize the numerical modelling by improving the quality of the bed level data (at which point this task would extend up until model construction);
3. Variable selection: The variables which are to be simulated in the stochastic modelling should be selected based on existing literature (regarding, for example, sensitivity analysis of similar situations) and on an analysis of the data collected (depending on the variability of the data regarding a given variable, that variable's uncertainty may or may not be included in the study). The variables chosen for uncertainty modelling should obey the following criteria:
    a. Simulated variables should be demonstrably relevant for the uncertainty of fluvial morphodynamics. Virtually unrelated variables or variables whose uncertainty is solely epistemic in nature (i.e., which pertain solely to the numerical representation of otherwise deterministic morphodynamical processes) should be excluded from the stochastic modelling;
    b. The independent representation of the uncertainty from significantly linearly related variables (such as sediment grain size, density and angle of repose) should be avoided. This is because their respective uncertainties may be dependent/correlated and/or not

individually representable (e.g., when certain combinations of the variables' values are not realistic, despite the individual values being within the variables' likely variability ranges). Unless the dependent variables' dependencies can be clearly represented from a statistical or deterministic perspective, the consideration of only one of such variables is the more cautious alternative (while still likely representing a large portion of the variables' effects on fluvial morphodynamics).

c. Where the definition of a variable's uncertainty range is difficult (or even impossible), the corresponding variable should be excluded from consideration (due to the significant danger of over/under-estimating the variable's effects of fluvial morphodynamics). Naturally, the selection of a given variable therefore implies the definition of the corresponding statistical characteristics and (in most cases) the corresponding series/curve/value generation approach.

4. Model construction: At this stage, the numerical HM models to be used should be selected and the data (in particular the bed level data and some initial values of the variables and parameters of the models) should be introduced in the numerical model. Naturally, the selected model should be as fast and as accurate as possible, with an emphasis on the former (given the large number of simulations that must be performed). Amongst other priorities, implicit models are often preferable because the larger time-steps which they allow for are often suitable for the representation of morphodynamical processes while being typically faster than explicit models. Finally, it is preferable for the selected model to possesses some form of interface (e.g., the R code used in this study to interact with the CCHE2D program), in order to enable the automation and acceleration of the simulation process, as well as to reduce the chance of human error;
5. Selection and stochastic modelling of the variables' uncertainty: In most situations, the available computational capacity will not allow for a full crude MCS-based representation of the variables' uncertainty ranges. Accordingly, a set of representative values must be selected for the variables in accordance with the approach adopted in section 5. Given the multiple steps involved in this task (and the interdependency of their results, described in Figure 122), the automation of this process (accomplished in this study by using the R language) is advised. The stochastic modelling of fluvial morphodynamics was split into three stages:
    a. A Direct Simulation (DS) stage, where the observed/initially-estimated values of each variable are simulated individually (i.e., for the mean/central values of the other variables). If a given variable can be directly related with morphodynamics (if their relationship is relatively simple/linear and continuously defined in terms of its probability space), then a suitable number of representative values (e.g., quantiles) can be directly sampled from that variables' estimated, historical or recorded values;
    b. A Complete Simulation (CS) stage, where new values of the variables who could not be directly sampled in the DS stage are generated, in accordance with the corresponding generation approach, in order to produce a continuum of values from which to sample

the representative values. In this stage, a large number of values should be generated and their respective effects in terms of morphodynamical change assessed. The number of generated values which can be considered as large enough is one which produces a continuum in terms of the *dH*'s probability distribution. After a continuum is developed, the variable's values which correspond to evenly spaced quantiles of the *dH*'s (and not of the variables') probability distribution can be used as the representative values (e.g., the variable's values which produce the 10^{th}, 20^{th}, etc. quantiles of *dH*);

c. A Final Simulation (FS) stage which conceptually corresponds to the stochastic modelling of fluvial morphodynamics. The combinations of the representative values selected in the previous two stages are here to be simulated in order to represent the uncertainty of fluvial morphodynamics. At this stage, the user may reasonably perform the simulation of all possible combinations of the representative values (for n^v simulations corresponding to n values of v variables) or, taking advantage of the generalization procedure developed in section 7, simulate only the matching quantile values of each variable (for n simulations corresponding to n values of v variables). This last option is only possible if the intended application of the stochastic modelling's results is mainly only focused on the study of erosion profiles/magnitudes (which have been observed to have a generalizable/extrapolatable structure).

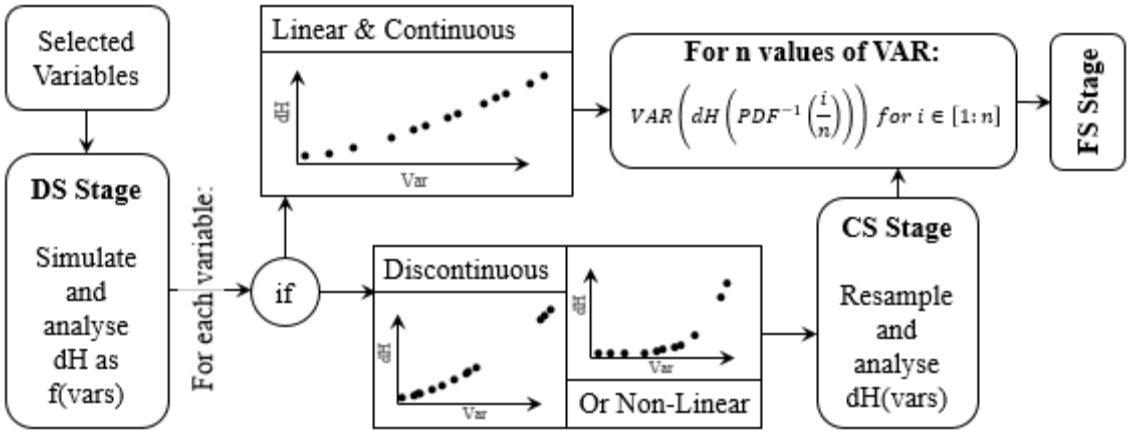

Figure 122 – Generation and resampling process for selection of the representative variables' values (which are to be simulated in the FS stage).

NOTE: Task 5 should be developed in parallel with a selection and validation process regarding the variables' and the morphodynamics' representative statistics. These statistics should be selected in the DS stage (where they are used to summarize and represent the corresponding quantities for the comparison between morphodynamics and each of the variables) and validated in the CS and FS stages. While in some cases the appropriate statistic may appear obvious (such as in the case of bed roughness), the same is not true for variables represented by a complex and dependent set of values (as is the case of granulometry, streamflow and *dH* itself). Selecting the appropriate statistics will greatly improve the quality of the selection of the variables' representative values.

6. Validation of the stochastic modelling: As has been previously stated, the validation of the stochastic modelling in a fluvial context is a complex subject given the singularity of each unique case study (particularly in terms of their respective variables' variability ranges). Nonetheless, this validation can still be performed by comparing the results of the sensitivity analysis for this case study with the results of sensitivity analyses performed on similar case studies, namely, in terms of TEIs and of the behaviour of fluvial morphodynamics. Where no other option is available, a comparison of the simulated sensitivities with the characteristics of the different variables can still provide some indication as to the quality of the simulations (e.g., a variable with a bounded variability range should have a smaller importance than a variable with a semi-unbounded variability range);
7. Application of the results of the stochastic modelling: In most cases, this application can be done directly, by applying the results of the stochastic modelling in accordance with the intended goal of the study. If, during the stochastic modelling performed in task 5, only the matching quantile values of each variable were simulated (leading to a much reduced number of simulations), the generalization procedure must be applied at this stage in order to produce a good enough description of the uncertainty of fluvial morphodynamics for application.

This application methodology for the stochastic modelling of fluvial morphodynamics was developed with the purpose of systemising the corresponding approach and developing the foundations for future studies in this area. With extra development (e.g., by, wherever possible, seamelessy integrating the numerical models with the stochastic modelling methodology), a wide-spread generalization of the application of stochastic modelling in the area of fluvial morphodynamics is a possibility, where it may be of significant benefit for uncertainty modelling (such as in structural stability analysis or morphodynamical forecasting).

9.2. ASSESSMENT OF MORPHODYNAMICAL SENSITIVITIES

As part of the sensitivity analyses performed of this study, the natural sensitivities of fluvial morphodynamics were assessed for a real life case study (the Mondego Case Study) and a simplified case study (referred to as the Stylized Case Study and constructed based on a simplification of the Mondego Case Study). The application of sensitivity analysis in this context is meant to, on the one hand, characterize the statistical relations between the selected variables and morphodynamical change (which is the conceptual purpose of sensitivity analysis) and, on the other hand, validate the results of the stochastic modelling itself. Applications of stochastic modelling cannot, by their very nature be completely validated. This is mostly because each individual simulation has no inherent value and must be understood in the context of the whole of the simulations. Accordingly, analysing and comparing the results of sensitivity analysis with the characteristics of the variables involved and the results of other applications of sensitivity analysis in similar conditions is a common solution for approximately

validating the results of sensitivity analysis. The variables whose relevance for morphodynamical change was assessed in this study were streamflow, granulometry and bed roughness.

The most commonly used (in the literature) sensitivity measurement, namely, the range statistic, is often not the most suitable statistic for application in stochastic modelling, particularly in the context of fluvial morphodynamical modelling. This is because, amongst other things, the discrete nature of this statistic is incapable of taking into consideration the probability distribution of the variables' effects on morphodynamics, thereby likely disregarding the otherwise important complexities in their relationships with morphodynamical change. The variance-based estimates of sensitivities (applied, to a significant extent, in this study) allow one to bypass these effects, defining the global sensitivities based on global measurements such as variance. The analysis of sensitivity performed in this study was also based on multiple statistics (to represent the complexities of morphodynamical change) and a few different approaches to define sensitivity (including variance-based measurements and graphical representations).

Finally, the representation of the effects of a variable's uncertainty requires a complete description of the probability distribution of that variable's effects on morphodynamics. If this description is lacking (i.e., if the description is incomplete or misrepresents this probability distribution), this would greatly reduce the quality of the stochastic modelling and, inherently, the corresponding sensitivity analysis. With this obstacle in mind, the DS and CS stages of stochastic modelling were aimed at construction of a complete description of the variables' effects (morphologically speaking) for use in the stochastic modelling. By using this approach, the selection of the variables' representative series/curves/values is more appropriate for the purpose of representing morphodynamical uncertainty. These carefully selected values provide significantly clearer results in both sensitivity analysis and the stochastic modelling's later applications.

The Stylized Case Study's purpose was to provide a simplified case study with which to compare the results of the Mondego Case Study. Concurrently, the Stylized Case Study's results were much simpler to analyse and the relationships represented by it were much easier to interpret, be it due to the simplistic nature of the channel (a stylized channel), the variables (defined by representative single parameters) or the simulations (based on a single flood event). Nevertheless, based on the comparison with the Mondego Case Study, these results allowed for the development of a likely description of the relationships between the selected variables in the context of fluvial morphodynamics. The effects of the streamflow in particular was observed to have a significant influence on the other two variables' effects on morphodynamics (potentially due to its importance for the definition of the flooded area). While, given the complexity of morphodynamical models, no two variables can be considered as forcefully independent, the results of the Mondego Case Study showed that the influence of the Granulometry and Bed Roughness may appear independent (as described by their chaotic relationship presented, for example, in Figure 75b). This fact is most likely due the complexity of morphodynamical processes superseding the Bed Roughness variable (determined as the least relevant variable for this case study) in terms of importance for the definition of bed morphodynamics. Additionally, the shape

and characteristics of the relationship between the selected variables and morphological change (the curvature, nature and positive or negative orientation of their dependency) are analogous, as would be expectable given that they are a result of the very nature of morphodynamical processes. However, on the other hand, despite these similarities between the two case studies, the variables' respective relative importance for morphodynamical uncertainty was observed to be strongly dependent on the corresponding variability ranges. Accordingly, while the overall behaviour of fluvial morphodynamics is in many aspects similar between the case studies (from a scale-independent perspective), the corresponding magnitudes can vary significantly.

The comparison of sensitivity analyses (including the two case studies analysed in this PhD study and in other studies in the literature) leads to one important conclusion: in the context of fluvial morphodynamics, the overall sensitivities quantified in sensitivity analysis, while providing interesting information on the corresponding case studies, cannot be (easily) generalized to other situations.

The validation of stochastic modelling's results (using sensitivity analysis) is most commonly performed by analysing the resulting sensitivities and determine if the modelled natural tendencies, the models' overall behaviour or the interaction between the variables is in consonance with what should be expected in that situation. In many study areas, where the characteristics of the variables involved have reasonably well defined and universally-accepted criteria for defining their corresponding variability ranges, the comparison of sensitivities for different case studies is a reasonable solution for validating the results of stochastic modelling. This is because their respective sensitivities should be very similar across a wide range of cases. However, in the case of uncertainty in fluvial morphodynamics, independently of how well-defined are a case study's variables' variability ranges, the corresponding sensitivities are naturally case-specific (the only – partial – exception to this statement is bed roughness, because it's uncertainty's variability range is usually defined – often due to the lack of an alternative – based on the data available in the literature). This of course renders nearly impossible the comparison of the morphodynamical sensitivities' magnitudes across significantly distinct case studies. Despite these limitations, the validation of the stochastic modelling performed for the Mondego Case Study was still validated using the methods and information available. Within the natural limitations of sensitivity analysis applications in the context of fluvial morphodynamics, the simulations can be deemed to be validated. *Per se*, a numerical model cannot be "proven true" but it can be corroborated, which was the purpose of this part of the study. The validity of the stochastic modelling can be stated because:

- The fluvial morphodynamics' sensitivities (expressed in terms of the TEI) are very similar in magnitude to the corresponding values obtained in a parallel study also developed for the Mondego Case Study (Santos, 2018), as represented in Figure 123. The small differences which exist between the two studies are likely to be due to the 2D nature of the present study, which is capable of capturing complex aspects of fluvial morphodynamics which are not present in a 1D analysis;
- The sensitivities calculated using the numerical HM modelling are in accordance with the variables' natures (i.e., infinite, semi-infinite and bounded) and variability ranges (i.e., their respective widths).

Streamflow, which is semi-infinite in terms of its range of variability was observed to have the highest impact in the morphodynamics overall uncertainty. Concurrently, granulometry (which was deemed to be uniformly variable over the entire range of historical measurements) and bed roughness (which was represented as a partial uncertainty around its estimated mean spatial distribution – and therefore possessed only a relatively small level of uncertainty) displayed the second least and the least impact on morphodynamical uncertainty.

Nonetheless, certain aspects of the relationships between the variables' effects and morphodynamical change, such as the curvature and other shape characteristics (of the relationships between the variables and morphodynamics and the variables' effects on fluvial morphodynamics), due to their relative nature, have a significant potential for generalization and may offer an alternative solution for sensitivity analysis-based validation of stochastic modelling. This solution for validating the stochastic application of fluvial morphodynamics models, however, requires further validation with different case studies in order to correctly determine which characteristics of the referred relationships are universal and which are not.

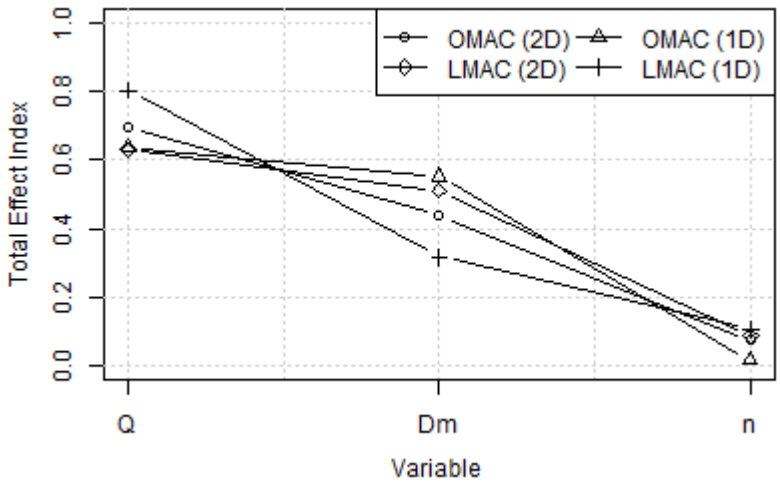

Figure 123 – TEIs obtained in the sensitivity analysis of fluvial morphodynamics for the Mondego Case Study using a 1D (Santos, 2018) and a 2D (present study) numerical HM model.

As far as the sensitivities go, the results show that the variables' hierarchy is significantly dependent on their respective variability ranges and the characteristics of the individual situations being studied. Streamflow and granulometry were observed to have a large importance for morphodynamical uncertainty. The bed roughness variable however was recurrently observed to be of lesser importance. Additionally, different components/aspects of fluvial morphodynamics are affected in different intensities by different variables. For example, the bed roughness and granulometry's variables' importance hierarchy (in the Mondego Case Study) changed depending on the specific component/statistic of morphological change which was analysed. Using different statistics to represent different aspects of morphological change is therefore necessary to fully represent the complexities of fluvial morphodynamics.

9.3. STATISTICAL CHARACTERIZATION OF FLUVIAL MORPHODYNAMICS

The statistical characterization of fluvial morphodynamics aimed to investigate the spatial patterns of fluvial morphodynamics. Apart from the obvious clarification of some important aspects of the morphodynamical processes, the analysis is also intended as a support for the application of the results of the stochastic modelling, namely, by clarifying the limitations and requirements for the application itself. The characterization of fluvial morphodynamics was based on the data from the Mondego Case Study.

Regarding the overall statistical patterns of fluvial morphodynamics, the objective of the analysis was to assess directional tendencies in the longitudinal and transversal direction in order to produce an understanding on how to translate the results of the stochastic modelling into useful data for other applications. This assessment was performed in terms of the directional serial dependency/correlation of *dH* and of the symmetry and peakdness of local and global maxima and minima of *dH*. The directional serial correlation showed a much more significant correlation in the longitudinal direction (0.67) than in the transversal direction (0.25) of the channel. Graphical evaluations of this characteristic additionally indicated that this correlation is particularly pronounced where erosion is present (and not so much where sedimentation is the predominant process). Symmetry (of peaks in *dH* – i.e., local maxima and minima of *dH*, relative to the near-peak values) was observed to be very significant in both the longitudinal and transversal direction. Larger peak values of *dH* on the other hand (as opposed to smaller peak values of *dH*) were observed to have a significant spatial coherency, with near-peak values having a relatively similar magnitude as the peak values themselves (although less significant in the longitudinal direction regarding the sedimentation occurrences). These results show that fluvial morphodynamical behaviour has a very significant spatial structure/coherency. This spatial structure is particularly pronounced in the longitudinal direction in erosion-prone areas. This information is very useful in the application of *dH* data, as is explained below.

Where the application of the data on *dH*'s uncertainty is performed in a 3D model, the results of the stochastic modelling can be directly used. However, if the application in question is performed in 2D (as would be the case with a vast majority of near-river infrastructures with a significant longitudinal orientation and development), the main question becomes whether it is possible to translate and interpret the 3D data in 2D without a sharp decrease in the application's reliability. This question could be answered by the previously referred statistical characterization of fluvial morphodynamics, where significant spatial patterns in the morphodynamical change were observed. In accordance with these results, it was concluded, that, at the very least, approximating areas of the channel prone to erosion with transversal profiles is a reasonable solution (due to the very significant longitudinal correlation of erosion occurrences – observable in Figure 91 and the similarity between peak and near-peak *dH* values – observable in Figure 93). Fortunately, this type of case studies (where a cross-sectional profile is used to represent the system/terrain/structure, often referring to near-river infrastructures with a significant

longitudinal development) is quite common, encompassing in fact the risk analysis application analysed in section 8.

Additionally, a preliminary study was performed on the potential convolution of *dH* data from one year into multiple years, namely by analysing the composite effect of multiple years' worth of streamflow on morphology. The objective was to assess the potential of using a reduced number of simulations (or one year-long instead of two year-long simulations) to represent the effects of fluvial morphodynamics over a long period of time. This study was mostly exploratory in nature and was intended to check for the convergence or divergence potential of fluvial morphodynamics and potential approaches for *dH* convolution. The results show a good potential for the convolution of the *dH*'s global tendencies (with the overall composite effects of the streamflow series being easily reproducible with a simple multi-linear fitting approach) but only with a limited potential for local applications. The complexity of the local *dH* was observed to invalidate the possibility of the convolution of the effects of consecutive years on a local scale. A simplified approach was adopted (solely from a tentative, not-comprehensive standpoint) to extrapolate the results of the stochastic modelling of the Mondego Case Study from a 1Y horizon to a 2Y horizon for application in the risk analysis case study.

Based on the information from the statistical characterization of fluvial morphodynamics, the 2D cross section profiles considered as representative for each simulation were defined, along with the corresponding selection/definition procedure. Regarding sedimentation, the lack of strong spatial pattern makes it harder to apply a generalization procedure, even in a strongly 2D application case. Erosion on the other hand has a clear pattern which can be used for extrapolating the results of stochastic modelling. The selection procedure for the representative 2D cross section varies depending on whether the target application is a localized structure/system (where the system to be analysed is generally small or has a small longitudinal development) or a longitudinally extensive structure (or one whose most hazardous cross-section is uncertain or hard to define). In the first instance, the representative cross-section simply corresponds to the section where the system in question is located, while in the second instance, the profile with the highest overall erosion in the likely area of the system (where erosion is situated or likely to be situated) should be taken as representative of the corresponding simulations. The generalization procedure was developed for the first case (although it is also theoretically applicable to the second) and consists of using a stylized/characteristic shape (viz., a hyperbolic tangent equation) to represent the standardized outline of erosion progression in the river bank and two fitted theoretical probability density functions to sample new values of the standardization parameters, thereby generating new, realistic erosion profiles.

The collection of selected or defined 2D cross sections for each simulation (i.e., which are representative of said simulation) correspond to the profiles which will reproduce the morphodynamical uncertainty for the corresponding application. Taking advantage of the spatial patterns of morphodynamical change, a functional generalization procedure for the 2D cross sections defined by the stochastic modelling was produced. This procedure shows great potential for reducing the number of simulations required to

represent morphodynamical uncertainty (depending on the characteristics of the targeted application of the stochastic modelling) by n^{v-1} simulations (for n representative values for each of the v variables).

9.4. RISK ANALYSIS OF MORPHODYNAMICS

The risk analysis application developed in this study was intended to provide the foundations for future applications of stochastic modelling of fluvial morphodynamics, by establishing (and exemplifying) the methodology for applying the results of the stochastic modelling.

Given that a significant number of parameters in this application were estimated based on the literature and the known or estimated characteristics of the terrain, the results obtained may differ from the exact real life conditions of the case study (as no direct measurements were performed regarding a few of the parameters). Nonetheless, this example provides a realistic demonstration of the potential effect and importance of the morphodynamical uncertainty in a system's reliability and risk.

As with most risk applications, the case study analysed in this application is a structure/terrain stability case where the occurrence of erosion adds to the instability of the system. The case in question (as is defined in section 8) consists of a retention wall and an embankment situated in the proximity of the Mondego river's bank. In this application of risk analysis, the system's stability was analysed and compared under three different scenarios, namely, (1) disregarding the effects of *dH* (modelling only the uncertainty in the terrain's and the structure's variables), (2) considering the simulated effects of *dH* for the 1Y horizon (estimated based on the simulations performed in section 5) and (3) considering the extrapolated effects of *dH* for the 2Y horizon (extrapolated from the simulated *dH* for the 1Y horizon in section 7.4).

The results of the reliability/stability analysis show a very significant increase in the failure probability of the system from the inclusion of the morphodynamical uncertainty. In terms of the mean safety factor, from the 1st to the 2nd and to the 3rd scenario there is a reduction of 5.6% and 4.3%, respectively. However, in terms of failure probability, while the 1st scenario has a virtual zero failure probability (considering a safety factor of 1 as the failure criteria), this value rises to 0.89% and 6.2% for the 2nd and 3rd scenarios. These failure probabilities are much more significant than most commonly used failure probabilities in terrain/structural design, which are often of around 0.01%. These results show the significant potential relevance of morphodynamical uncertainty in any system which is vulnerable to the morphodynamical change of nearby rivers and streams. As the magnitude of morphodynamical change increases, the critical failure surfaces move towards the river, growing more extensive and longer (i.e., more unsafe) relative to the 1st scenario (which is unaffected by morphodynamical change) This effect is clearly is observable in Figure 115. This indicates that the failure likelihood of the simulations can change significantly depending on the morphodynamical change scenario considered.

The most significant approximation in this risk analysis application is the multi-year extension of the erosion profiles (at the 2Y horizon) and the failure likelihood curves (at the 3 to 10Y horizon). This

extension was approximated and only intended as a representation of the potential composite effects of multiple years' worth of morphodynamical uncertainty in the risk analysis. Using this data, it was possible to perform a risk analysis of multiple scenarios of fluvial interventions and to compare the different solutions for different failure criteria. Nevertheless, even if only the 1Y horizon was considered, the effects of morphodynamical change and its uncertainty have been shown to clearly affect the stability of near-bank infrastructures – as in fact has been observed in multiple real events of structural collapse throughout the years – by increasing the system's failure probability. Morphodynamical change can therefore be clearly stated to be capable of producing a relevant effect on the stability of nearby infrastructures or terrain.

9.5. FUTURE WORK

Regarding the necessary future developments for the stochastic modelling of fluvial morphodynamics, they generally pertain to improvements which are intended to facilitate and extend the applicability of the stochastic modelling of fluvial morphodynamics. The areas which still required some development are:

- The systematization of the proposed pre-modelling approach into a more quantitative technique, possibly using one or more representative statistics (based on an evaluation of the continuity of the bed level corrections introduced by the pre-modelling approach, in accordance with the criteria presented in section 5.3.4) to estimate the optimal level of dH to be introduced (or, from a different perspective, the optimal *Q'* value to use in the application of the proposed approach).
- The validation process of the stochastic modelling, namely, by way of systematizing the characteristics of the relationships between the different variables and morphodynamics and the relationships between the different variables effects on morphodynamics. The systematization of these aspects is the best option for the validation of general purpose applications of stochastic modelling as it avoids the necessity of performing additional simulations with other models in order to establish comparison cases;
- The generalization procedure applied in section 7, which can reduce the number of simulations required for the appropriate stochastic modelling of fluvial morphodynamics. While most of this approach has already been fully developed, without further validation, it is impossible to blindly guarantee the appropriateness of the choice of the theoretical probability distributions which best fit the erosion profiles' characteristic values. For corroboration purposes, the characteristic/standardized shape of the erosion profiles should also be confirmed using other, different case studies;
- The convolution of 1Y simulations into multi-year simulations or, at least, the clarification of the tendencies and the morphodynamical behaviour produced by the composite effect of hydrodynamic forcings over multiple years. The simulations performed in this study showed a significant increase

in the complexity of the streamflow's relation with *dH* as the simulations moved from single events (in the Stylized Case Study) to 1Y and 2Y simulations (for the Mondego Case Study), indicating a divergence in the behaviour of fluvial morphology. Concurrently, even if a convolution procedure cannot be accomplished (due to this divergence), this much should be confirmed using other case studies as a base. This confirmation can be obtained by way of the simulation and analysis of the results of the stochastic modelling of fluvial morphodynamics, not just for a 1Y horizon, but also for 2Y and 3Y horizons. The potential compounding of uncertainties between the streamflow's and the other variables' uncertainties over multi-year simulations should also be taken into consideration.

Some questions which should merit significant attention in future studies in this area would be:

- Would simulating a large number of quantile-matched values of the variables (as per the generalization procedure applied in section 7) be equivalent to Crude Monte Carlo of the numerical models? Which is the more efficient solution?
- Can the results of the simulations be extrapolated (i.e., convoluted) over time? Is this possible on a local scale (even if with some approximations) or is it solely restricted to global/average quantities?
- What are the best probability distributions for morphodynamical quantities (namely for extreme, localized and global values)?
- How significant are the errors introduced by the extrapolation applied in this study in the context of the performed risk analysis (the consideration of a geometrical decay to the failure likelihood of the retention wall)? Would this be (or not) the most reasonable assumption in most situations?

Despite the significant amount of work necessary in order to accomplish these tasks, the work developed so far in this study will provide a good, complete foundation for their development, namely by way of the systematization of the methodology for the stochastic modelling of fluvial morphodynamics.

BIBLIOGRAPHY

Albertsen, P. C., Hanley, J. A., Gleason, D. F. & Barry, M. J., 1998. Competing risk analysis of men aged 55 to 74 years at diagnosis managed conservatively for clinically localized prostate cancer. *Journal of the American Medical Association,* 280(11), pp. 975-980.

Ancey, C., 2010. Stochastic modeling in sediment dynamics: Exner equation for planar bed incipient bed load transport conditions. *Journal of Geophysical Research: Earth Surface,* 115(F2).

Anderson, A. G., Paintal, A. S. & Davenport, J. T., 1970. *Tentative Design Procedure for Riprap-Lined Channels,* s.l.: Highway Research Board.

Anderson, M. p., Woessner, W. W. & Hunt, R. J., 2015. *Applied groundwater modeling: simulation of flow and advective transport.* 2nd ed. s.l.:Academic press.

Arcement, G. J. & Schneider, V. R., 1984. *Guide for Selecting Manning's Roughness Coefficients for Natural Channels and Flood Plains,* Washington, D.C.: Federal Highway Administration.

ARH Centro, 2011. *Plano de Gestão das Bacias Hidrográficas dos Rios Vouga, Mondego e Lis integrados na Região Hidrográfica 4,* s.l.: Ministério da Agricultura, Mar, Ambiente e Ordenação do Território.

Ashofteh, P.-S., Haddad, O. B. & Marino, M. A., 2014. Risk Analysis of Water Demand for Agricultural Crops under Climate Change. *Journal of Hydrologic Engineering ,* 20(4).

Ayyub, B. M., 2014. *Risk analysis in engineering and economics.* 2nd ed. s.l.:Chapman and Hall/CRC.

Ballio, F. & Menoni, S., 2009. The treatment of uncertainty in risk mitigation: the case of mountain floods. Em: M. Editore, ed. *Città, salute, sicurezza. Strumenti di governo e casi studio. La gestione del rischio*. Milano: s.n., pp. 668-692.

Beckers, F., Noack, M. & Wieprecht, S., 2016. *Reliability analysis of a 2D sediment transport model: An example of the lower river Salzach.* Stuttgart, Germany, s.n.

Bedford, T. & Cooke, R. M., 2001. *Probabilistic Risk Analysis: Foundations and Methods.* 1st ed. New York: Cambridge University Press.

Bertin, X., Fortunato, A. B. & Oliveira, A., 2007. *Sensitivity analysis of a morphodynamic modeling system applied to a Portuguese tidal inlet.* s.l., s.n.

Bishop, A. W., 1955. The Use of the Slip Circle in the Stability Analysis of Slopes. *Geotechnique,* Volume 5, pp. 7-17.

Blodgett, J. C., 1986. *Rock riprap design for protection of stream channels near highway structures; Volume 1, Hydraulic characteristics of open channels,* s.l.: US Geological Survey.

Bohorquez, P. & Ancey, C., 2015. Stochastic-deterministic modeling of bed load transport in shallow water flow over erodible slope: Linear stability analysis and numerical simulation. *Advances in water resources ,* Volume 83, pp. 36-54.

Bosompemaa, P., Yidana, S. M. & Chegbeleh, L. P., 2016. Analysis of transient groundwater flow through a stochastic modelling approach. *Arabian Journal of Geosciences,* 9(694).

Bray, D. I., 1979. Estimating average velocity in gravel-bed rivers. *Journal of the Hydraulics Division,* 105(9), pp. 1103-1122.

Chatfield, C., 2016. *The analysis of time series: an introduction*. s.l.:CRC press.

Chen, D. & Chen, H. W., 2013. Using the Köppen classification to quantify climate variation and change: An example for 1901-2010. *Environment Development,* pp. 69-79.

Chen, X. Y., Chau, K. W. & Busari, A. O., 2015. A comparative study of population-based optimization algorithms for downstream river flow forecasting by a hybrid neural network model. *Engineering Applications of Artificial Intelligence,* Volume 46, pp. 258-268.

Chow, V. T., 1959. *Open-channel hydraulics*. New York: McGraw-Hill.

Cloke, H. L., Pappenberger, F. & Renaud, J.-P., 2008. Multi-Method Global Sensitivity Analysis (MMGSA) for modelling floodplain hydrological processes. *Hydrological Processes,* Volume 22, pp. 1660-1674.

Courant, R., Friedrichs, K. & Lewy, H., 1928. On the Partial Difference Equations of Mathematical Physics. *Mathematische Annalen,* Volume 100, pp. 32-74.

de Kok, J.-L. & Grossmann, M., 2010. Large-scale assessment of flood risk and the effects of mitigation measures along the Elbe River. *Natural Hazards,* 52(1), p. 143–166.

Dolgos, D., Meier, H., Schenk, A. & Witzigmann, B., 2012. Full-band Monte Carlo simulation of high-energy carrier transport in single photon avalanche diodes with multiplication layers made of InP, InAIAs and GaAs. *Journal of Applied Physics*.

Einstein, H. A., 1942. Formulas for the transport of bed sediment. *Transactions of the American Society of Civil Engineers*.

Faber, M. H., 2012. *Statistics and Probability Theory - In Pursuit of Engineering Decision Support*. s.l.:Springer.

FEUP, APA & ARH, 2016. *Estudo de Reabilitação do Rio Mondego - Intervenção margem direita junto à Estrada Nacional N110,* s.l.: s.n.

FHWA, 2000. *Hydraulic Engineering Circular Nº 11 - Design of Riprap Revetment,* s.l.: Federal Highway Administration.

Fisher, N. I. & Switzer, P., 2001. Graphical Assessment of Dependence. *The American Statistician,* 55(3), pp. 233-239.

Flokstra, C. & Koch, F. G., 1981. *Numerical aspects of bed level predictions for alluvial river bends,* Netherlands: Delft Hydraulics Laboratory.

French, J. R. & Clifford, N. J., 2000. Hydrodynamic modelling as a basis for explaining estuarine environmental dynamics: some computational and methodological issues. *Hydrological Processes,* Volume 14, pp. 2089-2108.

Genest, C. & Boies, J.-C., 2003. Detecting Dependence With Kendall Plots. *The American Statistician,* 57(4), pp. 275-284.

Gentle, J. E., 2003. *Random Number Generation and Monte Carlo Methods.* 2nd ed. New York: Springer-Verlag.

Geweke, J., 1989. Bayesian Inference in Econometric Models using Monte Carlo Integration. *Econometrica,* 57(6), pp. 1317-1339.

Gilks, W. R., Richardson, S. & Spiegelhalter, D., 1995. *Markov chain Monte Carlo in practice*. s.l.:Chapman and Hall/CRC.

Grimaldi, S., 2004. Linear Parametric Models Applied to Daily Hydrological Series. *Journal of Hydrologic Engineerging,* pp. 383-391.

Guyon, I. & Elisseeff, A., 2003. An Introduction to Variable and Feature Selection. *Journal of Machine Learning Research,* Volume 3, pp. 1157-1182.

Hey, R. D., 1979. Flow resistance in gravel-bed rivers. *Journal of the Hydraulics Division,* 105(4), pp. 365-379.

Howard, A. K., 1984. The Revised ASTM Standard on the Unified Soil Classification System. *Geotechnical Testing Journal,* 7(4), pp. 216-222.

Hu, C. & Guo, Q., 2010. Near-bed sediment concentration distribution and basic probability of sediment movement. *Journal of Hydraulic Engineering,* pp. 1269-1275.

Huthoff, F., van Vuren, S., Barneveld, H. J. & Scheel, F., 2010. *On the importance of discharge variability in the morphodynamic modeling of rivers.* s.l., s.n., pp. 985-991.

Ikeda, S., Parker, G. & Sawai, K., 1981. Bend theory of river meanders. Part 1. Linear development. *Journal of Fluid Mechanics,* Volume 112, pp. 363-377.

Instituto da Água, s.d. *Plano específico de gestão da extração de inertes em domínio hídrico nas bacias do Mondego e do Vouga,* s.l.: s.n.

Jia, Y. & Culver, T. B., 2006. Bootstrapped artificial neural networks for synthetic flow generation with a small data sample. *Journal of Hydrology,* pp. 580-590.

Jia, Y. & Wang, S. S. Y., 2001. *CCHE2D:Two-dimensional Hydrodynamic and Sediment Transport ,* s.l.: University of Mississippi - School of Engineering.

Kalra, A. & Ahmad, S., 2011. Evaluating changes and estimating seasonal precipitation for the Colorado River Basin using a stochastic nonparametric disaggregation technique. *WATER RESOURCES RESEARCH,* Volume 47.

Kasvi, E. et al., 2015. Two-dimensional and three-dimensional computational models in hydrodynamic and morphodynamic reconstructions of a river bend: sensitivity and functionality. *Hydrological processes,* 29(6), pp. 1604-1629.

Kasyi, E. et al., 2015. Two-dimensional and three-dimensional computational models in hydrodynamic and morphodynamic reconstructions of a river bend: sensitivity and functionality. *Hydrological Processes,* 29(6), pp. 1604-1629.

Kim, Y.-S., Jang, C.-L., Lee, G.-H. & Jung, K.-S., 2010. Investigation of Flow Characteristics of Sharply Curved Channels by Using CCHE2D Model. *Korean Society of Hazard Mitigation,* 10(5), pp. 125-133.

Kleijnen, J. P. C., 1999. *Validation of models: statistical techniques and data availability.* s.l., s.n.

Kopmann, R., Merkel, U. & Riehme, J., 2012. *Using reliability analysis in morphodynamic simulation with TELEMAC-2D/SISYPHE.* s.l., XIXth TELEMAC-MASCARET User Conference 2012.

Kopmann, R. & Schmidt, A., 2014. *Comparison of different reliability analysis methods for a 2D morphodynamic numerical model of River Danube.* s.l., s.n., pp. 1615-1620.

Kristiansen, S., 2013. *Maritime transportation: safety management and risk analysis.* s.l.:Routledge.

Lall, U. & Sharma, A., 1996. A nearest neighbor bootstrap for resampling hydrologic time series. *Water Resources Research,* 32(3), pp. 679-693.

Lambeek, J., Jagers, H. & Van der Klis, H., 2004. *Monte Carlo method applied to a two-dimensional morphodynamic model.* s.l., s.n., pp. 191-196.

Lane, E. W. & Carlson, E. J., 1953. *Some factors affecting the stability of canals constructed in coarse granular materials.* s.l., Minnesota International Hydraulic Convention.

Lee, T. & Salas, J. D., 2011. Copula-based stochastic simulation of hydrological data applied to the Nile River flows. *Hydrology Research,* pp. 318-330.

Lempert, R. J. & Groves, D. G., 2010. Identifying and evaluating robust adaptive policy responses to climate change for water management agencies in the American west. *Technological Forecasting and Social Change,* 77(6), pp. 960-974.

Lettenmaier, D. P., 1984. Synthetic Streamflow Forecast Generation. *Jounal of Hydraulic Engineering,* pp. 277-289.

Limerinos, J. T., 1970. *Determination of the Manning coefficient from measured bed roughness in natural channels,* s.l.: California Department of Water Resources.

Li, W., Wang, Z., de Vriend, H. J. & van Maren, D. S., 2014. Long-Term Effects of Water Diversions on the Longitudinal Flow and Bed Profiles. *Journal of Hydraulic Engineering,* 140(6).

Maia, R. et al., 2014. *Development of a Methodology to Integrate Climate Change Effects in Water Resources Management on a Portuguese River Basin. Final Report from the Research Project (PTDC/AAC-AMB/115587/2009),* s.l.: Fundação para a Ciência e Tecnologia (FCT).

Matos Fernandes, M., 2011. *Mecânica dos Solos–Introdução à engenharia geotécnica.* Porto: Universidade do Porto, FEUP .

McNeil, B. J., 1985. Probabilistic Sensitivity Analysis Using Monte Carlo Simulation: A Practical Approach. *Medical Decision Making,* 5(2), pp. 157-177.

Melchers, R. E. & Beck, A. T., 2018. *Structural reliability analysis and prediction.* s.l.:John Wiley & Sons.

Meyer-Peter, E. & Müller, R., 1948. *Formulas for bed-load transport.* Stockholm, IAHR.

Milly, P. C. D. et al., 2008. Stationarity is dead: Whither water management. *Science,* 319(5863), pp. 573-574.

Moges, E. M., 2010. *Evaluation of sediment transport equations and parameter sensitivity analysis using the SRH-2D Model,* s.l.: Diss. MS Thesis in Universität Stuttgart.

Morway, E. D., Niswonger, R. G. & Triana, E., 2016. Toward improved simulation of river operations through integration with a hydrologic model. *Environmental Modelling & Software,* Volume 82, pp. 255-274.

Moser, B. A. & Gallus Jr., W. A., 2015. An Initial Assessment of Radar Data Assimilation on Warm Season Rainfall Forecasts for Use in Hydrologic Models. *American Meteorological Society,* pp. 1491-1520.

Mouradi, R. S. et al., 2016. *Sensitivity analysis and uncertainty quantification in 2D morphodynamic models using a newly implemented API for TELEMAC2D/SISYPHE.* s.l., s.n.

Mueller, J. E., 1968. An introduction to the hydraulic and topographic sinuosity indexes. *Annals of the Association of American Geographers,* 58(2), pp. 371-385.

Musa, J. J., 2013. Stochastic Modelling of Shiroro River Stream flow Process. *American Jounal of Engineering Research,* 2(6).

Nassar, M. A., 2011. Multi-parametric sensitivity analysis of CCHE2D for channel flow simulations in Nile River. *Journal of Hydro-environment Research,* 5(3), pp. 187-195.

Nathwani, J. S., Lind, N. C. & Pandey, M. D., 1997. *Affordable safety by choice: the life quality method,* WATERLOO, CANADA: INSTITUTE FOR RISK RESEARCH.

NCCHE, 2017. *National Center for Computational Hydroscience and Engineering.* [Online] Available at: https://www.ncche.olemiss.edu/ [Acedido em 05 05 2017].

NCCHE, 2017. *National Center for Computational Hydroscience and Engineering.* [Online] Available at: https://www.ncche.olemiss.edu/ [Accessed 05 05 2017].

Negm, A. M., Abdulaziz, T., Nassar, M. & Fathy, I., 2010. *PREDICATION OF LIFE TIME SPAN OF HIGH ASWAN DAM RESERVOIR USING CCHE2D SIMULATION MODEL.* Cairo, Egypt, s.n.

Nelson, J. M. et al., 2016. Modelling flow, sediment transport and morphodynamics in rivers. Em: G. M. Kondolf & H. Piégay, edits. *Tools in Fluvial Geomorphology.* s.l.:John Wiley & Sons, Ltd.

Neyman, J., 1934. On the two different aspects of the representative method: the method of stratified sampling and the method of purposive selection. *Journal of the Royal Statistical Society,* 97(4), pp. 558-625.

Niederreiter, H., 2010. Quasi-Monte Carlo Methods. Em: R. Cont, ed. *Encyclopedia of Quantitative Finance.* s.l.:John Wiley & Sons.

Nones, M. & Di Silvio, G., 2016. Modeling of River Width Variations Based on Hydrological, Morphological, and Biological Dynamics. *Journal of Hydraulic Engineering,* 142(7).

Noordam, D., van der Klis, H. & Hulscher, S., 2006. *Expert opinion: uncertainties in hydraulic roughness.* Zwijndrecht, s.n.

Nowak, K., Prairie, J. & Rajagopalan, B., 2008. Development of Stochastic Flow Sequences Based on Observed Data.

Oliveira, B. & Maia, R., 2018. Stochastic Generation of Streamflow Time Series. *Journal of Hydrologic Engineering,* 23(10).

Oliveira, B. & Maia, R., 2019. Pre-modelling as a tool for the optimization of morphodynamical numerical simulations. *International Journal of River Basin Management,* p. in press.

Oliveira, B., Maia, R. & Ballio, F., s.d. Numerical Sensitivity Analysis of Morphodynamics in a Straight Channel. *(under review).*

Organization for Economic Co-operation and Development, 2017. *Health at a Glance 2017,* Paris: OECD Publishing.

Ortiz, E., De Michele, C., Todini, E. & Cifres, E., 2016. *Global system for hydrological monitoring and forecasting in real time at high resolution.* s.l., EGU General Assembly 2016.

Papadrakakis, M., Papadopoulos, V. & Lagaros, N. D., 1996. Structural reliability of elastic-plastic structures using neural networks and Monte Carlo simulation. *Computer Methods in Applied Mechanics and Engineering,* Volume 136, pp. 145-163.

Pender, D., Patidar, S., Hassan, K. & Haynes, H., 2016. Method for incorporating morphological sensitivity into flood inundation modeling. *Journal of Hydraulic Engineering,* 142(6).

Phillips, B. C. & Sutherland, A. J., 1989. Spatial lag effects in bed load sediment transport. *Journal of Hydraulic Research,* 27(1), pp. 115-133.

Pinto, L., Fortunato, A. B. & Freire, P., 2006. Sensitivity analysis of non-cohesive sediment transport formulae. *Continental Shelf Research,* Volume 26, pp. 1826-1839.

Plecha, S. et al., 2010. Sensitivity analysis of a morphodynamic modelling system applied to a coastal lagoon inlet. *Ocean Dynamics,* 60(2), pp. 275-284.

Portela, M. M., Zeleňákpvá, M., Silva, A. T. & Santos, A. C., 2017. *Obtenção de Séries Sintéticas de Escoamentos Diários por Desagregação Direta de Escoamentos Anuais.* Porto, Silusba.

Posner, A. J. & Duan, J. G., 2012. Simulating river meandering processes using stochastic bank erosion coefficient. *Geomorphology,* Volume 163, pp. 26-36.

Prairie, J., Rajagopalan, B., Lall, U. & Fulp, T., 2007. A stochastic nonparametric technique for space-time disaggregation of streamflows. *Water Resources Research,* Volume 43.

Renka, R. J., Renka, R. L. & CLINE, A. K., 1984. A triangle-based C^1 interpolation method. *The Rocky Mountain journal of mathematics*, pp. 223-237.

Ricardo, A. M., Franca, M. J. & Ferreira, R. M. L., 2013. Characterization of turbulent flow within boundaries covered by rigid and emergent vegetation. *Journal of Water Resources*, 34(2), pp. 55-67.

Rocha, J. S. & Freitas, H., 1998. *O Rio Mondego. O ambiente fluvial e a sua ecologia*. Lisbon, s.n.

Saltelli, A. et al., 2008. *Global Sensitivity Analysis: The Primer.* s.l.:John Wiley & Sons.

Saltelli, A., Tarantola, S., Campolongo, F. & Ratto, M., 2004. *Sensitivity analysis in practice: a guide to assessing scientific models.* s.l.:John Wiley & Sons.

Santos, R., 2018. *Sensitivity of the Fluvial Morphodynamics to Hydromorphological Factors: Application to a Case Study,* s.l.: Faculty of Engineering of the University of Porto.

Sargent, R. G., Goldsman, D. M. & Yaacoub, T., 2016. *A TUTORIAL ON THE OPERATIONAL VALIDATION OF SIMULATION MODELS.* s.l., s.n.

Savvides, S., 1998. *Risk analysis in investment appraisal,* s.l.: s.n.

Schall, J. D., Richardson, E. V. & Morris, J. L., 2008. *Introduction to Highway Hydraulics: Hydraulic Design Series Number 4,* Washington, D.C.: Federal Highway Administration.

Scheel, F. et al., 2014. On the Generic Utilization of Probabilistic Methods for Quantification of Uncertainty in Process-Based Morphodynamic Model Applications. *Coastal Engineering Proceedings,* 1(34).

Schielen, R. M. J., Jesse, P. & Botwidt, L. J., 2007. On the use of flexible spillways to control the discharge ratio of the Rhine in the Netherlands: hydraulic and morphological observations. *Netherlands Journal of Geosciences,* 86(1), pp. 77-88.

Schuurman, F., Marra, W. A. & Kleinhans, M. G., 2013. Physics-based modeling of large braided sand-bed rivers: Bar pattern formation, dynamics, and sensitivity. *Journal of geophysical research: Earth Surface,* 118(4), pp. 2509-2527.

Scott, D. W., 2015. *Multivariate density estimation: theory, practice, and visualization.* 2nd ed. s.l.:John Wiley & Sons.

Sirangelo, B., Caloiero, T., Coscarelli, R. & Ferrari, E., 2017. A stochastic model for the analysis of maximum daily temperature. *Theoretical and Applied Climatology,* 130(1-2), p. 275–289.

Smith, R. E. & Hebbert, R. H. B., 1979. A Monte Carlo Analysis of the Hydrologic Effects of Spatial Variability of Infiltration. *Water Resources Research,* 15(2), pp. 419-429.

Snyder, N. P., Whipple, K. X., Tucker, G. E. & Merritts, D. J., 2003. Importance of a stochastic distribution of floods and erosion thresholds in the bedrock river incision problem. *Journal of Geophysiscal Research,* 108(B2).

Srinivas, V. V. & Srinivasan, K., 2001. Post-blackening approach for modeling periodic streamflows. *Jounal of Hydrology,* pp. 221-269.

Srinivas, V. V. & Srinivasan, K., 2005. Hybrid moving block bootstrap for stochastic simulation of multi-site multi-season streamflows. *Journal of Hydrology,* pp. 307-330.

Strickler, A., 1923. *Beiträge zur Frage der Geschwindigkeitsformel und der Rauhigkeitszahlen für Ströme, Kanäle und geschlossene Leitungen: mit... Tab,* s.l.: Selbstverlag.

Throne, C. R., Allen, R. G. & Simon, A., 1996. Geomorphological River Channel Reconnaissance for River Analysis, Engineering and Management. *Transactions of the Institute of British Geographers,* 21(3), pp. 469-483.

Tiwari, K. M. & Chatterjee, C., 2010. Development of an accurate and reliable hourly flood forecasting model using wavelet–bootstrap–ANN (WBANN) hybrid approach. *Journal of Hydrology,* pp. 458-470.

Topping, D. J., Rubin, D. M. & Vierra, L. E., 2000. Colorado River sediment transport: 1. Natural sediment supply limitation and the influence of Glen Canyon Dam. *Water Resources Research,* 36(2), pp. 515-542.

Tritthart, M., Schober, B. & Habersack, H., 2011. Non-uniformity and layering in sediment transport modelling 1: flume simulations. *Journal of Hydraulic Research,* 49(3), pp. 325-334.

Trivedi, P. K. & Zimmer, D. M., 2005. Copula Modelling: An Introduction for Practitioners. *Foundations and Trends in Econometrics,* 1(1), pp. 1-111.

Turowski, J. M., 2011. Probability distributions for bed form–dominated bed load transport: The Hamamori distribution revisited.. *Journal of Geophysical Research: Earth Surface,* p. 116(F2).

U.S. Army Core of Engineers Institute for Water Resources, 2016. *HEC- RAS User's Manual,* s.l.: s.n.

Van Beek, E. et al., 2005. *Water resources systems planning and management: an introduction to methods, models and applications.* Paris: UNESCO.

van Vliet, J. et al., 2016. A review of current calibration and validation practices in land-changemodeling. *Environmental Modelling & Software,* Volume 82, pp. 174-182.

van Vuren, B. G., 2005. *Stochastic modelling of river morphodynamics,* s.l.: s.n.

van Vuren, S., de Vriend, H. & Barneveld, H., 2016. A stochastic model approach for optimisation of lowland river restoration works. *Journal of Earth Science,* 27(1), p. 55–67 .

van Vuren, S., Paarlberg, A. & Havinga, H., 2015. The aftermath of "Room for the River" and restoration works: Coping with excessive maintenance dredging. *Journal of Hydro-environment Research,* 9(2), pp. 172-186.

Venables, W. N. & Smith, D. M., 2018. *An Introduction to R.* [Online]
Available at: https://cran.r-project.org/doc/manuals/r-release/R-intro.pdf
[Acedido em 02 07 2018].

Villaret, C. et al., 2016. First-order uncertainty analysis using Algorithmic Differentiation of morphodynamic models. *Computers & Geosciences,* Volume 90, pp. 144-151.

Visconti, F., Camporeale, C. & Ridolfi, L., 2010. Role of discharge variability on pseudomeandering channel morphodynamics: Results from laboratory experiments. *Journal of Geophysiscal Research: Earth Surface,* 115(F4).

Wang, W.-c.et al., 2017. The annual maximum flood peak discharge forecasting using Hermite projection pursuit regression with SSO and LS method. *Water resources management,* Volume 31.1, pp. 461-477.

Wang, W., Li, Y. & Hu, S., 2011. Wavelet Tranform Method for Synthetic Generation of Daily Streamflow. *Water Resources Management,* pp. 41-57.

World Bank, 2017. *GDP per capita (current US$) | Data.* [Online]
Available at: data.worldbank.org/indicator/NY.GDP.PCAP.CD?locations=PL-GR-DE-EU
[Acedido em 06 2018].

Wu, W., 2007. *Computational River Dynamics.* s.l.:Taylor & Francis/Balkema.

Wu, W., Wang, S. S. Y. & Jia, Y., 2000. Nonuniform sediment transport in alluvial rivers. *Journal of Hydraulic Research,* 38(6), pp. 427-434.

You, G. J.-Y., Thum, B.-H. & Lin, F.-H., 2014. The examination of reproducibility in hydro-ecological characteristics by daily synthetic flow models. *Jounal of Hydrology,* pp. 904-919.

Yurekli, K. & Kurunc, A., 2005. Performance of Stochastic Approaches in Generating Low Streamflow Data for Drought Analysis. *Journal of Spatial Hidrology*.

Zhang, Q., Hillebrand, G., Moser, H. & Hinkelmann, R., 2015. *Simulation of non-uniform sediment transport in a German reservoir with the SSIIM model and sensitivity analysis.* s.l., s.n.

Zhang, Q. et al., 2016. *Sensitivity of deposition and erosion to bed composition in the Iffezheim reservoir*. Germany, s.n.

Zhang, Y., 2005. *graphical user interface for the CCHE2D model user's manual—version 2.2,* Mississippi, US: National Center for Computational Hydroscience and Engineering.

Annex

Annex 1 – Photograph of the Mondego Case Study's upstream boundary (taken from a high location on the right bank of the river, downstream from the boundary).

Annex 2 – Photograph of the Mondego Case Study's downstream boundary (taken towards the upstream direction from one of the bridges situated on boundary iself).

Annex 3 – Photograph of the risk analysis' case study (i.e., a retention wall) taken from the opposite bank of the river.

Annex 4 – Photograph of the risk analysis' case study taken from the top of the retention wall towards the river (form the edge of the N110 national road).